AGP Accelerated Geoscience Program

RECORD 2021/4

ACCELERATED GEOSCIENCE PROGRAM EXTENDED ABSTRACTS

Government of **Western Australia**
Department of **Mines, Industry Regulation and Safety**

Geological Survey of Western Australia

Government of **Western Australia**
Department of **Mines, Industry Regulation and Safety**

RECORD 2021/4

ACCELERATED GEOSCIENCE PROGRAM EXTENDED ABSTRACTS

PERTH 2021

Geological Survey of Western Australia

MINISTER FOR MINES AND PETROLEUM
Hon Bill Johnston MLA

DIRECTOR GENERAL, DEPARTMENT OF MINES, INDUSTRY REGULATION AND SAFETY
Richard Sellers

EXECUTIVE DIRECTOR, GEOLOGICAL SURVEY AND RESOURCE STRATEGY
Jeff Haworth

REFERENCE

The recommended reference for this publication is:

(a) For reference to an individual contribution
Phillips, C, Haines, P, Martin, DMcB and Howard, HM 2021, Interpreted bedrock geology of the Far East Yilgarn, *in* Accelerated Geoscience Program extended abstracts: Geological Survey of Western Australia, Record 2021/4, p. 56–63.

(b) For reference to the publication
Geological Survey of Western Australia 2021, Accelerated Geoscience Program extended abstracts: Geological Survey of Western Australia, Record 2021/4, 217p.

ISBN 978-1-74168-931-0
ISSN 2204-4345

Isotope and element analyses were conducted using the GeoHistory laser-ablation ICP-MS and SHRIMP ion microprobe facilities at the John de Laeter Centre (JdLC), Curtin University, with the financial support of the Australian Research Council and AuScope National Collaborative Research Infrastructure Strategy (NCRIS).

The TESCAN Integrated Mineral Analyser (TIMA) instrument was funded by a grant from the Australian Research Council (LE140100150) and is operated by the JdLC with the support of the Geological Survey of Western Australia, The University of Western Australia and Murdoch University.

Based on consultation with the Western Desert Lands Aboriginal Corporation (WDLAC) on the cultural significance of the name, Waukarlycarly, it has been agreed to change the name of the well to Barnicarndy 1 and the tectonic subdivision to Barnicarndy Graben. This and all future publications will now refer to the Barnicarndy 1 stratigraphic drillhole (formerly Waukarlycarly 1) and the Barnicarndy Graben (formerly Waukarlycarly Embayment).

Published 2021 by the Geological Survey of Western Australia
This Record is published in digital format (PDF) and is available online at <www.dmirs.wa.gov.au/GSWApublications>.

Further details of geoscience products are available from:
Information Centre
Department of Mines, Industry Regulation and Safety
100 Plain Street
EAST PERTH WESTERN AUSTRALIA 6004
Telephone: +61 8 9222 3459 Email: publications@dmirs.wa.gov.au
www.dmirs.wa.gov.au/GSWApublications

Cover image: Wave and wind sculpted stromatolites at Flagpole Landing, Hamelin Pool in the world heritage site of Shark Bay, Western Australia (photo by Heidi Allen, DMIRS)

Contents

Statewide critical minerals prospectivity study

Energy systems including petroleum, geothermal, and carbon capture and storage

Accelerated Geoscience Program overview

The Geological Survey of Western Australia (GSWA) reprioritized its 2020–21 work program due to the impact of travel and operational restrictions imposed by the COVID-19 pandemic. By using its extensive, geoscience datasets and outstanding rock and paleontology collections, GSWA's Accelerated Geoscience Program (AGP) aims to aid economic recovery and stimulate the exploration industry. GSWA has delivered new interpretive datasets across all areas of geoscience in key regions of the State, accelerating understanding of the regions' geology and mineral prospectivity.

AGP main projects

Dedicated geoscientists from across GSWA have concentrated their efforts on four main projects:

1. Publication of existing data into GIS layers
2. Data integration and analyses — the Yilgarn Craton
3. Statewide critical minerals prospectivity study
4. Energy systems including petroleum, geothermal, and carbon capture and storage.

To date, the AGP has delivered close to a hundred new interpreted datasets across the four projects, consisting of about 1080 interpreted data layers that comprise original work by GSWA and repurposed or reprocessed data originating from other organizations. Many of the layers have been published online and are available through the Data and Software Centre, GeoVIEW.WA and the Petroleum and Geothermal Information management system (WAPIMS). However, most of the data are available within three standalone Geological Exploration Packages:

- Southwest Yilgarn, 2021
- Far East Yilgarn, 2021
- Critical minerals, 2021.

These standalone packages facilitate use for all levels of technical competency and software, from prospectors to Tier 1 companies. As these datasets formed part of the State's economic recovery from COVID-19, the three Geological Exploration Packages will be available at no cost from the 1st floor counter in Mineral House and at other events attended by GSWA.

Publication of existing data into GIS layers

This project has delivered previously non-digital datasets as new spatial datasets. The majority of the 13 new datasets (160 layers) are delivered at the state scale and provide a significantly improved understanding of the prospectivity of Western Australia. These new results feed into other projects in the AGP.

Data integration and analyses — the Yilgarn Craton

The Yilgarn Craton is one of Western Australia's most prospective regions and contains significant deposits of gold, nickel, lithium, copper–zinc, iron ore, tantalum, aluminium and uranium. Recent high-grade gold and nickel discoveries in the craton's far eastern (Gruyere, Tropicana, Neale) and southwestern margins (Julimar), have shown that these two poorly exposed and geologically not well-understood regions are likely to be as prospective as the craton's interior (i.e. Eastern Goldfields). Despite both regions being covered by a thick blanket of regolith, GSWA holds a vast amount of geoscientific data relating to the bedrock and regolith geology with the potential for uncovering significant, new mineral deposits.

The minerals industry is increasingly aware that the new era of Tier 1 deposits is likely to be under deep cover. Working to the UNCOVER plan, the AGP has delivered 55 new integrated geoscience datasets (500 layers) for the southwestern and far eastern Yilgarn Craton margins. The program has also incorporated the results of ongoing work in the Eastern Goldfields, and performed new analyses on archived samples.

Statewide critical minerals prospectivity study

Both the State and Federal Governments have outlined a list of minerals that are deemed critical for emerging high-tech applications and are considered essential for economic and industrial development over the next decade. Western Australia is well placed to capitalize on increasing demand for critical minerals as we transition globally to low-carbon technologies. Knowledge of the geological settings where these deposits are likely to be located not only reveals emerging exploration plays but allows the government the foresight to manage land for strategic industrial purposes such as downstream processing.

The aim of this project was to catalogue the known critical mineral resources of the State to better understand the mineral systems in which they occur and the associated alteration systems. The program has delivered 20 new datasets consisting of 251 new layers that will help to define new exploration targets and to stimulate and increase investment in the critical minerals sector by releasing new parts of the State to exploration.

Energy systems including petroleum, geothermal, and carbon capture and storage

This project has created 12 new datasets consisting of 129 data layers that critically define elements of petroleum and geothermal systems to enhance regional understanding of the prospectivity of the State's potential energy resources, including low-carbon technology.

The petroleum industry has been one of the most affected by COVID-19, having a simultaneous supply and demand shock caused by an oil price war that coincided with the start of the pandemic. The goals of this project were to produce a graphic summary of the State's well data, in addition to other GIS layers, that will directly benefit petroleum industry exploration.

AGP Accelerated Geoscience Program

Publication of existing data into GIS layers

McNaughton Legacy SHRIMP Mount Collection

by

E Blereau*, A Bellenger*, NJ McNaughton*, BIA McInnes* and MTD Wingate

Abstract

The McNaughton Legacy SHRIMP Mount Collection data layer represents a collection of geochronology samples and associated digital information donated to the Geological Survey of Western Australia (GSWA) by Professor Neal McNaughton of the John de Laeter Centre (JdLC) at Curtin University, and provided as part of the Curtin University Preservation of Legacy Collections Project (Fig. 1).

Neal McNaughton served in the role of sensitive high-resolution ion microprobe (SHRIMP) geochronologist at the Centre for Global Metallogeny (1994–2005) and the Centre for Exploration Targeting (2005–07), both at The University of Western Australia and at the JdLC (2007–19).

How to access

The data layer is best accessed using GeoVIEW.WA. This online interactive mapping system allows data to be viewed and searched together with other datasets, including GSWA and Geoscience Australia geochronology data, geological maps and mineral exploration datasets. The McNaughton collection data layer is also available for download from the Data and Software Centre, as ESRI Shape files and MapInfo Tab files.

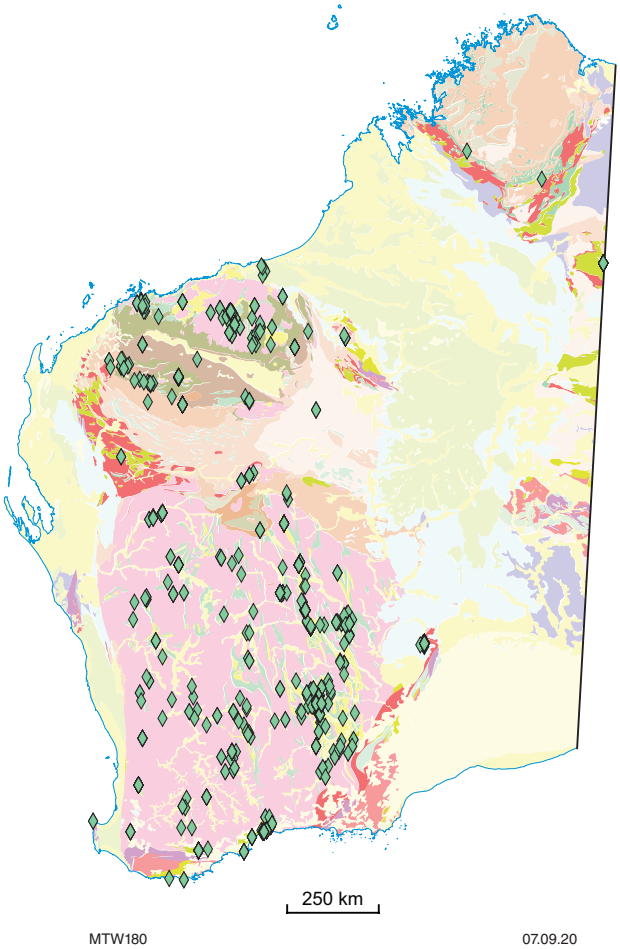

Figure 1. Locations of Western Australian samples represented in the McNaughton Legacy SHRIMP Mount Collection

* John de Laeter Centre, Curtin University, Kent Street, Bentley WA 6102

Western Australian mineral samples in the form of SHRIMP mounts in the McNaughton collection are curated by GSWA. These samples, as well as about 1700 GSWA geochronology samples listed in the accompanying GSWA geochronology layer, are available for access by researchers via email request to GSWA (geochronology@dmirs.wa.gov.au).

The geochronology samples and associated data were compiled as part of the Curtin University Preservation of Legacy Collections Project, which was responsible for the content. Limited editing has been undertaken by GSWA. The project was jointly funded by AuScope, GSWA and Curtin University. Project sponsor was Brent McInnes (JdLC Director) and data were collated by Eleanore Blereau (JdLC), with project support from Amanda Bellenger (Curtin Library), and technical support and advice from Peter Green, David Lewis, John Brown and Colin Meikle (Curtin Library) and Michael Wingate (GSWA). The digitization team included Shereen Roy, Ravi Patel, Nicole Nevill, Hannah Whitaker, Brendon Lynn and Payal Panchal.

Download additional information about the McNaughton Legacy SHRIMP Mount Collection, including samples not listed in the data layer due to their origin outside Western Australia or incomplete contextual data here (opens MS Excel worksheet, 1.08 MB). This listing provides additional location, publication and analytical details, where available.

Recommended reference

Blereau, E, Bellenger, A, McNaughton, NJ, McInnes, BIA and Wingate, MTD 2020, McNaughton Legacy SHRIMP Mount Collection, Curtin University Preservation of Legacy Collections Project: Geological Survey of Western Australia, digital data layer.

Isostatic residual gravity of Western Australia, 2020

by

JW Brett

Abstract

The gravity datasets used to generate the Isostatic residual gravity of Western Australia, 2020 are the Complete Bouguer Gravity Anomaly Grid of Onshore Australia (Nakamura, 2016), the Isostatic Residual Gravity Anomaly Grid of Onshore Australia (Nakamura, 2016) and the Bouguer gravity anomaly grid of Western Australia (Brett, 2020).

Topography was used to calculate depth to Moho using the Airy-Heiskanen crustal root model. An initial average depth to Moho at a sea level of 37 km was used. Depth to Moho was then forward modelled to produce a gravity response using a crustal density of 2.67 g/cm^3 and crust/mantle density contrast of 0.4 g/cm^3. This isostatic correction was then subtracted from the Bouguer anomaly to produce the isostatic residual gravity anomaly.

How to access

The data layer is best accessed using GeoVIEW.WA. This online interactive mapping system allows data to be viewed and searched together with other datasets, including Geological Survey of Western Australia and Geoscience Australia geochronology data, geological maps and mineral exploration datasets.

References

Nakamura, A 2016, Complete Bouguer Gravity Anomaly Grid of Onshore Australia 2016: Geoscience Australia, Canberra, doi:10.4225/25/579AB5FC3CAD7.

Nakamura, A 2016, Isostatic Residual Gravity Anomaly Grid of Onshore Australia 2016: Geoscience Australia, Canberra, doi:10.4225/25/57A0243A36A9F.

Brett, JW 2020, 400 m Bouguer gravity merged grid of Western Australia 2020 – version 1: Geological Survey of Western Australia, <www.dmirs.wa.gov.au/geophysics>.

Recommended reference

Brett, JW 2020, Isostatic residual gravity of Western Australia, 2020: Geological Survey of Western Australia, digital data layer.

Multi-scale edges for Western Australia from gravity and magnetics

by

JW Brett

Abstract

Multi-scale edges have been generated from Bouguer gravity and Reduced-to-Pole (RTP) magnetic data.

The Intrepid v5.6.3 Multi-scale edge detection module uses potential field geophysical data to provide a starting point for an interpretation of structural geology. Detection of multi-scale edges proceeds by finding local maxima points of the total horizontal derivative for many upward continuations of data. Neighbouring points are then joined together to create strings (also referred to as 'worms') that define the edges of features.

Upward continuation levels used are as follows:

gravity (11 levels): 6.2, 8.3, 11, 15, 21, 28, 38, 50, 68, 92, 124 km

magnetics (10 levels): 6.2, 8.3, 11, 15, 21, 28, 38, 50, 68, 92 km

The gravity data used to generate the multi-scale edges is the Gravity anomaly grid (400 m) of Western Australia (Brett, 2020a). The magnetic data used to generate the multi-scale edges is the Magnetic anomaly RTP grid (80 m) of Western Australia (Brett, 2020b).

The following products have been generated:

- ArcGIS shape files of multi-scale edges from gravity and magnetic data.

How to access

The data layer is best accessed using GeoVIEW.WA. This online interactive mapping system allows data to be viewed and searched together with other datasets, including Geological Survey of Western Australia and Geoscience Australia geochronology data, geological maps and mineral exploration datasets.

References

Brett, JW 2020a, 400 m Bouguer gravity merged grid of Western Australia 2020 – version 1: Geological Survey of Western Australia, <www.dmirs.wa.gov.au/geophysics>.

Brett, JW 2020b, 80 m magnetic RTP merged grid of Western Australia 2020 – version 1: Geological Survey of Western Australia, <www.dmirs.wa.gov.au/geophysics>.

Recommended references

Brett, JW 2020, Multi-scale edges for Western Australia from gravity and magnetics: Geological Survey of Western Australia, digital data layer.

1:100 000 regolith geology regimes of Western Australia

by

N de Souza Kovacs and S Jakica

Abstract

The 1:100 000 regolith geology regimes of Western Australia digital layer is a compilation of existing Geological Survey of Western Australia (GSWA) regolith and surface geology maps and new regolith interpretation using radiometric ternary KTU (potassium, thorium, uranium) imagery.

This new product incorporates all regolith coverage available at 1:100 000 scale and uses a revised regolith classification scheme. Regolith geology from 1:100 000 and 1:250 000-scale maps has been compiled to produce a seamless digital regolith coverage (Fig. 1). The coding of regolith units in the layer follows GSWA's regolith classification scheme (GSWA, 2013) with the addition of a depositional regime unit (_D-WAD). The suffix (-WAD) represents the Western Australia Division, a major physiographic division based on Pain et al. (2011). Earlier maps that did not conform to the current scheme were recoded accordingly.

Regolith codes consist of two parts: the regolith regime code and the physiographic division (-WAD). Regolith units are assigned to three regolith regime codes: _X-WAD, _R-WAD and _D-WAD based on the RED scheme of Anand et al. (1993), which classifies regolith–landform units as residual–relict (R), exposed bedrock (E) or depositional transported regolith (D).

In this digital map layer, areas of exposed bedrock outcrops are termed _X-WAD. Residual or relict materials are termed R-WAD, representing residual regolith including deposits derived from in situ weathering of underlying rocks, deposits of uncertain origin and relict reworked regolith deposits. Areas of transported depositional regolith are termed D-WAD, which comprise sediments derived from residual or erosional landforms including colluvial, sheetwash, alluvial, lacustrine, sandplain, eolian and marine deposits.

Sources for the digital layer are published in GSWA Geological Information Series (GIS) packages that include digital 1:100 000 and 1:250 000 regolith and/or surface geology. The final product is a digital map layer containing three distinct levels of reliability (Fig. 2). The highest level of reliability is in areas where additional regolith interpretation using radiometric KTU imagery is available, including the southwest Yilgarn Craton and the Far East Yilgarn Craton Accelerated Geoscience Program areas, extending to the Great Victorian Desert, the Gibson Desert, the Great Sandy Desert, and the Albany–Fraser Orogen. High to variable levels of reliability are in areas of 1:100 000 and 1:250 000 regolith-only maps, and 1:100 000 surface geology maps. These maps cover most of the southwestern Capricorn Orogen and the Nicholls 1:100 000 sheet in the eastern Capricorn Orogen; most of the Pilbara Craton and Paterson Orogen; the Tanami–Arunta region; the Kimberley Basin and Halls Creek Orogen; the west Musgrave Province; and the Yilgarn Craton. Reliability and accuracy for the northeast Pilbara polygons are variable, as the digital coverage derives from 1:100 000 to 1:500 000 regolith and surface geology maps.

For performance purposes, large polygons have been split creating long linear lines in the map. This does not affect the interpretation of regolith geology. The nomenclature and hierarchy for the regolith units are based on the Explanatory Notes System, a database that incorporates a seamless, current summary of the regolith, bedrock, tectonic units and events of Western Australia.

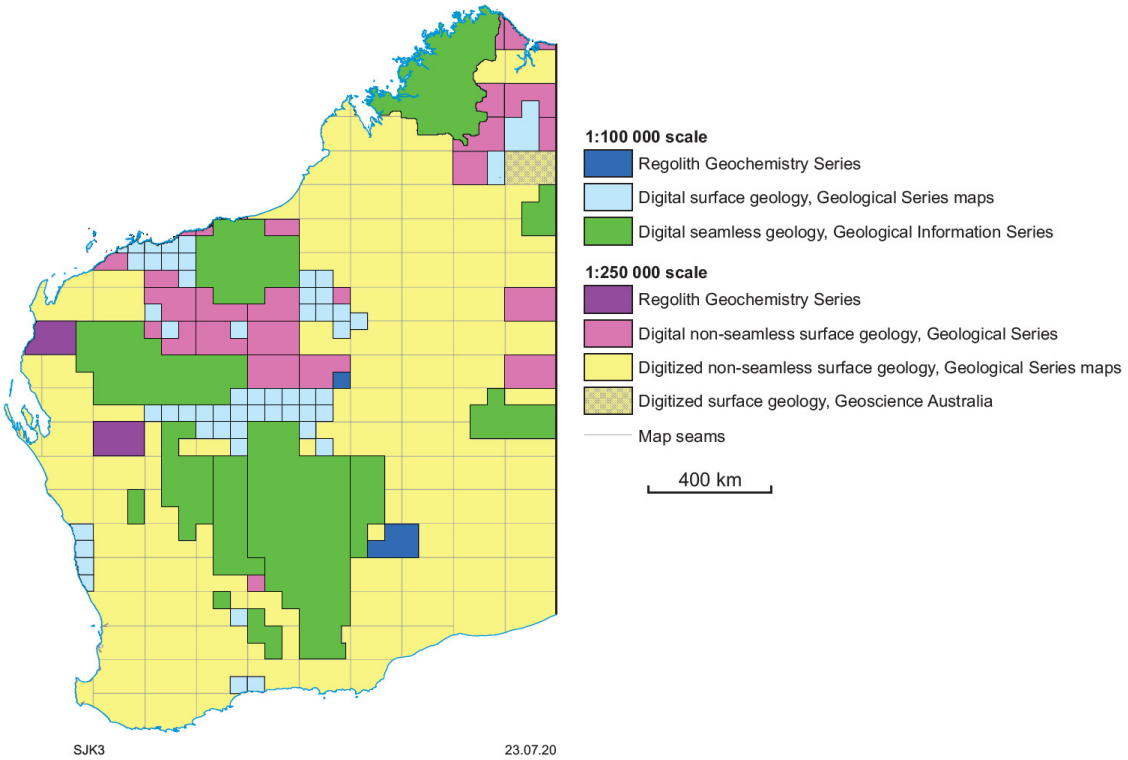

Figure 1. Map and data sources used to compile the 1:100 000-scale regolith geology regimes of Western Australia digital map layer. Figure source: Jakica et al. (2020)

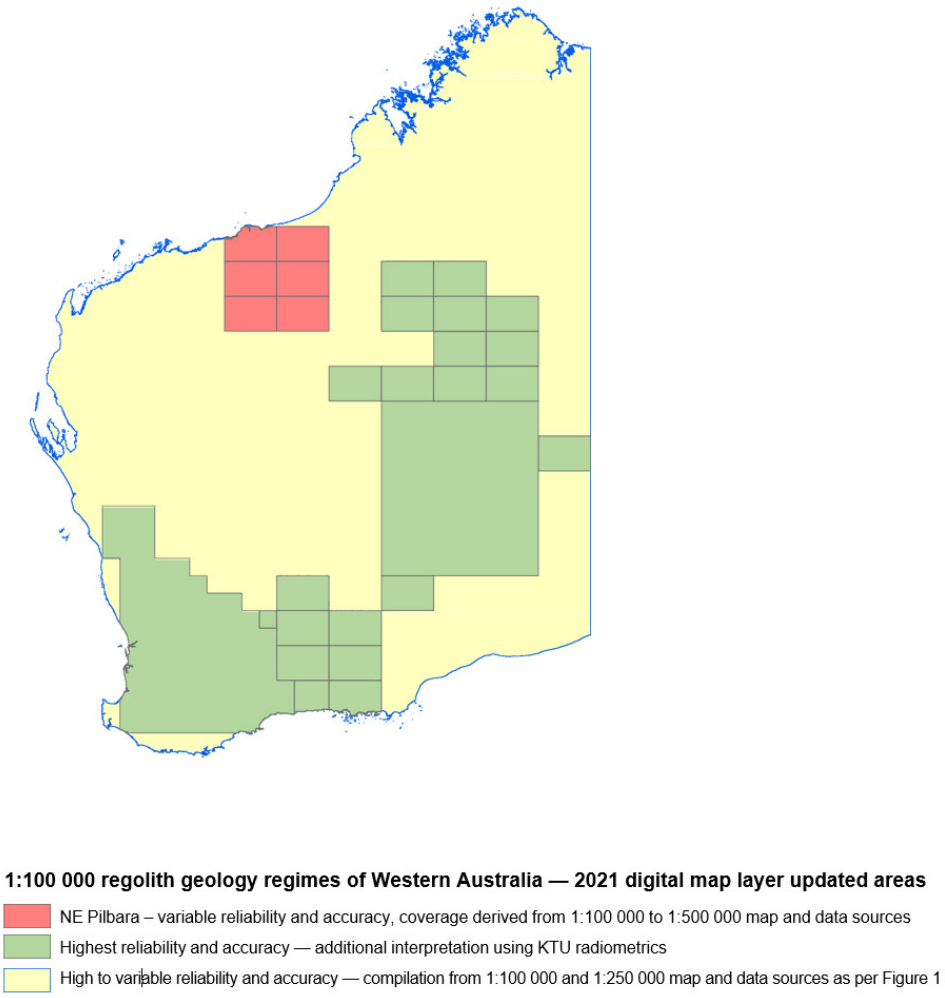

Figure 2. Updated areas and reliability in 2021 for the 1:100 000 regolith geology regimes of Western Australia digital map layer

How to access

The 1:100 000 regolith geology regimes of Western Australia digital data is available as a free download from the Data and Software Centre.

References

Anand, RR, Churchward, HM, Smith, RE, Smith, K, Gozzard, JR, Craig, MA and Munday, TJ 1993, Classification and atlas of regolith landform mapping units, Exploration perspectives for the Yilgarn Craton, Australia: CSIRO Division of Exploration and Mining, Restricted Report 440R (unpublished).

Geological Survey of Western Australia 2013, Revised classification system for regolith in Western Australia, and the recommended approach to regolith mapping: Geological Survey of Western Australia, Record 2013/7, 26p.

Jakica, S, de Souza Kovacs, N, Hogen-Esch, J and Granado, IMT 2020, 1:500 000 State regolith geology of Western Australia — compilation methodologies: Geological Survey of Western Australia, Record 2020/10, 22p

Pain, C, Gregory, L, Wilson, P and McKenzie, N 2011, The physiographic regions of Australia – Explanatory notes 2011, Australian Collaborative Land Evaluation Program and National Committee on Soil and Terrains.

Recommended reference

de Souza Kovacs, N and Jakica, S 2021, 1:100 000 regolith geology regimes of Western Australia: Geological Survey of Western Australia, digital data layer.

Samarium–neodymium isotope map of Western Australia

by

Y Lu, MTD Wingate, DC Champion[1], RH Smithies, SP Johnson, DR Mole[2], M Poujol[3], J Zhao[4], R Maas[5] and RA Creaser[6]

Abstract

Isotope maps are used to characterize lithospheric architecture through time, to understand crustal evolution and mineral system distributions, and play an increasingly important role in exploration targeting.

These Sm–Nd isotope maps of Western Australia (Fig. 1) are based on whole-rock Sm–Nd data for felsic igneous rocks, which provide a window into the middle and lower continental crust, and are used for isotope mapping. Although mafic to intermediate igneous and sedimentary rocks were not used in constructing the contoured isotope maps, Sm–Nd data for those samples are included with those for felsic igneous rocks in the data table.

The maps show two-stage depleted mantle model ages (T_{DM}^2, proxy for the age of the crustal source of the igneous rocks) and crustal residence time (the difference between T_{DM}^2 and magmatic crystallization age, i.e. the length of time the source of the igneous rocks has resided in the crust). The model age gradients are typically associated with major crustal structures and are potentially important for localizing mineral systems. Map colours in areas with no sample reflect interpolated values and may have little or no relationship with underlying crust.

The isotope maps were created using the Natural Neighbor interpolation tool in ArcGIS Spatial Analyst. The isotope maps are presented as both stretched (Histogram Equalize type, Fig. 1a,c) and classified (natural breaks classification, Fig. 1b,d) raster datasets. Some isotope gradients may not be as pronounced in the statewide map as they might be on more detailed maps of individual regions. It is therefore recommended that users download the isotope data and create their own contour maps for particular areas, to enhance the isotope gradients in those areas.

The Sm–Nd isotope samples and associated data were compiled as part of a collaboration between Geological Survey of Western Australia (GSWA) and Geoscience Australia (GA). Acquisition of GSWA's Sm–Nd isotope data involved collaboration with several university research laboratories and was funded by the Exploration Incentive Scheme.

How to access

The data layer is best accessed using GeoVIEW.WA. This online interactive mapping system allows data to be viewed and searched together with other datasets, including GSWA and GA geochronology data, geological maps and mineral exploration datasets. Data for individual sample points can be viewed by selecting the symbols. The Samarium—neodymium isotope map data layer is are also available as a free download from the Data and Software Centre via Datasets — Statewide spatial datasets — Geochronology & Isotope Geology — Samarium—neodymium isotope map, as ESRI shapefiles and MapInfo TAB files. These datasets are subject to ongoing updates as new data are generated.

1 Geoscience Australia, GPO Box 378, Canberra, ACT 2601, Australia
2 Mineral Exploration Research Centre, Harquail School of Earth Sciences, Laurentian University, 935 Ramsey Lake Road, Sudbury, ON P3E 2C6, Canada
3 GeOHeLiS, Géosciences Rennes, UMR 6118, Université Rennes 1, 35042 Rennes cedex, France
4 Radiogenic Isotope Facility, School of Earth Sciences, University of Queensland, Brisbane, QLD 4072, Australia
5 School of Earth Sciences, University of Melbourne, Parkville, VIC 3010, Australia
6 Department of Earth and Atmospheric Sciences, University of Alberta, Edmonton, AB T6G 2E3, Canada

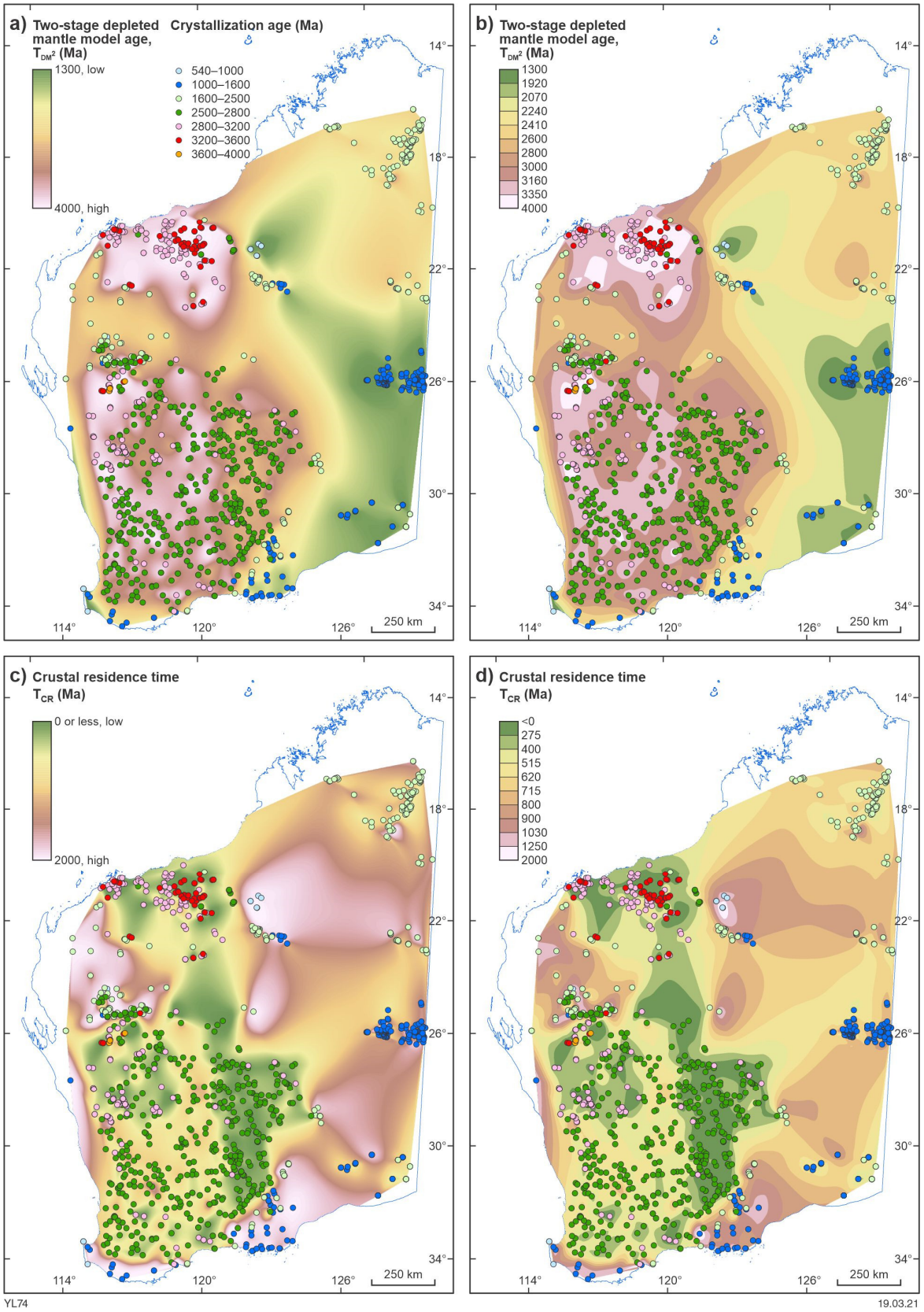

Figure 1. **Sm–Nd isotope maps for whole-rock samples of felsic igneous rocks in Western Australia. Two-stage depleted mantle model age (T_{DM}^2) and crustal residence time (T_{CR}) maps are presented as stretched (a and c) and classified (b and d) raster images. Symbols show the locations of Sm–Nd samples used for isotope mapping and are colour-coded to indicate their magmatic crystallization ages**

Recommended reference

Lu, Y, Wingate, MTD, Champion, DC, Smithies, RH, Johnson, SP, Mole, DR, Poujol, M, Zhao, J, Maas, R and Creaser RA 2021, Samarium–neodymium isotope map of Western Australia: Geological Survey of Western Australia, digital data layer, <https://www.dmirs.wa.gov.au/geoview>.

Zircon lutetium–hafnium isotope map of Western Australia

by

Y Lu, MTD Wingate, SS Romano, DR Mole[1], CL Kirkland[2], AIS Kemp[3], EA Belousova[4], RH Smithies, K Gessner and SP Johnson

Abstract

Time-constrained isotope maps are used to characterize the evolution of lithospheric architecture as well as understand crustal development and mineralization. Such isotope maps play an increasingly important role in exploration targeting, and statistically significant relationships between different types of mineralization and isotopic signatures over time have been found. The Lu–Hf isotope maps of Western Australia (Fig. 1) are based on Lu–Hf data for dated magmatic zircons from felsic igneous rocks, which provide a window into evolution and architecture of the middle and lower continental crust. Zircons from granitic rocks are used because they provide a useful tool to sample the deeper sections of lithosphere that form the foundations of our continents.

Initial $^{176}Hf/^{177}Hf$ and εHf values of all zircons were calculated using the ^{176}Lu decay constant of Söderlund et al. (2004) and the CHUR (CHondritic Uniform Reservoir) value of Bouvier et al. (2008). For each analysis, a two-stage depleted mantle model age (T_{DM}^2) is calculated, which assumes that the parental magma of the zircon was produced from a volume of average continental crust ($^{176}Lu/^{177}Hf$ ratio of 0.015) extracted from depleted mantle (Griffin et al., 2000, 2002). T_{DM}^2 estimates the average age of the crustal source of the igneous rocks (Griffin et al., 2002). Crustal residence time (T_{CR}), the difference between T_{DM}^2 and magmatic crystallization age, is also calculated for each analysis, and provides an estimate of the average length of time the source of the igneous rocks has resided in the crust.

The evolution of the mantle is a topic of debate in isotope geoscience (including whether mantle depletion occurred at 4.56 or 3.8 Ga; Griffin et al., 2002; Kemp et al., 2015; Vervoort and Kemp, 2016; Fisher and Vervoort, 2018), and the model chosen affects values calculated for T_{DM}^2 and T_{CR}, particularly for zircons older than 3.8 Ga. Furthermore, the $^{176}Lu/^{177}Hf$ ratio used in isotopic evolution is solely an estimate and imparts significant uncertainty to any model age (see Vervoort and Kemp, 2016). Therefore, T_{DM}^2 and T_{CR} are used here mainly for qualitative comparative purposes because any gradients in T_{DM}^2 and T_{CR} may be more insightful than their absolute values. Moreover, model ages potentially highlight underlying patterns related to crustal composition and structure.

Lu–Hf isotope data for zircons from mafic igneous, sedimentary, and metamorphic rocks, and for xenocrystic zircons, were not used in constructing the isotope maps, although their sample-level information is included as a separate layer. Spot-level data for all samples are provided as a CSV file. The Lu–Hf isotope data have been filtered to exclude data with U–Pb age discordance >10%, $^{176}Yb/^{177}Hf$ >0.1, and εHf 2σ uncertainty >4 epsilon units (Belousova et al., 2010; Mole et al., 2019). The isotope maps are constructed from median T_{DM}^2 and T_{CR} values, using the Natural Neighbour interpolation tool in ArcGIS Spatial Analyst, and presented as both stretched (histogram equalize type, Fig. 1a,c) and classified (natural breaks classification, Fig. 1b,d) raster images.

[1] Geoscience Australia, GPO Box 378, Canberra, ACT 2601, Australia
[2] Timescales of Mineral Systems Group, School of Earth and Planetary Sciences, Curtin University, Bentley, WA 6102, Australia
[3] School of Earth Sciences, The University of Western Australia, Crawley, WA 6009, Australia
[4] ARC Centre of Excellence for Core to Crust Fluid Systems (CCFS) and GEMOC, Macquarie University, New South Wales 2109, Australia

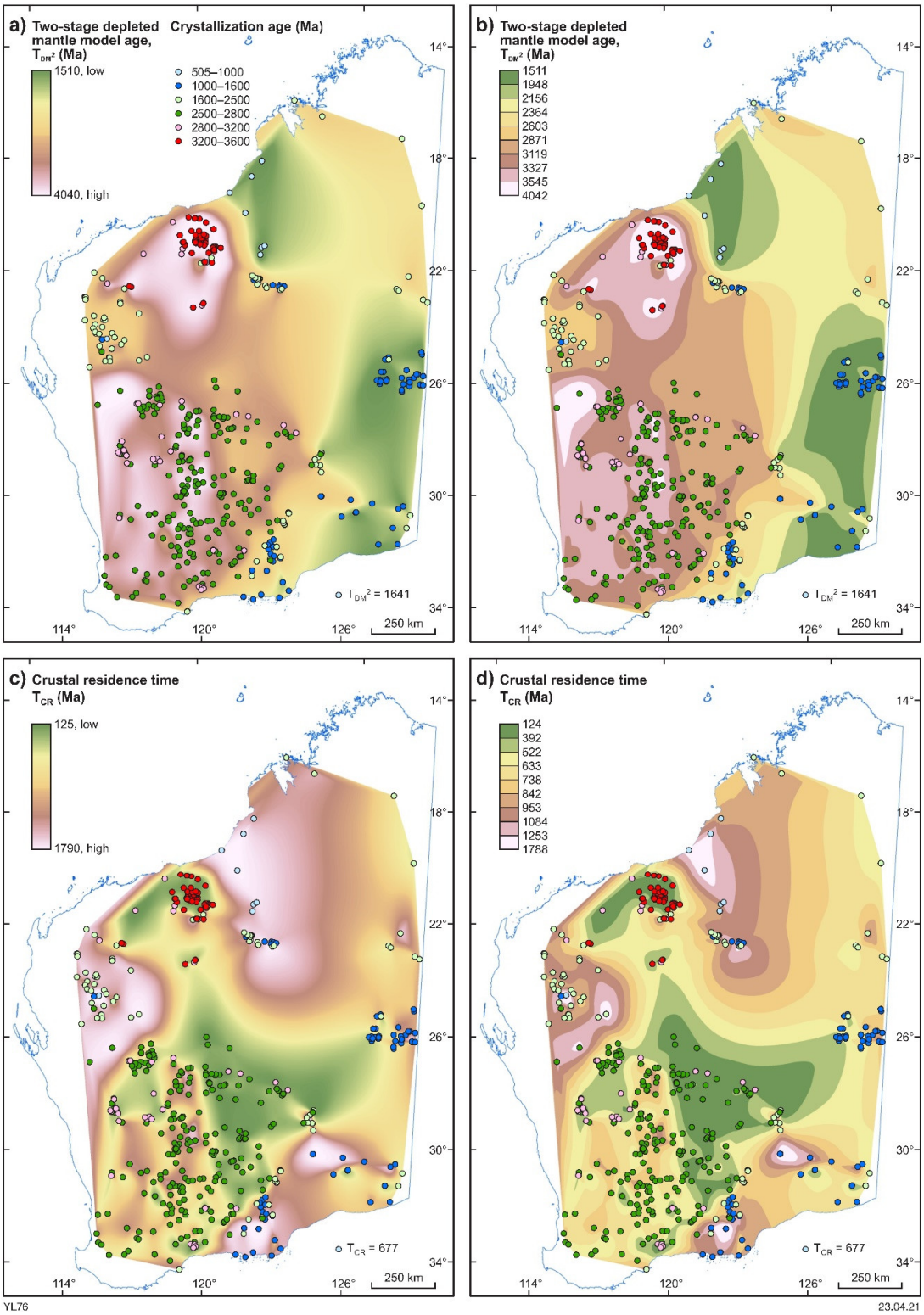

Figure 1. Zircon Lu–Hf isotope maps for felsic igneous rocks in Western Australia. Median two-stage depleted mantle model age (T_{DM}^2) and crustal residence time (T_{CR}) maps are presented as stretched (a and c) and classified (b and d) raster images. Symbols show the locations of Lu–Hf samples used for isotope mapping and are colour coded to indicate their magmatic crystallization ages

The model age (T_{DM}^2) maps highlight the distinction between Archean cratons (T_{DM}^2 >2.6 Ga) and Proterozoic orogens (T_{DM}^2 <2.4 Ga). T_{CR} maps highlight the predominance of moderate to short residence times (<0.5 Ga) for the Pilbara and Yilgarn Cratons, and much longer crustal residence times (>0.8 Ga) in the Paterson, Albany–Fraser, and Capricorn Orogens, consistent with an increased role for reworking of ancient crust in these orogens.

Granitic samples from basement rocks beneath the Canning Basin show similar T_{DM}^2 to those in the Musgrave, Madura and Coompana Provinces, but are different to those from the North and West Australian Cratons (NAC and WAC), suggesting the existence of a subsurface Proterozoic terrane between the NAC and WAC possibly related to the Mirning Ocean (Kirkland et al., 2017; Fig. 1a,b).

The isotope maps also image two rift-like structures in the Yilgarn Craton: the Kalgoorlie–Kurnalpi rift in the Eastern Goldfields and the Cue rift in the Murchison similar to those observed in whole-rock Sm–Nd isotope maps (Lu et al., 2021).

Map colours in areas where there are no samples reflect interpolated values and may have little or no relationship with underlying crust. Some isotope gradients may not be as pronounced in the statewide map as they might be on more detailed maps of individual regions. It is therefore recommended that users download the isotope data and create their own contour maps for particular areas to examine the isotope gradients in those areas.

Acquisition of Lu–Hf isotope data by the Geological Survey of Western Australia (GSWA) was funded by the Exploration Incentive Scheme (EIS), and conducted using multi-collector inductively coupled plasma mass spectrometry (MC-ICPMS) in the Centre for Geochemical Evolution and Metallogeny of Continents (GEMOC) and ARC Centre of Excellence for Core to Crust Fluid Systems (CCFS) at Macquarie University and in the Centre for Microscopy, Characterization and Analysis (CMCA) at The University of Western Australia.

How to access

The data layer is best accessed using GeoVIEW.WA. This online interactive mapping system allows data to be viewed and searched together with other datasets, including Geological Survey of Western Australia and Geoscience Australia geochronology data, geological maps and mineral exploration datasets. The Zircon lutetium–hafnium isotope map digital data are also available as a free download from the Data and Software Centre via Datasets — Statewide spatial datasets — Geochronology & Isotope Geology — Zircon lutetium-hafnium isotope map, as ESRI shapefiles and MapInfo TAB files. All spot-level zircon data are provided as a CSV file. These datasets are subject to ongoing updates as new data are generated.

References

Belousova, EA, Kostitsyn, YA, Griffin, WL, Begg, GC, O'Reilly, SY and Pearson, NJ 2010, The growth of the continental crust: Constraints from zircon Hf-isotope data: Lithos, v. 119, p. 457–466.

Bouvier, A, Vervoort, JD and Patchett, PJ 2008, The Lu-Hf and Sm-Nd isotopic composition of CHUR: constraints from unequilibrated chondrites and implications for the bulk composition of terrestrial planets: Earth and Planetary Science Letters, v. 273, p. 48–57.

Fisher, CM and Vervoort, JD 2018, Using the magmatic record to constrain the growth of continental crust–The Eoarchean zircon Hf record of Greenland: Earth and Planetary Science Letters, v. 488, p. 79–91.

Griffin, WL, Pearson, NJ, Belousova, EA, Jackson, SE, O'Reilly, SY, van Achterberg, E and Shee, SR 2000, The Hf isotope composition of cratonic mantle: LAM-MC-ICPMS analysis of zircon megacrysts in kimberlites: Geochimica
et Cosmochimica Acta, v. 64, p. 133–147.

Griffin, WL, Wang, X, Jackson, SE, Pearson, NJ, O'Reilly, SY, Xu, X and Zhou, X 2002, Zircon chemistry and magma genesis, SE China: in-situ analysis of Hf isotopes, Pingtan and Tonglu igneous complexes: Lithos, v. 61, p. 237–269.

Kemp, AIS, Hickman, AH, Kirkland, CL and Vervoort, JD 2015, Hf isotopes in detrital and inherited zircons of the Pilbara Craton provide no evidence for Hadean continents: Precambrian Research, v. 261, p. 112–126.

Kirkland, CL, Smithies, RH, Spaggiari, CV, Wingate, MTD, Quentin de Gromard, R, Clark, C, Gardiner, NJ and Belousova, EA 2017, Proterozoic crustal evolution of the Eucla basement, Australia: Implications for destruction of oceanic crust during emergence of Nuna: Lithos, v. 278–281, p. 427–444.

Lu, Y, Wingate, MTD, Champion, DC, Smithies, RH, Johnson, SP, Mole, DR, Poujol, M, Zhao, J, Maas, R and Creaser RA 2021, Samarium–neodymium isotope map of Western Australia: Geological Survey of Western Australia, digital data layer, <www.dmirs.wa.gov.au/geoview>.

Mole, DR, Kirkland, CL, Fiorentini, ML, Barnes, SJ, Cassidy, KF, Isaac, C, Belousova, EA, Hartnady, M and Thébaud, N 2019, Time-space evolution of an Archean craton: A Hf-isotope window into continent formation: Earth-Science Reviews, v. 196, 102831.

Söderlund, U, Patchett, PJ, Vervoort, JD and Isachsen, CE 2004, The 176Lu decay constant determined by Lu-Hf and U-Pb isotope systematics of Precambrian mafic intrusions: Earth and Planetary Science Letters, v. 219, p. 311–324.

Vervoort, JD and Kemp, AIS 2016, Clarifying the zircon Hf isotope record of crust–mantle evolution: Chemical Geology, v. 425, p. 65–75.

Recommended reference

Lu, Y, Wingate, MTD, Romano, SS, Mole, DR, Kirkland, CL, Kemp, AIS, Belousova, EA, Smithies, RH, Gessner, K and Johnson, SP 2021, Zircon lutetium–hafnium isotope map of Western Australia: Geological Survey of Western Australia, digital data layer, <www.dmirs.wa.gov.au/geoview>.

The author, DR Mole, publishes with the permission of the Chief Executive Officer, Geoscience Australia.

Zircon oxygen isotope map of Western Australia

by

Y Lu, MTD Wingate, RH Smithies, L Martin[1], H Jeon[1,2], DC Champion[3], SP Johnson and DR Mole[4]

Abstract

The oxygen isotope compositions of igneous rocks are preserved in zircon crystals from the time of crystallization. The $^{18}O/^{16}O$ ratios are reported in delta notation as $\delta^{18}O$ (‰) values, normalized to Vienna Standard Mean Ocean Water (V-SMOW). Zircons crystallized from uncontaminated mantle-derived magmas have homogeneous $\delta^{18}O$ values (5.3 ± 0.6‰, 2σ). Low-temperature interaction with surface waters leads to elevated $\delta^{18}O$ values, and high-temperature (≥350 °C) interaction with meteoric water or seawater leads to lower $\delta^{18}O$ values. Therefore, zircon $\delta^{18}O$ values can be used to fingerprint reworking and recycling of supracrustal rocks that have interacted with the hydrosphere of the Earth, and can be related to geodynamic processes.

The oxygen isotope map of Western Australia (Fig. 1) is based on primary zircon $\delta^{18}O$ data from igneous rocks. Zircon $^{16}O^{1}H/^{16}O$ ratios, together with cathodoluminescence texture and zircon age discordance, are used to assess whether the measured oxygen isotope ratios represent primary magmatic compositions, or if they potentially reflect alteration, weathering or contamination by inclusions. After filtering, the zircon $\delta^{18}O$ data show no correlation with $^{16}O^{1}H/^{16}O$, U, Th, Th/U and discordance on an individual sample basis, attesting to retention of primary magmatic compositions. Although zircon oxygen isotope data from altered, xenocrystic, metamorphic and detrital grains were not used in constructing the isotope map, this sample-level information is presented as a separate layer. All spot-level zircon data are provided as a CSV file.

The median $\delta^{18}O$ values of primary magmatic zircons from each igneous rock sample are visualized spatially using graduated symbols in a Manual Interval Classification in ArcGIS (Fig. 1). The Archean Pilbara and Yilgarn Cratons are dominated by mantle-like $\delta^{18}O$ values (4.7 – 5.9‰), consistent with reworking of igneous material that had not been exposed at the surface. Some igneous rocks in the Pilbara and Yilgarn Cratons exhibit weakly elevated zircon $\delta^{18}O$ values (6.0 – 6.5‰) which, together with trace element enrichment, are attributed to hydrous sanukitoids or to derivation from a sanukitoid-enriched source. The Capricorn, Paterson and Albany–Fraser Orogens and the Eucla Basin basement contain rocks that mainly indicate elevated $\delta^{18}O$ values (6.6 – 10.4‰), suggesting significant reworking of upper crustal material subjected to weathering or low-temperature hydrothermal alteration. Submantle $\delta^{18}O$ values (1.7 – 4.6‰) were found in zircons from igneous rocks in the Pilbara Craton, the Narryer and South West Terranes of the Yilgarn Craton, and the Albany–Fraser Orogen and Musgrave Province, and suggest reworking of crustal material subjected to high-temperature hydrothermal alteration, such as observed in rift systems or calderas.

The oxygen isotope data were compiled as part of a collaboration between the Geological Survey of Western Australia (GSWA) and Geoscience Australia (GA). Acquisition of GSWA's oxygen isotope data was funded by the Exploration Incentive Scheme (EIS), and was conducted using a Cameca IMS 1280 ion microprobe with the scientific and technical assistance of Microscopy Australia at the Centre for Microscopy, Characterization and Analysis (CMCA), a facility at The University of Western Australia (UWA) funded by UWA and by State and Commonwealth Governments.

1 Centre for Microscopy, Characterization and Analysis, University of Western Australia, 35 Stirling Highway, Perth, WA 6009, Australia
2 Swedish Museum of Natural History, PO Box 50007, SE-104 05 Stockholm, Sweden
3 Geoscience Australia, GPO Box 378, Canberra, ACT 2601, Australia
4 Mineral Exploration Research Centre, Harquail School of Earth Sciences, Laurentian University, 935 Ramsey Lake Road, Sudbury, ON P3E 2C6, Canada

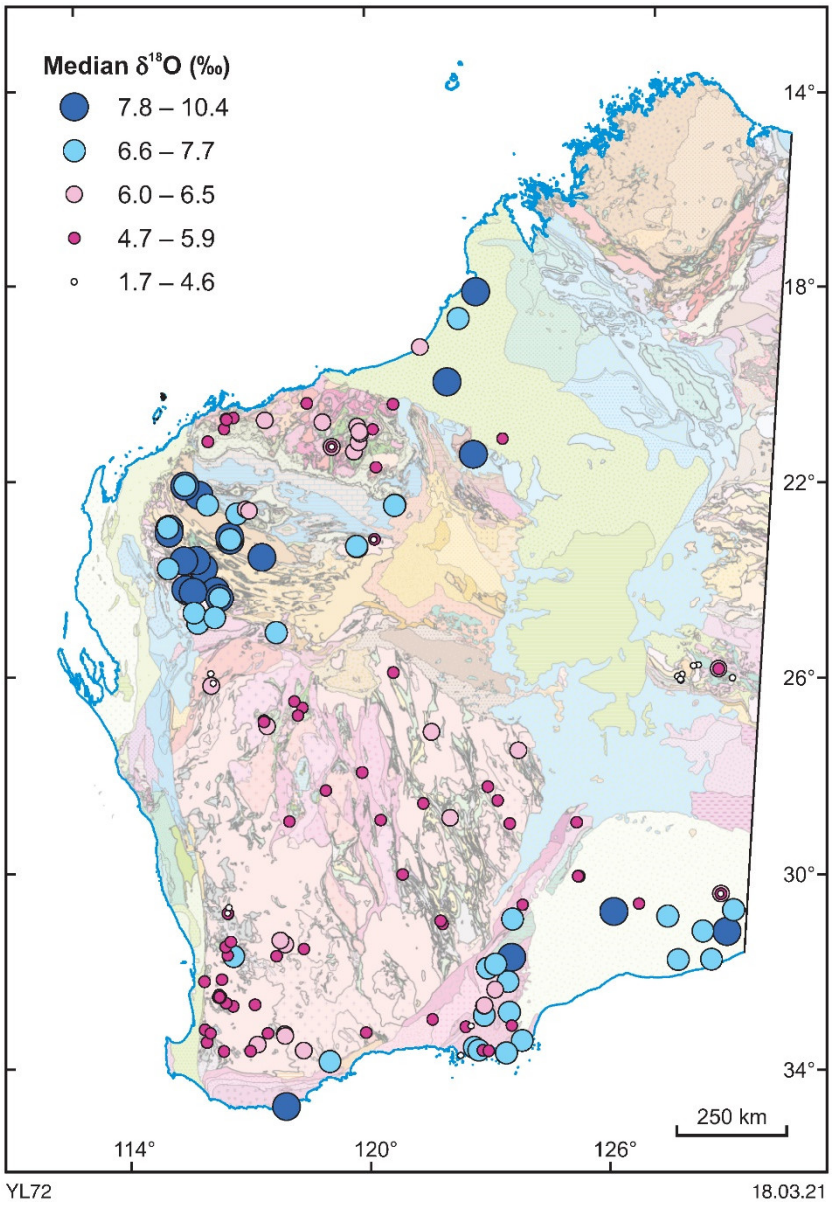

Figure 1. **Zircon oxygen isotope map for igneous rocks in Western Australia. Median $\delta^{18}O$ values of primary magmatic zircons from each igneous rock sample are presented on top of the 1:2.5M interpreted bedrock geology map**

How to access

The data layers are best accessed using GeoVIEW.WA. This online interactive mapping system allows data to be viewed and searched together with other datasets, including GSWA and GA geochronology data, geological maps and mineral exploration datasets. The Zircon oxygen isotope map data layer is also available as a free download from the Data and Software Centre via Datasets — Statewide spatial datasets — Geochronology & Isotope Geology — Zircon oxygen isotope map, as ESRI shapefiles and MapInfo TAB files. All spot-level zircon data are provided as a CSV file. These datasets are subject to ongoing updates as new data are generated.

Recommended reference

Lu, Y, Wingate, MTD, Smithies, RH, Martin, L, Jeon, H, Champion, DC, Johnson, SP and Mole, DR 2021, Zircon oxygen isotope map of Western Australia: Geological Survey of Western Australia, digital data layer, <https://www.dmirs.wa.gov.au/geoview>.

THE UNIVERSITY OF WESTERN AUSTRALIA

Australian Government
Geoscience Australia

1:2 500 000 major crustal boundaries of Western Australia

by

DMcB Martin, RE Murdie, HN Cutten, DE Kelsey, CM Thomas, R Quentin de Gromard, Y Zhan and P Haines

Abstract

Major crustal boundaries that potentially tap the upper mantle are a major component of some important mineral systems (Korsch and Doublier, 2016). Australia-wide interpretations of such boundaries, or lithospheric architecture, are commonly presented in schematic form in the academic literature and are based mainly on the interpretation of high-resolution potential field geophysical datasets (Kennett et al., 2018) as well as the extensive national network of deep seismic reflection profiles (Kennett et al., 2016). However, the most recent Australia-wide interpretation (Korsch and Doublier, 2015) is now over five years old and does not include some critical new geophysical datasets, and due to the national scale of these interpretations, they also seldom capture the nuances of State-based geological interpretations.

The Major crustal boundaries map of Western Australia (Fig. 1) integrates the most recent geophysical data with current understanding of the geological evolution of the State at a significantly improved level of detail. For the purposes of this interpretation, a major crustal boundary is defined as 'a lithospheric-scale structure that is interpreted to transect the crust to the Moho, and/or a structure within the crust that forms the boundary between interpreted tectonic units at the terrane or province scale'. The primary data sources for identifying these structures are the State tectonic units map and a network of 25 deep seismic reflection profiles. Structures were first identified on seismic reflection profiles then extrapolated along strike and projected to surface following a similar methodology to Korsch and Doublier (2016), although exposed structures have been snapped to mapped faults. Multiscale edge analysis of gravity data was also used to estimate dip and dip direction in areas without seismic coverage. Each feature has a detailed suite of attributes that are described in the associated data dictionary and metadata statement. Following compilation in 2D, the structures were also modelled in 3D in order to validate the crustal architecture and to ensure internal geometric consistency. The 3D model is available as a separate product (Murdie, 2021).

The most useful potential field datasets for interpreting major crustal boundaries were found to be the isostatic residual gravity anomaly map and the map of total magnetic intensity reduced to pole and upward continued to 10 km. Individual boundaries consist of multiple segments according to the specific attributes that define them but individual boundaries can be selected using the 'NAME' or 'DESCRIPTN' field. The depiction of dipping crustal-scale structures in 2D that are largely interpreted from potential field data is a significant limitation of the dataset. The various uncertainties in both the nature, location and timing of structures is therefore conveyed in the 'FEAT_CONF', 'EV_CONF', 'CAP_SCALE' and 'PRECISN_KM' attributes. Links are provided to source data such as published literature and processed seismic sections, where possible. The map also attempts to capture the tectonic history of each structure by assigning up to five formal Tectonic Events as defined in the ENS database, although these are limited by uncertainties in understanding of the events themselves.

How to access

The 1:2 500 000 major crustal boundaries dataset is best accessed using GeoVIEW.WA. This online interactive mapping system allows data to be viewed and searched together with other datasets, including GSWA and Geoscience Australia geochronology data, geological maps and mineral exploration datasets. The 1:2 500 000 major crustal boundaries map is also available for download

from the Data and Software Centre in various formats. This digital product will be subject to ongoing updates as new data are acquired and tectonic interpretations are revised.

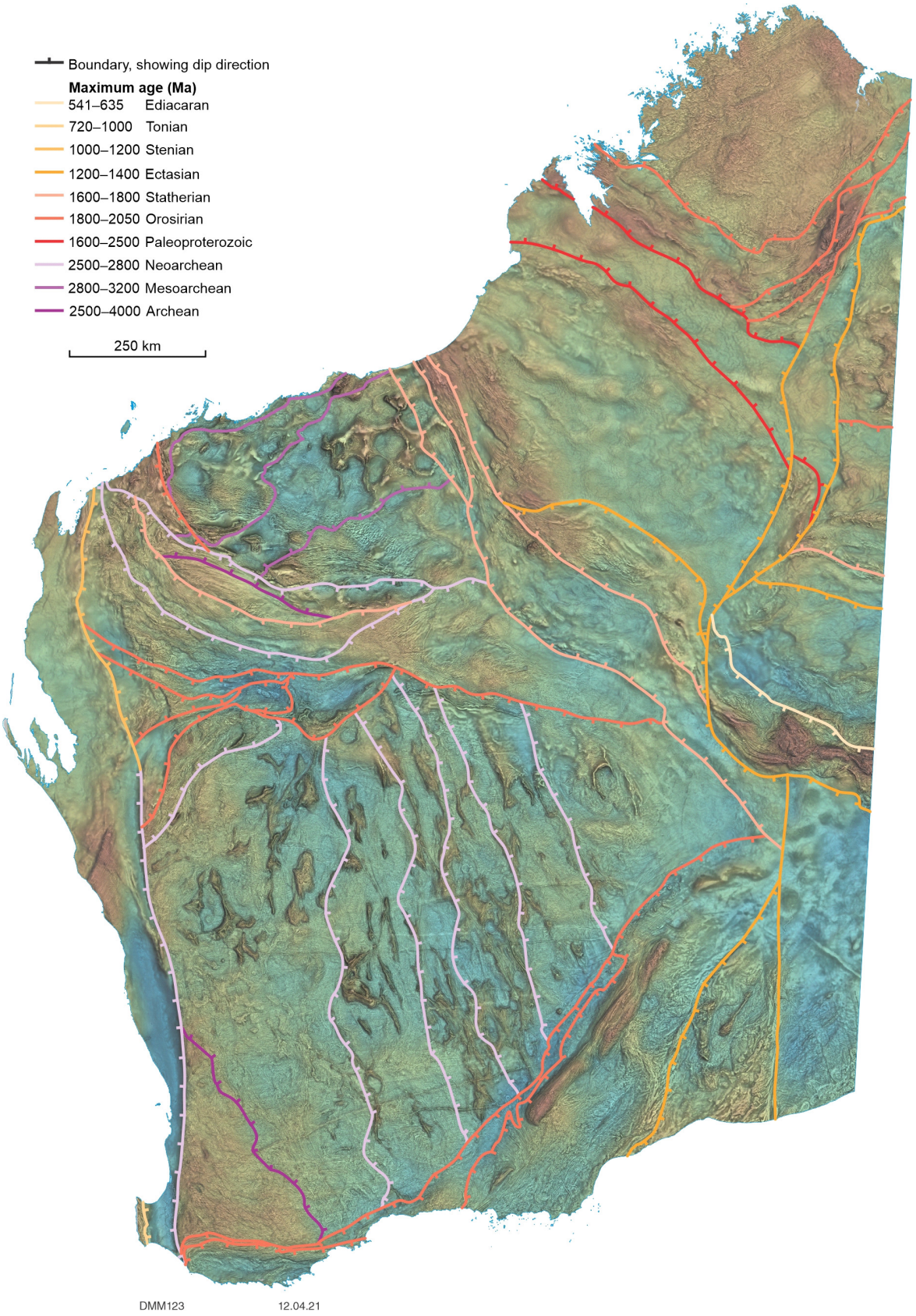

Figure 1. Major crustal boundaries of Western Australia overlain on composite potential field data consisting of isostatic residual gravity (colour) and first vertical derivative, reduced to pole aeromagnetics (texture). Boundaries are symbolized and coloured according to dip direction and maximum age, respectively

References

Kennett, BLN, Chopping, R and Blewett, R 2018, The Australian Continent: A Geophysical Synthesis: Australian National University Press and Geoscience Australia, Canberra.

Kennett, BLN, Saygin, E, Fomin, T and Blewett, R 2016, Deep Crustal Seismic Reflection Profiling: Australia 1978–2015: ANU Press; Geoscience Australia, Canberra, Australia, 224p.

Korsch, RJ and Doublier, MP 2015, Major crustal boundaries of Australia (1:2 500 000 scale): Geoscience Australia.

Korsch, RJ and Doublier, MP 2016, Major crustal boundaries of Australia, and their significance in mineral systems targeting: Ore Geology Reviews, v. 76, p. 211–228, doi:10.1016/j.oregeorev.2015.05.010.

Murdie, RE 2021, 3D geomodel of Western Australia, 2021: Geological Survey of Western Australia, 3D Geomodel Series, <www.dmirs.wa.gov.au/datacentre>.

Recommended reference

Martin, DMcB, Murdie, R, Cutten, HN, Kelsey, D, Thomas, C, Quentin de Gromard, R, Zhan, Y and Haines, P 2021, 1:2 500 000 major crustal boundaries of Western Australia, 2021: Geological Survey of Western Australia, digital data layer.

EXPLORATION INCENTIVE SCHEME

Selected mineralization sites of Western Australia

by

S Morin-Ka, WR Ormsby and TJ Beardsmore

Abstract

The provision of known mineralization sites for selected commodities assists with mineral exploration and other mineral-related studies. These sites provide further insight into the known spatial distribution of mineralized localities for specific commodities than has previously been readily available.

Many mineralized sites contain multiple commodities. These layers highlight where mineralization sites are known for specific commodities, even if they are a relatively minor component of the mineralization. Thus, they reflect the presence of mineralization for a commodity, not its endowment.

The mineralization sites are extracted from the MINEDEX database, which provides a coordinated, project-based inquiry system for textual information on mine, deposit, prospect and occurrence locations, as well as mineral resources and mine production. Data are collated from ASX reports, statutory exploration reports, mining proposals and production returns.

Mineralization sites are selected to exclude exploration targets and infrastructure not directly related to mineralization, such as tailings storage facilities and processing plants. They are derived from the SITE_COMMODITY field and are filtered to ensure that only the relevant commodities are selected.

The order of listing of the commodity in the SITE_COMMODITY field reflects its relative importance at that site. Only those identified as target commodities and listed in the TARGET_COMMODITY_GROUP field are classified in MINEDEX into four groups: mine, deposit, prospect and occurrence. Therefore, the SITE_TYPE_DESCRIPTION (i.e. mine, deposit, prospect or occurrence) is only applicable to the selected commodity if it is also listed in the TARGET_COMMODITY_GROUP field. If the commodity for a mineralization site is not listed in the TARGET_COMMODITY field then it is not possible to allocate the relevant SITE_TYPE_DESCRIPTION without further investigation of the source data. In these instances, the site remains unclassified with respect to SITE_TYPE_DESCRIPTION.

Site type	*Definition*
Mine	A deposit which is being mined, was previously mined, or is proposed to be mined
Deposit	A mineral occurrence with probable economic value and for which there is an established resource
Prospect	Any mineral occurrence where economic grades have been intersected over a significant width and strike length but for which there is not yet a resource, or any working or exploration activity that has found subeconomic mineral occurrences and from which there is no recorded production
Occurrence	An occurrence (excluding those defined as mines, deposits or prospects) can be defined if an economic mineral has been identified in outcrop, or if assay results exceed an agreed concentration and size.
Unclassified	Mineralization site for which the TARGET_COMMODITY_GROUP does not reflect the specified commodity, and hence the SITE_TYPE_DESCRIPTION is not applicable

How to access

The data layer is best accessed using GeoVIEW.WA. This online interactive mapping system allows data to be viewed and searched together with other datasets, including Geological Survey of Western Australia and Geoscience Australia geochronology data, geological maps and mineral exploration datasets. The Selected mineralization sites digital data are also available as a free download from the Data and Software Centre via Datasets — Statewide spatial datasets — Mineral information — Selected mineralization sites, as ESRI shapefiles and CSV files.

Recommended reference

Morin-Ka, S, Ormsby, W and Beardsmore TJ 2021, Selected mineralization sites of Western Australia: Geological Survey of Western Australia, digital dataset, <www.dmirs.wa.gov.au/geoview>.

3D geomodel of Western Australia, 2021

by

RE Murdie

Abstract

The 3D geomodel of Western Australia is an attempt to visualize the components of Earth's crust in Western Australia in three dimensions. The geomodel has been generated using the 1:2 500 000 major crustal boundaries of Western Australia, 2021 shapefile as the major input (Martin et al., 2021). This division of the crust into 3D volumes is the result of careful integration of geological and geophysical datasets and existing 3D geomodels. Surface geological mapping (Geological Survey of Western Australia [GSWA], 2016), aerial magnetic surveys (GSWA, 2020b), and ground and aerial gravity surveys (GSWA, 2020a) provide statewide coverage of the near surface geology and structures.

Early investigations into the layered nature of the crust were in the form of seismic refraction surveys (Everingham, 1965; Mathur, 1974; Dentith et al., 2000; Tassell and Goncharov, 2006), which showed a change in seismic velocity within the crust. Over the past 30 years, a dedicated campaign of active-source deep crustal seismic reflection and magnetotelluric (MT) profiles (see references associated with each survey in the List of components*) have been conducted by Geoscience Australia and GSWA. These profiles provide information on layering within the crust, the depth of the Moho and the dip of some major faults and seismic provinces (discrete volumes of middle to lower crust that cannot be traced to the surface, and whose crustal reflectivity is different to that of laterally or vertically adjoining provinces [Korsch and Kositcin, 2010]). Ambiguities are still present due to the fact that the profiles only sample a very small part of the State and are 2D profiles sampling 3D geology.

More recently, specific areas of the State have been covered by passive seismic campaigns focused on receiver functions and ambient noise tomography. Receiver functions are used to calculate the thickness and composition of the crust by examining how the waveforms of distant earthquakes are modified by the thickness, structure and composition of the crust directly below the station. Ambient noise tomography correlates the noise signals at across station pairs in an array to generate a tomographic image of the velocity structure. The two passive seismic methods are used to distinguish and define crustal domains and hence provide critical input to a geodynamic understanding of the continental crust in Western Australia.

Magnetotelluric surveys have been conducted along several profiles, often coincident with seismic reflection lines. These sample the electrical conductivity of the crust and upper mantle and have helped define crustal boundaries and character of the lower crust. Not all MT profiles are shown here, only ones that have been used in the interpretation. A full listing of state-registered MT, seismic reflection and passive seismic surveys can be found on the GSWA website.

Many parts of the State are covered by deep basins from the Archean, through the Proterozoic and younger. These are captured within the OZ SEEBASE model (Geognostics Australia, 2020) in conjunction with mapped geology and seismic and MT profiles. In this geomodel, the Basins volume is modified to only include Proterozoic and younger basins. The Archean Fortescue and Hamersley Basins are modelled as a separate unit. However in many places very little data exists away from the seismic lines. In these blank volumes, dips of the faults and surfaces have been extrapolated into the volume away from the imaged features to provide the best visualization given the limitations of the data.

* A list of components that better reflects the content of the model has been compiled in place of a standard data dictionary. Please refer to the Overview and list of components included with the geomodel

The major crustal boundaries have been determined by considering all the above geological and geophysical data (Martin et al., 2021). They have been named with regard to the rock unit adjoining the boundary or as being internal to a rock volume. Colours used here are non-standard GSWA colours as these often include overprints, which is not possible in these models. These internal faults and shear zones have been included as they are thought to be major transcrustal features. In many cases, the boundaries follow faults or shear zones as shown in the 1:500 000 interpreted bedrock geology of Western Australia structural layer (GSWA, 2016) and summarized in the list of components. More explanations about the kinematics, age and associated mapped faults and features of each boundary can be found in the 1:2 500 000 major crustal boundaries of Western Australia digital layer (Martin et al., 2021). The positional accuracy of these boundaries is low, due primarily to their crustal scale and uncertainties in interpreting the primary data sources, and consequently this map is best used at the nominal scale or larger. References given in the model refer to the paper in which the feature was imaged rather than the geological background of the feature. Please view this 3D geomodel of Western Australia as a geologically constrained, albeit a non-unique interpretation of sparse geoscience data rather than a precise geolocated 3D map.

How to access

The 3D geomodel of Western Australia, 2021 is available as a free download from the Data and Software Centre via Datasets — Statewide spatial datasets — 3D geology — 3D geomodel of Western Australia, 2021, and can be viewed using the free viewer software Geoscience ANALYST available from Mira Geoscience.

References

Dentith, MC, Dent, VF and Drummond, BJ 2000, Deep crustal structure in the southwestern Yilgarn Craton, Western Australia: Tectonophysics, v. 325, p. 227–255.

Everingham, IB 1965, The crustal structure of the south-west of Western Australia: Bureau of Mineral Resources, Geology and Geophysics, Record 1965/97.

Geognostics Australia Pty Ltd 2020, OZ SEEBASE 2020: Geognostics Australia Pty Ltd, web release, <https://www.geognostics.com/oz-seebase-2020>.

Geological Survey of Western Australia 2016, 1:500 000 State interpreted bedrock geology of Western Australia, 2016: Geological Survey of Western Australia; digital data layer, <www.dmirs.wa.gov.au/geoview>.

Geological Survey of Western Australia 2020a, Gravity anomaly grid (400 m) of Western Australia (2020 — version 1): Geological Survey of Western Australia, digital data layer, <www.dmirs.wa.gov.au/geophysics>.

Geological Survey of Western Australia 2020b, Magnetic anomaly grids (40 m) of Western Australia (2020 – version 1): Geological Survey of Western Australia, digital data layer, <www.dmirs.wa.gov.au/geophysics>.

Korsch, RJ and Kositcin, N (editors) 2010, South Australian Seismic and MT Workshop 2010: extended abstracts: Geoscience Australia, Record 2010/10, 124p.

Martin DMcB, Murdie, RE, Cutten, HN, Kelsey, D, Thomas, C, Quentin de Gromard, R, Zhan, Y and Haines, P 2021, 1:2 500 000 major crustal boundaries of Western Australia, 2021: Geological Survey of Western Australia, digital data layer, <www.dmirs.wa.gov.au/geoview>.

Mathur, SP 1974, Crustal structure in southwestern Australia from seismic and gravity data: Tectonophysics, v. 24, no. 1-2, p. 151–182, doi:10.1016/0040-1951(74)90135-8.

Tassell, H and Goncharov, A 2006, Geophysical evidence for a deep crustal root beneath the Yilgarn Craton and Albany–Fraser Orogen, Western Australia, *in* Conference abstracts: Australian Earth Sciences Convention, Melbourne, Victoria, 2–8 July 2006: Geological Society of Australia, 6p.

Recommended reference

Murdie, RE 2021, 3D geomodel of Western Australia, 2021: Geological Survey of Western Australia, 3D Geomodel Series, <www.dmirs.wa.gov.au/3Dgeoscience>.

Western Australian Moho, 2021

by

RE Murdie and H Yuan

Abstract

The Western Australian Moho, 2021 is a depth contour map of the Mohorovičíć (Moho) discontinuity between the crust and mantle as determined from seismological methods. The base map is from the AuSREM model (Salmon et al., 2012) at half-degree gridded intervals with additional data from deep crustal seismic reflection lines Yilgarn 1999 (Goleby et al., 2000), Eastern Goldfields 1991 (Goleby et al., 1993), Northeastern Yilgarn 2001, (Goleby et al., 2003), Tanami 2005 (Goleby et al., 2009), Capricorn 2010 (Johnson et al., 2012), Youanmi 2010 (Wyche et al., 2014), Yilgarn Craton – Officer Basin – Musgrave Province 2011 (Neumann, 2013), Albany–Fraser and Tropicana 2012 (Spaggiari and Tyler, 2015), Eucla–Gawler 2013 (Dutch et al., 2015), Kidson Basin 2018 (Doublier et al., 2020a,b), New Norcia 1992 (Middleton et al., 1993), deep refraction lines South West Yilgarn 1983 (Dentith et al., 2000), offshore and onshore line GA280 (Tassell and Goncharov, 2006) and receiver function data from passive seismic deployments SKIPPY (Reading et al., 2003, 2012; Reading and Kennett, 2003), ALFREX (Sippl et al., 2018), COPA (Dentith et al., 2018), CWAS (Zhao et al., written comm.) and SWAN (Yuan et al., written comm).

How to access

The **Western Australian Moho, 2021** data layer forms part of the **Critical minerals, 2021 Geological Exploration Package**, available via the DMIRS eBookshop.

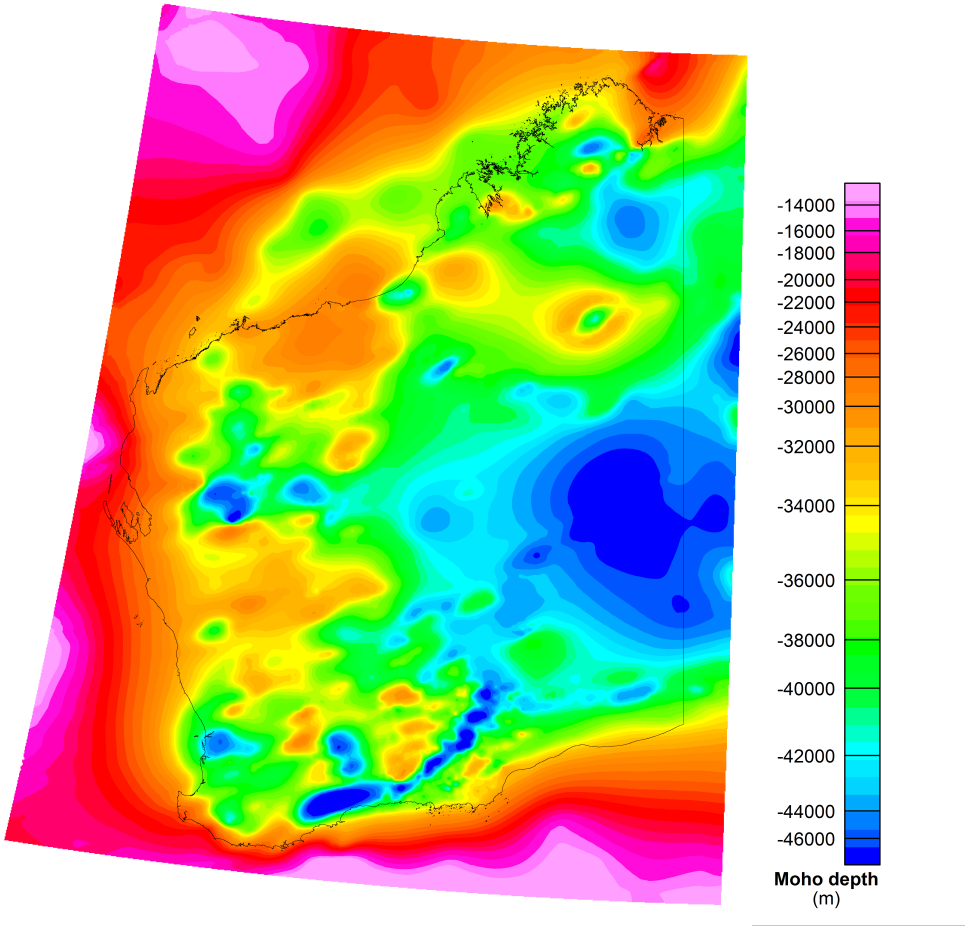

Figure 1. The Western Australian Moho, 2021 data layer

References

Dentith, M, Yuan, H, Murdie, RE, Pina-Varas, P, Johnson, SP, Gessner, K and Korhonen, FJ 2018, Improved interpretation of deep seismic reflection data in areas of complex geology through integration with passive seismic data sets: Journal of Geophysical Research: Solid Earth, v. 123, no. 12, p. 10 810–10 830, doi:10.1029/2018JB015795.

Dentith, MC, Dent, VF and Drummond, BJ 2000, Deep crustal structure in the southwestern Yilgarn Craton, Western Australia: Tectonophysics, v. 325, p. 227–255.

Doublier, MP, Gessner, K, Johnson, SP, Kelsey, DE, Haines, PW, Howard, HM, Chopping, R, Smithies, RH, Hickman, AH, Martin, DMcB, Southby, C, Champion, DC, Huston, DL, Calvert, AJ, Gorczyk, W, Kohanpour, F, Moro, P, Costelloe, R, Formin, T, Yuan, H and Kennett, BLN 2020a, Basement interpretation of the Kisdon seismic survey 18GA-KB1 (1:500 000 scale): Geological Society of Western Australia, non-series map.

Doublier, MP, Johnson, SP, Gessner, KT, Howard, HM, Chopping, R, Smithies, RH, Martin, DMcB, Kelsey, DE, Haines, PW, Hickman, AH, Czarnota, K, Southby, C, Champion, DC, Huston, DL, Calvert, AJ, Kohanpour, F, Moro, P, Costelloe, R, Fomin, T and Kennett, BLN 2020b, Basement architecture from the Pilbara Craton to the Aileron Province: new insights from deep seismic reflection line 18GA-KB1, *in* Exploring for the future: Extended Abstracts *edited by* K Czarnota, IC Roach, S Abbott, M Haynes, N Kositcin, A Ray and E Slatter, Geoscience Australia, Canberra, <www.ga.gov.au/eftf/extended-abstracts>.

Dutch, RA, Pawley, MJ and Wise, TW (editors) 2015, What lies beneath the Western Gawler Craton? 13GA-EG1 Seismic and Magnetotelluric Workshop 2015 — extended abstracts: Department of State Development, South Australia, Report Book 2015/00029, 84p.

Goleby, BR, Blewett, RS, Groenewald, PB, Cassidy, KF, Champion, DC, Jones, LEA, Korsch, RJ, Shevchenko, S and Apak, SN 2003, The 2001 northeastern Yilgarn deep seismic reflection survey: Geoscience Australia, Record 2003/28, 144p.

Goleby, BR and Drummond, BJ 2000, The 1991 deep seisimc survey, Eastern Goldfields, WA, in Crustal structure and fluid flow in the Eastern Goldfields, Western Australia: Results from the Australian Geodynamics Cooperative Research Centre's (AGRCRC) Yilgarn deep seismic refection survey and fluid flow modelling projects edited by BR Goleby, B Bell, RJ Korsch, P Sorjonen-Ward, PB Groenewald, S Wyche, R Bateman, T Fomin, W Witt, J Walshe, BJ Drummond and AJ Owen: Australian Geological Survey Organization, Record 2000/34, p. 53–57.

Goleby, BR, Huston, DL, Lyons, P, Vandenberg, L, Bagas, L, Davies, BM, Jones, LEA, Gebre-Mariam, M, Johnson, W, Smith, T and English, L 2009, The Tanami deep seismic reflection experiment: An insight into gold mineralization and Paleoproterozoic collision in the North Australian Craton: Tectonophysics, v. 472, no. 1-4, p. 169–182.

Goleby, BR, Rattenbury, MS, Swager, CP, Drummond, BJ, Williams, PR, Sheraton, JE and Heinrich, CA 1993, Archean crustal structure from seismic reflection profiling, Eastern Goldfields, Western Austalia: Australian Geological Survey Organization, Record 15, 54p.

Johnson, SP, Thorne, AM and Tyler, IM 2012, Capricorn Orogen seismic and magnetotelluric (MT) workshop 2011: Extended abstracts: Geological Survey of Western Australia, Record 2011/25, 120p.

Middleton, MF, Long, A, Wilde, SA, Dentith, M and Evans, BA 1993, A preliminary interpretation of deep seismic reflection and other geophysical data from the Darling Fault Zone, Western Australia: Exploration Geophysics, v. 24, no. 3-4, p. 711–717, doi:10.1071/EG993711.

Neumann, NL (editor) 2013, Yilgarn Craton – Officer Basin – Musgrave Province seismic and MT workshop: Geoscience Australia, Record 2013/28, 210p.

Reading, AM and Kennett, BLN 2003, Lithospheric structure of the Pilbara Craton, Capricorn Orogen and northern Yilgarn Craton, Western Australia, from tele-seismic receiver functions: Australian Journal of Earth Sciences, v. 50, p. 439–445.

Reading, AM, Kennett, BLN and Dentith, MC 2003, Seismic structure of the Yilgarn Craton, Western Australia: Australian Journal of Earth Sciences, v. 50, no. 3, p. 427–438, doi:10.1046/j.1440-0952.2003.01000.x.

Reading, AM, Tkalčić, H, Kennett, BLN, Johnson, SP and Sheppard, S 2012, Seismic structure of the crust and uppermost mantle of the Capricorn and Paterson Orogens and adjacent cratons, Western Australia, from passive seismic transects: Precambrian Research, v. 196–197, p. 295–308, doi:10.1016/j.precamres.2011.07.001.

Salmon, M, Kennett, BLN and Saygin, E 2012, Australian Seismological Reference Model (AuSREM): Crustal component: Geophysical Journal International, v. 192, p. 190–206.

Sippl, C, Tkalčić, H, Kennett, BLN, Spaggiari, CV and Gessner, K 2018, Crustal and uppermost mantle structure of the east Albany–Fraser Orogen from passive seismic data: Geological Survey of Western Australia, Report 177, 51p.

Spaggiari, CV and Tyler, IM (editors) 2015, Albany–Fraser Orogen seismic and magnetotelluric (MT) workshop 2014: Geological Survey of Western Australia, Record 2014/6.

Tassell, H and Goncharov, A 2006, Geophysical evidence for a deep crustal root beneath the Yilgarn Craton and Albany–Fraser Orogen, Western Australia, *in* Conference abstracts: Australian Earth Sciences Convention, Melbourne, Victoria, 2–8 July 2006: Geological Society of Australia, 6p.

Wyche, S, Ivanic, TJ and Zibra, I (editors) 2014, Youanmi and southern Carnarvon seismic and magnetotelluric (MT) workshop 2013: Geological Survey of Western Australia, Record 2013/6, 180p.

Yuan, H, Murdie, RE, Miller, M, Allen, T, Salmon, M and Whitney, J 2021 South West Australia Network, initial results: Written communication, February 2021.

Zhao L, Yuan H, Tyler I, Gorczyk W, Murdie RE, Gessner K, Lu Y, Smithies RH, Li T, Yang J, Zhan A, Wan B and China – Western Australia passive seismic group 2021, Geophysical imaging of a 1.9 Ga hidden orogen in the northern West Australian Craton and implications for early cratonization: Written communication, April 2021.

Recommended reference

Murdie, RE and Yuan, H 2021, Western Australian Moho, 2021: Geological Survey of Western Australia, digital data layer.

Maximum grade in-hole drilling data

by

WR Ormsby, J Thom, SHD Howard, D Then, S De Biran and B Tapping

Abstract

Images and processed maximum grade in-hole data for the most commonly analysed elements can assist with mineral exploration and other mineral-related studies by providing a spatial overview of known mineralization locations, trends and patterns. This digital product has been made possible by extracting analytes from the Western Australian Mineral Exploration reports (WAMEX) database from the many disparate submission names and units into flat tables using a common set of units. This is the first time that this process has been attempted by the Geological Survey of Western Australia (GSWA) and despite being incomplete and incorporating significant known errors, data processing has enabled valuable information to be derived.

Publicly available industry drillhole data provided in digital format (generally from the late 1990s to more than five years old) were used in this compilation. The compilation process is acknowledged to be problematic and incomplete for a variety of reasons. The automated identification of all possible analytes and units of measurement had limitations resulting in the loss of about 15% of the data. Furthermore, the compilation contains significant erroneous data with the main contributor being incorrectly recorded units, resulting in excessively large or small values when converted to the common set. For example, results incorrectly reported as being a percentage (when actually in parts per million) would be incorrect by a factor of 10 000. To partly address these issues, low and high cuts were applied to the data to remove the most obvious erroneous values. This resulted in a further reduction in the dataset by between 7 and 20% (see Table 1) and in addition, the loss of valid data. Furthermore, results from all analytical techniques were combined in the same table, so not all are directly comparable, particularly those derived from portable XRF instruments.

Table 1. Statistics and grade threshold summary for the maximum grade in-hole drilling data

Analyte	No. compiled samples	Minimum grade	Maximum grade	Mineralized threshold	Units	No. samples used	% of compiled samples
Au	1 325 000	1	10 000	500	ppb	1 061 936	80
As	868 250	1	10 000	1000	ppm	697 369	80
Cu	779 385	1	50 000	2500	ppm	720 363	92
Zn	689 186	1	100 000	10 000	ppm	638 546	93
Pb	553 224	1	100 000	10 000	ppm	473 849	86
Ni	677 691	1	50 000	3000	ppm	628 488	93
Co	468 501	1	5 000	1000	ppm	414 946	89

Maximum grade in-hole was identified and attributed to the relevant drill collar coordinates irrespective of drillhole type, depth, orientation or downhole interval. As over 85% of all drillholes are less than 200 m deep, even if inclined at 60 °, the maximum horizontal location error for most results is therefore +/- 100 m.

Data were processed using the point neighbourhood statistics tool in ESRI ArcGIS software to obtain the maximum in-hole grade and density of mineralized drillholes for three different cell sizes (5 km, 300 m and 100 m) smoothed over the adjoining eight cells. These cell sizes enable visualization of mineralization trends at different scales ranging from statewide, through to regional and district scale.

Note that the smoothing effect of this approach, while a powerful visualization tool, does exaggerate the apparent spatial extent of mineralization. This effect is readily evident by comparing the imagery for the different cell sizes at any specific location.

To further visualize mineralization trends, smoothed images of maximum in-hole grade overlaying a hill-shaded density of mineralized drillholes were generated using ER Mapper software. Mineralized drillholes were defined as those with a maximum grade corresponding to the definition of a mineral occurrence for greenfields areas in MINEDEX (see 'mineralized threshold' in Table 1).

Noting the above data qualifications, it is strongly recommended that the source data in the original exploration reports (identified by the unique 'A-Number' in the Mineral Exploration Drillholes layer in GeoVIEW.WA) are examined closely to verify the results before using this information for any detailed work, including exploration targeting.

Despite the significant limitations of the dataset, the resultant mineralization footprints agree with the relevant mineralization sites data and provide further detail and information on statewide, regional and district scale mineralization trends.

How to access

Selected data are available as a free download from the Data and Software Centre via Datasets — Statewide spatial datasets — Mineral information — Maximum grade in-hole drilling data.

Smoothed images can also be viewed using GeoVIEW.WA. This online interactive mapping system allows data to be viewed and searched together with other datasets, including orthophotography, geological maps, geophysical images, and mineral exploration datasets.

Recommended reference

Ormsby, WR, Thom, J, Howard, SHD, Then, D, De Biran, S and Tapping, B 2021, Maximum grade in-hole drilling data: Geological Survey of Western Australia, digital dataset.

Mean soil sample geochemical data

by

WR Ormsby, J Thom, SHD Howard, D Then, N Gardiner and B Tapping

Abstract

Images and processed mean soil sample geochemical data for the most commonly analysed elements can assist with mineral exploration and other mineral-related studies by providing a spatial overview of elevated soil geochemical locations, trends and patterns. This digital product has been made possible by compiling analytes from the Western Australian Mineral Exploration reports (WAMEX) database from the many disparate submission names and units into flat tables using a common set of units. This is the first time that this process has been attempted by the Geological Survey of Western Australia (GSWA) and despite being incomplete and incorporating significant known errors, data processing has enabled valuable information to be derived.

Publically available industry soil sample geochemical data provided in digital format (generally from the late 1990s to more than five years old) were used in this compilation. The compilation process is acknowledged to be problematic and incomplete for a variety of reasons. The automated identification of all possible analytes and units of measure had limitations, resulting in the loss of about 15% of the data. Furthermore, the compilation contains significant erroneous data with the main contributor being incorrectly recorded units resulting in excessively large or small values when converted to the common set. For example, results incorrectly reported as being in parts per million (when actually in parts per billion) would be incorrect by a factor of 1000. Also, in some cases, the assay range for data points imported as soils would be more typical of rock chip samples. Soil sampling datasets, which combine subsets of analytical results for different sized fractions or analytical techniques could also introduce variability. To partly address these issues, low and high cuts were applied to the data to remove the most obvious erroneous values. This resulted in a further reduction in the dataset by between 7 and 20% (see Table 1) and in addition, the loss of valid data.

Table 1. Statistics and grade threshold summary for the mean soil sample geochemical data

Analyte	No. compiled samples	Minimum grade	Maximum grade	Anomalous threshold	Units	No. samples used	% of compiled samples
Au	3 492 899	1	1000	10	ppb	2 777 932	80
As	3 039 130	1	600	20	ppm	2 761 295	91
Cu	3 583 553	1	2500	50	ppm	3 337 739	93
Zn	3 023 924	1	2500	50	ppm	2 753 631	91
Pb	2 833 759	1	2500	25	ppm	2 584 689	91
Ni	2 962 658	1	2500	100	ppm	2 666 225	90
Co	2 148 242	1	2000	25	ppm	1 879 835	88

Data were processed using the point neighbourhood statistics tool in ESRI ArcGIS software to obtain the mean grade and density of 'anomalous' samples for two different cell sizes (5 km and 300 m) smoothed over the adjoining eight cells. These cell sizes enable visualization of actual and potential mineralization trends at different scales ranging from state-wide, through to regional and district scale. Note that the smoothing effect of this approach, while a powerful visualization tool, does exaggerate the apparent spatial extent of mineralization. This effect is readily evident by comparing the imagery for the two cell sizes at any specific location.

To further visualize mineralization trends, smoothed images of mean grade overlaying a hill-shaded density of 'anomalous' samples were generated using ER Mapper software. For the purpose of visualization, thresholds for 'anomalous' samples (see Table 1) were identified in comparison with the known mineralization sites, the maximum grade in-hole and statistical data. All selected thresholds ranged from between 0.1 and 0.5 times the mean plus one standard deviation and between 1.7 and 3.9 times the median grades.

Noting the above data qualifications, it is strongly recommended that the source data in the original exploration reports (identified by the unique 'A-Number' in the Company Surface Sample Geochemistry layer in GeoVIEW.WA) are examined closely to verify the results before using this information for any detailed work, including exploration targeting.

Despite the significant limitations of the dataset, the resultant mineralization footprints agree well with the relevant known mineralization sites and maximum grade in-hole drilling data and provide further detail and information on state-wide, regional and district scale mineralization trends.

How to access

Selected data are available as a free download from the Data and Software Centre via Datasets — Statewide spatial datasets — Mineral information — Mean soil sample geochemical data.

Smoothed images can also be viewed using GeoVIEW.WA. This online interactive mapping system allows data to be viewed and searched together with other datasets, including orthophotography, geological maps, geophysical images, and mineral exploration datasets.

Recommended reference

Ormsby, WR, Thom, J, Howard, SHD, Then, D, Gardiner, N and Tapping, B 2021, Mean soil sample geochemical data: Geological Survey of Western Australia, digital dataset.

AGP Accelerated Geoscience Program

Data integration and analyses — the Yilgarn Craton

Far East Yilgarn

Far East Yilgarn, 2021 Geological Exploration Package

project managed by

R Chopping and HM Howard

Abstract

The Geological Survey of Western Australia (GSWA) reprioritized its 2020–21 work program because of the impact of current travel and operational restrictions imposed by the COVID-19 pandemic. By using GSWA's extensive, pre-competitive geoscience datasets and outstanding rock and paleontology collection, the organization's aim was to aid economic recovery and stimulate the exploration industry. GSWA's objective was to deliver new interpretive datasets across all areas of geoscience in key regions of the State to accelerate understanding of the region's geology and mineral prospectivity.

A key area where data integration and analyses can assist in an increased understanding of geology and mineral prospectivity is the Yilgarn Craton. The Yilgarn Craton is one of Western Australia's most prospective regions and contains significant deposits of gold, nickel, lithium, copper, zinc, iron ore, tantalum, aluminium and uranium. Recent high-grade gold and nickel discoveries in the craton's far eastern (Gruyere, Tropicana, Neale) and southwestern margins (Julimar), have shown that these two poorly exposed and geologically not well-understood regions are likely to be as prospective as the craton's interior (i.e. Eastern Goldfields). Despite both regions being covered by a thick blanket of regolith, GSWA holds a vast amount of geoscientific data relating to the bedrock and regolith geology with the potential for uncovering significant, new mineral deposits.

The minerals industry is increasingly aware that the next generation of Tier 1 deposits is likely to be under deep cover. Working to the UNCOVER plan, the aim of the Accelerated Geoscience program has been to deliver new integrated geoscience datasets for the southwestern and far eastern Yilgarn Craton margins. The program has incorporated results of ongoing work in the Eastern Goldfields and has performed new analyses on archived samples, which will accelerate understanding of these regions and will define new areas of high mineral prospectivity.

The Far East Yilgarn, 2021 Geological Exploration Package is a compilation of data of use by those interested in understanding the eastern margin of the Yilgarn Craton, where it adjoins the Musgrave Province or the Albany–Fraser Orogen. A number of existing GSWA products are included, and some extracts from new products within the region of interest are also provided. Abstracts are incorporated into this product for individual layers or groups of thematically similar layers (such as geophysical imagery).

How to access

The Far East Yilgarn, 2021 Geological Exploration Package is available via the DMIRS eBookshop.

Recommended reference

Chopping, R and Howard, HM 2021, Far East Yilgarn, 2021 Geological Exploration Package: Geological Survey of Western Australia, digital data layers.

Multi-scale edges for the Far East Yilgarn from gravity and magnetics

by

JW Brett

Abstract

Multi-scale edges have been generated from Bouguer gravity and Reduced-to-Pole magnetic data. The Intrepid v5.6.3 Multi-scale edge detection module uses potential field geophysical data to provide a starting point for an interpretation of structural geology. Detection of multi-scale edges proceeds by finding local maxima points of the total horizontal derivative for many upward continuations of data. Neighbouring points are then joined together to create strings (also referred to as 'worms') that define the edges of features.

Upward continuation levels used are as follows:

gravity (15 levels): 0.8, 1, 1.5, 2.1, 3, 4.2, 6, 8, 12, 16, 22, 32, 44, 62, 85 km

magnetics (13 levels): 0.8, 1, 1.5, 2.1, 3, 4.2, 6, 8, 12, 16, 22, 32, 44 km

The gravity data used to generate the multi-scale edges is the Gravity anomaly grid (400 m) of Western Australia (Brett, 2020a). The magnetic data used to generate the multi-scale edges is the Magnetic anomaly grid (80 m) of Western Australia (Brett, 2020b).

The following products have been generated:

- ArcGIS shape files of multi-scale edges from gravity and magnetic data.

How to access

The data layer is best accessed using GeoVIEW.WA. This online interactive mapping system allows data to be viewed and searched together with other datasets, including Geological Survey of Western Australia and Geoscience Australia geochronology data, geological maps and mineral exploration datasets.

References

Archibald, N, Gow, P and Boschetti, F 1999, Multi-scale edge analysis of potential field data: Exploration Geophysics, 30, p. 38–44, doi:10.1071/EG999038.

Brett, JW 2020a, 400 m Bouguer gravity merged grid of Western Australia 2020 – version 1: Geological Survey of Western Australia, <www.dmirs.wa.gov.au/geophysics>.

Brett, JW 2020b, 80 m magnetic merged grid of Western Australia 2020 – version 1: Geological Survey of Western Australia, <www.dmirs.wa.gov.au/geophysics>.

Recommended reference

Brett, JW 2021, Multi-scale edges for the Far East Yilgarn from gravity and magnetics: Geological Survey of Western Australia, digital data layer, <www.dmirs.wa.gov.au/geoview>.

Geochemical pathfinders for gold-rich mineralizing systems in the Far East Yilgarn

by

P Duuring, JN Guilliamse and S Morin-Ka

Abstract

Multiple layers show the distribution and abundance of selected elements or element ratios for rock, soil, stream, and laterite samples within the Far East Yilgarn. The displayed geochemical data are relevant for mineral exploration because they either directly identify gold mineralization (e.g. Au layers), or they may be considered proxies for hydrothermal fluid alteration associated with mineralization (e.g. S layers).

The derivative GIS layers were created from existing primary geochemical datasets. These parent datasets include WACHEM, OZCHEM (WA subset), CRCLEME-laterite, and WAMEX (i.e. the surface rock chip, surface stream sediment, surface shallow drillhole, surface soil, and maximum grade in drillhole). In each dataset, the samples have been analysed for a range of elements. A variety of analytical approaches has been used at commercial and government laboratories, so that a user must take care when comparing element value ranges between different datasets. Element ratios have been created as a normalization tool to avoid some of these laboratory procedure-induced differences between datasets. The WACHEM, OZCHEM, and CRCLEME-laterite data have high fidelity because strict quality controls were in place at the time of sampling, rock preparation, and laboratory analysis. In contrast, WAMEX geochemical data are derived from exploration and mining activities in Western Australia, reported by companies to the Geological Survey of Western Australia (GSWA). GSWA applies quality control measures at the time of data submission, but there is likely to be some inclusion of spurious results (e.g. errors in unit reporting, multiple field names for the same analyte, incorrect assignment of analytes). For each geochemical layer, a unique legend and colour scheme has been chosen to best highlight geochemical trends. Higher element abundance values are drawn on top of lower values to more clearly show spatial gradients in element concentrations.

How to access

These data form part of the Far East Yilgarn, 2021 Geological Exploration Package, available via the DMIRS eBookshop.

Recommended reference

Duuring, P, Guilliamse, JN and Morin-Ka, S 2021, Geochemical pathfinders for gold-rich mineralizing systems in the Far East Yilgarn: Geological Survey of Western Australia, digital data layers.

Alteration minerals potentially diagnostic of mineral systems fertile for gold in the Far East Yilgarn

by

P Duuring, S Morin-Ka and JN Guilliamse

Abstract

These data layers show the distribution of non-sulfide minerals that may indicate altered rocks (or their metamorphosed equivalents) and are potentially associated with gold-rich mineral systems in the Far East Yilgarn. Each layer shows the occurrence of a specific target mineral (e.g. andalusite).

The parent WAROX database contains geoscientific data related to observations and samples collected in the field. The data include information about outcrop geology, regolith geology, field photographs, geological samples, rock physical properties, petrography, paleontology and geochronology.

The derived layer shows site locations where minerals that indicate alteration have been recorded (Table 1). Results show that no specific non-sulfide mineral is strongly correlated with known MINEDEX gold occurrences in the Far East Yilgarn. A simple explanation is that there is strong lithological control on the presence or absence of non-sulfide minerals in the study area.

Table 1. Query operation

Operation	Query
For the 'alteration minerals' layers, WAROX data are queried to select specific minerals from any field in the WAROX database	Any field = 'andalusite' OR Any field = 'anhydrite' OR Any field = 'ankerite' OR Any field = 'barite' OR Any field = 'biotite' OR Any field = 'calcite' OR Any field = 'cordierite' OR Any field = 'diopside' OR Any field = 'dolomite' OR Any field = 'garnet' OR Any field = 'gypsum' OR Any field = 'kyanite' OR Any field = 'magnetite' OR Any field = 'prehnite' OR Any field = 'rutile' OR Any field = 'siderite' OR Any field = 'sillimanite' OR Any field = 'staurolite' OR Any field = 'titanite' OR Any field = 'tourmaline' OR Any field = 'wollastonite'

How to access

These data form part of the Far East Yilgarn, 2021 Geological Exploration Package, available via the DMIRS eBookshop.

Recommended reference

Duuring, P, Morin-Ka, S and Guilliamse, JN 2021, Alteration minerals potentially diagnostic of mineral systems fertile for gold in the Far East Yilgarn: Geological Survey of Western Australia, digital data layers.

MINEDEX observations of gold sites in the Far East Yilgarn

by

P Duuring, S Morin-Ka and JN Guilliamse

Abstract

This data layer shows the distribution of known gold-rich sites in the Far East Yilgarn. Gold mineralization sites are extracted from the MINEDEX database, which provides a coordinated, project-based inquiry system for textual information on mine, deposit, prospect and occurrence locations (coordinates, etc.), as well as mineral resources and mine production. Data are collated from ASX reports, statutory exploration reports, mining proposals and production returns.

The derived gold mineralization sites are selected to exclude exploration targets and infrastructure not directly related to mineralization, such as tailings storage facilities and processing plants. Gold sites are derived from the SITE_COMMODITY field in the MINEDEX database.

The order of listing of the commodity in the SITE_COMMODITY field reflects its relative importance at that site. Only those identified as target commodities and listed in the TARGET_COMMODITY_GROUP field are classified in MINEDEX into four groups: mine, deposit, prospect and occurrence (Table 1). Therefore, the SITE_TYPE_DESCRIPTION (i.e. mine, deposit, prospect or occurrence) is only applicable to the selected commodity if it is also listed in the TARGET_COMMODITY_GROUP field. When the commodity for a mineralization site is not listed in the TARGET_COMMODITY field, then it is not possible to allocate the relevant SITE_TYPE_DESCRIPTION without further investigation of the source data. In these instances, the site remains unclassified with respect to SITE_TYPE_DESCRIPTION.

The distribution of known gold sites in the Far East Yilgarn correlate with the mapped location of greenstone belts, shear zones and faults.

Table 1. Legend description

Site type	Definition
Au Mine	A deposit which is being mined, was previously mined, or is proposed to be mined
Au Deposit	A mineral occurrence with probable economic value and for which there is an established resource
Au Prospect	Any mineral occurrence where economic grades have been intersected over a significant width and strike length but for which there is not yet a resource, or any working or exploration activity that has found subeconomic mineral occurrences and from which there is no recorded production
Au Occurrence	An occurrence (excluding those defined as mines, deposits or prospects) can be defined if an economic mineral has been identified in outcrop, or if assay results exceed an agreed concentration and size
Au Unclassified	Mineralization site for which the TARGET_COMMODITY_GROUP does not reflect the specified commodity, and hence the SITE_TYPE_DESCRIPTION is not applicable

How to access

These data form part of the Far East Yilgarn, 2021 Geological Exploration Package, available via the DMIRS eBookshop.

Recommended reference

Duuring, P, Morin-Ka, S and Guilliamse, JN 2021, MINEDEX observations of gold sites in the Far East Yilgarn: Geological Survey of Western Australia, digital data layers.

MINEDEX observations of silver sites in the Far East Yilgarn

by

P Duuring, S Morin-Ka and JN Guilliamse

Abstract

This data layer shows the distribution of known silver-rich sites in the Far East Yilgarn. Silver mineralization sites are extracted from the MINEDEX database, which provides a coordinated, project-based inquiry system for textual information on mine, deposit, prospect and occurrence locations (coordinates, etc.), as well as mineral resources and mine production. Data are collated from ASX reports, statutory exploration reports, mining proposals and production returns.

The derived silver mineralization sites are selected to exclude exploration targets and infrastructure not directly related to mineralization, such as tailings storage facilities and processing plants. Silver sites are derived from the SITE_COMMODITY field in the MINEDEX database.

The order of listing of the commodity in the SITE_COMMODITY field reflects its relative importance at that site. Only those identified as target commodities and listed in the TARGET_COMMODITY_GROUP field are classified in MINEDEX into four groups: mine, deposit, prospect and occurrence (Table 1). Therefore, the SITE_TYPE_DESCRIPTION (i.e. mine, deposit, prospect or occurrence) is only applicable to the selected commodity if it is also listed in the TARGET_COMMODITY_GROUP field. When the commodity for a mineralization site is not listed in the TARGET_COMMODITY field, then it is not possible to allocate the relevant SITE_TYPE_DESCRIPTION without further investigation of the source data. In these instances, the site remains unclassified with respect to SITE_TYPE_DESCRIPTION.

The distribution of known silver sites in the Far East Yilgarn correlates with gold sites and the mapped location of greenstone belts, shear zones and faults.

Table 1. Legend description

Site type	Definition
Ag Mine	A deposit which is being mined, was previously mined, or is proposed to be mined
Ag Deposit	A mineral occurrence with probable economic value and for which there is an established resource
Ag Prospect	Any mineral occurrence where economic grades have been intersected over a significant width and strike length but for which there is not yet a resource, or any working or exploration activity that has found subeconomic mineral occurrences and from which there is no recorded production
Ag Occurrence	An occurrence (excluding those defined as mines, deposits or prospects) can be defined if an economic mineral has been identified in outcrop, or if assay results exceed an agreed concentration and size
Ag Unclassified	Mineralization site for which the TARGET_COMMODITY_GROUP does not reflect the specified commodity, and hence the SITE_TYPE_DESCRIPTION is not applicable

How to access

These data form part of the Far East Yilgarn, 2021 Geological Exploration Package, available via the DMIRS eBookshop.

Recommended reference

Duuring, P, Morin-Ka, S and Guilliamse, JN 2021, MINEDEX observations of silver sites in the Far East Yilgarn: Geological Survey of Western Australia, digital data layers.

Sulfide minerals commonly associated with gold-rich mineral systems in the Far East Yilgarn

by

P Duuring, S Morin-Ka and JN Guilliamse

Abstract

These data layers show the distribution of sulfide minerals in the Far East Yilgarn based on observations recorded in the WAROX database. Each layer shows the occurrence of a specific sulfide mineral (e.g. arsenopyrite) commonly associated with gold-rich mineral systems. The 'Sulfides' layer shows occurrences of undifferentiated sulfide minerals resulting from a search query for 'sulfide' or 'sulphide' (Table 1).

The distribution of sulfide minerals is important for mineral exploration because their presence is potentially indicative of hydrothermal alteration associated with gold-rich mineralizing systems. Certain sulfide minerals may in some cases be part of multiple types of mineralizing systems (e.g. pyrite is commonly part of gold-rich hydrothermal systems, as well as some magmatic systems).

The parent WAROX database contains geoscientific data related to observations and samples collected in the field. The data include information about outcrop geology, regolith geology, field photographs, geological samples, rock physical properties, petrography, paleontology and geochronology.

The derived layers show site locations where a variety of sulfide minerals have been documented.

In this instance, the mapped distribution of sulfide minerals shows strong spatial correlation with gold sites reported by MINEDEX.

Table 1. Query operation

Operation	Query
WAROX data are queried to select particular sulfide minerals from any field in the WAROX database	Any field = 'arsenopyrite' OR Any field = 'bornite' OR Any field = 'chalcocite' OR Any field = 'chalcopyrite' OR Any field = 'galena' OR Any field = 'pyrite' OR Any field = 'pyrrhotite' OR Any field = 'sphalerite' OR Any field = 'sulfide' OR 'sulphide'

How to access

These data form part of the Far East Yilgarn, 2021 Geological Exploration Package, available via the DMIRS eBookshop.

Recommended reference

Duuring, P, Morin-Ka, S and Guilliamse, JN 2021, Sulfide minerals commonly associated with gold-rich mineral systems in the Far East Yilgarn: Geological Survey of Western Australia, digital data layers.

Far East Yilgarn earthquakes 1940–2020

original data by

Geoscience Australia

Abstract

Far East Yilgarn earthquakes 1940–2020 digital layer contains the location and magnitude of earthquakes of the Far East Yilgarn from 1940 to December 2020 (Fig. 1). The data are a subset of the Geoscience Australia catalogue, which is a nationwide dataset. Earthquake location markers are coloured by depth and scaled by preferred magnitude (usually M_L, local magnitude).

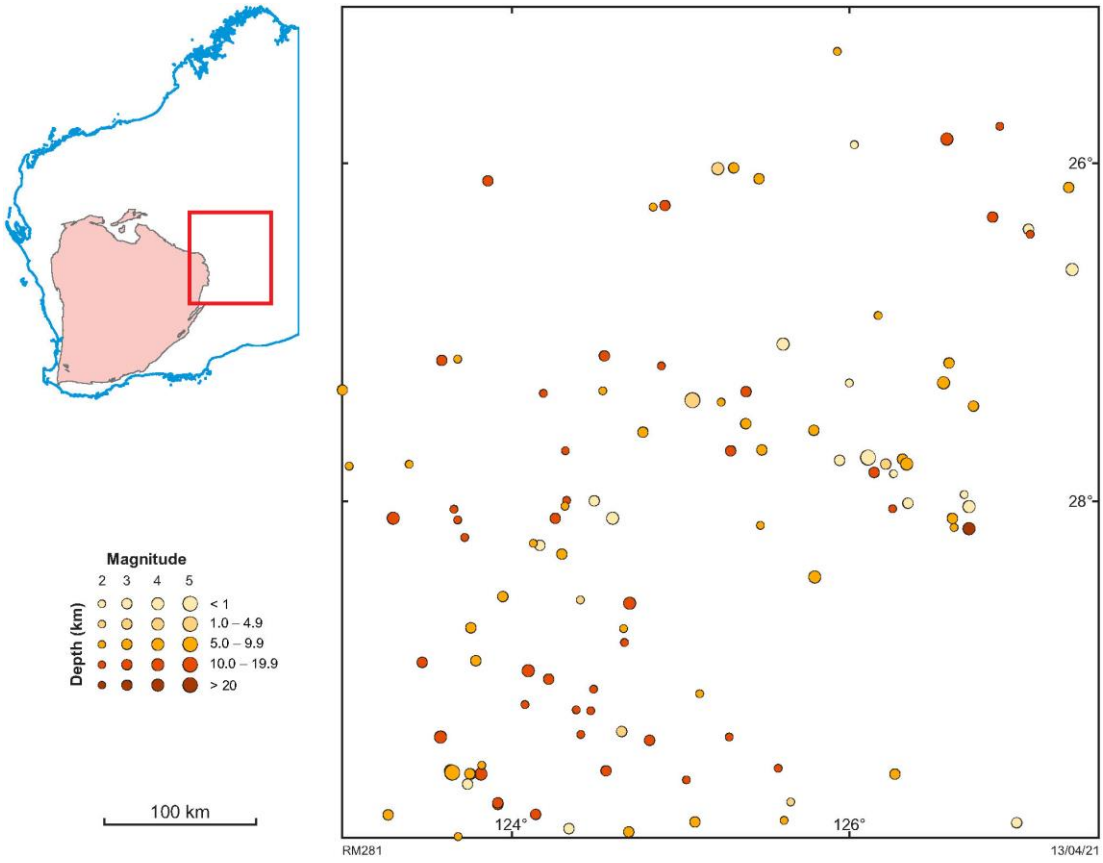

Figure 1. Far East Yilgarn earthquakes 1940–2020 digital layer

How to access

Far East Yilgarn earthquakes 1940–2020 digital data are available on a USB via the DMIRS eBookshop.

Recommended reference (to original data)

Geoscience Australia 2020, Earthquakes@GA: Geoscience Australia, accessed December 2020, <https://earthquakes.ga.gov.au>.

Recommended reference (to this abstract)

Geoscience Australia 2021, Far East Yilgarn earthquakes 1940–2020: Geological Survey of Western Australia, digital data layer.

Neotectonic fault scarps of the Far East Yilgarn

original data by

Geoscience Australia

Abstract

The Neotectonic fault scarps map of the Far East Yilgarn (Fig. 1) is extracted from the Geoscience Australia database 'Neotectonic Features' layer. It comprises fault scarps, lineaments and fault zones, which are believed to relate to large earthquakes during the Neotectonic era, that is, the past 5–10 million years.

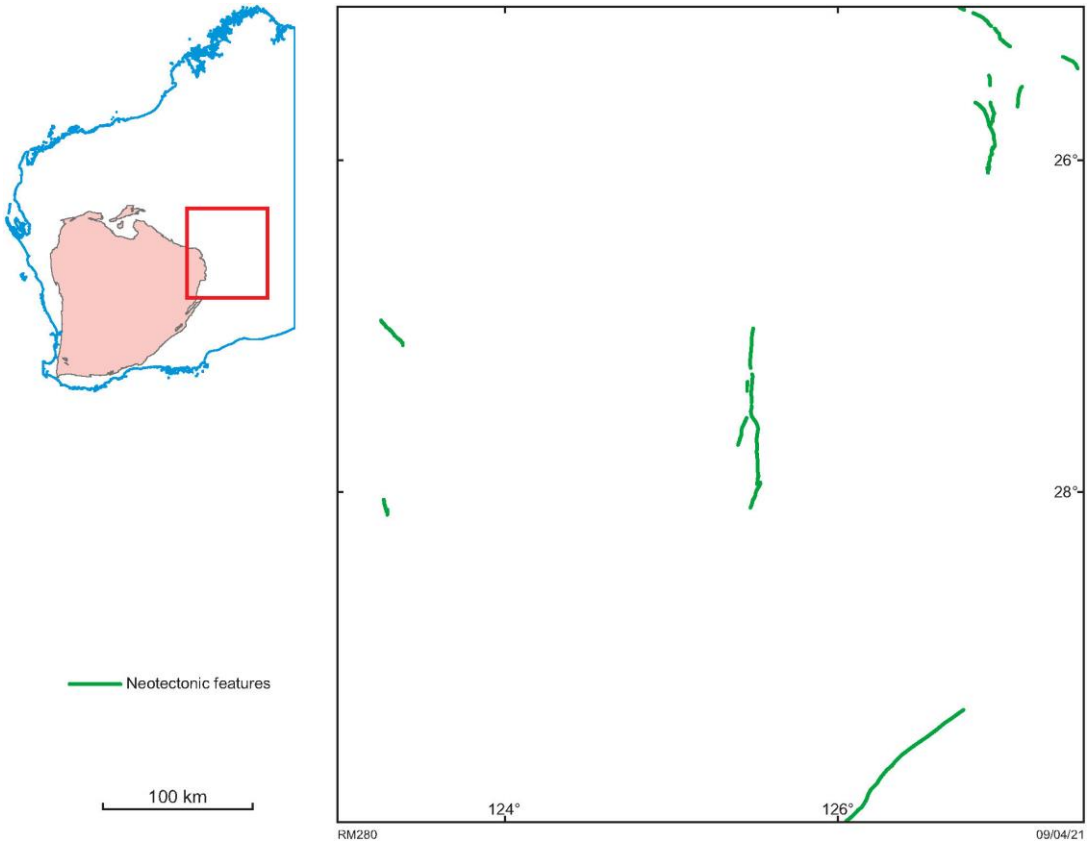

Figure 1. Map of the Neotectonic fault scarps of the Far East Yilgarn

How to access

The Neotectonic fault scarps of the Far East Yilgarn map layers are available on a USB via the DMIRS eBookshop.

Recommended reference (to original data)

Geoscience Australia 2020, Neotectonic Features: Geoscience Australia, <https://neotectonics.ga.gov.au/>.

Recommended reference (to this abstract)

Geoscience Australia 2021, Neotectonic features of the Far East Yilgarn: Geological Survey of Western Australia, digital data layer.

WAROX observations of minerals potentially diagnostic of phyllic alteration in the Far East Yilgarn

by

LL Grech and P Duuring

Abstract

These data layers show the distribution of minerals that are commonly associated with phyllic alteration related to porphyry Cu–Au–Mo mineral systems (e.g. Sillitoe, 2010; Safari et al., 2018). Each layer shows the occurrence of a specific target mineral (e.g. white mica; Table 1).

The parent WAROX database contains geoscientific data related to observations and samples collected in the field. The data include information about outcrop geology, regolith geology, field photographs, geological samples, rock physical properties, petrography, paleontology and geochronology.

The derived layer shows site locations where minerals that are indicative of alteration have been recorded.

Table 1. Query operation

Operation	Query
For the 'phyllic alteration' layers, WAROX data are queried to select specific minerals from any field in the WAROX database	Any field = 'quartz' OR Any field = 'white mica' OR Any field = 'pyrite'

How to access

These data form part of the Far East Yilgarn, 2021 Geological Exploration Package, available via the DMIRS eBookshop.

References

Safari, M, Maghsoudi, A and Beiranvand Pour, A 2018, Application of Landsat-8 and ASTER satellite remote sensing data for porphyry copper exploration: a case study from Shahr-e-Babak, Kerman, south of Iran: Geocarto International, v. 33, no. 11, p. 1186–1201.

Sillitoe, RH 2010, Porphyry copper systems: Economic Geology, v. 105, p. 3–41.

Recommended reference

Grech, LL and Duuring, P 2021, WAROX observations of minerals potentially diagnostic of phyllic alteration in the Far East Yilgarn: Geological Survey of Western Australia, digital data layers.

WAROX observations of minerals potentially diagnostic of potassic alteration in the Far East Yilgarn

by

LL Grech and P Duuring

Abstract

These data layers show the distribution of minerals that are commonly associated with potassic alteration related to porphyry Cu–Au–Mo mineral systems (e.g. Sillitoe, 2010; Safari et al., 2018). Each layer shows the occurrence of a specific target mineral (e.g. K-feldspar; Table 1).

The parent WAROX database contains geoscientific data related to observations and samples collected in the field. The data include information about outcrop geology, regolith geology, field photographs, geological samples, rock physical properties, petrography, paleontology and geochronology.

The derived layer shows site locations where minerals that are indicative of alteration have been recorded.

Table 1. Query operation

Operation	Query
For the 'potassic alteration' layers, WAROX data are queried to select specific minerals from any field in the WAROX database	Any field = 'biotite' OR Any field = 'bornite' OR Any field = 'chalcocite' OR Any field = 'chalcopyrite' OR Any field = 'k-feldspar' OR Any field = 'quartz' OR Any field = 'magnetite'

How to access

These data form part of the Far East Yilgarn, 2021 Geological Exploration Package, available via the DMIRS eBookshop.

References

Safari, M, Maghsoudi, A and Beiranvand Pour, A 2018, Application of Landsat-8 and ASTER satellite remote sensing data for porphyry copper exploration: a case study from Shahr-e-Babak, Kerman, south of Iran: Geocarto International, v. 33, no. 11, p. 1186–1201.

Sillitoe, RH 2010, Porphyry copper systems: Economic Geology, v. 105, p. 3–41.

Recommended reference

Grech, LL and Duuring, P 2021, WAROX observations of minerals potentially diagnostic of potassic alteration in the Far East Yilgarn: Geological Survey of Western Australia, digital data layers.

WAROX observations of minerals potentially diagnostic of propylitic alteration in the Far East Yilgarn

by

LL Grech and P Duuring

Abstract

These data layers show the distribution of minerals that are commonly associated with propylitic alteration related to porphyry Cu–Au–Mo mineral systems (e.g. Sillitoe, 2010; Safari et al., 2018). Each layer shows the occurrence of a specific target mineral (e.g. epidote). Users may integrate these layers to show sites with containing specific mineral combinations.

The parent WAROX database contains geoscientific data related to observations and samples collected in the field. The data include information about outcrop geology, regolith geology, field photographs, geological samples, rock physical properties, petrography, paleontology and geochronology.

The derived layer shows site and secthole WAROX locations where minerals that are indicative of alteration have been recorded. The query logic is provided in Table 1.

Table 1. Query operation

Operation	Query
For the 'propylitic alteration' layers, WAROX data are queried to select specific minerals from any field in the WAROX database	Any field = 'albite' OR Any field = 'ankerite' OR Any field = 'calcite' OR Any field = 'chlorite' OR Any field = 'dolomite' OR Any field = 'epidote' OR Any field = 'galena' OR Any field = 'siderite' OR Any field = 'sphalerite' OR Any field = 'sulfides'

How to access

These data form part of the Far East Yilgarn, 2021 Geological Exploration Package, available via the DMIRS eBookshop.

References

Safari, M, Maghsoudi, A and Beiranvand Pour, A 2018, Application of Landsat-8 and ASTER satellite remote sensing data for porphyry copper exploration: a case study from Shahr-e-Babak, Kerman, south of Iran: Geocarto International, v. 33, no. 11, p. 1186–1201.

Sillitoe, RH 2010, Porphyry copper systems: Economic Geology, v. 105, p. 3–41.

Recommended reference

Grech, LL and Duuring, P 2021, WAROX observations of minerals potentially diagnostic of propylitic alteration in the Far East Yilgarn: Geological Survey of Western Australia, digital data layers.

Geochemical pathfinders for porphyry Cu–Au–Mo mineralizing systems in the Far East Yilgarn

by

LL Grech, P Duuring, JN Guilliamse and S Morin-Ka

Abstract

These data layers show the abundance of selected elements or element ratios for rock, soil, stream, and laterite samples within the Far East Yilgarn. The displayed geochemical data are relevant for mineral exploration because they are directly associated with copper–gold mineralization (e.g. Cu and Au abundance).

These derivative GIS layers were created from larger primary geochemical datasets. The parent datasets include WACHEM, OZCHEM (WA subset), CRCLEME-laterite, and WAMEX (i.e. the surface rock chip, surface stream sediment, surface shallow drillhole, surface soil, and maximum grade in drillhole). In each dataset, the samples have been analysed for a range of elements. A variety of analytical approaches have been used at commercial and government laboratories, so that a user must take care when comparing element value ranges between different datasets. Element ratios have been created as a normalization tool to avoid some of these laboratory procedure-induced differences between datasets. The WACHEM, OZCHEM, and CRCLEME-laterite data have high fidelity because strict quality controls were in place at the time of sampling, rock preparation, and laboratory analysis. In contrast, WAMEX geochemical data are derived from exploration and mining activities in Western Australia, reported by companies to the Geological Survey of Western Australia (GSWA). GSWA applies quality control measures at the time of data submission, but there is likely to be some inclusion of spurious results (e.g. errors in unit reporting, multiple field names for the same analyte, incorrect assignment of analytes).

For each derived geochemical layer, a unique legend colour scheme has been applied to best elucidate geochemical trends. Higher element abundance values are plotted on top of lower values to more clearly show spatial gradients in element concentrations.

How to access

These data form part of the Far East Yilgarn, 2021 Geological Exploration Package, available via the DMIRS eBookshop.

Recommended reference

Grech, LL, Duuring, P, Guilliamse, JN and Morin-Ka, S 2021, Geochemical pathfinders for porphyry Cu–Au–Mo mineralizing systems in the Far East Yilgarn: Geological Survey of Western Australia, digital data layers.

WAROX observations of alteration minerals diagnostic of mineral systems for volcanogenic massive sulfide deposits in Western Australia

by

JN Guilliamse and P Duuring

Abstract

These data layers show the distribution of minerals that may be indicative of altered rocks (or their metamorphosed equivalents) associated with volcanogenic massive sulfide (VMS) deposits in Western Australia. Each layer shows the occurrence of a specific target mineral (e.g. andalusite). The geographically located occurrences of the diagnostic minerals depicted in this package are extracted from the Geological Survey of Western Australia's WAROX database, which contains site-specific geoscientific observations collected during field and subsequent laboratory work, on themes such as bedrock and regolith geology, field photographs, geological samples, rock physical properties, petrographic descriptions, palaeontology and geochronology. Such observations include those made on drillcore and rock chips, stored in the 'Secthole' subset of WAROX. The query logic is provided in Table 1.

Table 1. Query operation

Operation	Query
'Sericitic alteration Low grade metamorphism' occurrence layers are extracted by querying for selected alteration minerals from any field in the WAROX database	Any field = 'illite' OR Any field = 'quartz' OR Any field = 'white mica'
'Sericitic alteration High grade metamorphism' occurrence layers are extracted by querying for selected metamorphic minerals from any field in the WAROX database	Any field = 'biotite' OR Any field = 'cordierite' OR Any field = 'garnet' OR Any field = 'K-feldspar' OR Any field = 'kyanite' OR Any field = 'quartz' OR Any field = 'sillimanite'
'Chloritic alteration Low grade metamorphism' occurrence layer is extracted by querying for this mineral from any field in the WAROX database	Any field = 'chlorite'
'Chloritic alteration High grade metamorphism' occurrence layers are extracted by querying for selected metamorphic minerals from any field in the WAROX database	Any field = 'anthophyllite' OR Any field = 'cordierite' OR Any field = 'gedrite' OR Any field = 'kyanite' OR Any field = 'orthopyroxene' OR Any field = 'phlogopite' OR Any field = 'sillimanite'

How to access

These data form part of the Far East Yilgarn, 2021 Geological Exploration Package, available via the DMIRS eBookshop.

Recommended reference

Guilliamse, JN and Duuring, P 2021, WAROX observations of alteration minerals diagnostic of mineral systems for volcanogenic massive sulfide deposits in Western Australia: Geological Survey of Western Australia, digital data layers.

WAROX observations of exhalative minerals and rocks diagnostic of mineral systems for volcanogenic massive sulfide deposits in Western Australia

by

JN Guilliamse and P Duuring

Abstract

These data layers show the distribution of minerals and rock types that may be indicative of exhalative formations associated with volcanogenic massive sulfide (VMS) deposits in Western Australia. Each layer shows the occurrence of a specific target mineral or rock (e.g. gypsum).

The geographically located occurrences of the diagnostic minerals and rocks depicted in this package are extracted from the Geological Survey of Western Australia's WAROX database, which contains site-specific geoscientific observations collected during field and subsequent laboratory work, on themes such as bedrock and regolith geology, field photographs, geological samples, rock physical properties, petrographic descriptions, palaeontology and geochronology. Such observations include those made on drill core and rocks chips, stored in the 'Secthole' subset of WAROX. The query logic is provided in Table 1.

Table 1. Query operation

Operation	Query
'Carbonates' occurrence layers are extracted by querying for selected carbonate minerals from any field in the WAROX database	Any field = 'ankerite' OR Any field = 'calcite' OR Any field = 'dolomite' OR Any field = 'siderite'
'Oxides' layers are extracted by querying for selected oxide minerals from any field in the WAROX database	Any field = 'chert' OR Any field = 'jasper' OR Any field = 'hematite' OR Any field = 'magnetite'
'Sulfates' occurrence layers are extracted by querying for selected sulfate minerals from any field in the WAROX database	Any field = 'anhydrite' OR Any field = 'barite' OR Any field = 'gypsum'

How to access

These data form part of the Far East Yilgarn, 2021 Geological Exploration Package, available via the DMIRS eBookshop.

Recommended reference

Guilliamse, JN and Duuring, P 2021, WAROX observations of exhalative minerals diagnostic of mineral systems for volcanogenic massive sulfide deposits: Geological Survey of Western Australia, digital data layers.

WAROX observations of minerals diagnostic of weathering and oxidation of volcanogenic massive sulfide deposits in Western Australia

by

JN Guilliamse and P Duuring

Abstract

These data layers show the distribution of minerals that may be indicative of exposed or near-surface weathered and oxidized zones of volcanogenic massive sulfide (VMS) deposits in Western Australia. Each layer shows the occurrence of a specific target mineral (e.g. malachite).

The geographically located occurrences of the diagnostic minerals depicted in this package are extracted from the Geological Survey of Western Australia's WAROX database, which contains site-specific geoscientific observations collected during field and subsequent laboratory work, on themes such as bedrock and regolith geology, field photographs, geological samples, rock physical properties, petrographic descriptions, palaeontology and geochronology. Such observations include those made on drillcore and rock chips, stored in the 'Secthole' subset of WAROX. The query logic is provided in Table 1.

Table 1. Query operation

Operation	Query
'Weathered and oxidized mineral' occurrence layers are extracted by querying for selected minerals from any field in the WAROX database	Any field = 'ankerite' OR Any field = 'atacamit" OR Any field = 'azurite' OR Any field = 'barite' OR Any field = 'cerrusite' OR Any field = 'chlorite' OR Any field = 'cuprite' OR Any field = 'goethite' OR Any field = 'gypsum' OR Any field = 'hematite' OR Any field = 'kaolinite' OR Any field = 'malachite' OR Any field = 'montmorillonite' OR Any field = 'pyromorphite' OR Any field = 'quartz' OR Any field = 'scorodite' OR Any field = 'siderite' OR Any field = 'smectite'

How to access

These data form part of the Far East Yilgarn, 2021 Geological Exploration Package, available via the DMIRS eBookshop.

Recommended reference

Guilliamse, JN and Duuring, P 2021, WAROX observations of minerals diagnostic of weathering and oxidation of volcanogenic massive sulfide deposits: Geological Survey of Western Australia, digital data layers.

MINEDEX observations of copper sites in the Far East Yilgarn

by

JN Guilliamse, P Duuring and S Morin-Ka

Abstract

This data layer shows the distribution of known copper-rich sites in the Far East Yilgarn. Copper mineralization sites are extracted from the MINEDEX database, which provides a coordinated, project-based inquiry system for textual information on mine, deposit, prospect and occurrence locations (coordinates, etc.), as well as mineral resources and mine production. Data are collated from ASX reports, statutory exploration reports, mining proposals and production returns.

The derived copper mineralization sites are selected to exclude exploration targets and infrastructure not directly related to mineralization, such as tailings storage facilities and processing plants. Copper sites are derived from the SITE_COMMODITY field in the MINEDEX database.

The order of listing of the commodity in the SITE_COMMODITY field reflects its relative importance at that site. Only those identified as target commodities and listed in the TARGET_COMMODITY_GROUP field are classified in MINEDEX into four groups: mine, deposit, prospect and occurrence (Table 1). Therefore, the SITE_TYPE_DESCRIPTION (i.e. mine, deposit, prospect or occurrence) is only applicable to the selected commodity if it is also listed in the TARGET_COMMODITY_GROUP field. When the commodity for a mineralization site is not listed in the TARGET_COMMODITY field, then it is not possible to allocate the relevant SITE_TYPE_DESCRIPTION without further investigation of the source data. In these instances, the site remains unclassified with respect to SITE_TYPE_DESCRIPTION. The distribution of known copper sites in the Far East Yilgarn correlate with the mapped location of greenstone belts, shear zones and faults.

Table 1. Legend description

Site type	Definition
Cu Mine	A deposit which is being mined, was previously mined, or is proposed to be mined
Cu Deposit	A mineral occurrence with probable economic value and for which there is an established resource
Cu Prospect	Any mineral occurrence where economic grades have been intersected over a significant width and strike length but for which there is not yet a resource, or any working or exploration activity that has found subeconomic mineral occurrences and from which there is no recorded production
Cu Occurrence	An occurrence (excluding those defined as mines, deposits or prospects) can be defined if an economic mineral has been identified in outcrop, or if assay results exceed an agreed concentration and size
Cu Unclassified	Mineralization site for which the TARGET_COMMODITY_GROUP does not reflect the specified commodity, and hence the SITE_TYPE_DESCRIPTION is not applicable

How to access

These data form part of the Far East Yilgarn, 2021 Geological Exploration Package, available via the DMIRS eBookshop.

Recommended reference

Guilliamse, JN, Duuring, P and Morin-Ka, S 2021, MINEDEX observations of copper sites in the Far East Yilgarn: Geological Survey of Western Australia, digital data layers.

MINEDEX observations of lead sites in the Far East Yilgarn

by

JN Guilliamse, P Duuring and S Morin-Ka

Abstract

This data layer shows the distribution of known lead-rich sites in the Far East Yilgarn. Lead mineralization sites are extracted from the MINEDEX database, which provides a coordinated, project-based inquiry system for textual information on mine, deposit, prospect and occurrence locations (coordinates, etc.), as well as mineral resources and mine production. Data are collated from ASX reports, statutory exploration reports, mining proposals and production returns.

The derived lead mineralization sites are selected to exclude exploration targets and infrastructure not directly related to mineralization, such as tailings storage facilities and processing plants. Lead sites are derived from the SITE_COMMODITY field in the MINEDEX database.

The order of listing of the commodity in the SITE_COMMODITY field reflects its relative importance at that site. Only those identified as target commodities and listed in the TARGET_COMMODITY_GROUP field are classified in MINEDEX into four groups: mine, deposit, prospect and occurrence (Table 1). Therefore, the SITE_TYPE_DESCRIPTION (i.e. mine, deposit, prospect or occurrence) is only applicable to the selected commodity if it is also listed in the TARGET_COMMODITY_GROUP field. When the commodity for a mineralization site is not listed in the TARGET_COMMODITY field, then it is not possible to allocate the relevant SITE_TYPE_DESCRIPTION without further investigation of the source data. In these instances, the site remains unclassified with respect to SITE_TYPE_DESCRIPTION. The distribution of known lead sites in the Far East Yilgarn correlate with the mapped location of greenstone belts, shear zones and faults.

Table 1. Legend description

Site type	Definition
Pb Mine	A deposit which is being mined, was previously mined, or is proposed to be mined
Pb Deposit	A mineral occurrence with probable economic value and for which there is an established resource
Pb Prospect	Any mineral occurrence where economic grades have been intersected over a significant width and strike length but for which there is not yet a resource, or any working or exploration activity that has found subeconomic mineral occurrences and from which there is no recorded production
Pb Occurrence	An occurrence (excluding those defined as mines, deposits or prospects) can be defined if an economic mineral has been identified in outcrop, or if assay results exceed an agreed concentration and size
Pb Unclassified	Mineralization site for which the TARGET_COMMODITY_GROUP does not reflect the specified commodity, and hence the SITE_TYPE_DESCRIPTION is not applicable

How to access

These data form part of the Far East Yilgarn, 2021 Geological Exploration Package, available via the DMIRS eBookshop.

Recommended reference

Guilliamse, JN, Duuring, P and Morin-Ka, S 2021, MINEDEX observations of lead sites in the Far East Yilgarn: Geological Survey of Western Australia, digital data layers.

MINEDEX observations of zinc sites in the Far East Yilgarn

by

JN Guilliamse, P Duuring and S Morin-Ka

Abstract

This data layer shows the distribution of known zinc-rich sites in the Far East Yilgarn. Zinc mineralization sites are extracted from the MINEDEX database, which provides a coordinated, project-based inquiry system for textual information on mine, deposit, prospect and occurrence locations (coordinates, etc.), as well as mineral resources and mine production. Data are collated from ASX reports, statutory exploration reports, mining proposals and production returns.

The derived zinc mineralization sites are selected to exclude exploration targets and infrastructure not directly related to mineralization, such as tailings storage facilities and processing plants. Zinc sites are derived from the SITE_COMMODITY field in the MINEDEX database.

The order of listing of the commodity in the SITE_COMMODITY field reflects its relative importance at that site. Only those identified as target commodities and listed in the TARGET_COMMODITY_GROUP field are classified in MINEDEX into four groups: mine, deposit, prospect and occurrence (Table 1). Therefore, the SITE_TYPE_DESCRIPTION (i.e. mine, deposit, prospect or occurrence) is only applicable to the selected commodity if it is also listed in the TARGET_COMMODITY_GROUP field. When the commodity for a mineralization site is not listed in the TARGET_COMMODITY field, then it is not possible to allocate the relevant SITE_TYPE_DESCRIPTION without further investigation of the source data. In these instances, the site remains unclassified with respect to SITE_TYPE_DESCRIPTION. The distribution of known zinc sites in the Far East Yilgarn correlate with the mapped location of greenstone belts, shear zones and faults.

Table 1. Legend description

Site type	Definition
Zn Mine	A deposit which is being mined, was previously mined, or is proposed to be mined
Zn Deposit	A mineral occurrence with probable economic value and for which there is an established resource
Zn Prospect	Any mineral occurrence where economic grades have been intersected over a significant width and strike length but for which there is not yet a resource, or any working or exploration activity that has found subeconomic mineral occurrences and from which there is no recorded production
Zn Occurrence	An occurrence (excluding those defined as mines, deposits or prospects) can be defined if an economic mineral has been identified in outcrop, or if assay results exceed an agreed concentration and size
Zn Unclassified	Mineralization site for which the TARGET_COMMODITY_GROUP does not reflect the specified commodity, and hence the SITE_TYPE_DESCRIPTION is not applicable

How to access

These data form part of the Far East Yilgarn, 2021 Geological Exploration Package, available via the DMIRS eBookshop.

Recommended reference

Guilliamse, JN, Duuring, P and Morin-Ka, S 2021, MINEDEX observations of zinc sites in the Far East Yilgarn: Geological Survey of Western Australia, digital data layers.

Far East Yilgarn Moho, 2021

by

RE Murdie and H Yuan[1,2]

Abstract

The Far East Yilgarn Moho, 2021 digital data layer is a depth contour map of the Mohorovičíć (Moho) discontinuity between the crust and mantle as determined from seismological methods (Fig. 1). The map is based on the AuSREM model (Salmon et al., 2012) at half degree-gridded intervals with additional data from the Yilgarn Craton – Officer Basin – Musgrave Province (Neumann, 2013) and the northeastern Yilgarn deep crustal seismic reflection lines (Goleby et al., 2003). Receiver function data is from passive seismic deployments (Reading et al., 2003).

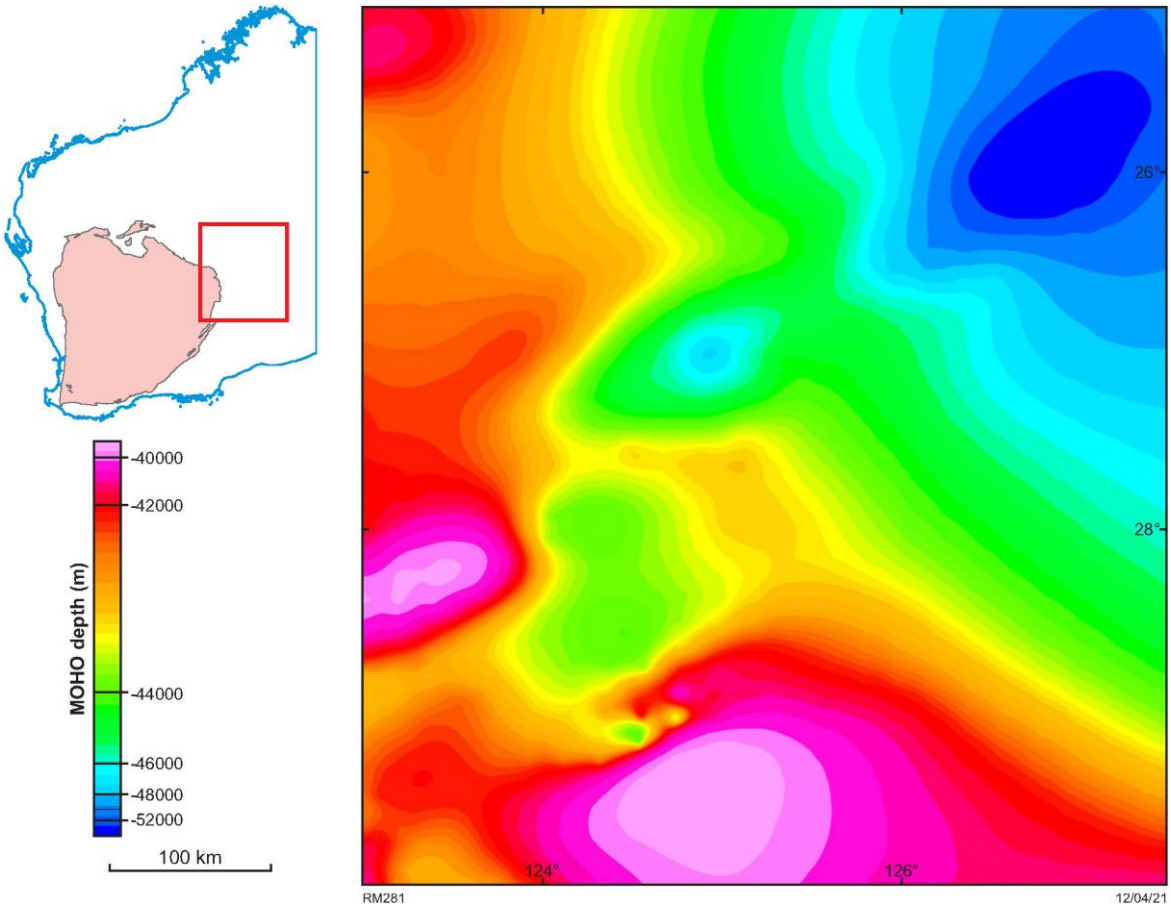

Figure 1. Far East Yilgarn Moho, 2021 digital data layer

How to access

The Far East Yilgarn Moho, 2021 digital data layer is available on a USB via the DMIRS eBookshop.

1 ARC Centre of Excellence for Core to Crust Fluid Systems, Macquarie University, Balaclava Road, North Ryde NSW 2019
2 Centre of Exploration Targeting, The University of Western Australia, Stirling Highway, Crawley WA 6009

References

Goleby, BR, Blewett, RS, Groenewald, PB, Cassidy, KF, Champion, DC, Jones, LEA, Korsch, RJ, Shevchenko, S and Apak, SN 2003, The 2001 northeastern Yilgarn deep seismic reflection survey: Geoscience Australia, Record 2003/28, 144p.

Neumann, NL (editor) 2013, Yilgarn Craton – Officer Basin – Musgrave Province seismic and MT workshop: Geoscience Australia, Record 2013/28, 210p.

Reading, AM, Kennett, BLN and Dentith, MC 2003, Seismic structure of the Yilgarn Craton, Western Australia: Australian Journal of Earth Sciences, v. 50, no. 3, p. 427–438, doi:10.1046/j.1440-0952.2003.01000.x.

Salmon, M, Kennett, BLN and Saygin, E 2012, Australian Seismological Reference Model (AuSREM): Crustal component: Geophysical Journal International, v. 192, p. 190–206.

Recommended reference

Murdie, RE and Yuan, H 2021, East Yilgarn Moho, 2021: Geological Survey of Western Australia, digital data layer.

Interpreted bedrock geology of the Far East Yilgarn

by

C Phillips, P Haines, DMcB Martin and H Howard

Abstract

The interpreted basement geology of the Far East Yilgarn is a data package consisting of 10 new geology layers that together show the geology of the project area in a novel way as a series of thematic layers at the 1:250 000 scale. These layers are arranged so as to extend the known outcrop geology under younger basin cover to produce a quasi-3D rendering of the geology. This approach follows that which has previously been used for the Geological Survey of Western Australia (GSWA) State tectonic units layers since 2015, and accounts for differing bedrock geology of interest for users of the map.

The bulk of the Archean and Proterozoic crystalline basement interpretation is derived from published GSWA Geological Information Series packages, including West Musgrave 2019 (GSWA, 2019), East Albany–Fraser Orogen (GSWA, 2020a) and East Yilgarn 2020 (GSWA, 2020b). For the purpose of this compilation, the Precambrian component of these earlier interpretations has been extended under the shallow cover of the Paleoproterozoic and younger basins, where possible, using drillhole data and interpretation of field data. Largely undivided granites and greenstones of the Burtville and Yamarna Terranes of the Eastern Goldfields Superterrane have been extended beneath the Grant Group of the Canning Basin to the concealed margins of the Earaheedy Basin and Officer Basin Phase 1 in the southwest of the project area. In order to conform to the internal logic and layered approach of this map product, the available interpretation of the Albany–Fraser Orogen (GSWA, 2020a) beneath younger basins has been clipped to the margin of the Officer Basin Phase 1.

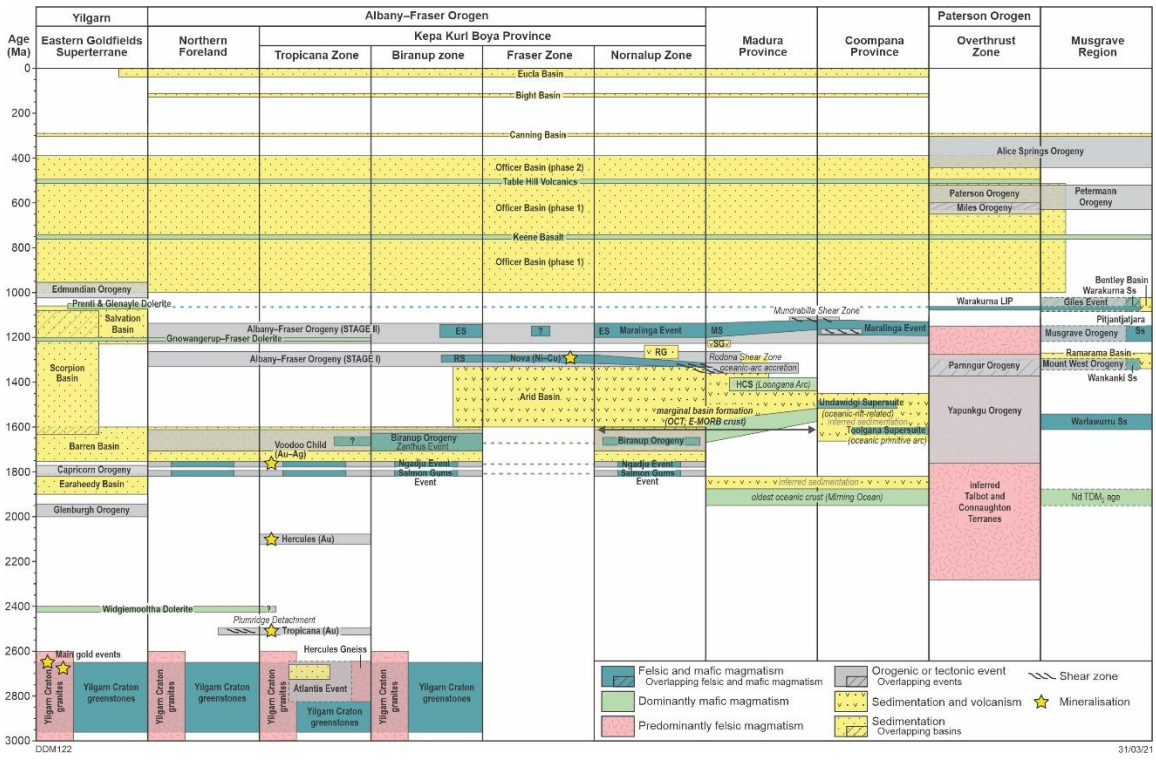

Figure 1. Time–space plot summarizing the geology covering the Far East Yilgarn Accelerated Geoscience Program. The plot represents a rough transect through the project area from southwest (Yilgarn Craton) to northeast (Musgrave Province). Modified after Spaggiari et al. (2020). Abbreviations: ES, Esperance Supersuite; LIP, Large Igneous Province; MS, Moodini Supersuite; RS, Recherche Supersuite; Ss, Supersuite

The Musgrave region within the project area is dominated by the Mesoproterozoic volcano-sedimentary units of the Bentley Supergroup and igneous rocks of the Warakurna Supersuite that were all generated during the 1085–1030 Ma Giles Event. At the southern margin of the Musgrave region, the Bentley Supergroup dips moderately (30°) to the southwest on TALBOT 1:250 000 and extends to the south beneath the Grant Group cover to the edge of the Officer Basin Phase 1. The exposed rock units have been extended under Grant Group cover to the margins of Officer Basin Phase 1. Previous structural interpretations have been preserved and extended under younger cover, and the mapped extent of the numerous dolerite dyke suites has also been extended under cover.

Proterozoic and Phanerozoic basins overlying Yilgarn, Musgrave and Albany–Fraser crystalline basement geology have been divided into seven lithostratigraphic layers. The stratigraphy discussed below is presented in the time–space plot on Figure 1. These lithostratigraphic layers include:

- Eucla Basin (c. 48 Ma to Pliocene and younger)
- Bight Basin (175–66 Ma)
- Canning Basin (c. 488 Ma to Late Cretaceous)
- Officer Basin Phase 2 (510–359 Ma)
- Officer Basin Phase 1 (1000–510 Ma)
- Salvation Basin (1338–1066 Ma)
- Earaheedy Basin (1990–1648 Ma)
- Basement geology (>1990 Ma)

The interpreted bedrock geology of the Far East Yilgarn data package was compiled using numerous datasets that allow the interpretation of mapped geological units under cover. These layers have been compiled using data from petroleum well logs (WAPIMS), mineral drillhole (WAMEX), geological field observations (WAROX), detrital zircon geochronology, existing 1:250 000-scale geological mapping (GSWA), gravity imagery, magnetic imagery (including upward continued magnetic imagery), Landsat imagery and radiometric imagery. This package presents interpretations from these data in a new format, with individual time slices presenting and extending basin boundaries. Each layer can be viewed separately or interlayered with other datasets. The sections below present a brief rationale on how each of the basin layers were drawn and the constraints on their extent. Geological field observations are useful for interpreting the subsurface in areas adjacent to the observation point but drillhole data becomes a more diagnostic tool in areas of relatively shallow cover. However, drillholes are less abundant away from exposed basement due to increasing basin thickness. In areas of thickest sedimentary basin cover, petroleum well log data and geophysical imagery are the paramount interpretive tool.

Earaheedy Basin

The Earaheedy Basin (Bunting, 1986; Jones et al., 2000; Pirajno et al., 2004; Sheppard et al., 2016) has an exposed area of 35 300 km^2 from the eastern end of the Capricorn Orogen (Myers et al., 1996; Tyler et al., 1998; Cawood and Tyler, 2004; Sheppard et al., 2016) along the northeast margin of the Yilgarn Craton. The basin contains the dominantly siliciclastic Tooloo and Miningarra Groups separated by the Frere Formation, deposited in a coastal to outer shelf setting interpreted by Jones et al. (2000) and Pirajno et al. (2004) as a passive continental margin.

In the Far East Yilgarn project area, the Earaheedy Basin is exposed along the western border on ROBERT and THROSSELL 1:250 000 map sheets and consists of the Tooloo Group (Yelma Formation only), unconformably overlain by the Frere Formation which in turn is unconformably overlain by the Miningarra Group (Chiall Formation, Wongawol Formation, Kulele Limestone, and Mulgarra Sandstone). The age of the Tooloo Group is constrained by the 1990 ± 6 Ma Imbin Porphyry (Nelson, 2001) interpreted by Sheppard et al. (2016) to be contemporaneous with the lower Yelma Formation.

The minimum age of the Earaheedy Basin is poorly constrained using an Ar–Ar date of 1648 ± 12 Ma (Pirajno et al., 2009) from metamorphic muscovite in the Tooloo Group. The actual minimum age is probably much older than c. 1648 Ma with Sheppard et al. (2016) and Occhipinti et al. (2017) suggesting a cessation of sedimentation across the southern Capricorn Orogen with onset of the intracratonic 1820–1770 Ma Capricorn Orogeny.

The Prenti Dolerite (Warakurna Supersuite) intruded the Earaheedy Basin at c. 1066 Ma (Wingate, 2003). These voluminous mafic intrusions are visible in outcrop on KINGSTON and ROBERT 1:250 000 map sheets continuing under the Canning and Officer Basins (interpreted from magnetic imagery), thus extending the Earaheedy Basin to the east. These geophysical extrapolations are consistent with the recovery of Earaheedy-like sedimentary rocks from drillholes EGD001 and EDG002 on southeast ROBERT 1:250 000 map sheet where sedimentary rocks are intercalated with dolerite sills above the interpreted Archean basement (Baxter, 2011). MRG Metals recovered strongly magnetic mafic extrusive and volcaniclastic rocks from drillhole EY4001 on eastern ROBERT 1:250 000 map sheet which they postulated to be Table Hills Volcanics of the Officer Basin Phase 2 (Weston and Eggo, 2015). However, stromatolitic carbonates under the basalt-bearing interval are consistent with Earaheedy-like lithologies recovered from EGD001 and EDG002 to the west (Baxter, 2011). The succession above the basalt (probably unconformable), is consistent with Browne Formation lithofacies in the Officer Basin. Thus, the basalt is probably pre-Officer, here reassigned to the Prenti Dolerite.

The Earaheedy Basin is commonly unconformable or in fault contact with the overlying Salvation Basin on STANLEY 1:250 000 map sheet to the immediate northwest of the project area. On STANLEY 1:250 000 map sheet, roughly northwest-trending structures place the Salvation Basin in thrust-contact with the Earaheedy Basin. Similar northwest-trending structures can be traced under the Canning and Officer Basins to the southeast into HERBERT and ROBERT 1:250 000 map sheets. These concealed structures are used to constrain the eastern extent of the Earaheedy Basin.

The southern extent of the Earaheedy Basin is largely unknown but there is evidence from outcropping geology and detrital zircon geochronology (discussed later) of a sub-basin between the present-day exposures of the Yilgarn Craton and Albany–Fraser Orogen. A pronounced gravity and magnetic ridge straddling the border of the THROSSELL and WESTWOOD 1:250 000 map sheets suggests the two sub-basins are not joined. This gravity and magnetic ridge is interpreted to represent the Yilgarn Craton under a shallow cover of sedimentary rocks, principally the Canning Basin.

Outcropping units of the Turkey Hill Formation on northeast RANSON 1:250 000 map sheet are reinterpreted. Jackson and van den Graaff (1981) described the Turkey Hill Formation on RASON 1:250 000 map sheet as an unmetamorphosed unit of mudstone and fine-grained sandstone, locally dipping up to 65°, unconformable on granitic (Yilgarn) basement and unconformably overlain by Canning Basin glacial units. This description led Grey et al. (2005) to interpret the unit as probably Neoproterozoic/Officer Basin Phase 1 and an assumed correlative of the Lupton Formation. This package has reassessed the Turkey Hill Formation based on the deformation and steep dips being inconsistent with Officer Basin stratigraphy elsewhere except on the Rudall, Musgrave or Pilbara margins or proximate to diapirs but is consistent with the bottom-of-hole succession in petroleum wells NJD-1 and MI-1. The unconformable contact with Yilgarn basement rocks also suggests a Pre-Officer Basin unit. Consequently, the Turkey Hills Formation is tentatively assigned to the Earaheedy Basin.

Elkington (1988) describes lithologies recovered from the bottom of MI-1 (drilled by Osino on northeast MINIGWAL 1:250 000 map sheet) as steeply dipping (45° to 70°) graphitic and locally pyritic, brecciated shale and minor sandstone consistent with lithofacies in the Turkey Hill Formation (named Turkey Hills Beds by Elkington). These steeply dipping units are here interpreted as pre-Officer Basin, tentatively assigned to the Earaheedy Basin. Consequently, the southern Earaheedy Basin sub-basin is drawn from the Turkey Hill Formation units on RANSON 1:250 000 map sheet to drillhole MI-1 on MINIGWAL 1:250 000 map sheet, infilling a gravity low indicative of thick sedimentary

cover. The eastern extent of the Earaheedy Basin is defined by the Gunbarrel Fault along the western edge of the Albany–Fraser Orogen.

Salvation Basin

The Mesoproterozoic (1338–1066 Ma) Salvation Basin is limited to the Salvation Group (Coonabildie Formation and Brassey Range Formation) and the Oldham Sandstone in the northwest of the project area. The minimum age of the Salvation Basin is provided by the Glenayle Dolerite (Warakurna Supersuite) which intruded the basin at 1066 ± 14 Ma (Wingate, 2003).

The Glenayle Dolerite extensively intrudes the Salvation Group to the immediate west of the project area on STANLEY and TRAINOR 1:250 000 map sheets. Using magnetic imagery, the west-northwesterly trending corridor of outcropping mafic intrusions on STANLEY 1:250 000 map sheet can be extended eastwards into the project area beneath cover of the Canning and underlying Officer Basins. These interpreted units of Glenayle Dolerite are here used to likewise extrapolate the Salvation Group (Coonabildie Formation and Brassey Range Formation) eastwards under the Canning and Officer Basins.

The extent of the Salvation Basin under cover is constrained by detrital zircon geochronology from stratigraphic wells GSWA Lancer 1 and GSWA Empress 1A and Western Mining Corporation drillhole NJD-1. A quartz sandstone (GSWA 181873) sampled from beneath the Officer Basin in Lancer 1 yielded a weighted mean $^{207}Pb^*/^{206}Pb^*$ detrital zircon date of 1305 ± 14 Ma, interpreted as a maximum depositional age (Wingate and Bodorkos, 2007) and consistent with the age of the Salvation Basin. Pre-Officer Basin units in Empress 1A were recovered from 1540.2 to 1624.6 m (TD) and consist of siltstone, sandstone, minor conglomerate and basalt (Stevens and Apak, 1999). A K–Ar age of 1058 ± 13 Ma was obtained from the basalt at the base of this well (Stevens and Apak, 1999), indicating it most likely belongs to the 1085–1031 Ma Warakurna Supersuite of the Musgrave region (Edgoose et al., 2004; Wingate et al., 2017). Two sandstone samples from the pre-Officer Basin succession yielded $^{207}Pb^*/^{206}Pb^*$ detrital zircon dates of c. 1310 (GA 2152079) and c 1315 Ma (GA 2152080), interpreted as maximum depositional ages (Korsch et al., 2013) consistent with their inclusion into the Salvation Basin.

Heterolithic siltstone–sandstone rocks under the Officer Basin Phase 1 at the base of NJD-1 have been correlated with numerous Mesoproterozoic units such as the Collier, Edmund, Scorpion and Salvation Groups (Hocking, 2002). A sandstone sample (GA 2152078) from an assumed Mesoproterozoic unit at the bottom of NJD-1 yielded a $^{207}Pb^*/^{206}Pb^*$ detrital zircon date of c. 1310 Ma, interpreted as a maximum depositional age (Korsch et al., 2013). Based on the consistency of age and lithology, these pre-Officer units have been tentatively assigned to the Salvation Basin and therefore the Mesoproterozoic units at the base NJD-1 mark the southern extent of the Salvation Basin. The eastern extent of the Salvation Basin is defined by the major crustal boundary between the Yilgarn Craton and Rudall Province.

Officer Basin Phase 1

Phase 1 of the Officer Basin (Centralian Superbasin) is defined as a Neoproterozoic to early Cambrian succession of mixed siliciclastic and carbonate sedimentary units deposited from 1000–510 Ma (Grey et al., 2005). In the project area, Phase 1 is dominated by the Buldya Group which primarily comprises siltstone, mudstone, sandstone, dolomite and halite. The Buldya Group is divided into a lower Buldya Group (Townsend Quartzite overlain by the Lefroy Formation and Browne Formation) and an upper Buldya Group (Hussar Formation overlain by the Kanpa Formation which is overlain by the Steptoe Formation) (Grey et al., 2005). Petroleum well GSWA Lancer 1 intersects the Keene Basalt, a highly magnetic unit, erupted during deposition of the Kanpa Formation in the upper Buldya Group (Hocking, 2002; Haines et al., 2004; Pirajno et al., 2006). The Keene Basalt has been dated at 752 ± 4 Ma (Ar–Ar pyroxene) and 753 ± 1 Ma (Ar–Ar plagioclase) by Zi et al. (2019).

Around the southern margin of the Musgrave Province on BENTLEY and TALBOT 1:250 000 map sheets, the lower Buldya Group, including the Townsend Quartzite and overlying succession is exposed with post-Buldya Group units restricted to the Lupton Formation (GSWA, 2019). Undercover, drillhole data recognize post-Buldya Group units including the Wahlgu Formation (Cryogenian) and Lungkarta Formation (Ediacaran to Early Cambrian).

Magnetic imagery defines a semicontinuous magnetic unit here interpreted as Keene Basalt which has been confidently mapped throughout the extent of the Officer Basin Phase 1. Using magnetic characteristics to identify the Keene Basalt at depth allows the interpretation of the Officer Basin Phase 1 close to the margin of the exposed Yilgarn Craton. As stated above, the reassignment of the Turkey Hill Formation to be tentatively included in the Earaheedy Basin has constrained the Officer Basin to the east of locally steeply dipping, unmetamorphosed mudstone and fine-grained sandstone, on northeast RASON 1:250 000 map sheet. On this data package, Officer Basin Phase 1 is mapped under Officer Basin Phase 2 as generic Buldya Group; however, petroleum well log and seismic data allows for subdivision and interpretation of formations at depth (Simeonova and Iasky, 2005).

Officer Basin Phase 2

The 510–359 Ma Officer Basin Phase 2 is a Paleozoic volcano-sedimentary succession which overlies the Officer Basin Phase 1. In the project area, Phase 2 consists of three outcropping units: the basal Table Hill Volcanics overlain by the shallow-marine to eolian Lennis and Wanna Formations (GSWA, 2019). The 508–505 Ma Table Hill Volcanics consists of widespread flood basalts with lesser volcaniclastic and siliciclastic units (Jackson and van de Graaff, 1981; Stevens and Apak, 1999) which form the southern part of the Kalkarindji Large Igneous Province (Glass and Phillips, 2006). The formation has been dated at 509 ± 2.6 Ma in the project area (Jourdan et al., 2014).

The Table Hill Volcanics are exposed south of the Musgrave Province on central TALBOT 1:250 000 map sheet and locally on the western edge of the extent of Phase 2 on the boundary of ROBERT and YOWALGA 1:250 000 map sheets. The unit is highly magnetic so despite its limited outcrop, the Table Hill Volcanics can be interpreted along strike and under cover. The convolute pattern at the southern margin of the Officer Basin Phase 2 is defined by flows of Table Hills Volcanics interpreted to infill troughs between longitudinal eolian dunes developed within the underlying Lungkarta Formation (Mory, 2017). This bold magnetic texture can be interpreted northeast of the Albany–Fraser Orogen on WESTWOOD, NEALE and VERNON 1:250 000 map sheets but becomes more diffuse under thicker cover to the northwest and east.

Canning Basin

The Canning Basin is an extensive Phanerozoic basin deposited from the Early Ordovician to Late Cretaceous (onshore) covering a total area of about 595 000 km^2. In the project area, the Canning Basin consists of the Late Carboniferous to Early Permian Grant Group overlain by the Lower Cretaceous Samuel Formation and Bejah Claystone. The extent of the Canning Basin units is well constrained by outcrop data and can be mapped using remotely sensed surface data including Landsat and Radiometric imagery. Most of the geology in this layer has been extracted from the 1:500 000 State Geology layer with very few alterations except for some added detail on the extent of the Samuel Formation and Bejah Claystone under thin regolith.

Bight Basin

The Bight Basin is a Late Cretaceous sedimentary succession which in the project area is exclusively populated by carbonaceous sandstone, siltstone, claystone and shale of the 129.4–113 Ma Madura Formation. The geology of the Bight Basin has been extracted from the existing 1:500 000 State Geology layer and covers the southeast corner of the project area adjacent to the exposed Albany–Fraser Orogen. The basin covers the Canning and Officer Basins. No interpretations were made to the existing data for the Bight Basin and the Madura Formation for this data package.

Eucla Basin

The Eucla Basin is the youngest exposed unit in the project area, which on this data package includes bioclastic limestones of the 28–14 Ma Eucla Group (Li et al., 1996; McGowran et al., 1997; O'Connell, 2011). Units labelled as GE-xk-s-WA on the 1:500 000 Cenozoic Geology layer consist of Eocene marine limestone and lesser sandstone as well as lignite and spongolite. Hou et al. (2011) suggested these features represent a strand line from a c. 38 and 36 Ma coastline adjacent to marine deposition in the Eucla Basin. This package considers these units to be coeval with deposition in the Eucla Basin, and are therefore included in this layer.

How to access

The Interpreted Bedrock Geology of the Far East Yilgarn data layer is part of the Far East Yilgarn, 2021 Geological Exploration Package, available on a USB via the DMIRS eBookshop.

References

Baxter, C 2011, Annual Report for EL38/2205 Calanchini Hills for the Period 13 May 2010 to 12 May 2011: Greatland Pty Ltd: Geological Survey of Western Australia, Statutory mineral exploration report A090664, 39p. (Open file).

Bunting, JA 1986, Geology of the eastern part of the Nabberu Basin, Western Australia: Geological Survey of Western Australia, Bulletin 131, 130p.

Cawood, PA and Tyler, IM 2004, Assembling and reactivating the Proterozoic Capricorn Orogen: Lithotectonic elements, orogenies, and significance: Precambrian Research, v. 128, p. 201–218.

Edgoose, CJ, Scrimgeour, IR and Close, DF 2004, Geology of the Musgrave Block, Northern Territory: Northern Territory Geological Survey, Report 15, 46p.

Elkington, CR 1988, Meinya Gravity Prospect Final Report: Osino Pty Ltd: Geological Survey of Western Australia, Statutory mineral exploration report A022769, 41p. (Open File).

Geological Survey of Western Australia 2019, West Musgrave, 2019: Geological Society of Western Australia, Geological Information Series.

Geological Survey of Western Australia 2020a, East Albany–Fraser Orogen, 2020: Geological Society of Western Australia, Geological Information Series.

Geological Survey of Western Australia 2020b, East Yilgarn, 2020: Geological Society of Western Australia, Geological Information Series.

Glass, LM and Phillips, D 2006, The Kalkarindji continental flood basalt province: A new Cambrian large igneous province in Australia with possible links to faunal extinctions: Geology, v. 34, no. 6, p. 461–464, doi:10.1130/G22122.1.

Grey, K, Hocking, RM, Stevens, MK, Bagas, L, Carlsen, GM, Irimies, F, Pirajno, F, Haines, PW and Apak, SN 2005, Lithostratigraphic nomenclature of the Officer Basin and correlative parts of the Paterson Orogen, Western Australia: Geological Survey of Western Australia, Report 93, 89p.

Haines, PW, Mory, AJ, Stevens, MK and Ghori, KAR 2004, GSWA Lancer 1 well completion report (basic data), Officer and Gunbarrel Basins, Western Australia: Geological Survey of Western Australia, Record 2004/10, 39p.

Hocking, RM 2002, Drillhole WMC NJD1, Western Officer Basin, Western Australia: Stratigraphy and petroleum geology: Geological Survey of Western Australia, Record 2002/18, 26p.

Hou, B, Keeling, J, Reid, A, Fairclough, MC, Warland, I, Belousova, E, Frakes, LA and Hocking, R 2011, Heavy mineral sands in the Eucla Basin, South Australia: Deposition and province-scale prospectivity: Economic Geology, v. 106, p. 687–712.

Jackson, MJ and van de Graaff, WJE 1981, Geology of the Officer Basin, Western Australia: Bureau of Mineral Resources, Geology and Geophysics, Bulletin 206, 102p.

Jones, JA, Pirajno, F and Hocking, RM 2000, Stratigraphy, tectonic evolution, and mineral potential of the Earaheedy Basin, in GSWA 2000 extended abstracts: geological data for WA explorers in the new millennium compiled by Geological Survey of Western Australia: Geological Survey of Western Australia, Record 2000/8, p. 11–13.

Jourdan, F, Hodges, K, Sell, B, Schaltegger, U, Wingate, MTD, Evins, LZ, Söderlund, U, Haines, PW, Phillips, D and Blenkinsop, T 2014, High-precision dating of the Kalkarindji large igneous province, Australia, and synchrony with the Early-Middle Cambrian (Stage 4-5) extinction: Geology, v. 42, p. 543–546, doi:10.1130/G35434.1.

Korsch, RJ, Blewett, RS, Pawley, MJ, Carr, LK, Hocking, RM, Neumann, NL, Smithies, RH, Quentin de Gromard, R, Howard, HM, Kennett, BLN, Aitken, ARA, Holzschuh, J, Duan, J, Goodwin, JA, Jones, T, Gessner, K and Gorczyk, W 2013, Geological setting and interpretation of the southwest half of deep seismic reflection line 11GA-YO1: Yamarna Terrane of the Yilgarn Craton and the western Officer Basin, *in* Yilgarn Craton – Officer Basin – Musgrave Province seismic and MT workshop *edited by* NL Neumann: Geoscience Australia, Record 2013/28, p. 24–50.

Li, Q, James, NP, Bone, Y and McGowran, B 1996, Foraminiferal biostratigraphy and depositional environments of the mid-Cenozoic Abrakurrie Limestone, Eucla Basin, southern Australia: Australian Journal of Earth Sciences, v. 43, no. 4, p. 437–450.

McGowran, B, Li, Q and Moss, G 1997, The Cenozoic neritic record in southern Australia: the biogeohistorical framework, in Cool-water carbonates edited by NP James and J Clarke: Society for Sedimentary Geology, Tulsa, Oklahoma, US, SEPM Special Publication 56, p. 185–203.

Mory, AJ 2017, A Paleozoic perspective of Western Australia: Geological Survey of Western Australia, 58p.

Myers, JS, Shaw, RD and Tyler, IM 1996, Tectonic evolution of Proterozoic Australia: Tectonics, v. 15, p. 1431–1446.

Nelson, DR 2001, 132415: quartz–feldspar porphyry, Inbim Rockhole; Geochronology Record 444: Geological Survey of Western Australia, 4p.

Occhipinti, S, Hocking, R, Lindsay, M, Aitken, A, Copp, I, Jones, J, Sheppard, S, Pirajno, F and Metelka, V 2017, Paleoproterozoic basin development on the northern Yilgarn Craton, Western Australia: Precambrian Research, v. 300, p. 121–140, doi:10.1016/j.precamres.2017.08.003.

O'Connell, LG 2011, Sedimentology of the Miocene Nullarbor Limestone; southern Australia: Geological Survey of Western Australia, Report 111, 211p.

Pirajno, F, Haines, PW and Hocking, RM 2006, Keene Basalt, northwest Officer Basin, Western Australia: tectonostratigraphic setting and implications for possible submarine mineralisation: Australian Journal of Earth Sciences, v. 53, p. 1013–1022.

Pirajno, F, Hocking, RM, Reddy, SM and Jones, JA 2009, A review of the geology and geodynamic evolution of the Palaeoproterozoic Earaheedy Basin, Western Australia: Earth-Science Reviews, v. 94, p. 39–77.

Pirajno, F, Jones, JA, Hocking, RM and Halilovic, J 2004, Geology and tectonic evolution of Palaeoproterozoic basins of the eastern Capricorn Orogen, Western Australia: Precambrian Research, v. 128, no. 3–4, p. 315–342.

Sheppard, S, Fletcher, IR, Rasmussen, B, Zi, J-W, Muhling, JR, Occhipinti, SA, Wingate, MTD and Johnson, SP 2016, A new Paleoproterozoic history of the eastern Capricorn Orogen, Western Australia, revealed by U-Pb dating of micro-tuffs: Precambrian Research, v. 286, p. 1–19, doi:10.1016/j.precamres.2016.09.026.

Simeonova, AP and Iasky, RP 2005, Seismic mapping, salt deformation, and hydrocarbon potential of the central western Officer Basin, Western Australia: Geological Survey of Western Australia, Report 98, 51p.

Spaggiari, CV, Smithies, RH, Kirkland, CL, Wingate, MTD, England, RN and Lu, Y 2020, Stratigraphic and co-funded drilling of the Eucla basement — the Proterozoic geology beneath the Nullarbor Plain: Geological Survey of Western Australia, Report 204, 147p.

Stevens, MK and Apak, SN (compilers) 1999, GSWA Empress 1 and 1A well completion report, Yowalga Sub-basin, Officer Basin, Western Australia: Geological Survey of Western Australia, Record 1999/4, 110p.

Tyler, IM, Pirajno, F, Bagas, L, Myers, JS and Preston, WA 1998, The geology and mineral deposits of the Proterozoic in Western Australia: AGSO Journal of Australian Geology & Geophysics, v. 17, p. 223–244.

Weston, K and Eggo, A 2015, Final Report for the Government Co-Funded Drilling Application DAG2014/00296174: East Yilgarn Project EL38/2553 & E38/2773: MRG Metals (Exploration) Pty Ltd: Geological Survey of Western Australia, Statutory mineral exploration report A105254, 18p. (Open File).

Wingate, MTD 2003, Age and palaeomagnetism of dolerite intrusions of the southeast Collier Basin and the Earaheedy and Yerrida Basins, Western Australia: Geological Survey of Western Australia, Record 2003/3, 34p.

Wingate, MTD and Bodorkos, S 2007, 181873: quartz sandstone, Lancer 1; Geochronology Record 685: Geological Survey of Western Australia, 6p.

Wingate, MTD, Lu, Y, Quentin de Gromard, R and Howard, HM 2017, 208486: migmatitic metasyenogranite, south of Mount Deering; Geochronology Record 1438: Geological Survey of Western Australia, 5p.

Zi, J-W, Haines, PW, Wang, X-C, Jourdan, F, Rasmussen, B, Halverson, GP, Sheppard, S and Li, C-F 2019, Pyroxene 40Ar/39Ar dating of basalt and applications to large igneous provinces and Precambrian stratigraphic correlations: Journal of Geophysical Research: Solid Earth, v. 124, 18p., doi:10.1029/2019JB017713.

Recommended reference

Phillips, C, Haines, P, Martin, D McB and Howard, H 2021, Interpreted Bedrock Geology of the Far East Yilgarn: Geological Survey of Western Australia, digital data layer.

Distribution in the Far East Yilgarn of greenstone lithologies sampled for geochemistry

by

RH Smithies and JR Lowrey

Abstract

This layer shows the location in the Far East Yilgarn where samples have been taken for whole rock major and trace element geochemistry since 2018. The accompanying geochemical dataset has been collated from WACHEM and includes samples from diamond drillcore co-funded through the Exploration Incentive Scheme (EIS), samples from company diamond drillcore and outcrop samples recently extracted from the Geological Survey of Western Australia (GSWA) rock archive.

How to access

The Far East Yilgarn greenstone geochemistry digital data are available on a USB via the DMIRS eBookshop and as a free download from the Data and Software Centre.

Recommended reference

Smithies, RH and Lowrey, JR 2021, Distribution in the Far East Yilgarn of greenstone lithologies sampled for geochemistry: Geological Survey of Western Australia, digital data layer, <www.dmirs.wa.gov.au/geoview>.

Far East Yilgarn depth of weathering

original data by

J Wilford, R Searle, M Thomas and M Grundy

Abstract

These data are extracted from the CSIRO national depth of weathering product for the area of interest encompassing the Far East Yilgarn, 2021 Geological Exploration Package. There are three layers that comprise this dataset:

- FEY_min_weathering_depth is the minimum weathering depth from the original ensemble and represents the 5th percentile of the ensemble of estimated depths
- FEY_median_weathering_depth represents the median, or 50th percentile, from the original ensemble
- FEY_max_weathering_depth represents the 95th percentile from the original ensemble.

Generally, these layers should be utlized together to provide both an average and measure of uncertainty of the depth estimates on the thickness of weathered material and should only be used as a guide as to the likely thickness of regolith within the Far East Yilgarn region of interest.

These layers are rendered in three different colour palettes to distinguish between the data and to better represent the differences in data range for each dataset.

Layer	Colour range	Minimum value	Maximum value	Colour ramp
FEY_min_weathering_depth	Bright yellow through green to dark blue	0 m	0.5 m	
FEY_median_weathering_depth	Light green to dark green	0 m	100 m	
FEY_max_weathering_depth	Light brown to dark brown	0 m	200 m	

How to access

These data form part of the Far East Yilgarn, 2021 Geological Exploration Package, which is available via the DMIRS eBookshop.

Recommended reference (to original data)

Wilford, J, Searle, R, Thomas, M, and Grundy, M 2015, Soil and Landscape Grid National Soil Attribute Maps - Depth of Regolith (3" resolution) Release 2 v6: CSIRO, Data Collection, https://doi.org/10.4225/08/55C9472F05295.

Recommended reference (to this abstract)

Wilford, J, Searle, R, Thomas, M, and Grundy, M 2021, Far East Yilgarn depth of weathering: Geological Survey of Western Australia, digital data layers.

AGP Accelerated Geoscience Program

Data integration and analyses — the Yilgarn Craton

Southwest Yilgarn

Southwest Yilgarn, 2021 Geological Exploration Package

project managed by

RH Smithies and HM Howard

Abstract

The Geological Survey of Western Australia (GSWA) reprioritized its 2020–21 work program because of the impact of travel and operational restrictions imposed by the COVID-19 pandemic. By using GSWA's extensive, pre-competitive geoscience datasets and outstanding rock and paleontology collection, the organization's aim was to aid economic recovery and stimulate the exploration industry. GSWA's objective was to deliver new interpretive datasets across all areas of geoscience in key regions of the State to accelerate understanding of the region's geology and mineral prospectivity.

A key area where data integration and analyses can assist in an increased understanding of geology and mineral prospectivity is the Yilgarn Craton. The Yilgarn Craton is one of Western Australia's most prospective regions and contains significant deposits of gold, nickel, lithium, copper, zinc, iron ore, tantalum, aluminium and uranium. Recent high-grade gold and nickel discoveries in the craton's far eastern (Gruyere, Tropicana, Neale) and southwestern margins (Julimar), have shown that these two poorly exposed and geologically not well-understood regions are likely to be as prospective as the craton's interior (i.e. Eastern Goldfields). Despite both regions being covered by a thick blanket of regolith, GSWA holds a vast amount of geoscientific data relating to the bedrock and regolith geology with the potential for uncovering significant, new mineral deposits.

The minerals industry is increasingly aware that the next generation of Tier 1 deposits is likely to be under deep cover. Working to the UNCOVER plan, the aim of the Accelerated Geoscience program has been to deliver new integrated geoscience datasets for the southwestern and far eastern Yilgarn Craton margins. The program has incorporated results of ongoing work in the Eastern Goldfields and has performed new analyses on archived samples, which will accelerate understanding of these regions and will define new areas of high mineral prospectivity.

The southwest Yilgarn, 2021 Geological Exploration Package is a compilation of data for use by those interested in understanding this portion of the Yilgarn Craton. A number of existing GSWA products are included, and some extracts from new products within the region of interest are also provided. Abstracts are incorporated into this product for individual layers or groups of thematically similar layers (such as geophysical imagery).

How to access

The Southwest Yilgarn, 2021 Geological Exploration Package is available via the DMIRS eBookshop.

Recommended reference

Smithies, RH and Howard, HM 2021, Southwest Yilgarn, 2021 Geological Exploration Package: Geological Survey of Western Australia, digital data package.

Peak ground acceleration map for the southwest Yilgarn

original data by

TI Allen

Abstract

The Peak ground acceleration (PGA) map for the southwest Yilgarn has been extracted from the National Seismic Hazard Assessment map 2018 (NHSA18).

The NSHA18 hazard map shows the horizontal PGA (expressed as a proportion of the gravitational acceleration, g) for a 10% probability that is, it exceeded in 50 years, equivalent to 1 in 475 probability of exceedance in a given year. This assumes a substrate of soil of Standards Australia AS1170.4 Soil Class Be which has a shear wave velocity of 760 m/s in the uppermost 30 m of the crust. The data is gridded at 15 km spacing (Fig. 1).

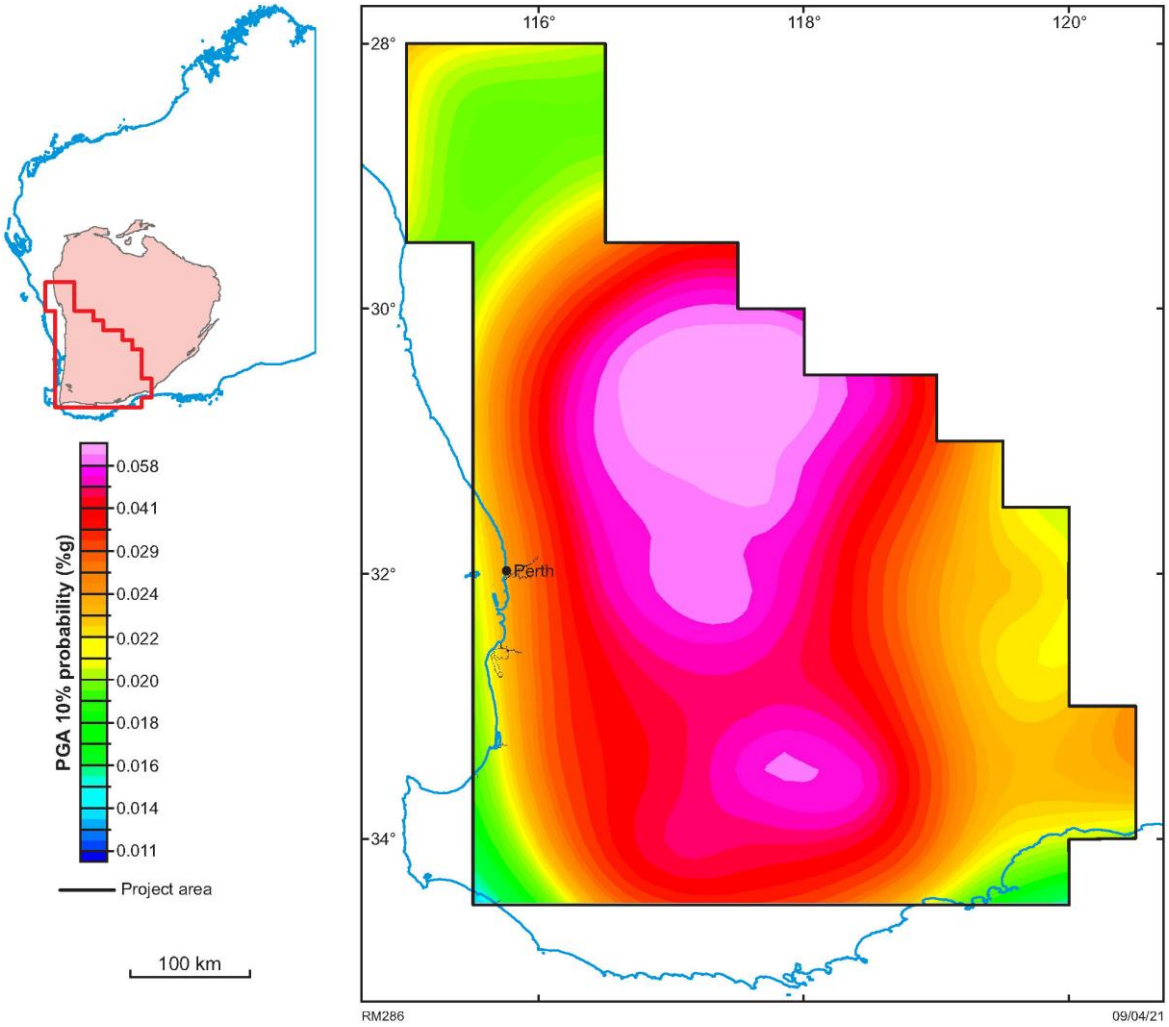

Figure 1. The Peak ground acceleration (PGA) map for the southwest Yilgarn

How to access

The Peak ground acceleration map, southwest Yilgarn digital data are available on a USB via the DMIRS eBookshop.

Recommended reference (to original data)

Allen, TI 2018, The 2018 National Seismic Hazard Assessment for Australia: Data package, maps and grid values, Geoscience Australia, Record 2018/33, doi:10.11636.

Recommended reference (to this abstract)

Allen, TI 2021, Peak ground acceleration map for the southwest Yilgarn: Geological Survey of Western Australia, digital data layer.

Multi-scale edges for the southwest Yilgarn from gravity and magnetics

by

JW Brett

Abstract

Multi-scale edges have been generated from Bouguer gravity and Reduced-to-Pole magnetic data.

The Intrepid v5.6.3 Multi-scale edge detection module uses potential field geophysical data to provide a starting point for an interpretation of structural geology. Detection of multi-scale edges proceeds by finding local maxima points of the total horizontal derivative for many upward continuations of data. Neighbouring points are then joined together to create strings (also referred to as 'worms') that define the edges of features.

Upward continuation levels used are as follows:

gravity (15 levels): 0.8, 1, 1.5, 2.1, 3, 4.2, 6, 8, 12, 16, 22, 32, 44, 62, 85 km

magnetics (13 levels): 0.8, 1, 1.5, 2.1, 3, 4.2, 6, 8, 12, 16, 22, 32, 44 km

The gravity data used to generate the multi-scale edges is the Gravity anomaly grid (400 m) of Western Australia (Brett, 2020a). The magnetic data used to generate the multi-scale edges is the Magnetic anomaly grid (80 m) of Western Australia (Brett, 2020b).

The following products have been generated:

- ArcGIS shape files of multi-scale edges from gravity and magnetic data.

How to access

The data layer is best accessed using GeoVIEW.WA. This online interactive mapping system allows data to be viewed and searched together with other datasets, including Geological Survey of Western Australia and Geoscience Australia geochronology data, geological maps and mineral exploration datasets.

References

Archibald, N, Gow, P and Boschetti, F 1999, Multi-scale edge analysis of potential field data: Exploration Geophysics, v. 30, p. 38–44, doi:10.1071/EG999038.

Brett, JW 2020a, 400 m Bouguer gravity merged grid of Western Australia 2020 – version 1: Geological Survey of Western Australia, <www.dmirs.wa.gov.au/geophysics>.

Brett, JW 2020b, 80 m magnetic merged grid of Western Australia 2020 – version 1: Geological Survey of Western Australia, <www.dmirs.wa.gov.au/geophysics>.

Recommended reference

Brett, JW 2021, Multi-scale edges for the southwest Yilgarn from gravity and magnetics: Geological Survey of Western Australia, digital data layer, <www.dmirs.wa.gov.au/geoview>.

Southwest Yilgarn 3D, 2021

by

L Brisbout

Abstract

Selected datasets from the southwest Yilgarn Accelerated Geoscience Program (AGP) have been compiled in the free 3D viewer, Geoscience ANALYST (Fig. 1). The aim of this 3D compilation is to assist with the visualization of data (map, section and 3D) and to present some of the 3D datasets produced for the southwest Yilgarn AGP.

Some of the datasets in the 3D project include:

- the geology (Geology_polygons), structure (Structure_lines) and dyke layers (Geology_lines) (Geological Survey of Western Australia [GSWA], 2021)
- extracts from the State potential field grids (GSWA, 2020a,b)
- three P-wave velocity profiles (AOB_velocity, Perth_Jubilee_velocity, Perth_Albany_velocity) (Mathur et al., 1977; Dentith et al., 2000)
- the reprocessed New Norcia seismic reflection data (New_Norcia_seismic_data_shallow)
- multi-scale edges (Gravity_worms) (Brett, 2020).

A prominent feature of the southwest Yilgarn is a large (~55 000 km^2), long-wavelength, Bouguer gravity high. The eastern edge of this anomaly has a distinct northwesterly trend that has been named the Yandanooka/Cape Riche Lineament (Everingham, 1965). To improve our understanding of the source of this gravity anomaly, 2D gravity forward modelling and 3D gravity inversions have been completed.

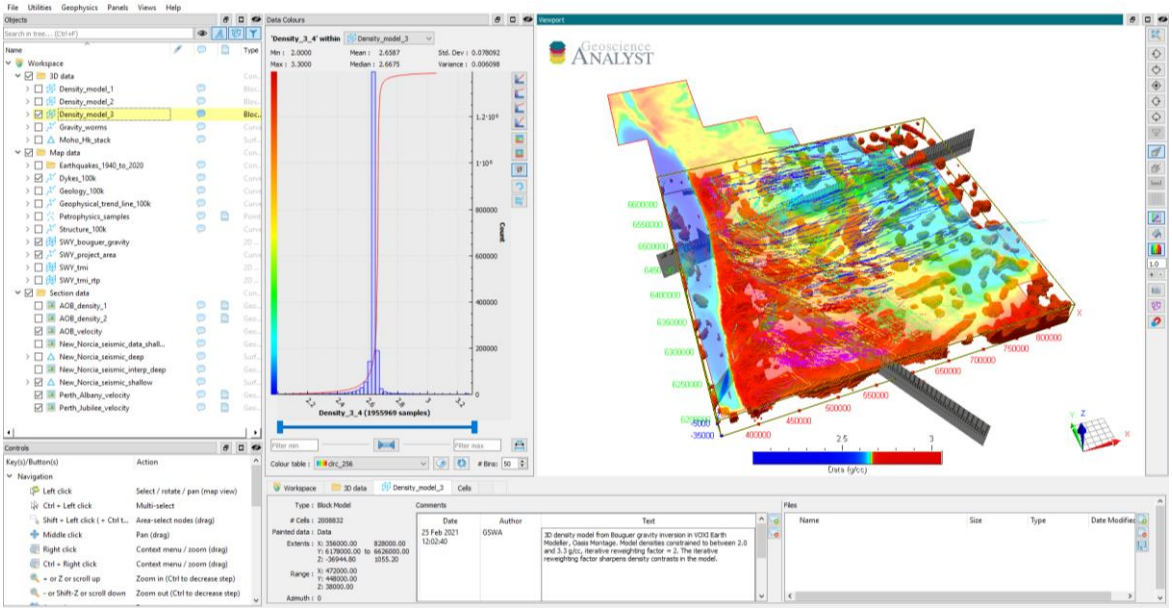

Figure 1. Typical view of the southwest Yilgarn project area in Geoscience ANALYST

Some of the density models in the 3D project include:

- the P-wave velocity model AOB of Dentith et al. (2000) has been converted to density, using the Nafe–Drake equation in Brocher (2005) (AOB_density_1)
- AOB_density_1 has been modified to fit the long wavelength gravity data, using gravity forward modelling (AOB_density _2)
- 3D density models from gravity inversion, in Geosoft's VOXI Earth Modeller (Density_model_1, Density_model_2 and Density_model_3)

How to access

The Southwest Yilgarn 3D, 2021 3D geomodel is available as a free download from the Data and Software Centre via Datasets — Statewide spatial datasets — 3D geology — Southwest Yilgarn 3D, 2021, and can be viewed using free viewer software Geoscience ANALYST available from Mira Geoscience.

References

Brett, JW 2020, Multi-scale edges for Western Australia from Bouguer gravity 2020: Geological Survey of Western Australia, <www.dmirs.wa.gov.au/geophysics>.

Brocher, TM 2005, Empirical relations between elastic wavespeeds and density in the Earth's crust: Bulletin of the Seismological Society of America, v. 95, no. 6, p. 2081–2092.

Dentith, MC, Dent, VF and Drummond, BJ 2000, Deep crustal structure in the southwestern Yilgarn Craton, Western Australia: Tectonophysics, v. 325, p. 227–255.

Everingham, IB 1965, The crustal structure of the south-west of Western Australia: Bureau of Mineral Resources, Geology and Geophysics, Record 1965/97.

Geological Survey of Western Australia 2020a, Gravity anomaly grid (400 m) of Western Australia (2020 — version 1): Geological Survey of Western Australia, digital data layer, <www.dmirs.wa.gov.au/geophysics>.

Geological Survey of Western Australia 2020b, Magnetic anomaly grids (40 m) of Western Australia (2020 – version 1): Geological Survey of Western Australia, digital data layer, <www.dmirs.wa.gov.au/geophysics>.

Geological Survey of Western Australia 2021, Southwest Yilgarn Geological Exploration Package, 2021: Geological Survey of Western Australia, Geological Exploration Package.

Mathur, SP, Moss, FJ and Branson JC 1977, Seismic and gravity investigation along the geotraverse, Western Australia, 1969: a BMR contribution to the Upper Mantle Project: Bureau of Mineral Resources, Geology and Geophysics, Bulletin 191.

Recommended reference

Brisbout, L 2021, Southwest Yilgarn 3D, 2021: Geological Survey of Western Australia; 3D Geomodel Series.

HyLogger spectral mineralogy of regolith from the central southwest Yilgarn

by

N de Souza Kovacs, MJ Wawryk and EA Hancock

Abstract

This spatial dataset results from a collaborative project between the Geological Survey of Western Australia (GSWA) of the Department of Mines, Industry Regulation, and Safety (DMIRS), and the Agricultural Resource Management and Assessment branch of the Department of Primary Industries and Regional Development of Western Australia (DPIRD). The dataset displays interpreted spectral reflectance data from 58 regolith profiles distributed throughout the central southwest Yilgarn. The spectral reflectance data were compiled by scanning drilling aircore samples using the GSWA HyLogger-3 system at the Perth Core Library. The aircore samples derive from historic groundwater bores drilled by DPIRD. The drillholes are vertical, with a maximum depth of 68 m. The aircore samples are stored in plastic chip trays and were scanned using HyChips mode. This spatial dataset is a GIS feature class point shapefile containing the drillhole locations coordinates, and a feature class attribute table holding spectral measurements taken at 2 m intervals for each of the 58 drillholes.

The HyLogger-3 system captures reflectance data in the visible-near infrared (VNIR, 360–1000 nm), short-wave infrared (SWIR, 1000–2500 nm) and thermal infrared (TIR, 6000 – 14 500 nm) wavelength intervals. The measured data were interpreted using the latest mineral reference library and full-pattern unmixing algorithms (SWIR: TSAS+ 7.05; TIR: jCLST 7.08) in The Spectral Geologist (8.0.7.4) software package. Absorption features in the VNIR region are associated with characteristic electronic transitions, including crystal bound ferrous and ferric ions (Karr, 1975). Most absorption features in the SWIR region are associated with hydroxyl (OH) absorptions around 1400 nm, and water (H_2O) absorption at 1900 nm. Other important indicative absorption features in SWIR are AlOH around 2200 nm, FeOH 2250 nm, and MgOH at or near 2330 nm (Pontual et al., 1997). Most reflectance features in the TIR region are associated with lattice vibrations of silicate and carbonate minerals (Hancock et al., 2013). Table 1 lists the identified minerals and absorption features.

The minerals identified in the 58 regolith profiles are clays (smectite, kaolinite), iron oxides and sulfate minerals, known as products of weathering. Mineral indicators of parent bedrock lithology include quartz, white mica, dark mica, amphibole, plagioclase, garnet, pyroxene, olivine; and minerals commonly found in alteration zones such as chlorite, white mica, serpentine, MgOH group minerals, tourmaline, epidote and carbonates.

Stratigraphic discontinuities in the regolith profile appear as distinct variations of the diagnostic absorption features in the spectral data. The change from poor to well-ordered crystalline kaolinite indicates a stratigraphic boundary between depositional-transported regolith and in situ saprolithic regolith (Anand and Paine, 2002). The kaolinite crystallinity diagnostic feature can be used by pairing with the 'water feature depth', as depositional-transported regolith commonly show spectra with broader 'water feature depth' than in situ regolith. The 'water feature depth' (1900 nm) corresponds to a common strong absorption feature of bound and unbound water present in various minerals (Pontual et al., 1997). The presence of abundant hematite together with poor crystalline kaolinite in the regolith profile can be used to map transported material, including paleochannels.

This 2D spatial dataset contains 3D data created for export and visualized as downhole regolith profiles showing mineral distribution based on variations in wavelengths as shown in Figure 1, and or used to build 3D models.

Table 1. Mineral classes and spectral features identified in the 58 regolith profiles. The HyLogger-3 system captures reflectance data in the visible-near infrared (VNIR, 360–1000 nm), short-wave infrared (SWIR, 1000–2500 nm) and thermal infrared (TIR 6000 – 14 500 nm) wavelength intervals

VNIR–SWIR region (360–2500 nm)	TIR region (6000 – 14 500 nm)
Kaolin	Silica
White mica	K-feldspar
Smectite	Plagioclase
Other AlOH class minerals	Garnet
Chlorite	Pyroxene
Dark mica	Olivine
Amphibole	Zeolite
Serpentine	Kaolin
Other MgOH class minerals	White mica
Epidote	Smectite
Tourmaline	Other AlOH class minerals
Carbonate	Chlorite
Sulfate	Dark mica
Aspectral	Amphibole
1900 nm water feature depth	Serpentine
2200 nm AlOH feature depth	Other mgoh class minerals
2200 nm AlOH feature wavelength	Epidote
2250 nm FeOH feature depth	Tourmaline
2250 nm FeOH feature wavelength	Carbonate
Kaolinite crystallinity	Sulfate
Ferric oxide abundance	Phosphate
Hematite goethite distribution	Oxide
	Aspectral
	8625 nm quartz feature depth
	6500 nm carbonate feature height
	6500 nm carbonate feature wavelength
	11 300 nm carbonate feature height
	11 300 nm carbonate feature wavelength

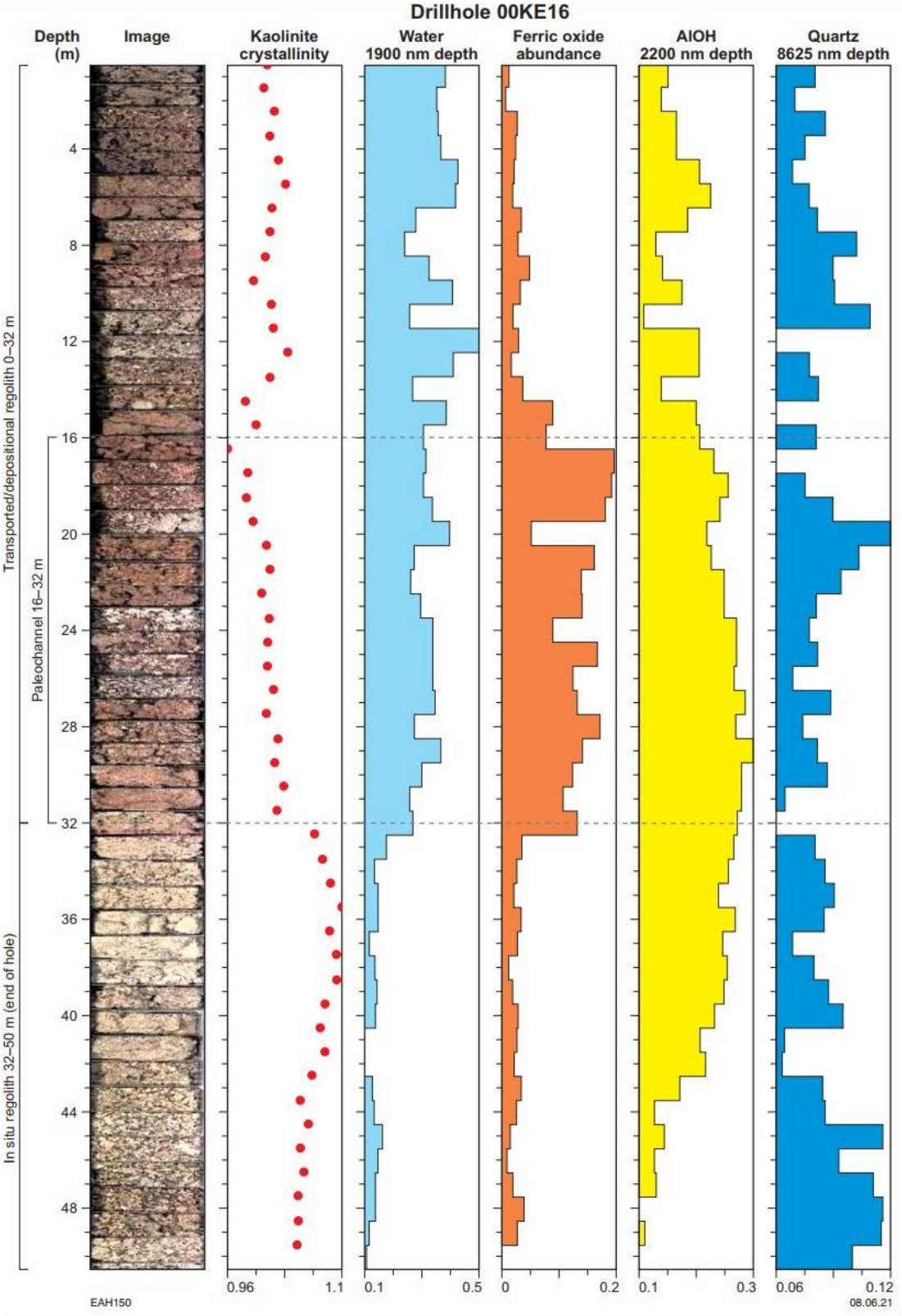

Figure 1. Regolith profile for the vertical drillhole 00KE16 showing the downhole distribution for SWIR kaolinite crystallinity, SWIR depth of bound water 1900 nm absorption feature, SWIR ferric oxide abundance, SWIR depth of the 2200 nm AlOH absorption feature, and TIR depth of the 8625 nm quartz absorption feature. The displayed measurements are derived from ratios of depths of the absorption features (minimum reflectivity) normalized against background hull reflectivity at those wavelengths. A distinct change in kaolinite crystallinity from poor to well-ordered is observed at 32 m deep, where there is also a distinct change in the depth of bound water absorption, and a decrease in ferric oxide abundance. This sharp change in hyperspectral data is characteristic of the discontinuity horizon between the transported depositional regolith above and the in situ weathering profile below. In this case for drillhole 00KE16, the base of the transported regolith is at 32 m deep. The 16–32 m interval in this regolith profile shows abundant hematite and can be investigated as a potential paleochannel

How to access

The HyLogger regolith digital data is available as a free download from the Data and Software Centre, and via the DMIRS eBookshop.

References

Anand, RR and Paine, M 2002. Regolith geology of the Yilgarn Craton, Western Australia: Implications for exploration: Australian Journal of Earth Sciences, 49 (1), 3–162pp, doi:10.1046/j.1440-0952.2002.00912x.

Hancock, EA, Green, AA, Huntington, JF, Schodlok, MC and Whitbourn, LB 2013, HyLogger-3: implications of adding thermal-infrared sensing: Geological Survey of Western Australia, Record 2013/3, 24p.

Karr, C 1975, Infrared and Raman spectroscopy of lunar and terrestrial minerals: Academic Press, Inc. ISBN 0-12-399950-2.

Pontual, S, Merry, N and Gamson, P 1997, Spectral interpretation field manual: Spectral analysis guides for mineral exploration. G-MEX, version 1.0, AusSpec International.

Recommended reference

de Souza Kovacs, N, Wawryk, MJ and Hancock, EA 2021, HyLogger spectral mineralogy of regolith from the central southwest Yilgarn: Geological Survey of Western Australia, digital data layers.

EXPLORATION INCENTIVE SCHEME

GOVERNMENT OF WESTERN AUSTRALIA
Department of Primary Industries and Regional Development

Soil-landscape mapping Western Australia – Best available soils

original data by

Department of Primary Industries and Regional Development

Abstract

This data layer comprises soil-landscape mapping covering Western Australia at the best available scale. It is a compilation of various surveys at different scales between 1:20 000 and 1:3 000 000. Mapping conforms to a nested hierarchy established to deal with the varying levels of information resulting from the variety of scales. Land capability and land quality attribution are included. For a description of the methodology employed, please refer to Technical Report No. 280 d (Purdie et al., 2004).

Data were collected through field observations and sampling, and interpretation of aerial photography and satellite imagery at a variety of scales. Soil surveys were carried out according to Gunn et al. (1988). Soil maps produced between 1987 and 1999 were scanned, vectorized and added to aerial photography and satellite images, and further georeferenced for digitizing using Microstation. Surveys were edge-matched to ensure that joins and overlaps between datasets were rationalized. Further individual survey datasets were imported into GeoMedia and combined into one dataset. During 2011 and 2012, topological errors were identified and corrected using GeoMedia Professional and checked using ArcGIS 10. The data were then written to the Department of Agriculture and Food Oracle Spatial database. Attribute data is stored in a separate Oracle map unit database, but key attribute data is provided with the spatial data. Attribute and spatial data are subject to change, hence the need for regular updates to this dataset. Positional and attribution accuracy are variable, depending upon survey scale, ranging from ±25 to ±500 m. The reliability map is mainly used for land capability and land quality values outside the southwest agricultural area where these have not been assessed. (Figs 1 and 2).

How to access

These data were extracted for the relevant area of interest for the Southwest Yilgarn, 2021 Geological Exploration Package, available on a USB via the DMIRS eBookshop. The original data can be accessed through https://catalogue.data.wa.gov.au/dataset/soil-landscape-mapping-best-available. For further information refer to Department of Agriculture Resource Management Technical Reports No. 280 and 313.

References

Gunn, RH, Beattie, JA, Reid, RE and van de Graaff, RHM 1988, Australian soil and land survey handbook: guidelines for conducting surveys: Inkata Press, Melbourne, Victoria, 293p, <http://hdl.handle.net/102.100.100/266077>.

Purdie, BR, Tille, PJ and Schoknecht, NR 2004, Soil-landscape mapping in south-Western Australia: an overview of methodology and outputs: Department of Agriculture and Food, Perth, Western Australia, Report 280, 160p.

Western Australia soil-landscape mapping survey reliability

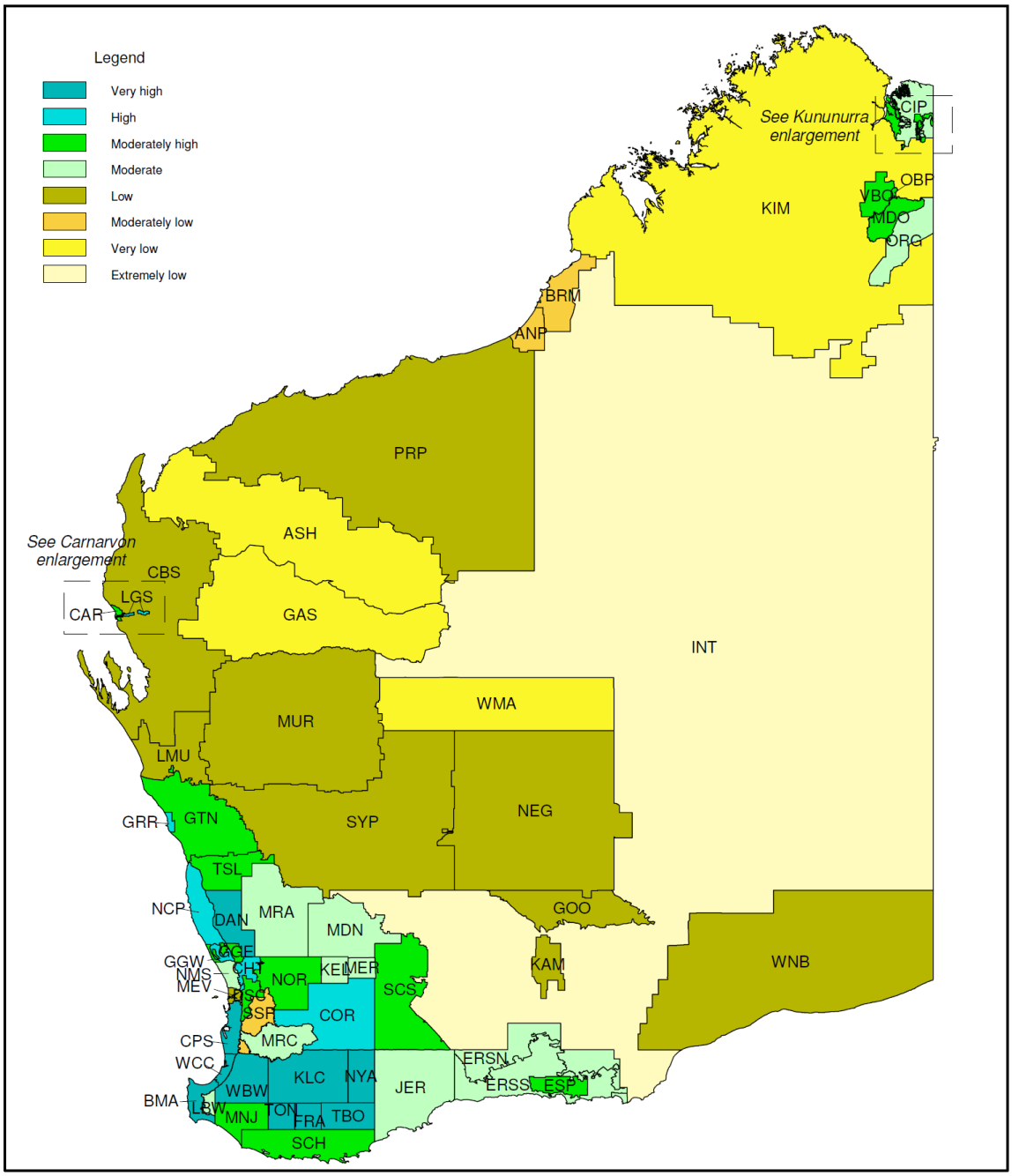

ANP	Anna Plains	GOO	Goongarrie	NCP	North Coastal Plain
ASH	Ashburton River	GRR	Geraldton Rural-residential	NEG	North-eastern Goldfields
BMA	Busselton Margaret River Augusta	GTN	Geraldton	NMS	North metropolitan surveys
BRM	Broome coastal	INT	Interior (Atlas of Australian Soils)	NOR	Northam
CAR	Carnarvon LCD	JER	Jerramungup	NYA	Nyabing Kukerin
CBS	Carnarvon basin	KAM	Kambalda	ORG	Ord River Regeneration
CHT	Chittering	KEL	Kellerberrin	PRP	Pilbara
CIP	Carlton Hill-Ivanhoe Plain	KIM	Kimberly	SCH	South Coast and hinterland
COR	Corrigin	KLC	Katanning	SCS	Southern Cross Hyden
CPS	Coastal plain south	LBW	Lower Blackwood	SSR	System 6 Residual
DAN	Dandaragan	LGS	Lower Gascoyne	SWV	Swan Valley vineyard
DSC	Darling Scarp	LMU	Lower Murchison	SYPS	Sandstone Yalgoo Paynes Find
ERSN	Esperance-Ravensthorpe-Salmon Gums (uncleared portion)	MDN	Bencubbin	TBO	Tambellup Borden
ERSS	Esperance-Ravensthorpe-Salmon Gums (Ag Land portion)	MDO	Mabel Downs-Osmond Valley	TON	Tonebridge
ESP	Esperance	MER	Merredin	TSL	Three Springs Latham
FRA	Frankland	MEV	Perth Metro Region Environmental Geology	VBO	Violet Valley-Bow River
GAS	Gascoyne	MNJ	Manjimup	WBW	Wellington Blackwood
GGE	Gingin East	MRA	Moora Wongan Hills	WCC	Harvey-Capel
GGF	Gingin Fill-in	MRC	Murray River catchment	WMA	Wiluna-Meekathara
GGW	Gingin West	MUR	Murchison River	WNB	Western Nullarbor

Figure 1. Reliability map. Positional and attribution accuracy are variable depending upon survey scale and can range from ±25 to ±500 m

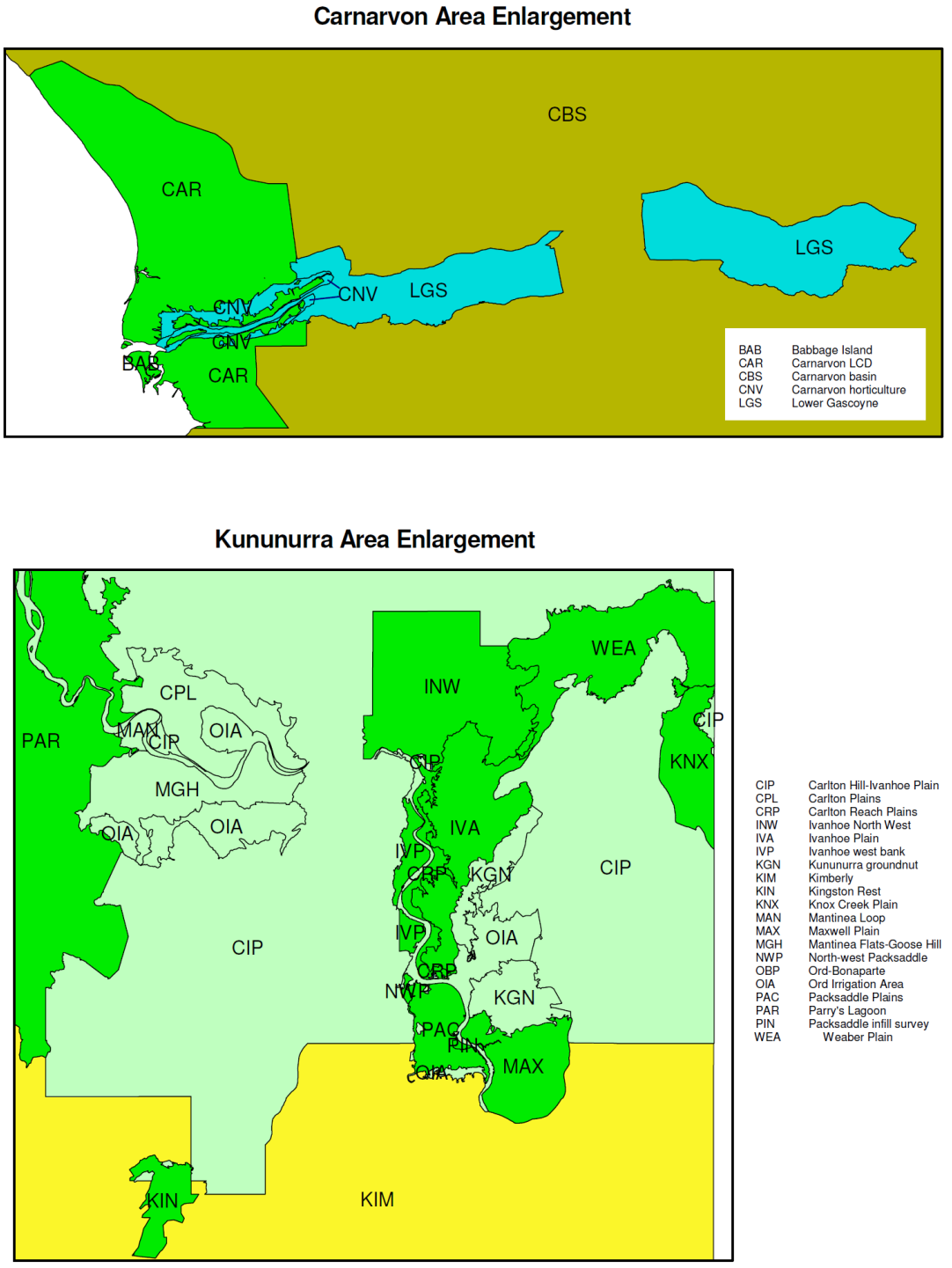

Figure 2. Inset reliability maps for the Carnarvon and Kununurra areas indicated on Figure 1

Recommended reference (to original data)*

Department of Primary Industries and Regional Development 2018, Soil-landscape mapping Western Australia — Best available soils: Department of Primary Industries and Regional Development, Western Australia, digital dataset, <https://catalogue.data.wa.gov.au/dataset/soil-landscape-mapping-best-available>.

Recommended reference (to this abstract)

Department of Primary Industries and Regional Development 2019, Soil-landscape mapping Western Australia — Best available soils: Geological Survey of Western Australia, digital data layers.

Soil-landscape mapping Western Australia — Western Australian Soil Group proportions

original data by

Department of Primary Industries and Regional Development

Abstract

The data layer comprises soil-landscape mapping covering Western Australia at the best available scale attributed with the proportional allocation of Western Australian Soil Groups to each map unit. It is a compilation of various surveys at different scales between 1:20 000 and 1:3 000 000.

The data were collected through field observations and sampling, and interpretation of aerial photography and satellite imagery. Soil surveys were carried out according to Gunn et al. (1988). Data were transferred to aerial photography or satellite images, or scanned, vectorized and georeferenced. Most data capture took place between 1987 and 1999. Surveys were edge-matched to ensure that joins and overlaps between datasets were rationalized. Individual survey datasets were imported into GeoMedia and combined into one dataset. During 2011 and 2012, topological errors were identified and corrected using GeoMedia Professional and checked using ArcGIS 10. The data were then written to the Department of Agriculture and Food Oracle Spatial database. The proportion of Western Australian Soil Groups occurring within each map unit are estimated based on field observations. Attribute and spatial data are subject to change, hence the need for regular updates to this dataset. Positional accuracy is variable depending upon the scale of the survey and can range from ±25 to ±500 m. Accuracy of attribution is also variable depending upon the scale of the survey (Fig. 1). Note that where a numerical value is stated as –99 or a text attribute value as 'NA', these attributes are not valid for the scale or type of mapping represented. The reliability map is mainly used for land capability and land quality values outside the southwest agricultural area where these have not been assessed.

How to access

These data were extracted for the Southwest Yilgarn, 2021 Geological Exploration Package, available on a USB via the DMIRS eBookshop. The original data can be accessed through https://catalogue.data.wa.gov.au/dataset/soil-landscape-mapping-western-australia-attributed-by-wa-soil-group. For further information about Western Australian Soil Groups refer to Department of Agriculture and Food Resource Management Technical Report No. 380.

Reference

Gunn, RH, Beattie, JA, Reid, RE and van de Graaff, RHM 1988, Australian soil and land survey handbook: guidelines for conducting surveys: Inkata Press, Melbourne, Victoria, 293p, <http://hdl.handle.net/102.100.100/266077>.

Recommended reference (to original data)*

Department of Primary Industries and Regional Development 2019, Soil-landscape mapping Western Australia — WA Soil Group proportions: Department of Primary Industries and Regional Development, Western Australia, digital dataset, <https://catalogue.data.wa.gov.au/dataset/soil-landscape-mapping-western-australia-attributed-by-wa-soil-group>.

Recommended reference (to this abstract)

Department of Primary Industries and Regional Development 2019, Soil-landscape mapping Western Australia — Western Australian Soil Group proportions: Geological Survey of Western Australia, digital data layers.

Western Australia soil-landscape mapping survey reliability

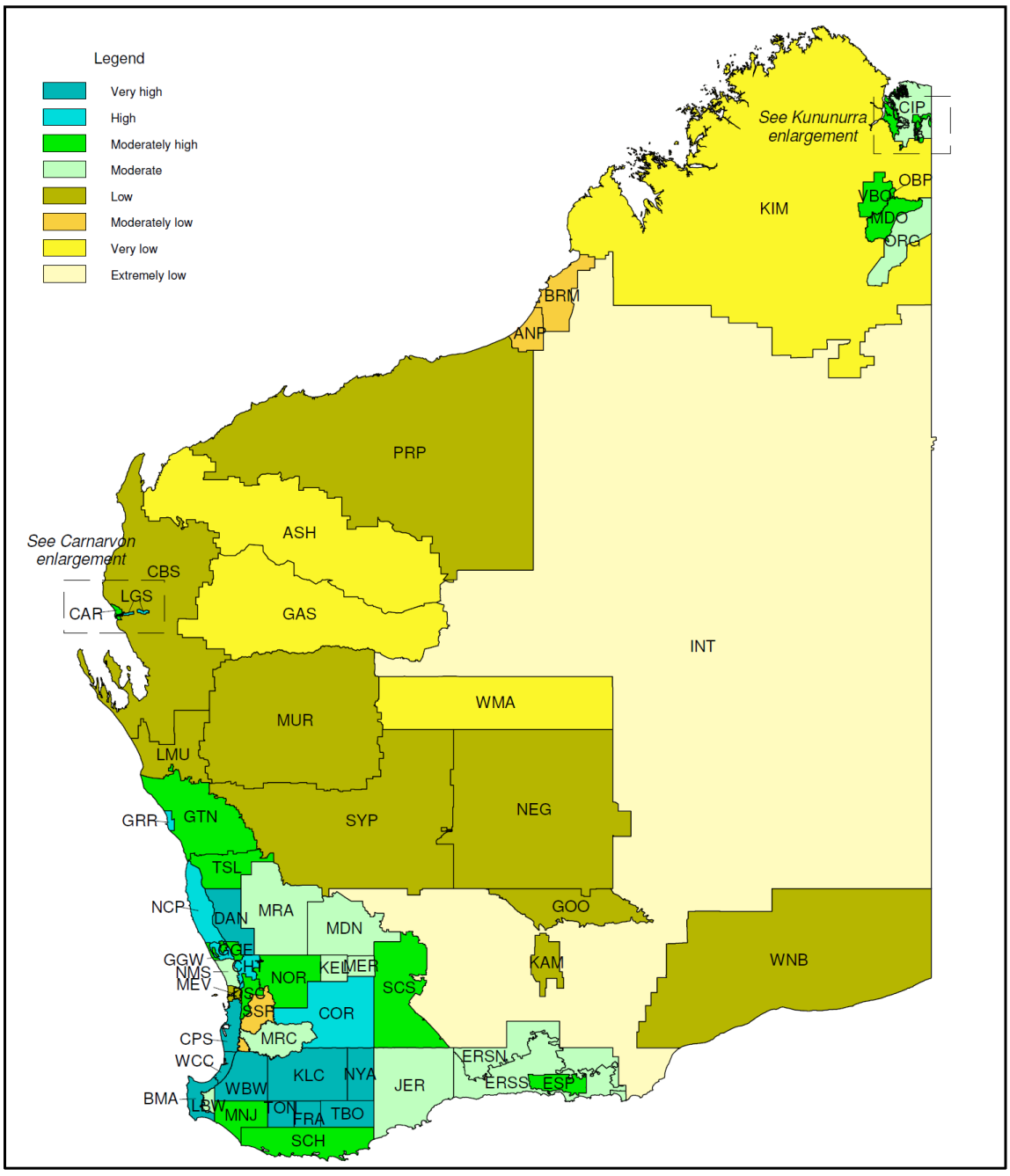

ANP	Anna Plains	GOO	Goongarrie	NCP	North Coastal Plain
ASH	Ashburton River	GRR	Geraldton Rural-residential	NEG	North-eastern Goldfields
BMA	Busselton Margaret River Augusta	GTN	Geraldton	NMS	North metropolitan surveys
BRM	Broome coastal	INT	Interior (Atlas of Australian Soils)	NOR	Northam
CAR	Carnarvon LCD	JER	Jerramungup	NYA	Nyabing Kukerin
CBS	Carnarvon basin	KAM	Kambalda	ORG	Ord River Regeneration
CHT	Chittering	KEL	Kellerberrin	PRP	Pilbara
CIP	Carlton Hill-Ivanhoe Plain	KIM	Kimberly	SCH	South Coast and hinterland
COR	Corrigin	KLC	Katanning	SCS	Southern Cross Hyden
CPS	Coastal plain south	LBW	Lower Blackwood	SSR	System 6 Residual
DAN	Dandaragan	LGS	Lower Gascoyne	SWV	Swan Valley vineyard
DSC	Darling Scarp	LMU	Lower Murchison	SYPS	Sandstone Yalgoo Paynes Find
ERSN	Esperance-Ravensthorpe-Salmon Gums (uncleared portion)	MDN	Bencubbin	TBO	Tambellup Borden
ERSS	Esperance-Ravensthorpe-Salmon Gums (Ag Land portion)	MDO	Mabel Downs-Osmond Valley	TON	Tonebridge
ESP	Esperance	MER	Merredin	TSL	Three Springs Latham
FRA	Frankland	MEV	Perth Metro Region Environmental Geology	VBO	Violet Valley-Bow River
GAS	Gascoyne	MNJ	Manjimup	WBW	Wellington Blackwood
GGE	Gingin East	MRA	Moora Wongan Hills	WCC	Harvey-Capel
GGF	Gingin Fill-in	MRC	Murray River catchment	WMA	Wiluna-Meekathara
GGW	Gingin West	MUR	Murchison River	WNB	Western Nullarbor

Figure 1. Reliability map. Positional and attribution accuracy are variable depending upon survey scale and can range from ±25 to ±500 m

Geochemical pathfinders for gold-rich mineralizing systems in the southwest Yilgarn

by

P Duuring, JN Guilliamse and S Morin-Ka

Abstract

Multiple layers show the distribution and abundance of selected elements or element ratios for rock, soil, stream, and laterite samples within the southwest Yilgarn. The displayed geochemical data are relevant for mineral exploration because they either directly identify gold mineralization (e.g. Au layers), or they may be considered proxies for hydrothermal fluid alteration associated with mineralization (e.g. S layers).

The derivative GIS layers were created from existing primary geochemical datasets. These parent datasets include WACHEM, OZCHEM (WA subset), CRCLEME-laterite, and WAMEX (i.e. the surface rock chip, surface stream sediment, surface shallow drillhole, surface soil, and maximum grade in drillhole). In each dataset, the samples have been analysed for a range of elements. A variety of analytical approaches have been used at commercial and government laboratories, so that a user must take care when comparing element value ranges between different datasets. Element ratios have been created as a normalization tool to avoid some of these laboratory procedure-induced differences between datasets. The WACHEM, OZCHEM, and CRCLEME-laterite data have high fidelity because strict quality controls were in place at the time of sampling, rock preparation, and laboratory analysis. In contrast, WAMEX geochemical data are derived from exploration and mining activities in Western Australia, reported by companies to the Geological Survey of Western Australia (GSWA). GSWA applies quality control measures at the time of data submission, but there is likely to be some inclusion of spurious results (e.g. errors in unit reporting, multiple field names for the same analyte, incorrect assignment of analytes).

For each geochemical layer, a unique legend and colour scheme has been chosen to best highlight geochemical trends. Higher element abundance values are drawn on top of lower values to more clearly show spatial gradients in element concentrations.

Several well-established element ratios and alteration indices have been calculated using the primary geochemical datasets to evaluate possible hydrothermal alteration in the southwest Yilgarn. However, all indices are likely influenced by precursor rock chemistry and are also strongly sensitive to the effects of overprinting hydrothermal fluids such as weathering. These factors need to be taken into consideration when interpreting alteration indices. Alternative methods, including normative methods and mass balance calculations (cf. Mathieu, 2018), are recommended.

1. Sulfidation index (S/Fe after Halley, 2020): sulfur may be added to rocks from hydrothermal fluids, whereas Fe is already present in the rock. When all the available Fe in a rock has reacted to form pyrite, samples have a molar ratio of S/Fe = 2:1. The S/Fe sulfidation index is considered to be an accurate measure of the intensity of pyrite alteration, more so than total S content (Halley, 2020). The sulfidation index for the southwest Yilgarn effectively highlights sites of known precious and base metal mineralization.
2. Carbonatization or Carbonate saturation index (CO_2/(CaO + MgO + FeO) after Kishida and Kerrich, 1987): carbonatization is associated with a CO_2 gain and results in the addition of carbonate alteration minerals in rocks. Carbon combines with Ca, Mg, or Fe; the latter are either introduced by hydrothermal fluids or are existing components of fresh rocks. Carbonate mineral abundance may depend on the composition of the precursor rock (Mathieu, 2018). There is a lack of point data available for this geochemical index in the southwest Yilgarn because CO_2 is

rarely included in laboratory analysis. However, the high carbonate saturation index values observed along the eastern margin of the study area coincide with known gold sites; other high values in central areas are unexplained.

3. Chlorite–carbonate–pyrite index (CCPI = 100 x (Fe_2O_{3T} + MgO)/(Fe_2O_{3T} + MgO + Na_2O + CaO) after Large et al., 2001): this product is severely affected by weathering. Values greater than 95% have not been shown in the map layer because these samples correspond with oxidized, iron-rich laterite samples in the geochemical datasets. Excluding the upper range of values, the remaining data demonstrate that higher index values are associated with greenstone belts in the study area. The higher index values overlap some of the target areas identified by the sulfidation index.

4. Ishikawa alteration index (AI = 100 x (K_2O + MgO)/(K_2O + MgO + Na_2O + CaO) after Ishikawa et al., 1976): the AI is commonly used to test for sericite and chlorite alteration in fresh rocks of common protolith. The distribution of AI values closely matches the distribution of chlorite–carbonate–pyrite index values in the southwest Yilgarn.

5. ACNK alteration index (Al_2O_3/(CaO+Na_2O+K_2O) after Hodges and Manojlovic, 1993): the ratio of Al_2O_3 vs CaO+Na_2O+K_2O is a measure of feldspar mineral destruction due to alteration. An index value of greater than 1.6 is considered to indicate the likely presence of alteration; while a value of greater than 3, such as that documented in the Snow Lake area of Manitoba, is correlated with strong alteration (Hodges and Manojlovic, 1993). A large proportion of samples in the southwest Yilgarn have ACNK indices greater than 3. The distribution of these high ACNK index values is strongly influenced by the common presence of supergene-altered samples, due to the removal of CaO+Na_2O+K_2O and residual concentration of the less mobile Al_2O_3.

6. Advanced argillic alteration index (AAAI = 100 x (SiO_2/(SiO_2 + 10(MgO + CaO + Na_2O)) after Williams and Davidson, 2004): argillic alteration is characterized by the increase in the proportion of quartz and clay minerals in rocks due to the addition of SiO_2 from hydrothermal fluids, plus the breakdown of feldspar and Mg-bearing primary minerals. This alteration index is strongly influenced by the distribution of supergene-altered samples in the southwest Yilgarn. An upper cut-off value of 97% has been applied to lessen the influence of these samples in the central–eastern parts of the study area.

7. K-feldspar saturation index (K/Al molar after Mathieu, 2018): measures gains in K vs the less mobile Al and estimates the degree of K-feldspar alteration in a fresh rock. Like albitization, it commonly occurs via the alteration of existing feldspars and may be accompanied by losses in Na, Ca, Fe, Mg, and possibly Si (Mathieu, 2018). The distribution of values in the southwest Yilgarn is strongly influenced by the distribution of supergene alteration, as well as felsic gneisses and granites.

8. Albite saturation index (Na/Al molar after Kishida and Kerrich, 1987): measures gains in Na vs the less mobile Al and estimates the degree of albitization in a fresh rock. Like potassic alteration, albitization commonly occurs via the alteration of existing feldspars and may be accompanied by losses in K, Ca, Fe, Mg, and possibly Si (Mathieu, 2018). The distribution of the albite saturation index closely matches that for the K-feldspar saturation index. Both are influenced by supergene alteration and precursor rock chemistry.

9. Sericite saturation index (3K/Al molar after Kishida and Kerrich, 1987): sericitization is an acid alteration that produces white mica, commonly via the destruction of feldspars. It commonly results in Ca- and Na-losses, combined with a gain or loss in K (Mathieu, 2018). The distribution of the albite saturation index closely matches the albite and K-feldspar saturation indices for the southwest Yilgarn.

How to access

These data form part of the Southwest Yilgarn, 2021 Geological Exploration Package, available on a USB via the DMIRS eBookshop.

References

Halley, S 2020, Mapping Magmatic and Hydrothermal Processes from Routine Exploration Geochemical Analyses: Economic Geology, v. 115, no. 3, p. 489–503, 15p., doi:10.5382/econgeo.4722.

Hodges, D and Manojlovic, P 1993, Application of lithogeochemistry to exploration for deep VMS deposits in high grade metamorphic rocks, Snow Lake, Manitoba: Journal of Geochemical Exploration, v. 48, no. 2, p. 201–224, doi:10.1016/0375-6742(93)90005-7.

Ishikawa, Y, Sawaguchi, T, Iwaya, S and Horiuchi, M 1976, Delineation of prospecting targets for Kuroko deposits based on modes of volcanism of underlying dacite and alteration haloes: Mining Geology, v. 26, p. 105–117.

Kishida, A and Kerrich, R 1987, Hydrothermal alteration zoning and gold concentration at the Kerr-Addison Archean lode gold deposit, Kirkland Lake, Ontario: Economic Geology, v. 82, no. 3, p. 649–690, doi:10.2113/gsecongeo.82.3.649.

Large, RR, Gemmell, JB, Paulick, H and Huston, DL 2001, The alteration box plot: A simple approach to understanding the relationship between alteration mineralogy and lithogeochemistry associated with volcanic-hosted massive sulfide deposits: Economic Geology, v. 96, no. 5, p. 957–971.

Mathieu, L 2018, Quantifying Hydrothermal Alteration: A Review of Methods: Geosciences, v. 8, no. 7, p. 245, doi:10.3390/geosciences8070245.

Williams, NC and Davidson, GJ 2004, Possible submarine advanced argillic alteration at the Basin Lake Prospect, western Tasmania, Australia: Economic Geology, v. 99, no. 5, p. 987–1002, doi:10.2113/gsecongeo.99.5.987.

Recommended reference

Duuring, P, Guilliamse, JN and Morin-Ka, S, 2021, Geochemical pathfinders for gold-rich mineralizing systems in the southwest Yilgarn: Geological Survey of Western Australia, digital data layers.

Alteration minerals potentially diagnostic of mineral systems fertile for gold in the southwest Yilgarn

by

P Duuring, S Morin-Ka and JN Guilliamse

Abstract

These data layers show the distribution of non-sulfide minerals that may indicate altered rocks (or their metamorphosed equivalents) and are potentially associated with gold-rich mineral systems in the southwest Yilgarn. Each layer shows the occurrence of a specific target mineral (Table 1).

The parent WAROX database contains geoscientific data related to observations and samples collected in the field. The data include information about outcrop geology, regolith geology, field photographs, geological samples, rock physical properties, petrography, paleontology and geochronology.

Table 1. Query operation

Operation	Query
For the 'alteration minerals' layers, WAROX data are queried to select specific minerals from any field in the WAROX database	Any field = 'andalusite' OR Any field = 'anhydrite' OR Any field = 'ankerite' OR Any field = 'barite' OR Any field = 'biotite' OR Any field = 'calcite' OR Any field = 'cordierite' OR Any field = 'diopside' OR Any field = 'dolomite' OR Any field = 'garnet' OR Any field = 'gypsum' OR Any field = 'kyanite' OR Any field = 'magnetite' OR Any field = 'prehnite' OR Any field = 'rutile' OR Any field = 'siderite' OR Any field = 'sillimanite' OR Any field = 'staurolite' OR Any field = 'titanite' OR Any field = 'tourmaline' OR Any field = 'wollastonite'

The derived layer shows site locations where minerals that indicate alteration have been recorded.

Results show that no specific non-sulfide mineral is strongly correlated with known MINEDEX gold sites in the southwest Yilgarn. A simple explanation is that there are strong lithological controls affecting non-sulfide mineral occurrences.

How to access

These data form part of the Southwest Yilgarn, 2021 Geological Exploration Package, available on a USB via the DMIRS eBookshop.

Recommended reference

Duuring, P, Morin-Ka, S and Guilliamse, JN 2021, Alteration minerals potentially diagnostic of mineral systems fertile for gold in the southwest Yilgarn: Geological Survey of Western Australia, digital data layers.

MINEDEX observations of gold sites in the southwest Yilgarn

by

P Duuring, S Morin-Ka and JN Guilliamse

Abstract

This layer shows the distribution of known gold-rich sites in the southwest Yilgarn. Gold mineralization sites are extracted from the MINEDEX database, which provides a coordinated, project-based inquiry system for textual information on mine, deposit, prospect and occurrence locations (coordinates, etc.), as well as mineral resources and mine production. Data are collated from ASX reports, statutory exploration reports, mining proposals and production returns.

The derived gold mineralization sites are selected to exclude exploration targets and infrastructure not directly related to mineralization, such as tailings storage facilities and processing plants. Gold sites are derived from the SITE_COMMODITY field in the MINEDEX database.

The order of listing of the commodity in the SITE_COMMODITY field reflects its relative importance at that site. Only those identified as target commodities and listed in the TARGET_COMMODITY_GROUP field are classified in MINEDEX into four groups: mine, deposit, prospect and occurrence (Table 1). Therefore, the SITE_TYPE_DESCRIPTION (i.e. mine, deposit, prospect or occurrence) is only applicable to the selected commodity if it is also listed in the TARGET_COMMODITY_GROUP field. When the commodity for a mineralization site is not listed in the TARGET_COMMODITY field, then it is not possible to allocate the relevant SITE_TYPE_DESCRIPTION without further investigation of the source data. In these instances, the site remains unclassified with respect to SITE_TYPE_DESCRIPTION.

The distribution of known gold sites in the southwest Yilgarn correlate with the mapped location of greenstone belts, shear zones and faults.

Table 1. Legend description

Site type	Definition
Au Mine	A deposit which is being mined, was previously mined, or is proposed to be mined.
Au Deposit	A mineral occurrence with probable economic value and for which there is an established resource.
Au Prospect	Any mineral occurrence where economic grades have been intersected over a significant width and strike length but for which there is not yet a resource, or any working or exploration activity that has found subeconomic mineral occurrences and from which there is no recorded production.
Au Occurrence	An occurrence (excluding those defined as mines, deposits or prospects) can be defined if an economic mineral has been identified in outcrop, or if assay results exceed an agreed concentration and size.
Au Unclassified	Mineralization site for which the TARGET_COMMODITY_GROUP does not reflect the specified commodity, and hence the SITE_TYPE_DESCRIPTION is not applicable.

How to access

These data form part of the Southwest Yilgarn, 2021 Geological Exploration Package, available on a USB via the DMIRS eBookshop.

Recommended reference

Duuring, P, Morin-Ka, S and Guilliamse, JN 2021, MINEDEX observations of gold sites in the southwest Yilgarn: Geological Survey of Western Australia, digital data layers.

MINEDEX observations of silver sites in the southwest Yilgarn

by

P Duuring, S Morin-Ka and JN Guilliamse

Abstract

This layer shows the distribution of known silver-rich sites in the southwest Yilgarn. Silver mineralization sites are extracted from the MINEDEX database, which provides a coordinated, project-based inquiry system for textual information on mine, deposit, prospect and occurrence locations (coordinates, etc.), as well as mineral resources and mine production. Data are collated from ASX reports, statutory exploration reports, mining proposals and production returns.

The derived silver mineralization sites are selected to exclude exploration targets and infrastructure not directly related to mineralization, such as tailings storage facilities and processing plants. Silver sites are derived from the SITE_COMMODITY field in the MINEDEX database.

The order of listing of the commodity in the SITE_COMMODITY field reflects its relative importance at that site. Only those identified as target commodities and listed in the TARGET_COMMODITY_GROUP field are classified in MINEDEX into four groups: mine, deposit, prospect and occurrence (Table 1). Therefore, the SITE_TYPE_DESCRIPTION (i.e. mine, deposit, prospect or occurrence) is only applicable to the selected commodity if it is also listed in the TARGET_COMMODITY_GROUP field. When the commodity for a mineralization site is not listed in the TARGET_COMMODITY field, then it is not possible to allocate the relevant SITE_TYPE_DESCRIPTION without further investigation of the source data. In these instances, the site remains unclassified with respect to SITE_TYPE_DESCRIPTION.

The distribution of known silver sites in the southwest Yilgarn correlate with gold sites and the mapped location of greenstone belts, shear zones and faults.

Table 1. Legend description

Site type	Definition
Ag Mine	A deposit which is being mined, was previously mined, or is proposed to be mined.
Ag Deposit	A mineral occurrence with probable economic value and for which there is an established resource.
Ag Prospect	Any mineral occurrence where economic grades have been intersected over a significant width and strike length but for which there is not yet a resource, or any working or exploration activity that has found subeconomic mineral occurrences and from which there is no recorded production.
Ag Occurrence	An occurrence (excluding those defined as mines, deposits or prospects) can be defined if an economic mineral has been identified in outcrop, or if assay results exceed an agreed concentration and size.
Ag Unclassified	Mineralization site for which the TARGET_COMMODITY_GROUP does not reflect the specified commodity, and hence the SITE_TYPE_DESCRIPTION is not applicable.

How to access

These data form part of the Southwest Yilgarn, 2021 Geological Exploration Package, available on a USB via the DMIRS eBookshop.

Recommended reference

Duuring, P, Morin-Ka, S and Guilliamse, JN 2021, MINEDEX observations of silver sites in the southwest Yilgarn: Geological Survey of Western Australia, digital data layers.

Sulfide minerals commonly associated with gold-rich mineral systems in the southwest Yilgarn

by

P Duuring, S Morin-Ka and JN Guilliamse

Abstract

These data layers show the distribution of sulfide minerals in the southwest Yilgarn based on observations recorded in the WAROX database. Each layer shows the occurrence of a specific sulfide mineral (e.g. arsenopyrite) commonly associated with gold-rich mineral systems. The 'Sulfides' layer shows occurrences of undifferentiated sulfide minerals resulting from a search query for 'sulfide' or 'sulphide' (Table 1).

The distribution of sulfide minerals is important for mineral exploration because their presence is potentially indicative of hydrothermal alteration associated with gold mineralization. Sulfide minerals may in some cases be part of multiple types of mineralizing systems (e.g. pyrite is commonly part of gold-rich hydrothermal systems, as well as some magmatic systems).

The parent WAROX database contains geoscientific data related to observations and samples collected in the field. The data include information about outcrop geology, regolith geology, field photographs, geological samples, rock physical properties, petrography, paleontology and geochronology.

The derived layers show site locations where a variety of sulfide minerals have been documented.

In this instance, the mapped distribution of sulfide minerals shows strong spatial correlation with gold sites reported by MINEDEX.

Table 1. Query operation

Operation	Query
WAROX data are queried to select particular sulfide minerals from any field in the WAROX database	Any field = 'arsenopyrite' OR Any field = 'bornite' OR Any field = 'chalcocite' OR Any field = 'chalcopyrite' OR Any field = 'galena' OR Any field = 'pyrite' OR Any field = 'pyrrhotite' OR Any field = 'sphalerite' OR Any field = 'sulfide' OR 'sulphide'

How to access

These data form part of the Southwest Yilgarn, 2021 Geological Exploration Package, available on a USB via the DMIRS eBookshop.

Recommended reference

Duuring, P, Morin-Ka, S and Guilliamse, JN 2021, Sulfide minerals commonly associated with gold-rich mineral systems in the southwest Yilgarn: Geological Survey of Western Australia, digital data layers.

Earthquakes of the southwest Yilgarn 1940–2020

original data by

Geoscience Australia

Abstract

A new digital layer has been created containing the location and magnitude of earthquakes of the southwest Yilgarn from 1940 to December 2020 (Fig. 1). The data are a subset of the Geoscience Australia catalogue, which is a nationwide dataset. Earthquake location markers are coloured by depth and scaled by preferred magnitude (usually M_L, local magnitude).

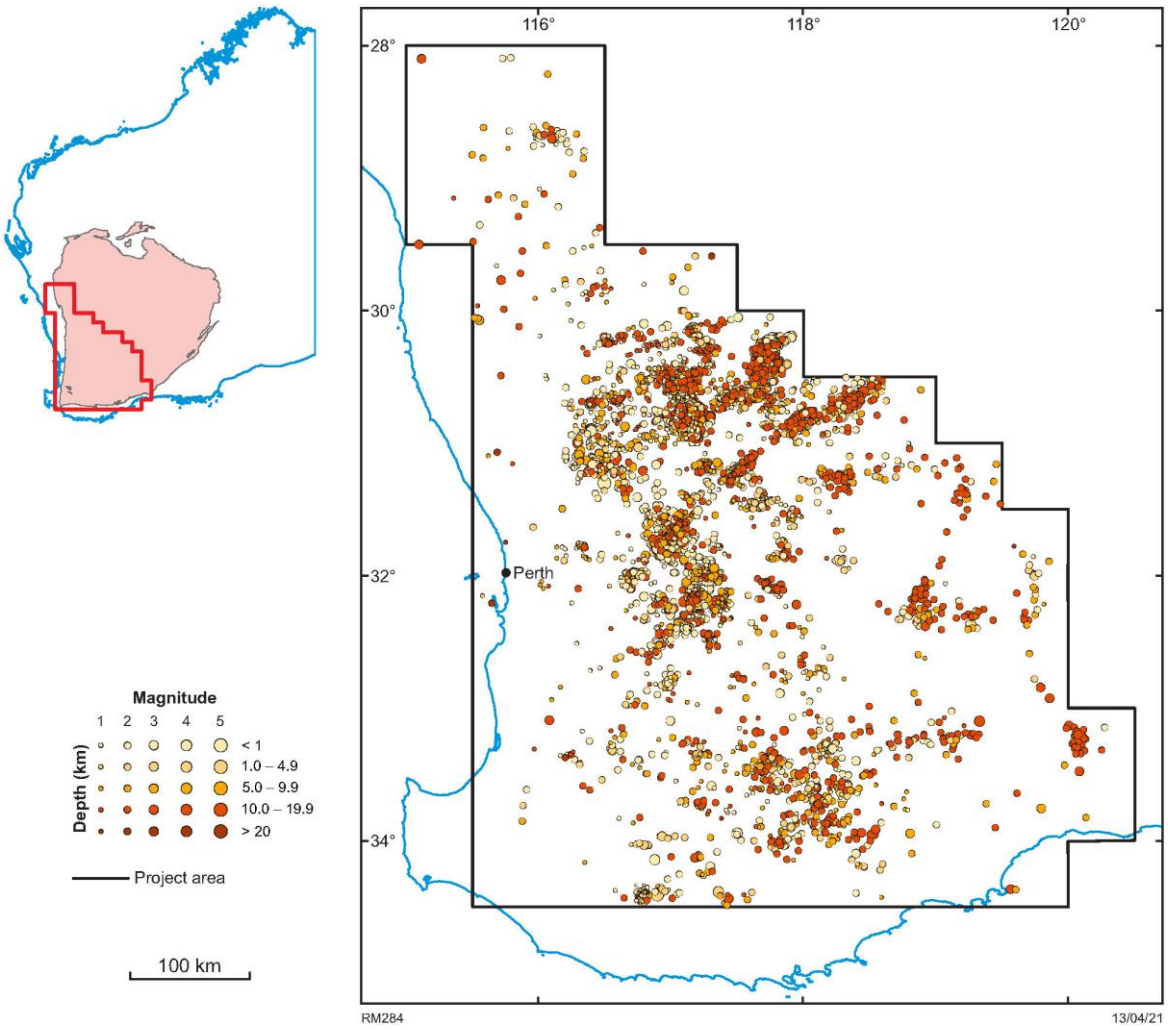

Figure 1. Earthquakes of the southwest Yilgarn 1940–2020 layer

How to access

Earthquakes of the southwest Yilgarn 1940–2020 digital data are available on a USB via the DMIRS eBookshop.

Recommended reference (to original data)

Geoscience Australia 2020, Earthquakes@GA: Geoscience Australia, accessed December 2020, <https://earthquakes.ga.gov.au>.

Recommended reference (to this abstract)

Geoscience Australia 2021, Earthquakes of the southwest Yilgarn 1940–2020: Geological Survey of Western Australia, digital data layer.

Neotectonic fault scarps of the southwest Yilgarn

original data by

Geoscience Australia

Abstract

The Neotectonic fault scarps map (Fig. 1) of the southwest Yilgarn is extracted from the Geoscience Australia database Neotectonic scarps layer. It comprises fault scarps which are believed to relate to large earthquakes during the Neotectonic era, i.e. the past 5–10 million years.

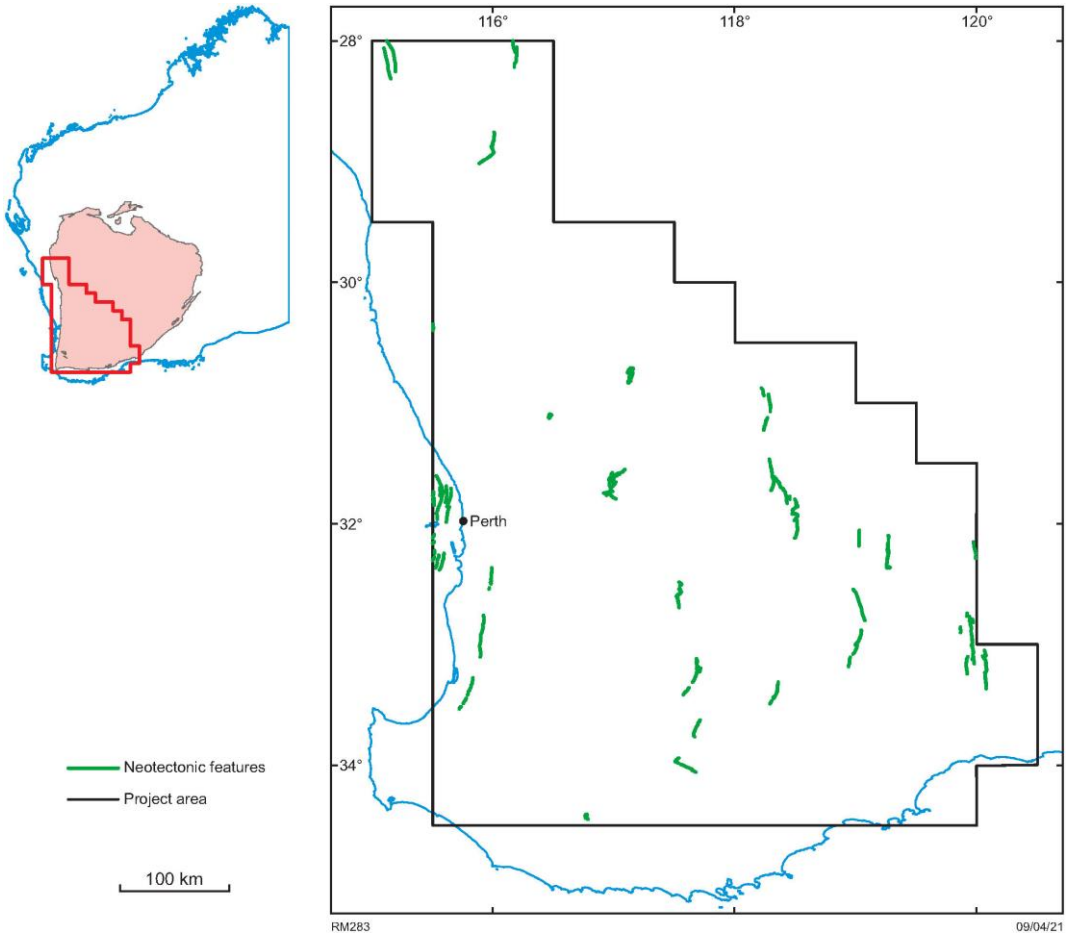

Figure 1. Neotectonic fault scarps of the southwest Yilgarn data layer

How to access

The Neotectonic fault scarps of the southwest Yilgarn data layer is available on a USB via the DMIRS eBookshop.

Recommended reference (to original data)

Geoscience Australia 2020, Neotectonic Features: Geoscience Australia, accessed December 2020, <https://neotectonics.ga.gov.au/>.

Recommended reference (to this abstract)

Geoscience Australia 2021, Neotectonic fault scarps of the southwest Yilgarn: Geological Survey of Western Australia, digital data layer.

WAROX observations of minerals potentially diagnostic of phyllic alteration in the southwest Yilgarn

by

LL Grech and P Duuring

Abstract

These data layers show the distribution of minerals that are commonly associated with phyllic alteration in porphyry Cu–Au–Mo mineral systems (e.g. Sillitoe, 2010; Safari et al., 2018). Each layer shows the occurrence of a specific target mineral (e.g. white mica) (Table 1).

The parent WAROX database contains geoscientific data related to observations and samples collected in the field. The data include information about outcrop geology, regolith geology, field photographs, geological samples, rock physical properties, petrography, paleontology and geochronology.

The derived layer shows site locations where minerals that are indicative of alteration have been recorded.

Results show that the distribution of pyrite overlaps many of the known Cu and Au sites in the southwest Yilgarn. The wide distribution of quartz and white mica is explained by their common presence in many precursor rocks (e.g. quartz in granites and felsic gneisses).

Table 1. Query operation

Operation	Query
For the 'phyllic alteration' layers, WAROX data are queried to select specific minerals from any field in the WAROX database	Any field = 'quartz' OR Any field = 'white mica' OR Any field = 'pyrite'

How to access

These data form part of the Southwest Yilgarn, 2021 Geological Exploration Package, available on a USB via the DMIRS eBookshop.

References

Safari, M, Maghsoudi, A and Beiranvand Pour, A 2018, Application of Landsat-8 and ASTER satellite remote sensing data for porphyry copper exploration: a case study from Shahr-e-Babak, Kerman, south of Iran: Geocarto International, v. 33, no. 11, p. 1186–1201.

Sillitoe, RH 2010, Porphyry copper systems: Economic Geology, v. 105, p. 3–41.

Recommended reference

Grech, LL and Duuring, P 2021, WAROX observations of minerals potentially diagnostic of phyllic alteration in the southwest Yilgarn: Geological Survey of Western Australia, digital data layers.

WAROX observations of minerals potentially diagnostic of potassic alteration in the southwest Yilgarn

by

LL Grech and P Duuring

Abstract

These data layers show the distribution of minerals that are commonly associated with potassic alteration in porphyry Cu–Au–Mo mineral systems (e.g. Sillitoe, 2010; Safari et al., 2018). Each layer shows the occurrence of a specific target mineral (e.g. K-feldspar) (Table 1).

The parent WAROX database contains geoscientific data related to observations and samples collected in the field. The data include information about outcrop geology, regolith geology, field photographs, geological samples, rock physical properties, petrography, paleontology and geochronology.

The derived layer shows locations where minerals that are indicative of alteration have been recorded.

Results show that the distribution of the target minerals overlaps known Cu sites in the southwest Yilgarn. However, the broad distribution of these minerals (e.g. quartz and biotite) suggests that they are also controlled by the precursor rock mineralogy (e.g. quartz in granites and felsic gneisses).

Table 1. Query operation

Operation	Query
For the 'potassic alteration' layers, WAROX data are queried to select specific minerals from any field in the WAROX database	Any field = 'biotite' OR Any field = 'bornite' OR Any field = 'chalcocite' OR Any field = 'chalcopyrite' OR Any field = 'k-feldspar' OR Any field = 'quartz' OR Any field = 'magnetite'

How to access

These data form part of the Southwest Yilgarn, 2021 Geological Exploration Package, available on a USB via the DMIRS eBookshop.

References

Safari, M, Maghsoudi, A and Beiranvand Pour, A 2018, Application of Landsat-8 and ASTER satellite remote sensing data for porphyry copper exploration: a case study from Shahr-e-Babak, Kerman, south of Iran: Geocarto International, v. 33, no. 11, p. 1186–1201.

Sillitoe, RH 2010, Porphyry copper systems: Economic Geology, v. 105, p. 3–41.

Recommended reference

Grech, LL and Duuring, P 2021, WAROX observations of minerals potentially diagnostic of potassic alteration in the southwest Yilgarn: Geological Survey of Western Australia, digital data layers.

WAROX observations of minerals potentially diagnostic of propylitic alteration in the southwest Yilgarn

by

LL Grech and P Duuring

Abstract

This layer shows the distribution of minerals that are commonly associated with propylitic alteration related to porphyry Cu–Au–Mo mineral systems (e.g. Sillitoe, 2010; Safari et al., 2018). Each layer shows the occurrence of a specific target mineral (e.g. epidote) (Table 1).

The parent WAROX database contains geoscientific data related to observations and samples collected in the field. The data include information about outcrop geology, regolith geology, field photographs, geological samples, rock physical properties, petrography, paleontology and geochronology.

The derived layer shows locations where minerals that are indicative of alteration have been recorded.

Table 1. Query operation

Operation	Query
For the 'propylitic alteration' layers, WAROX data are queried to select specific minerals from any field in the WAROX database	Any field = 'albite OR Any field = 'ankerite' OR Any field = 'calcite' OR Any field = 'chlorite' OR Any field = 'dolomite' OR Any field = 'epidote' OR Any field = 'galena' OR Any field = 'siderite' OR Any field = 'sphalerite' OR Any field = 'sulfides'

How to access

These data form part of the Southwest Yilgarn, 2021 Geological Exploration Package, available on a USB via the DMIRS eBookshop.

References

Safari, M, Maghsoudi, A and Beiranvand Pour, A 2018, Application of Landsat 8 and ASTER satellite remote sensing data for porphyry copper exploration: a case study from Shahr-e-Babak, Kerman, south of Iran: Geocarto International, v. 33, no. 11, p. 1186 1201.

Sillitoe, RH 2010, Porphyry copper systems: Economic Geology, v. 105, p. 3–41.

Recommended reference

Grech, LL and Duuring, P 2021, WAROX observations of minerals potentially diagnostic of propylitic alteration in the southwest Yilgarn: Geological Survey of Western Australia, digital data layers.

Geochemical pathfinders for porphyry Cu–Au–Mo mineralizing systems in the southwest Yilgarn

by

LL Grech, P Duuring, JN Guilliamse and S Morin-Ka

Abstract

These data layers show the abundance of selected elements or element ratios for rock, soil, stream, and laterite samples in the southwest Yilgarn. The included geochemical data are relevant for mineral exploration because they are directly associated with copper–gold mineralization (e.g. Cu and Au abundance).

These derivative GIS layers were created from larger primary geochemical datasets. The parent datasets include WACHEM, OZCHEM (WA subset), CRCLEME-laterite, and WAMEX (i.e. the surface rock chip, surface stream sediment, surface shallow drillhole, surface soil, and maximum grade in drillhole). In each dataset, the samples have been analysed for a range of elements. A variety of analytical approaches have been used at commercial and government laboratories, so that a user must take care when comparing element value ranges between different datasets. Element ratios have been created as a normalization tool to avoid some of these laboratory procedure-induced differences between datasets. The WACHEM, OZCHEM, and CRCLEME-laterite data have high fidelity because strict quality controls were in place at the time of sampling, rock preparation, and laboratory analysis. In contrast, WAMEX geochemical data are derived from exploration and mining activities in Western Australia, reported by companies to the Geological Survey of Western Australia (GSWA). GSWA applies quality control measures at the time of data submission, but there is likely to be some inclusion of spurious results (e.g. errors in unit reporting, multiple field names for the same analyte, incorrect assignment of analytes).

For each derived geochemical layer, a unique legend colour scheme has been applied to best elucidate geochemical trends. Higher element abundance values are plotted on top of lower values to more clearly show spatial gradients in element concentrations.

How to access

These data form part of the Southwest Yilgarn, 2021 Geological Exploration Package, available on a USB via the DMIRS eBookshop.

Recommended reference

Grech, LL, Duuring, P, Guilliamse, JN and Morin-Ka, S, 2021, Geochemical pathfinders for porphyry Cu–Au–Mo mineralizing systems in the southwest Yilgarn: Geological Survey of Western Australia, digital data layers.

MINEDEX observations of copper sites in the southwest Yilgarn

by

JN Guilliamse, P Duuring and S Morin-Ka

Abstract

This layer shows the distribution of known copper-rich sites in the southwest Yilgarn. Copper mineralization sites are extracted from the MINEDEX database, which provides a coordinated, project-based inquiry system for textual information on mine, deposit, prospect and occurrence locations (coordinates, etc.), as well as mineral resources and mine production. Data are collated from ASX reports, statutory exploration reports, mining proposals and production returns.

The derived copper mineralization sites are selected to exclude exploration targets and infrastructure not directly related to mineralization, such as tailings storage facilities and processing plants. Copper sites are derived from the SITE_COMMODITY field in the MINEDEX database.

The order of listing of the commodity in the SITE_COMMODITY field reflects its relative importance at that site. Only those identified as target commodities and listed in the TARGET_COMMODITY_GROUP field are classified in MINEDEX into four groups: mine, deposit, prospect and occurrence (Table 1). Therefore, the SITE_TYPE_DESCRIPTION (i.e. mine, deposit, prospect or occurrence) is only applicable to the selected commodity if it is also listed in the TARGET_COMMODITY_GROUP field. When the commodity for a mineralization site is not listed in the TARGET_COMMODITY field, then it is not possible to allocate the relevant SITE_TYPE_DESCRIPTION without further investigation of the source data. In these instances, the site remains unclassified with respect to SITE_TYPE_DESCRIPTION.

The distribution of known copper sites in the southwest Yilgarn correlate with the mapped location of greenstone belts, shear zones and faults.

Table 1. Legend description

Site type	Definition
Cu Mine	A deposit which is being mined, was previously mined, or is proposed to be mined.
Cu Deposit	A mineral occurrence with probable economic value and for which there is an established resource.
Cu Prospect	Any mineral occurrence where economic grades have been intersected over a significant width and strike length but for which there is not yet a resource, or any working or exploration activity that has found subeconomic mineral occurrences and from which there is no recorded production.
Cu Occurrence	An occurrence (excluding those defined as mines, deposits or prospects) can be defined if an economic mineral has been identified in outcrop, or if assay results exceed an agreed concentration and size.
Cu Unclassified	Mineralization site for which the TARGET_COMMODITY_GROUP does not reflect the specified commodity, and hence the SITE_TYPE_DESCRIPTION is not applicable.

How to access

These data form part of the Southwest Yilgarn, 2021 Geological Exploration Package, available on a USB via the DMIRS eBookshop.

Recommended reference

Guilliamse, JN, Duuring, P and Morin-Ka, S 2021, MINEDEX observations of copper sites in the southwest Yilgarn: Geological Survey of Western Australia, digital data layers.

MINEDEX observations of lead sites in the southwest Yilgarn

by

JN Guilliamse, P Duuring and S Morin-Ka

Abstract

This layer shows the distribution of known lead-rich sites in the southwest Yilgarn. Lead mineralization sites are extracted from the MINEDEX database, which provides a coordinated, project-based inquiry system for textual information on mine, deposit, prospect and occurrence locations (coordinates, etc.), as well as mineral resources and mine production. Data are collated from ASX reports, statutory exploration reports, mining proposals and production returns.

The derived lead mineralization sites are selected to exclude exploration targets and infrastructure not directly related to mineralization, such as tailings storage facilities and processing plants. Lead sites are derived from the SITE_COMMODITY field in the MINEDEX database.

The order of listing of the commodity in the SITE_COMMODITY field reflects its relative importance at that site. Only those identified as target commodities and listed in the TARGET_COMMODITY_GROUP field are classified in MINEDEX into four groups: mine, deposit, prospect and occurrence (Table 1). Therefore, the SITE_TYPE_DESCRIPTION (i.e. mine, deposit, prospect or occurrence) is only applicable to the selected commodity if it is also listed in the TARGET_COMMODITY_GROUP field. When the commodity for a mineralization site is not listed in the TARGET_COMMODITY field, then it is not possible to allocate the relevant SITE_TYPE_DESCRIPTION without further investigation of the source data. In these instances, the site remains unclassified with respect to SITE_TYPE_DESCRIPTION.

The distribution of known lead sites in the southwest Yilgarn correlate with the mapped location of greenstone belts, shear zones and faults.

Table 1. Legend description

Site type	Definition
Pb Mine	A deposit which is being mined, was previously mined, or is proposed to be mined.
Pb Deposit	A mineral occurrence with probable economic value and for which there is an established resource.
Pb Prospect	Any mineral occurrence where economic grades have been intersected over a significant width and strike length but for which there is not yet a resource, or any working or exploration activity that has found subeconomic mineral occurrences and from which there is no recorded production.
Pb Occurrence	An occurrence (excluding those defined as mines, deposits or prospects) can be defined if an economic mineral has been identified in outcrop, or if assay results exceed an agreed concentration and size.
Pb Unclassified	Mineralization site for which the TARGET_COMMODITY_GROUP does not reflect the specified commodity, and hence the SITE_TYPE_DESCRIPTION is not applicable.

How to access

These data form part of the Southwest Yilgarn, 2021 Geological Exploration Package, available on a USB via the DMIRS eBookshop.

Recommended reference

Guilliamse, JN, Duuring, P and Morin-Ka, S 2021, MINEDEX observations of lead sites in the southwest Yilgarn: Geological Survey of Western Australia, digital data layers.

MINEDEX observations of zinc sites in the southwest Yilgarn

by

JN Guilliamse, P Duuring and S Morin-Ka

Abstract

This layer shows the distribution of known zinc-rich sites in the southwest Yilgarn. Zinc mineralization sites are extracted from the MINEDEX database, which provides a coordinated, project-based inquiry system for textual information on mine, deposit, prospect and occurrence locations (coordinates, etc.), as well as mineral resources and mine production. Data are collated from ASX reports, statutory exploration reports, mining proposals and production returns.

The derived zinc mineralization sites are selected to exclude exploration targets and infrastructure not directly related to mineralization, such as tailings storage facilities and processing plants. Zinc sites are derived from the SITE_COMMODITY field in the MINEDEX database.

The order of listing of the commodity in the SITE_COMMODITY field reflects its relative importance at that site. Only those identified as target commodities and listed in the TARGET_COMMODITY_GROUP field are classified in MINEDEX into four groups: mine, deposit, prospect and occurrence (Table 1). Therefore, the SITE_TYPE_DESCRIPTION (i.e. mine, deposit, prospect or occurrence) is only applicable to the selected commodity if it is also listed in the TARGET_COMMODITY_GROUP field. When the commodity for a mineralization site is not listed in the TARGET_COMMODITY field, then it is not possible to allocate the relevant SITE_TYPE_DESCRIPTION without further investigation of the source data. In these instances, the site remains unclassified with respect to SITE_TYPE_DESCRIPTION.

The distribution of known zinc sites in the southwest Yilgarn correlate with the mapped location of greenstone belts, shear zones and faults.

Table 1. Legend description

Site type	Definition
Zn Mine	A deposit which is being mined, was previously mined, or is proposed to be mined.
Zn Deposit	A mineral occurrence with probable economic value and for which there is an established resource.
Zn Prospect	Any mineral occurrence where economic grades have been intersected over a significant width and strike length but for which there is not yet a resource, or any working or exploration activity that has found subeconomic mineral occurrences and from which there is no recorded production.
Zn Occurrence	An occurrence (excluding those defined as mines, deposits or prospects) can be defined if an economic mineral has been identified in outcrop, or if assay results exceed an agreed concentration and size.
Zn Unclassified	Mineralization site for which the TARGET_COMMODITY_GROUP does not reflect the specified commodity, and hence the SITE_TYPE_DESCRIPTION is not applicable.

How to access

These data form part of the Southwest Yilgarn, 2021 Geological Exploration Package, available on a USB via the DMIRS eBookshop.

Recommended reference

Guilliamse, JN, Duuring, P and Morin-Ka, S 2021, MINEDEX observations of zinc sites in the southwest Yilgarn: Geological Survey of Western Australia, digital data layers.

Dyke and structure density of the southwest Yilgarn

by

TJ Ivanic

Abstract

Two raster layers were produced covering the southwest Yilgarn. Vector layers for dykes and structural line work at 1: 100 000 (interp_geo_lne _100k and interp_struc_lne_100k) were the inputs for these layers. A line density operation was run on each layer in QGIS using a search radius of half a degree and an output pixel size of a quarter of a degree.

Caveats to bear in mind for these datasets are that in some areas, the intensity of line work (dykes and structures) drawn by geologists on the vector layers will vary significantly, according to the focus of the mapping, the availability of outcrop and the detail of magnetic surveys, and coverage may be incomplete. At the edges of the map area, density values drop to zero, which reflects the absence of mapped features outside of the study area.

Initial observations indicate that there is a higher density of dykes around the margins of the Yilgarn Craton (Fig. 1a), but also in a northwest-trending domain, located to the south of the Corrigin Tectonic Zone, coincident with a high-gravity gradient. In contrast, the density of mapped structures is high along the Corrigin Tectonic Zone; there are also highs at Southern Cross and Ravensthorpe and along the southern margin of the Yilgarn Craton (Fig. 1b).

How to access

The Dyke and structure density of the southwest Yilgarn digital data are available as a USB via the DMIRS eBookshop.

Recommended reference

Ivanic, TJ 2021, Dyke and structure density of the southwest Yilgarn: Geological Survey of Western Australia, digital data layer.

EXPLORATION INCENTIVE SCHEME

Australian Government
Geoscience Australia

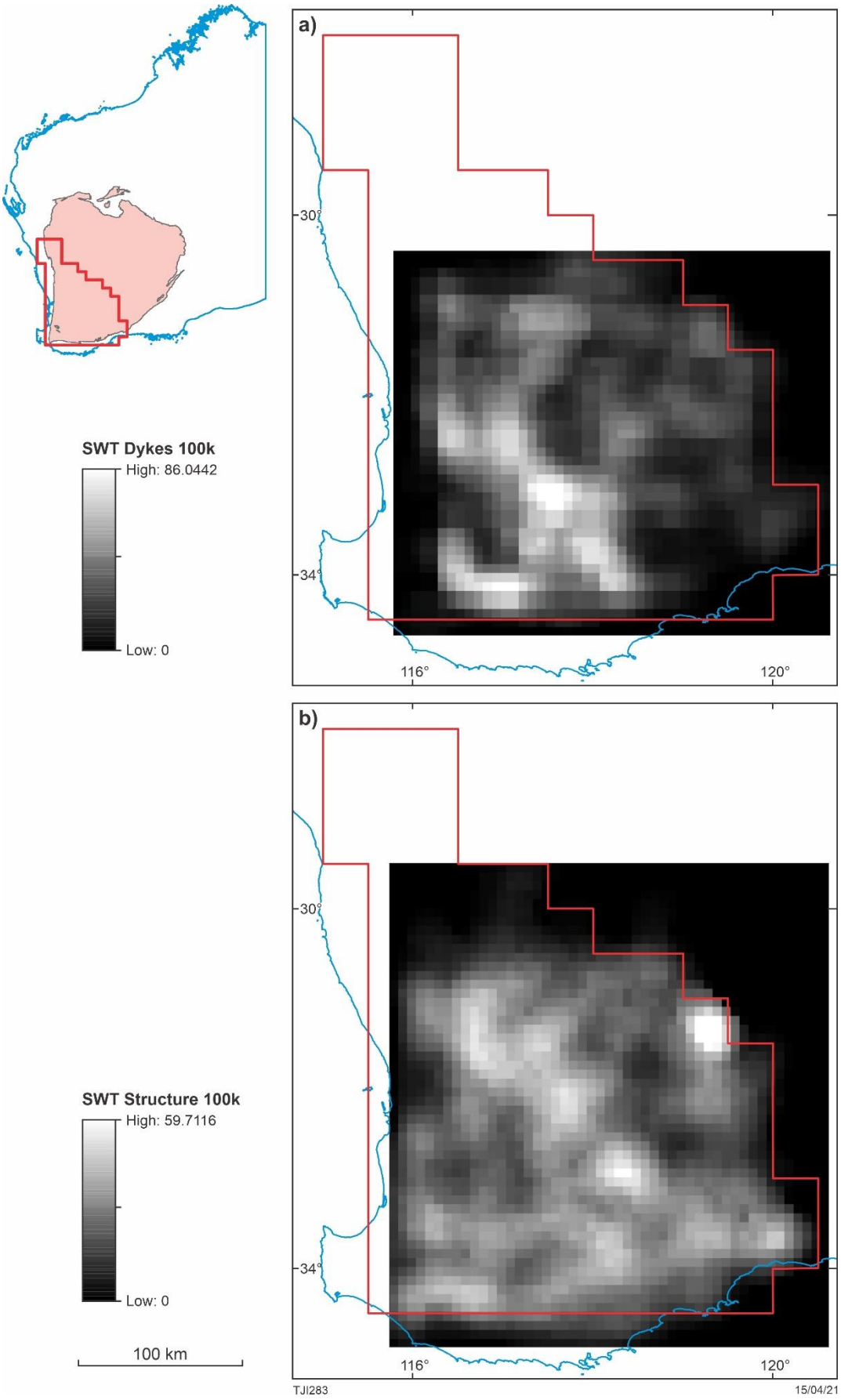

Figure 1. a) dyke density map; b) structure density map

Magmatic and stratigraphic WAROX text search results for the southwest Yilgarn

by

TJ Ivanic, DE Kelsey and P Duuring

Abstract

Specific text searches were conducted on lithological, textural and mineral-name categories from WAROX field observations in order to provide a spatial distribution of features relating to magmatic and stratigraphic mineral systems. The WAROX database contains geoscientific data related to observations and samples collected in the field. The data cover themes such as outcrop geology, regolith geology, field photographs, geological samples, rock physical properties, petrography, paleontology and geochronology.

A total of 26 text searches of the WAROX database were conducted in order to yield the distribution of various lithologies and lithological characteristics across the southwest Yilgarn (Fig. 1). Within the project area, the searches did not include the following 1:250 000-scale map sheets: RAVENSTHORPE, YALGOO, GERALDTON – HOUTMAN ABROLHOS and DONGARA – HILL RIVER. The results tables were converted into 26 shapefiles allocated to six groups: 'high-grade metamorphic', 'mafic', 'ultramafic', 'volcanic', 'special granitic' and 'sedimentary'.

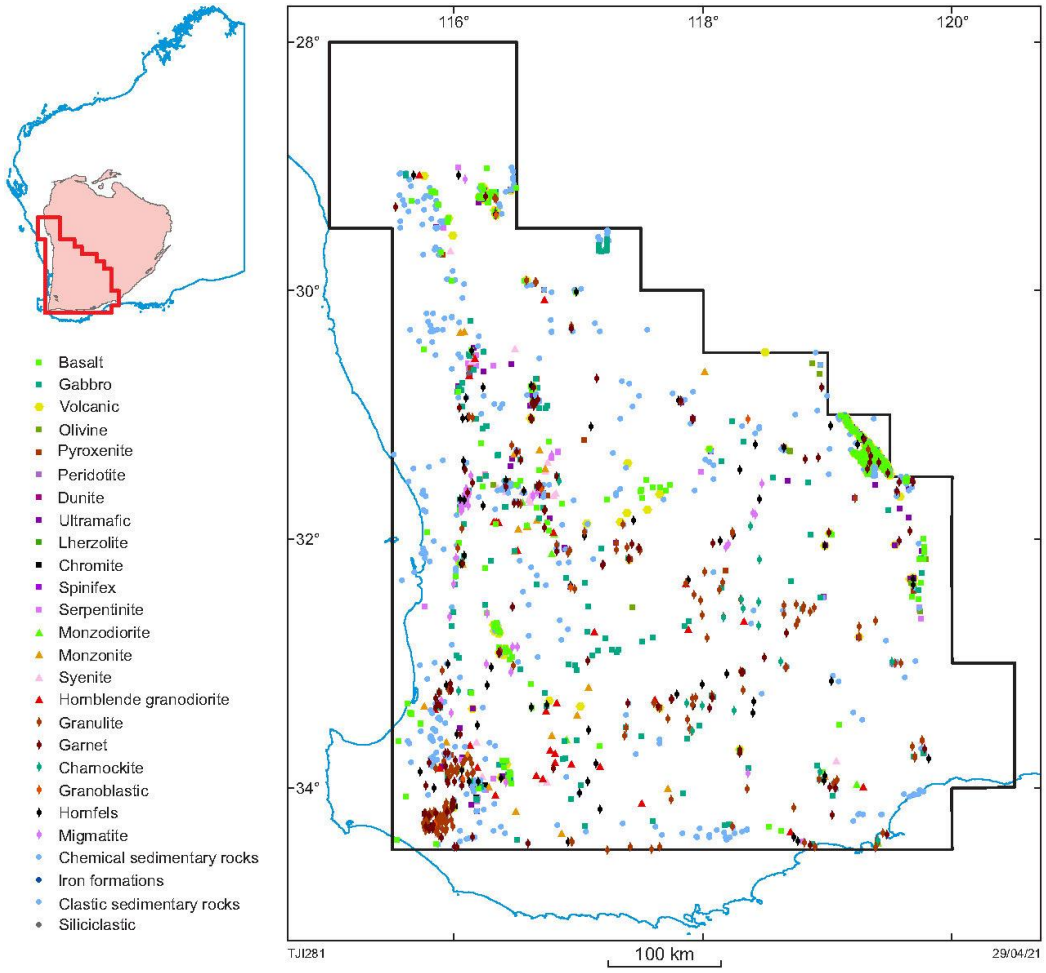

Figure 1. Distribution of WAROX text search results in the southwest Yilgarn

The "WAROX_{text string}" layers show the distribution of {text string} in the southwest Yilgarn (Table 1), where {text string} refers to the text-based search query (e.g. 'high-grade metamorphic'). The derived layer shows 'site' and 'secthole' WAROX locations where {text string} is recorded (Table 2).

Table 1. Description of the query performed on WAROX data to derive layers containing data matching the specific text string

Operation	*Query*
WAROX data are queried to select {text string} from any field in the WAROX database	Any field = '{text string}'

Table 2. WAROX text search layers and their text strings

Group	*Layer Name*	*Text string*
Mafic	WAROX_MF_Basalt	basalt
	WAROX_MF_Gabbro	gabbro
Volcanic	WAROX_Volcanic	volcan
Ultramafic	WAROX_UM_Olivine	olivine
	WAROX_UM_Pyroxenite	pyroxenit
	WAROX_UM_Peridotite	peridotite
	WAROX_UM_Dunite	dunite
	WAROX_UM_Ultramafic	ultramafic
	WAROX_UM_Lherzolite	lherzolite
	WAROX_UM_Chromite	chromit
	WAROX_UM_Spinifex	spinifex
	WAROX_UM_Serpentinite	serpentinite
Special granitic	WAROX_GR_Monzodiorite	monzod
	WAROX_GR_Monzonite	monzon
	WAROX_GR_Syenite	syenite
	WAROX_GR_HornblendeGranodiorite	hornblende gran
High-grade metamorphic	WAROX_MT_Granulite	granulit
	WAROX_MT_Garnet	garnet
	WAROX_MT_Charnockite	charn
	WAROX_MT_Granoblastic	granoblastic
	WAROX_MT_Hornfels	hornfels
	WAROX_MT_Migmatite	migmatit
Sedimentary	WAROX_SD_ChemicalSedimentaryRocks	chemical sedimentary
	WAROX_SD_IronFormations	iron formation
	WAROX_SD_ClasticSedimentaryRocks	clastic sedimentary
	WAROX_SD_Siliciclastic	siliciclastic

Caveats in utilizing the WAROX database are that different geologists may have used words differently or missed particular features in their rock descriptions, which means that the absence of a search result does not necessarily imply the absence of the feature.

'High-grade metamorphic' rock or mineral searches yielded a high concentration of occurrences along the Corrigin Tectonic Zone and in a 200 km-long, northwest-striking domain immediately east (wider in the south than the north). There is also a high density of observations recorded along the western margin of the Yilgarn Craton close to the Darling Fault. Notable absences of returned WAROX information are at Boddington and Wongan Hills, which are known to have reached greenschist or amphibolite grade at most.

'Mafic' search results are widespread and, as expected, are located in known greenstone belts. Basaltic rocks are not observed in strongly recrystallized domains (e.g. between Corrigin and Hyden), but this may be due to the inability to assign a protolith rather than the absence of fine-grained protoliths. Within the South West Terrane, notable clusters of 'basalt' occur at Boddington, Wongan Hills and Kellerberrin, with the latter due to observations of Proterozoic dykes. Similarly, a cluster of 'gabbro' results are distributed along the Jimberlana Dyke. A cluster of 'metabasalt' results occurs in the vicinity of Boyup Brook, which has not previously been recognized as a greenstone belt.

'Ultramafic' search results reveal three zones: (1) Youanmi Terrane greenstone belts, such as Ravensthorpe, Forrestania, Yalgoo–Singleton — these are the only areas where geologists have mentioned 'spinifex' textures; none are recorded in the South West Terrane; (2) New Norcia to Beverley, including areas around known Ni and V deposits such as Yarrawindah, Julimar and Coates Siding; (3) far southwest Yilgarn, including Yornup Ni and, notably, several mentions of 'chromite' between Bridgetown and Charnwood Forest.

'Volcanic' search results were rare, perhaps largely due to high-grade metamorphism across a wide expanse of the South West Terrane, where geologists were unable to establish the grain size of the protolith from recrystallized rocks. High concentrations are located at Boddington, Ravensthorpe and Forrestania.

'Special granitic' searches for 'hornblende granodiorite' and 'hornblende tonalite' show a distribution that is almost entirely confined to the southwest of the Corrigin Tectonic Zone. 'Syenite' returned results along the southern edge of the Yilgarn Craton and in a cluster around Chidlow.

'Sedimentary' searches reveal a band of scattered observations of 'iron formation' and 'chemical sedimentary' along the Corrigin Tectonic Zone, whereas to the southwest, they are largely absent. There is a higher abundance of siliciclastic rocks in the southwest corner of the South West Terrane, along the western margin of the Yilgarn Craton and within the Jimperding metamorphic belt.

How to access

The Magmatic and stratigraphic WAROX text search results for the southwest Yilgarn digital data are available on a USB via the DMIRS eBookshop.

Recommended reference

Ivanic, TJ, Kelsey, DE and Duuring, P 2021, Magmatic and stratigraphic WAROX text search results for the southwest Yilgarn: Geological Survey of Western Australia, digital data layer.

EXPLORATION INCENTIVE SCHEME

Australian Government
Geoscience Australia

New geochemical constraints on the mafic and ultramafic rocks of the southwest Yilgarn

by

TJ Ivanic, JR Lowrey and RH Smithies

Abstract

A total of 312 recently acquired whole-rock major and trace element analyses, of rocks collected mainly from drillcores in the southwest Yilgarn, have been examined and classified into preliminary geochemical groups. Samples were selected from representative rock types in each lithostratigraphic unit examined in core. Visibly weathered, altered or mineralized rocks were avoided. In addition, we show data from 51 samples of Proterozoic dykes collected by Stark et al. (2018, 2019) and Wang et al. (2014).

The dataset predominantly comprises Archean greenstone samples (n = 269), including metamorphosed mafic–ultramafic intrusive rocks (n = 167), volcanic rocks (n = 86) and sedimentary rocks (n = 16). There are also 40 samples of Proterozoic mafic dykes. The Archean samples are divided into those with an assumed age of either Meso- to Neoarchean or Neoarchean. The Meso- to Neoarchean samples from the northeastern part of the study area (northeast of the Corrigin Tectonic Zone) have tholeiitic compositions. Based on trace element concentrations, they are subdivided into those derived from a depleted mantle source (2.9 – 3.1 Ga, Mount Gibson, i.e. older Youanmi Terrane, affinity) and those with an enriched bulk source composition (2.75 – 2.82 Ga, Polelle Group, i.e. younger Youanmi Terrane, affinity). Samples of metagabbroic rocks from within the Corrigin Tectonic Zone, including samples from the Tampia Au deposit, have not been assigned to a suite. Samples southwest of the Corrigin Tectonic Zone (assumed to be Neoarchean) are tentatively grouped into Yarrawindah and Red Hill 'suites' based on low-Nb/Th vs Fe-rich tholeiitic compositions, respectively. Volcanic and plutonic rocks from Wheatley are not assigned to a suite owing to insufficient data. Figure 1a shows the distribution of samples and their assigned chemical group; Figure 1b shows the MgO wt% values for the samples.

The majority of mafic volcanic and plutonic rocks from Calingiri, Wongan Hills and Westonia have La_N/Gd_N <1 (N = normalized to primitive mantle), 45–54 wt% SiO_2, 5–9 wt% MgO and have low light rare earth elements (LREE; i.e. $[La/Gd]_N$ <1) and large ion lithophile elements (LILE) concentrations. The samples also contain up to 2.6 wt% TiO_2, 595 ppm V, 2570 ppm Cr and 1590 ppm Ni. They collectively form a steep trend on the Th/Yb vs Nb/Yb plot (Pearce, 2014), oblique to the mantle array, indicating mixing between N-MORB-like parent magmas and Th-enriched crust, widely interpreted to reflect assimilation of felsic crust in Archean greenstone terranes (Smithies et al., 2018).

Mafic to ultramafic volcanic and plutonic rocks from Woongaring and Lake King can be divided into three chemical groups. Collectively these groups form a tholeiitic trend on an AFM diagram (trivariate plot of alkalis, Fe and Mg.

1. A group of low-Th mafic rocks that contain 47.6 – 49.8 wt% SiO_2, 8 – 11.7 wt% MgO, 120–490 ppm Ni, 180–250 ppm Cr and 260–335 ppm V. The first group have moderate TiO_2 (mostly 0.8 – 1 wt%), subchondritic Al_2O_3/TiO_2 (13–18) and are LREE depleted ($[La/Gd]_N$ <0.9) with relatively flat middle to heavy REE patterns ($[Gd/Yb]_N$ ~1), comparable to NMORB.
2. A group of intermediate-Th ultramafic cumulate rocks containing 47.3 – 53.5 wt% SiO_2, 16–33.6 wt% MgO, higher Ni and Cr (560–1790 and 1840–2770 ppm respectively) and lower V (70–240 ppm; Ti/V ~19). Olivine cumulate samples from the second group show significant variation in their trace element patterns. However, samples containing <24 wt% MgO have more consistent mantle-normalized trace element patterns with flat LREE and depleted HREE

patterns ($[La/Gd]_N$ ~1, $[Gd/Yb]_N$ ~1.4), and lower Al_2O_3 at a given MgO concentration than MORB-like tholeiitic, or Al-undepleted komatiitic rocks. These lower-MgO rocks are chemically similar to those that dominate the Eastern Yilgarn Craton, and are therefore more compositionally similar to Al-depleted komatiites, similar to those along strike at Ravensthorpe and in the adjacent Southern Cross greenstone belt.

3. A group of ultramafic rocks containing 46.5 – 48.3 wt% SiO_2, 23–28 wt% MgO, 1420–1590 ppm Ni, 2390–2570 ppm Cr and 120–140 ppm V. They are LREE–MREE-depleted with low TiO_2 (0.4 wt%; Ti/V ~16) and Al_2O_3/TiO_2 ~17.

Ultramafic (and lesser mafic) plutonic rocks from the Yarrawindah and Yornup Ni–Cu prospects contain 8–37 wt% MgO and 37–55 wt% SiO_2 and are variably enriched in LILE and LREE; ultramafic rocks (serpentinized olivine-pyroxene cumulates) contain very low concentrations of LILE and REE and are LREE-depleted ($[La/Gd]_N$ <1) whereas plagioclase-bearing mafic–ultramafic cumulates contain higher relative abundances of LILE and REE, and are LREE-enriched ($[La/Gd]_N$ >1). The samples contain up to 2.7 wt% TiO_2, 506 ppm V, 8040 ppm Cr and 4240 ppm Ni. Although these rocks collectively show the effects of accumulation of mineral phases, they are all characterized by low Nb/Yb indicating a strongly depleted mantle source, while the presence of concave-up REE patterns, particularly in the plagioclase-bearing cumulates, also suggests an enriched (crustal) component. They collectively define a low-angle trend on the Th/Yb–Nb/Yb plot, parallel to the Phanerozoic mantle array and within the arc field, possibly indicating a metasomatized mantle source. We do note that the extent of the trend is almost certainly exaggerated due to fractionation and accumulation of various minerals that concentrate Yb, Th and Nb to very different degrees.

Mafic and ultramafic plutonic samples from Katanning (Red Hill deposit) are characteristically Fe-rich with 7–72 wt% Fe_2O_{3Total}, 1–11 wt% MgO, 34–51 wt% SiO_2, $[La/Gd]_N$ >1 and are slightly enriched in LILE. The samples contain up to 15.7 wt% TiO_2, 6600 ppm V, 572 ppm Cr and 284 ppm Ni. These rocks form a strong, steep tholeiitic trend on the AFM diagram. Their highly variable Th/Yb and Nb/Yb is likely due to alteration and mineral accumulation processes.

Unassigned rocks in this dataset show a variety of trace element patterns, some of which have a strong similarity to other suites described above. Additional trace element patterns and unique Th/Yb vs Nb/Yb compositions among unassigned rocks indicate the presence of several undefined suites. Furthermore, these additional compositions may have been the result of trace element mobility under granulite facies conditions across large parts of the South West Terrane.

Samples of mafic dykes (n = 110) are classified into Warakurna, Marnda Moorn, Biberkine and Boonadgin suites with 50 samples remaining unassigned due to unknown orientation or age. The Marnda Moorn suite (Gnowangerup–Fraser Dyke Suite; Group I, Wang et al., 2014) has the most Fe-rich, tholeiitic trend on the AFM diagram; however, most major elements do not discriminate clearly between the samples assigned to suites with 3–8 wt% MgO, 47–56 wt% SiO_2. In terms of trace elements, the Marnda Moorn suite has broadly chondritic REE ratios ($[La/Gd]_N$ ~1), while the other suites are typically LREE enriched ($[La/Gd]_N$ >1 and typically >4) and have moderate enrichments in LILE. In this dataset, Proterozoic mafic dykes contain up to 2.75 wt% TiO_2, 550 ppm V, 350 ppm Cr and 125 ppm Ni, with one lamprophyre containing 433 ppm Cr and 182 ppm Ni. The Gnowangerup–Fraser Dyke Suite (Group 1; Wang et al., 2014) plots on and immediately adjacent to the mantle array, close to E-MORB on the Th/Yb vs Nb/Yb plot, and the other suites plot above the mantle array, indicative of limited crustal contamination in the latter. Unassigned dykes yield compositions that overlap with the assigned suites in addition to other compositions indicative of unnamed suites.

The classifications of Archean greenstones in this dataset allow for tentative correlations to be made across large areas of previously poorly understood terrain. From east to west, we tentatively correlate magmatic rocks into four, north or northwesterly trending zones as follows: (1) a volcanic and intrusive, high-Mg suite, with Polelle Group affinity between Woongaring and Lake King, potentially coeval with Forrestania and Ravensthorpe; (2) a volcanic and intrusive, moderate-Mg suite with Mount Gibson affinity between Wongan Hills and Westonia, provisionally interpreted as magmatism

as the result of a protracted rifting event; (3) an intrusive, high-Fe suite at Red Hill (Red Hill suite), which is tholeiitic, and the result of a high degree of partial melting of the mantle, possibly coeval with the Coates Siding Gabbro at 2664 ± 6 Ma (Wilde and Pidgeon, 2006); (4) an intrusive high-Mg suite in the far west between Yarrawindah and Yornup, possibly coeval with the Red Hill suite and potentially indicative of the localized involvement of a metasomatized mantle source. This high-Mg suite shares lithological characteristics with rocks from the highly mineralized Julimar deposit, in particular the Gonneville intrusion, which has a magmatic crystallization age of 2668 ± 4 Ma (GSWA 203747; Wingate et al., 2021).

How to access

The New geochemical constraints on the mafic and ultramafic rocks of the southwest Yilgarn data layer forms part of the Southwest Yilgarn, 2021 Geological Exploration Package, available on a USB via the DMIRS eBookshop.

References

Pearce, J, 2014, Geochemical Fingerprinting of the Earth's Oldest Rocks: Geology, v. 42, p. 175–176.

Smithies, RH, Ivanic, TJ, Lowrey, JR, Morris, PA, Barnes, SJ, Wyche, S and Lu, Y-J 2018, Two distinct origins for Archean greenstone belts: Earth and Planetary Science Letters, v. 487, p. 106–116.

Stark, JC, Wang, X-C, Denyszyn, SW, Li, Z-X, Rasmussen, B, Zi, J-W, Sheppard, S and Liu, Y 2019, Newly identified 1.89 Ga mafic dyke swarm in the Archean Yilgarn Craton, Western Australia suggests a connection with India: Precambrian Research, v. 329, p. 156–169.

Stark, JC, Wang, X-C, Li, Z-X, Denyszyn, SW, Rasmussen, B and Zi, J-W 2018, 1.39 Ga mafic dyke swarm in southwestern Yilgarn Craton marks Nuna to Rodinia transition in the West Australian Craton: Precambrian Research, v. 316, p. 291–304, 14p., doi:10.1016/j.precamres.2018.08.014.

Wang, X-C, Li, Z-X, Li, J, Pisarevsky, SA and Wingate, MT 2014, Genesis of the 1.21 Ga Marnda Moorn large igneous province by plume–lithosphere interaction: Precambrian Research, v. 241, p. 85–103, 19p., doi:10.1016/j.precamres.2013.11.008.

Wilde, SA and Pidgeon, RT 2006, Nature and timing of Late Archaean arc magmatism along the western margin of the Yilgarn Craton: Goldschmidt Geochemistry Conference abstract, #670.

Wingate, MTD, Lu, Y, Ivanic, TJ 2021, Pegmatitic metagabbro, Wooroloo: Geological Survey of Western Australia Geochronology Report, 4pp.

Recommended reference

Ivanic, TJ, Lowrey, JR and Smithies, RH 2021, New geochemical constraints on the mafic and ultramafic rocks of the southwest Yilgarn: Geological Survey of Western Australia, digital data layer.

EXPLORATION INCENTIVE SCHEME

Australian Government
Geoscience Australia

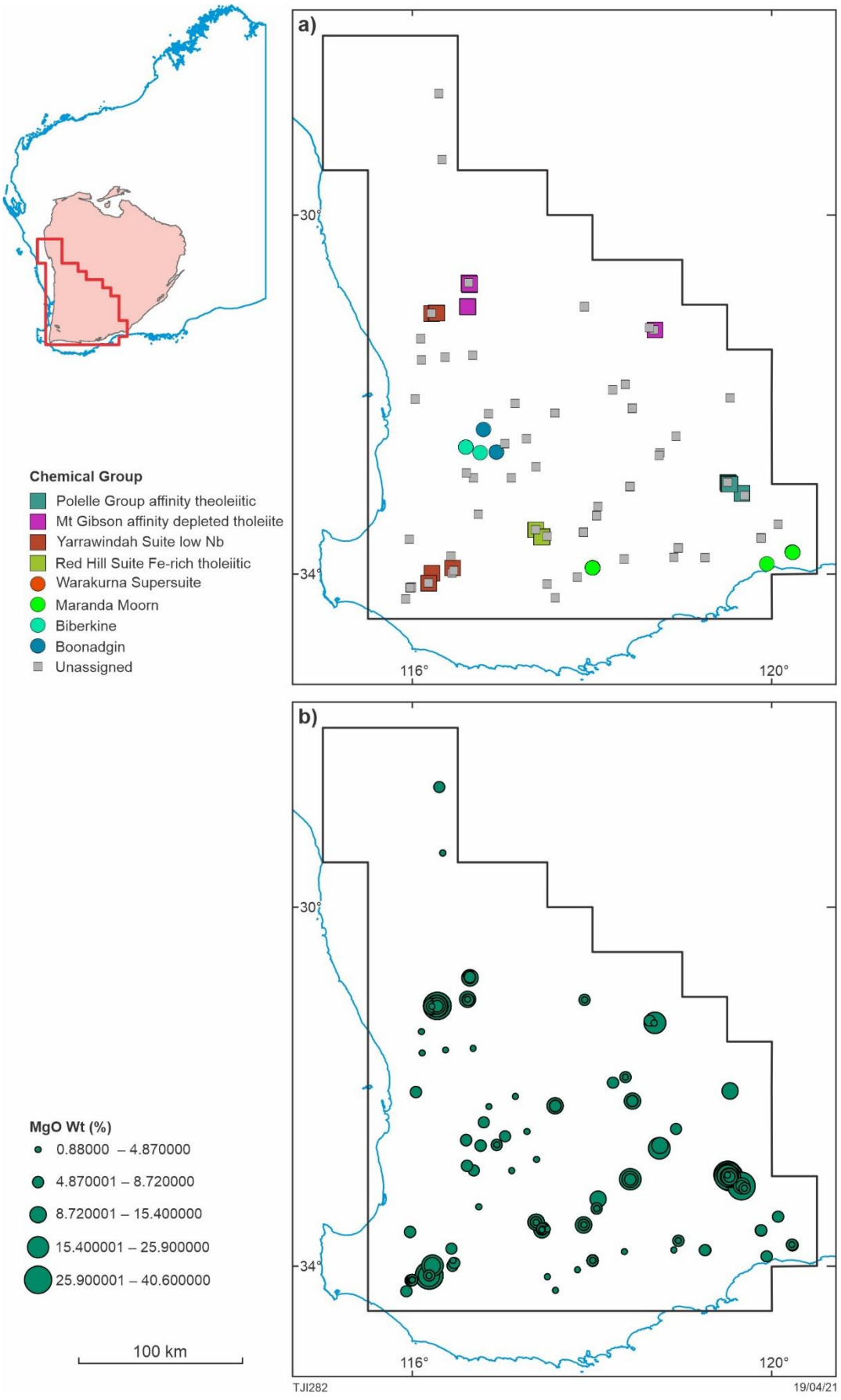

Figure 1. a) Distribution of samples and chemical group; (b) MgO wt.% values for the samples

Metamorphic evolution of the southwest Yilgarn

by

FJ Korhonen, ER Blereau, DE Kelsey, IOH Fielding and SS Romano

Abstract

Metamorphic rocks record information about their pressure (*P*)–temperature (*T*)–time (*t*) evolution in the mineral assemblages, the chemistry and variation in composition of these minerals, and the microstructural relationships among them. Our ability to interpret the evidence recorded by metamorphic rocks is critical to understanding their history and to constraining terrane evolution models. As part of the Accelerated Geoscience Program, quantitative *P–T* estimates were derived from an extensive sample set across the southwest Yilgarn. Such data provide powerful insight into the thermal structure of the crust over time, which, in concert with the expanded whole-rock geochemistry and new interpreted basement structure and geology datasets provided as part of the Accelerated Geoscience Program, provide an excellent foundation for understanding the tectonic and geodynamic framework in which the southwest Yilgarn evolved. The metamorphic data show that granulite and amphibolite facies conditions dominate the project area and corresponding apparent thermal gradients occur between 65 and 208 °C/kbar. Elevated apparent thermal gradients of Neoarchean regional metamorphism were likely partly facilitated by elevated crustal radiogenic heat production.

Methodology and layer details

As of April 2021, *P–T* constraints have been obtained from 28 samples across the southwest Yilgarn (Fig. 1), comprising 17 metasedimentary lithologies, three felsic gneisses and eight mafic lithologies. Metamorphic estimates were derived using phase equilibria modelling based on bulk rock chemical compositions (Fig. 2). These composition-specific phase diagrams were calculated using the software THERMOCALC version tc340 (Powell and Holland, 1988) and the internally consistent thermodynamic dataset of Holland and Powell (2011; dataset tc-ds62) for metasedimentary and felsic lithologies and Green et al. (2016; dataset tc-ds63) for mafic lithologies. The chemical systems used for the modelling were selected to include the key elemental components of each sample in order to most closely approximate the actual rock composition; however, the model system is a necessary simplification of the more complex natural system. The metasedimentary samples were generally modelled in the MnNCKFMASHTO ($MnO–Na_2O–CaO–K_2O–FeO–MgO–Al_2O_3–SiO_2–H_2O–TiO_2–O$) system, and mafic samples were modelled in the NCKFMASHTO system. The activity–composition relations used in the modelling for metasedimentary and felsic lithologies are detailed in White et al. (2014a,b), and those used for mafic lithologies are detailed in Green et al. (2016). The interpretation of phase diagrams utilizes detailed petrography to identify the peak assemblage and any possible metamorphic reactions preserved in the rock, manifest as overprinting relationships. Mineral chemistry, thermobarometry and in situ monazite geochronology for samples with such data were also used to further constrain the *P–T–t* evolution. Details for each sample, including location, geologic context, petrographic description, methodology, results, and interpretation, are summarized in the corresponding Metamorphic History Record. The results in this layer are considered to be preliminary until the Metamorphic History Record for a sample has been released. Future *P–T* estimates and age results from additional samples not included on the layer will be released on GeoVIEW.WA as they become available. Additional information on the workflow with relevant background and methodology are provided in Korhonen et al. (2020).

The layer captures several attributes that are relevant for understanding the metamorphic evolution of the southwest Yilgarn. These attributes are summarized in the data dictionary for this layer, but

key attributes are elaborated on here. Unless otherwise specified, reported metamorphic ages herein are based on in situ monazite geochronology using laser ablation inductively coupled plasma mass spectrometry (LA-ICP-MS), and details are or will be available in the corresponding Geochronology Record on GeoVIEW.WA. The *P–T* data for peak metamorphic conditions (M_{pk}) are based on the calculated stability of the peak phase assemblage (Fig. 2). The minimum and maximum values for *P* and *T* are recorded in the data layer, as well as the median value, which are defined by the size of the peak assemblage stability field. An assessment of uncertainty is also provided, which is defined as half of the data range (i.e. the difference between the median and the maximum or minimum values). An uncertainty of '1000' flags a result with only a minimum or maximum constraint, and thus has no data range or median value. For these samples, the minimum or maximum value is reported as the median. The apparent thermal gradient is also calculated for each sample using the minimum, maximum and median *P* and *T* values, defined as the *T/P* ratio, in °C/kbar. The median peak *P*, *T*, and apparent thermal gradient are plotted in three separate digital layers. Warm symbol colours represent higher values, decreasing to cooler colours. Five symbol sizes are used for each layer that correspond to the reliability of the result. Larger symbols represent samples that are more tightly constrained with smaller data ranges and therefore smaller uncertainty. The smallest symbol is for samples with only a minimum or maximum constraint.

Some samples preserve information on the post peak history (M_{rg}), which can be used to infer a retrograde *P–T* trajectory following conditions of peak metamorphism. For these samples, M_{rg} conditions are generally interpreted to be the *P–T* conditions of melt crystallization. The minimum, maximum and median values for M_{rg} *P*, *T* and apparent thermal gradient are reported for these samples, as well as the uncertainty defined as half of the data range for each parameter.

Many of the samples modelled in this study were collected and analysed as part of the unpublished Yilgarn Craton Metamorphic Project (2003–2014). The results from this project have not been released by the Geological Survey of Western Australia (GSWA), although select data are available in Goscombe et al. (2019) using an alternative sample number that is included in the data layer. The layer captures published *P–T* estimates from Goscombe et al. (2019), derived from multiple reaction thermobarometry (avPT in THERMOCALC; Powell and Holland, 1988) and/or conventional thermobarometry. Although these thermobarometric estimates are provided, they have not been integrated with the *P–T* estimates constrained by phase equilibria modelling and thus remain standalone. Any additional information regarding the metamorphic estimate or age for the sample are included in the 'COMMENTS' field.

P–T–t results

The quantitative *P–T* data from all the samples indicate peak metamorphism under amphibolite to granulite facies conditions, consistent with observations from previous studies (e.g. Gee et al., 1981). However, due to the limited exposure of lithologies that typically grow informative metamorphic minerals and low-variance mineral assemblages which can be used to constrain *P–T* conditions, there are data gaps across the project area, particularly in the northeast and southwest (Fig. 1). The majority of samples analysed thus far are from the northwest-trending Corrigin Tectonic Zone (CTZ), with others more proximal to the Youanmi Shear Zone to the east and to the Darling Fault in the west (Fig. 1).

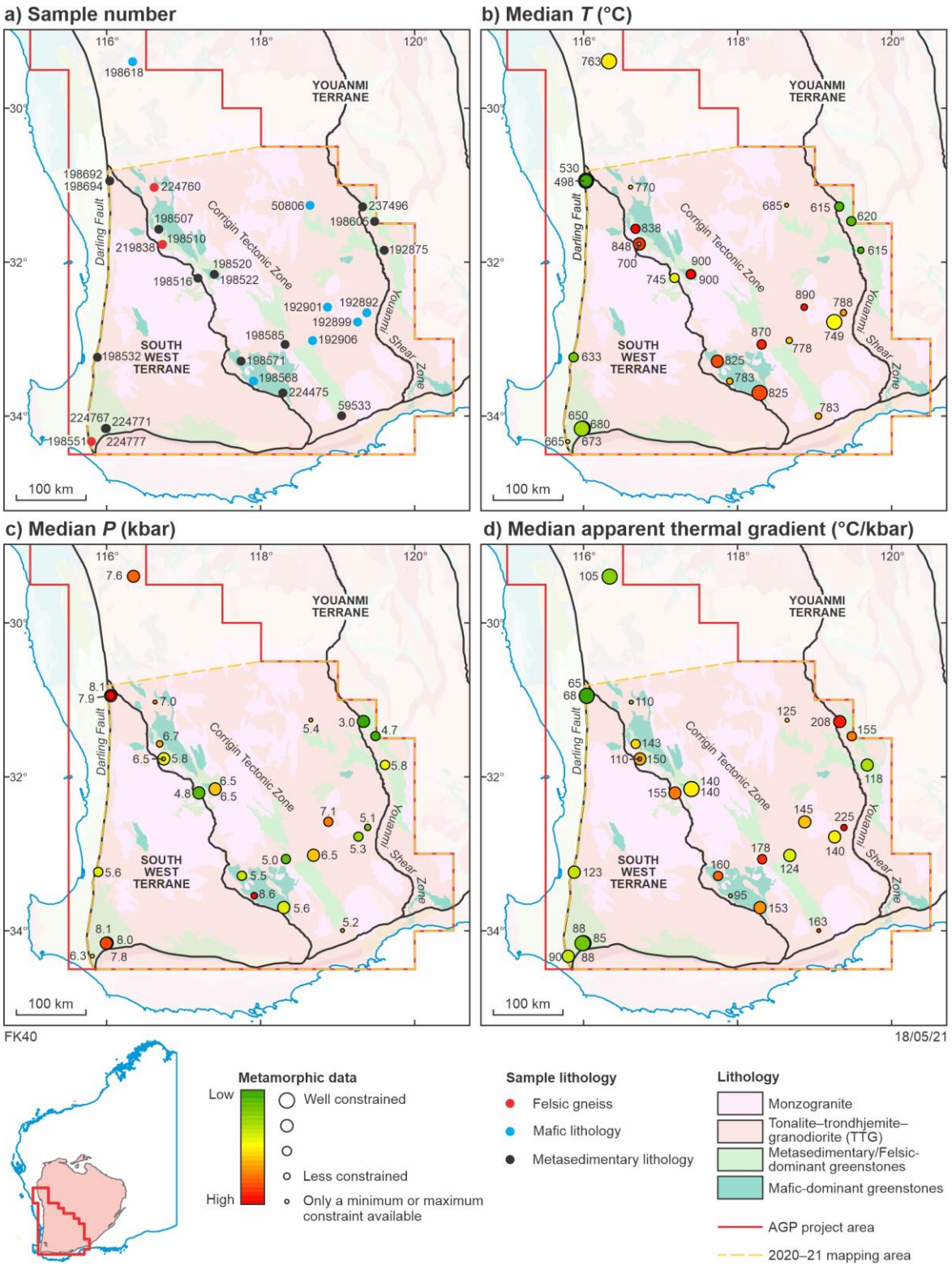

Figure 1. Sample locations and metamorphic data as of April 2021: a) sample location map; b) median *T*; c) median *P*; d) median apparent thermal gradient. Bedrock geology within the 2021–21 mapping area from Quentin de Gromard et al. (2021); other geology based on available 1:500 000 interpreted bedrock geology layers

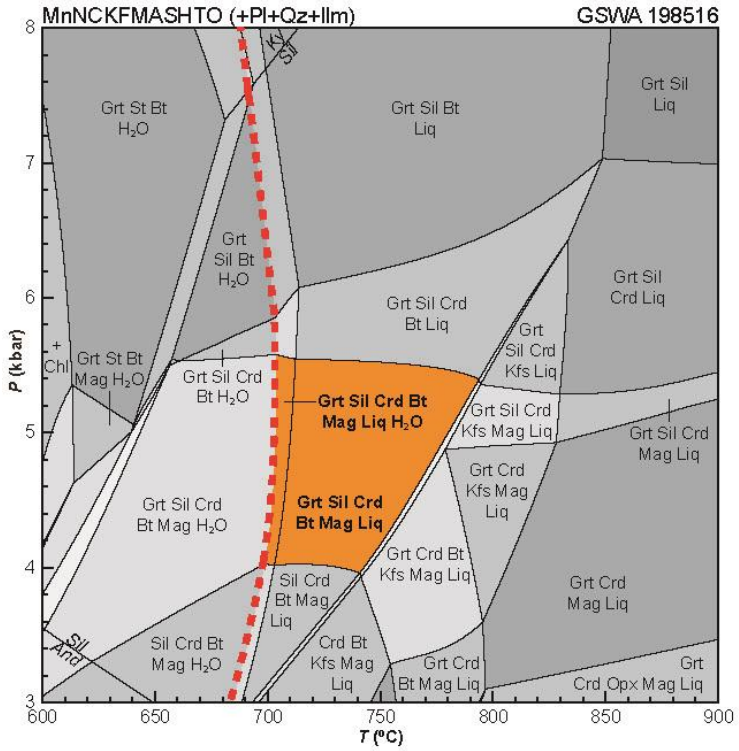

Figure 2. Example of *P–T* phase diagram calculated for a bulk rock chemical composition (GSWA 198516). The *P–T* data for peak metamorphic conditions are based on the calculated stability of the peak phase assemblage, and the minimum and maximum values are defined by the size of the peak assemblage stability field (shown in orange shading with bold text). Red dashed line represents the solidus. Mineral abbreviations provided in Korhonen et al. (2020)

Temperature

High-temperature granulites with median temperatures (T_{med}) between 700 and 900 °C occur within the CTZ (Fig. 1b), a broad zone of ductile transpressional shear zones (Ivanic, 2021; Quentin de Gromard et al., 2021) that forms the redefined boundary (Quentin de Gromard et al., 2021) between the Youanmi and South West Terranes. The timing of high-grade metamorphism and tectonism in this zone is estimated at 2665–2635 Ma, based on U–Pb analyses of monazite from several metamorphic samples (e.g. Fielding et al., 2021a–d) and ages obtained from metamorphic zircon rims (e.g. Wingate et al., 2008; 2021a,b; Lu et al., 2020). The *P–T* estimates for samples that record older ages of c. 2665 Ma (e.g. GSWA 219838) cannot be distinguished from samples that record younger ages of 2655–2635 Ma (e.g. GSWA 198522), supporting a model for a protracted high-*T* event over 30 Ma. This age range extends the timing of high-grade metamorphism previously estimated at 2649–2640 Ma (e.g. Nemchin et al., 1994). To the east of this zone, elevated metamorphic temperatures (>750 °C) are broadly similar to the results from the CTZ (Fig. 1b), although a full interpretation of this data is limited by poor spatial coverage and results with larger *P–T* uncertainties. There are also no metamorphic age constraints available for this part of the project area, as most of the samples are mafic granulites that do not contain datable metamorphic minerals. Distinctly lower temperatures are recorded from samples east of the Youanmi Shear Zone (620–615 °C) and along the western margin near the Darling Fault (680–500 °C; Fig. 1b). The metamorphic samples along the western margin yield a range of Proterozoic ages, with little evidence of the older Archean history preserved. The timing and significance of the Proterozoic reworking is currently being evaluated, although recent mapping within and just east of the Darling Fault supports a polyphase geological history spanning from the Archean to the Mesozoic (Zibra, 2021).

Pressure

Peak pressures (meaning pressures at the peak *T*) across the project area typically range from 4.7 to 6.8 kbar (Fig. 1c), corresponding to mid-crustal depths between about 16 and 24 km by c. 2665 Ma. The majority of the samples in the CTZ record peak pressures of 5.5 – 6.5 kbar, although lower and higher values are also reported. Samples to the east record broadly similar pressures indicating a similar exposed crustal level, although these results are subject to the same data caveats described

above. One sample to the east of the Youanmi Shear Zone in the Southern Cross greenstone belt records a distinctly lower *P* of 3.0 kbar (GSWA 237496). Monazite in a metapelitic schist from the same drillcore yields two age components at c. 2670 and 2630 Ma (Fielding et al., 2021e), suggesting a similar age of metamorphism to the CTZ in this part of the project area. Samples along the western margin near the Darling Fault record notably higher pressures, with peak Proterozoic pressures up to 8.1 kbar (Fig. 1c).

Apparent thermal gradients

Classifying *P–T* data in terms of apparent thermal gradients provides a way of normalizing variations in the crustal depth that is exposed, and instead focusing on the thermal regime that existed at the time of metamorphism. The apparent thermal gradients calculated from the peak *P–T* estimates show relatively uniform values across the project area. Within the CTZ and to the east, the most well constrained samples record apparent thermal gradients typically between 120 and 160 °C/kbar (Fig. 1d). These values straddle the upper limit for high *T/P* ('Barrovian') and lower limit of ultrahigh *T/P* (see Korhonen et al., 2020) and are generally higher than the range observed from other Neoarchean metamorphic events compiled by Brown and Johnson (2018; fig. 3). The two samples within the Southern Cross greenstone belt east of the Youanmi Shear Zone have values of 155 and 208 °C/kbar (Fig. 1d), which are broadly similar to the results from Dalstra et al. (1999). These conditions have been attributed to regional contact metamorphism during the emplacement of voluminous high Ca-granites (Dalstra et al., 1999) and synchronous granite doming and regional folding (Doublier et al., 2014).

Much lower thermal gradients are recorded by the Proterozoic samples along the western margin (65–90 °C/kbar; Fig. 1d). These values are within the range expected for high *T/P* ('Barrovian') metamorphism, but indicate significantly cooler conditions in the crust compared to the 2665–2635 Ma metamorphic event. The *P–T* conditions indicate crustal thickening and burial to depths up to about 28 km; however, metamorphic ages along this margin indicate a polyphase history and the timing of burial, peak metamorphism, and any subsequent reworking has not been firmly established or resolved.

Retrograde history

In this dataset, ten samples preserve evidence for post-peak (M_{rg}) conditions, and eight of those samples can be used to infer a retrograde *P–T* path. Of these eight samples, six are from within the CTZ, and two are located east of the Youanmi Shear Zone. Clockwise *P–T* paths were determined from six of the samples, including the two eastern samples, generally supporting a history of burial and heating. Two potential anticlockwise paths were independently retrieved from the same locality in the central CTZ (GSWA 198520, 198522), whereas a potential clockwise path was recorded in a sample located about 20 km to the west in the footwall of the CTZ (GSWA 198516). Monazite from these three samples yield similar peak metamorphic ages from c. 2656 to 2647 Ma. Although these contrasting trajectories might have tectonic significance, the results for all three samples are also compatible with near isobaric cooling paths. The apparent thermal gradients calculated for peak (M_{pk}) and retrograde (M_{rg}) conditions for the 10 samples are very similar, indicating little change to the thermal structure of the crust during cooling from peak conditions to melt crystallization.

Role of radiogenic heat production for Neoarchean metamorphism in the southwest Yilgarn

The crustal evolution of the southwest Yilgarn is characterized by voluminous granite magmatism between 3010 and 2610 Ma. A compilation of all inferred Archean rock types sampled in the southwest Yilgarn shows that the crustal rocks are elevated in radiogenic heat production (Fig. 3) with an average value in the dataset of 7.1 μWm^{-3} (n=1260) at 2640 Ma, compared to the global crustal average of 2.78 μWm^{-3} (calculated at 2640 Ma). The granites typically have the highest

concentrations of heat-producing elements (HPE) in the dataset, although granites with higher HPEs have whole rock major element compositions that are broadly similar to granites with lower HPEs

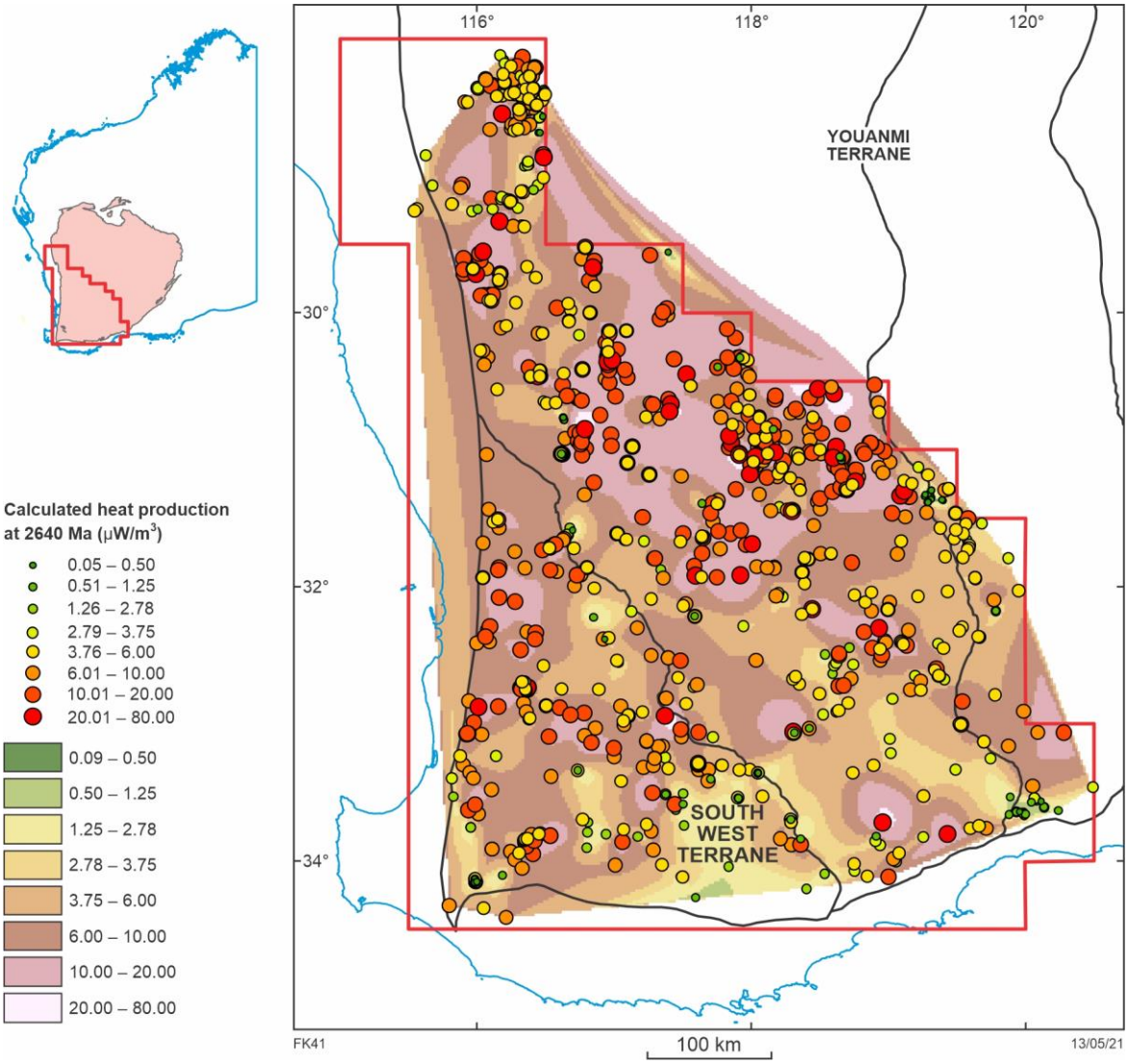

Figure 3. Calculated radiogenic heat production at 2640 Ma for samples of all lithologies within the project area, showing point data and contoured raster image using the Natural Neighbour interpolation tool in ArcGIS Spatial Analyst. The global whole crust average and upper crust average radiogenic heat production at 2640 Ma are 2.78 μWm^{-3} and 3.75 μWm^{-3}, respectively (from Wedepohl, 1995, geochemical data)

(Smithies et al., 2021), indicating that elevated heat production reflects the source characteristics, and is not restricted to low degree partial melts. A long history of elevated heat production in the crust is implied by the calculated heat production of granitic rocks that make up a significant portion of the southwest Yilgarn crust, which were emplaced prior to, synchronous with, and following the 2665–2635 Ma metamorphism. In addition, amphibolite to granulite facies supracrustal rocks in the southwest Yilgarn also have elevated radiogenic heat production values (on average 3.3 μWm^{-3}, n=27; Fig. 3). Together these imply that at the time of 2665–2635 Ma high-*T* metamorphism, and at the depth where amphibolite to granulite facies metamorphism was occurring, the crust was strongly enriched in HPEs, and that magmatism occurring during 2665–2635 Ma metamorphism was sourced from crust with elevated radiogenic heat production. These elevated thermal conditions are also exemplified by a northwest-trending belt of extreme heat production (>10 μWm^{-3}; Fig. 3) in the northern part of the study area that contain low-Ca, high-phosphorus granites with high zircon saturation temperatures (850–950 °C; Smithies et al., 2021), and chemical compositions that are

consistent with high-*T* felsic magmatism (Smithies et al., 2021). These results suggest that large regions of the project area reflect zones of unusually high heat flow both in the source and at the level of emplacement. The thermal drivers for these extreme conditions were likely a combination of elevated crustal heat production (Fig. 3), the effects of regional-scale granite magmatism, and a juvenile mantle contribution at depth.

How to access

The Compilation of metamorphic history information data layer is available on a USB via the DMIRS eBookshop.

References

Brown, M and Johnson, T 2018, Secular change in metamorphism and the onset of global plate tectonics: American Mineralogist, v. 103, no. 2, p. 181–196, doi:10.2138/am-2018-6166.

Dalstra, HJ, Ridley, JR, Bloem, EJM and Groves, DI 1999, Metamorphic evolution of the central Southern Cross Province, Yilgarn Craton, Western Australia: Australian Journal of Earth Sciences, v. 46, p. 765–784.

Doublier, MP, Thébaud, N, Wingate, MTD, Romano, SS, Kirkland, CL, Gessner, K, Mole, DR and Evans, N 2014, Structure and timing of Neoarchean gold mineralization in the Southern Cross district (Yilgarn Craton, Western Australia) suggest leading role of late Low-Ca I-type granite intrusions: Journal of Structural Geology, 67, Part B, p. 205–221, doi:10.1016/j.jsg.2014.02.009.

Fielding, IOH, Wingate, MTD, Korhonen, FJ and Rankenburg, K 2021a, 198516: pelitic granofels, Quajabin Peak; Geochronology Record 1764: Geological Survey of Western Australia, in prep.

Fielding, IOH, Wingate, MTD, Korhonen, FJ and Rankenburg, K 2021b, 198520: pelitic granofels, Tregenza Road; Geochronology Record 1765: Geological Survey of Western Australia, in prep.

Fielding, IOH, Wingate, MTD, Korhonen, FJ and Rankenburg, K, 2021c; 198522: pelitic granofels, Tregenza Road; Geochronology Record 1766: Geological Survey of Western Australia, in prep.

Fielding, IOH, Wingate, MTD, Korhonen, FJ and Rankenburg, K 2021d, 219838: granitic gneiss, Mount Mackie; Geochronology Record 1772: Geological Survey of Western Australia, in prep.

Fielding, IOH, Wingate, MTD, Lu, Y, Korhonen, FJ and Rankenburg, K 2021e, 237497: pelitic gneiss, Sunbeam pit; Geochronology Record 1773: Geological Survey of Western Australia, in prep.

Gee, RD, Baxter, JL, Wilde, SA and Williams, IR 1981, Crustal Development in the Archaean Yilgarn Block, Western Australia: Geological Society of Australia, Special Publication 7, p. 43–56.

Goscombe, B, Foster, DA, Blewett, R, Czarnota, K, Wade, B, Groenewald, B and Gray, D 2019, Neoarchaean metamorphic evolution of the Yilgarn Craton: a record of subduction, accretion, extension and lithospheric delamination: Precambrian Research, article no. 105441, doi:10.1016/j.precamres.2019.105441.

Green, ECR, White, RW, Diener, JFA, Powell, R, Holland, TJB and Palin, RM 2016, Activity–composition relations for the calculation of partial melting equilibria in metabasic rocks: Journal of Metamorphic Geology, v. 34, no. 9, p. 845–869.

Holland, TJB and Powell, R 2011, An improved and extended internally consistent thermodynamic dataset for phases of petrological interest, involving a new equation of state for solids: Journal of Metamorphic Geology, v. 29, no. 3, p. 333–383.

Ivanic, TJ 2021, Dyke and structure density of the southwest Yilgarn: Geological Survey of Western Australia, digital data layer, <https://www.dmirs.wa.gov.au/geoview>.

Korhonen, FJ, Kelsey, DE, Fielding IOH and Romano, SS 2020, The utility of the metamorphic rock record: constraining the pressure–temperature–time conditions of metamorphism: Geological Survey of Western Australia, Record 2020/14, 24p.

Lu, Y, Wingate, MTD and Smithies, RH 2020, 219902: metagranodiorite, Jinkas Hill mine; Geochronology Record 1686: Geological Survey of Western Australia, 5p.

Nemchin, AA, Pidgeon, RT and Wilde, SA 1994, Timing of Late Archaean granulite facies metamorphism in the southwestern Yilgarn Craton of Western Australia: Evidence from U–Pb of zircons from mafic granulites: Precambrian Research, v. 68, no. 3-4, p. 307–321.

Powell, R and Holland, TJB 1988, An internally consistent dataset with uncertainties and correlations: 3. Applications to geobarometry, worked examples and a computer program: Journal of Metamorphic Geology, v. 6, no. 2, p. 173–204.

Quentin de Gromard, R, Ivanic, TJ and Zibra, I 2021, Pre-Mesozoic Interpreted Bedrock Geology of the southwest Yilgarn, 2021: Geological Survey of Western Australia, digital data layer, <https://www.dmirs.wa.gov.au/geoview>.

Smithies, RH, Lu, Y, Lowrey, J, Ivanic, T, Champion, DC and Wilde, SA 2021, Variations in granite geochemistry in the southwest Yilgarn: Geological Survey of Western Australia, digital data layer, <http://www.dmirs.wa.gov.au/geoview>.

Wedepohl, KH 1995 The Composition of the Continental Crust. Geochimica et Cosmochimica Acta, v. 59, no. 7, p. 1217–1232.

White, RW, Powell, R, Holland, TJB, Johnson, TE and Green, ECR 2014a, New mineral activity–composition relations for thermodynamic calculations in metapelitic systems: Journal of Metamorphic Geology, v. 32, no. 3, p. 261–286.

White, RW, Powell, R and Johnson, TE 2014b, The effect of Mn on mineral stability in metapelites revisited: New a–x relations for manganese-bearing minerals: Journal of Metamorphic Geology, doi:10.1111/jmg.12095.

Wingate, MTD, Bodorkos, S, and Kirkland, CL, 2008, 177908: quartzite, Noondeening Hill; Geochronology dataset 742, in Compilation of geochronology data: Geological Survey of Western Australia.

Wingate, MTD, Fielding, IOH, Lu, Y and Korhonen, FJ 2021a, 219842: granitic gneiss, Yenyening Lakes; Geochronology Record: Geological Survey of Western Australia, in prep.

Wingate, MTD, Fielding, IOH, Lu, Y, Korhonen, FJ and Quentin de Gromard, R 2021b, 208381: quartzite; Geochronology Record: Geological Survey of Western Australia, in prep.

Zibra, I 2021, Lithostructural map of the Chittering Metamorphic Belt: Geological Survey of Western Australia, digital data layer, <https://www.dmirs.wa.gov.au/geoview>.

Recommended reference

Korhonen, FJ, Blereau, ER, Kelsey, DE, Fielding, IOH and Romano, SS 2021, Metamorphic evolution of the southwest Yilgarn: Geological Survey of Western Australia, digital data layer.

Southwest Yilgarn geochronology

by

Y Lu, MTD Wingate, IOH Fielding, RH Smithies, R Quentin de Gromard and TJ Ivanic

Abstract

The southwest Yilgarn Craton, particularly the South West Terrane, hosts world-class mineral deposits, including the Boddington Au–Cu mine and the Greenbushes Li mine. This region is highly prospective, as highlighted by the discovery of the Julimar PGE–Ni–Cu–Co deposit in 2020. However, the southwest Yilgarn Craton is not well understood geologically. The Southwest Yilgarn geochronology data layer combines 80 existing geochronology results by the Geological Survey of Western Australia (GSWA) with 23 new isotopic dates obtained as part of the Accelerated Geoscience Program (AGP). The new dataset provides an updated timeframe for understanding the geological evolution of this region (Fig. 1).

The project area mainly covers the South West Terrane and adjacent Youanmi Terrane. The recent interpretation by Quentin de Gromard et al., (2021) resulted in a significant south-westward shift of the boundary between these two terranes compared to the Yilgarn Craton subdivision by Cassidy et al. (2006). Therefore, some geochronology samples previously identified as originating in the South West Terrane, are now considered to be from the Youanmi Terrane.

The South West Terrane contains felsic magmatic rocks from c. 2704 to 2607 Ma, including two main pulses at c. 2670 and 2620 Ma (Fig. 2a). The South West Terrane is distinct from the Youanmi Terrane in the apparent absence of granitic rocks older than c. 2710 Ma and the presence of granitic rocks younger than 2620 Ma (Figs 1, 2). The youngest granitic rocks appear to be restricted to the southwest corner of the South West Terrane, and suggest a westward-younging magmatic trend (Fig. 2c). Metamorphism was Neoarchean in age in the terrane interior and along its eastern boundary, and Proterozoic on the western margin (Fig. 1). Maximum depositional ages for the few metasedimentary rocks dated in the South West Terrane are c. 3203, 3005, and 2597 Ma.

In contrast, the western Youanmi Terrane within the AGP project area contains felsic igneous rocks with crystallization ages between c. 3018 and 2622 Ma, which define four main magmatic stages, at about 3018–2914, 2800, 2721, and 2681–2622 Ma (Fig. 2b). The oldest granitic rock in the western Youanmi Terrane is a 3018 ± 4 Ma granitic gneiss from the Calingiri Cu–Mo–Ag deposit near Wongan Hills (GSWA 224760, Wingate et al., 2021d). Ages of metamorphism, based mainly on U–Pb monazite geochronology, range from c. 2671 to 2635 Ma, with main peaks at c. 2664, 2656, and 2636 Ma, for several samples distributed along the boundary with the South West Terrane (Fig. 1). Maximum depositional ages for metasedimentary rocks are 3158–3068, 2958, 2703, and 2675–2638 Ma (Fig. 1).

New geochronology data from the Julimar PGE–Ni–Cu–Co deposit in the South West Terrane define a new age of c. 2670 Ma for ultramafic magmatism and orthomagmatic mineralization in the Yilgarn Craton. A pegmatitic metagabbro from the ore-hosting Gonneville intrusion at Julimar yielded an igneous crystallization age of 2668 ± 4 Ma (GSWA 203747, Wingate et al., 2021a). A granodiorite that crosscuts the Gonneville intrusion crystallized at 2663 ± 8 Ma (GSWA 248207, Wingate et al., 2021c). Pendlandite in a sulfide ore sample produced a range of Re–Os model ages, which indicate that Proterozoic alteration or recrystallization of Archean sulfide ore was younger than c. 2356 Ma (GSWA 248203, Wingate et al., 2021b). The Julimar metagabbro is within uncertainty of the magmatic crystallization age of the Coates Siding gabbro (2664 ± 6 Ma) associated with the Morangup greenstone belt farther east (Wilde and Pidgeon, 2006). Together with a peak of granitic magmatism at c. 2670 Ma (Fig. 2a), these results may signify that c. 2670 Ma mafic–ultramafic and felsic magmatic rocks are more widespread in the South West Terrane and potentially prospective for mineralization.

Acquisition of geochronological data by GSWA was funded by the Exploration Incentive Scheme, and conducted using the SHRIMP ion microprobe and GeoHistory laser-ablation ICP-MS facilities in the John de Laeter Centre at Curtin University, which are operated with the financial support of the Australian Research Council and AuScope National Collaborative Research Infrastructure Strategy.

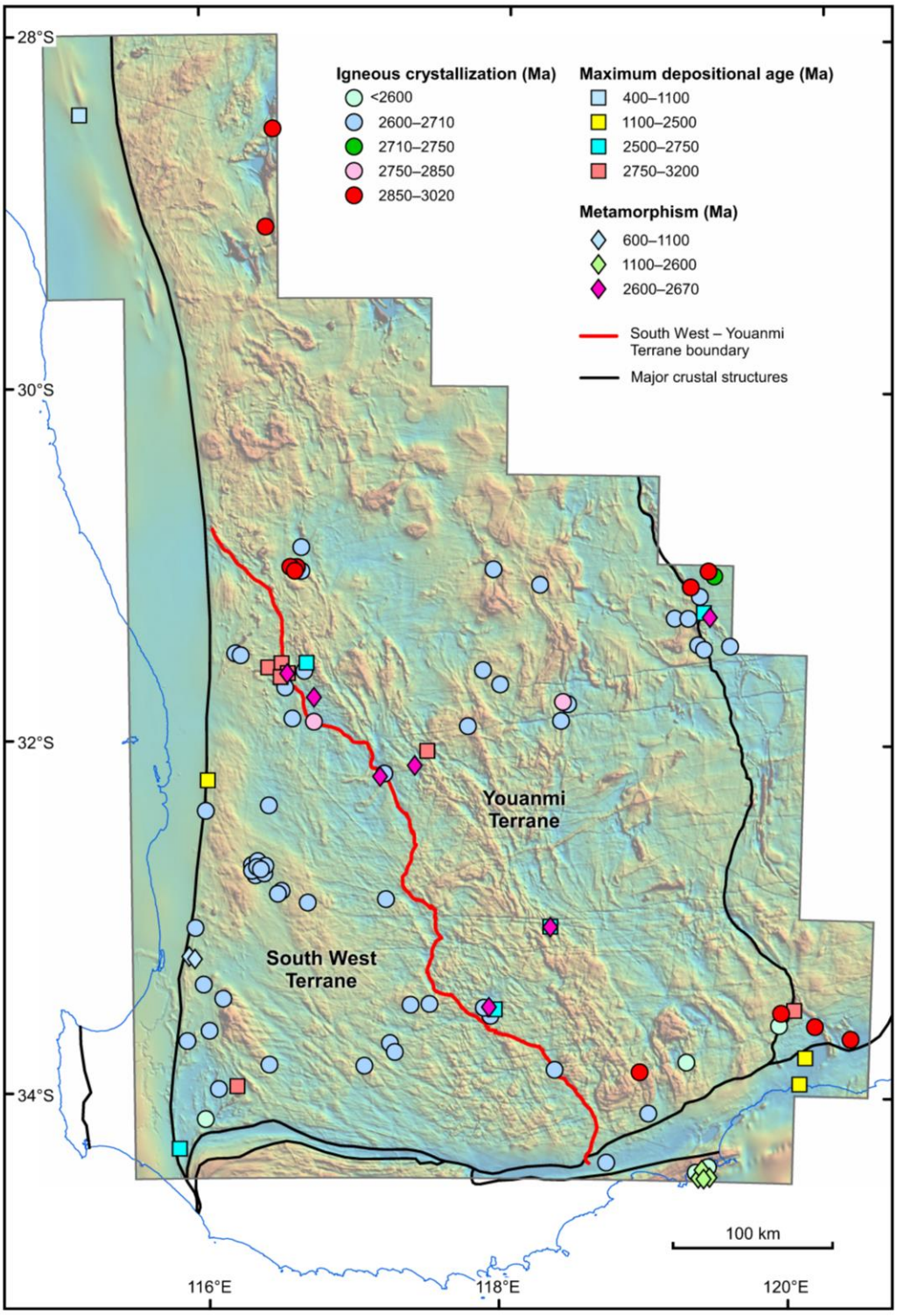

Figure 1. Geochronology samples in the southwest Yilgarn Craton, coded according to event dated and age. Background is the upwards-continued (500 m) reduced-to-pole magnetic anomaly map (GSWA, Southwest Yilgarn, 2021 Geological Exploration Package). The boundary between the South West and Youanmi Terranes is from Quentin de Gromard et al. (2021); major crustal structures are from Martin et al. (2021). Blue curve is the coastline

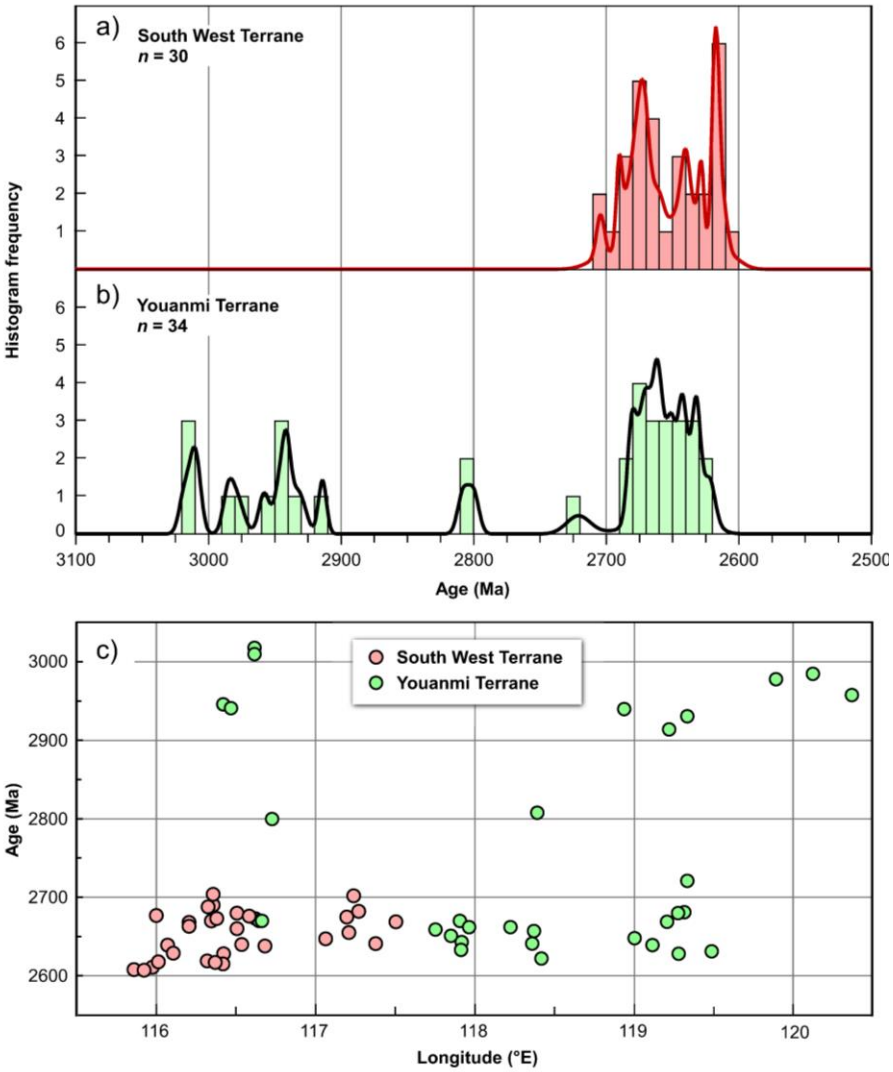

Figure 2. Probability density diagrams and histograms showing igneous crystallization ages in a) the South West Terrane and b) Youanmi Terrane; c) variation of igneous crystallization age with longitude

How to access

The Southwest Yilgarn geochronology data layer forms part of the Southwest Yilgarn, 2021 Geological Exploration Package, available on USB via the DMIRS eBookshop and is available for download from the Data and Software Centre. Geochronology and isotope results can also be accessed online using GeoVIEW.WA.

References

Cassidy, KF, Champion, DC, Krapež, B, Barley, ME, Brown, SJA, Blewett, RS, Groenewald, PB and Tyler, IM 2006, A revised geological framework for the Yilgarn Craton, Western Australia: Geological Survey of Western Australia, Record 2006/8, 8p.

Martin, DMcB, Murdie, R, Cutten, HN, Kelsey, D, Thomas, C, Quentin de Gromard, R, Zhan, Y and Haines, P 2021, 1:2 500 000 major crustal boundaries of Western Australia, 2021: Geological Survey of Western Australia, digital data layer.

Quentin de Gromard, R, Ivanic, TJ and Zibra, I 2021, Pre-Mesozoic interpreted bedrock geology of the southwest Yilgarn: Geological Survey of Western Australia, digital data layer.

Wilde, SA and Pidgeon, RT 2006, Nature and timing of Late Archaean arc magmatism along the western margin of the Yilgarn Craton: Goldschmidt Conference Abstracts 2006, A701, doi:10.1016/j.gca.2006.06.1522.

Wingate, MTD, Fielding, IOH, Lu, Y and Ivanic, TJ 2021a, 203747: pegmatitic leucogabbro, Julimar prospect; Geochronology Record 1784: Geological Survey of Western Australia.

Wingate, MTD, Fielding, IOH, Lu, Y and Ivanic, TJ 2021b, 248203: sulfide ore, Julimar prospect; Geochronology Record 1796: Geological Survey of Western Australia.

Wingate, MTD, Fielding, IOH, Lu, Y and Ivanic, TJ 2021c, 248207: granodiorite, Julimar prospect; Geochronology Record 1797: Geological Survey of Western Australia.

Wingate, MTD, Fielding, IOH, Lu, Y and Smithies, RH 2021d, 224760: granitic gneiss, Dasher prospect; Geochronology Record 1791: Geological Survey of Western Australia.

Recommended reference

Lu, Y, Wingate, MTD, Fielding, IOH, Smithies, RH, Quentin de Gromard, R and Ivanic, TJ 2021, Southwest Yilgarn geochronology: Geological Survey of Western Australia, digital data layer.

The southwest Yilgarn Moho, 2021

by

RE Murdie and H Yuan[1,2]

Abstract

The southwest Yilgarn Moho, 2021 is a depth contour map of the Mohorovičíć (Moho) discontinuity between the crust and mantle as determined from seismological methods (Fig. 1). The map is based on the AuSREM model (Salmon et al., 2012) at half degree-gridded intervals with additional data from seismic refraction lines (Dentith et al., 2000) and receiver function data from passive seismic deployments and permanent seismic stations (Reading et al., 2003).

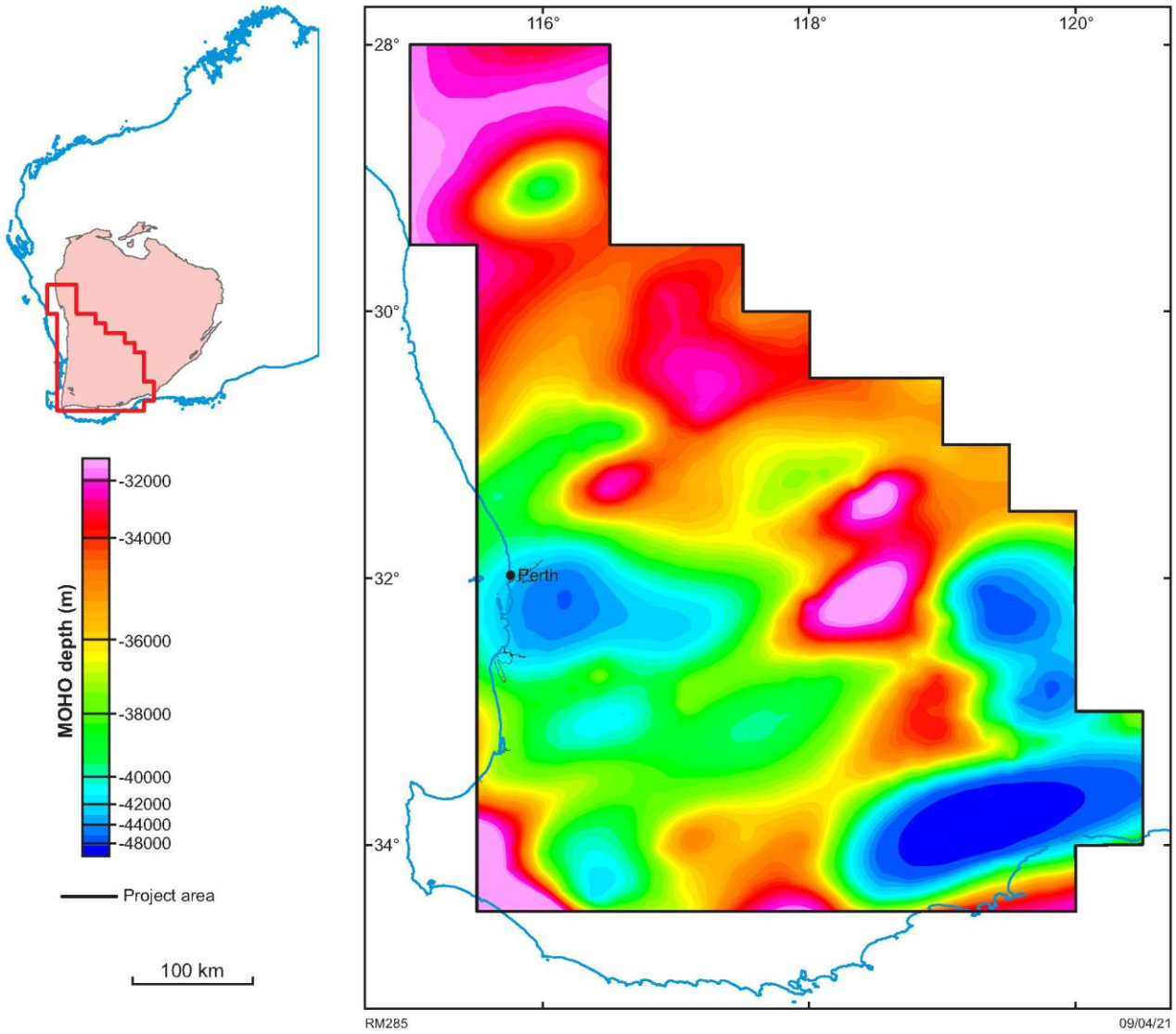

Figure 1. The southwest Yilgarn Moho 2021 data layer

1 ARC Centre of Excellence for Core to Crust Fluid Systems, Macquarie University, Balaclava Road, North Ryde NSW 2019
2 Centre of Exploration Targeting, The University of Western Australia, Stirling Highway, Crawley WA 6009

How to access

The southwest Yilgarn Moho, 2021 data layer is available on a USB via the DMIRS eBookshop.

References

Dentith, MC, Dent, VF and Drummond, BJ 2000, Deep crustal structure in the southwestern Yilgarn Craton, Western Australia: Tectonophysics, v. 325, p. 227–255.

Reading, AM, Kennett, BLN and Dentith, MC 2003, Seismic structure of the Yilgarn Craton, Western Australia: Australian Journal of Earth Sciences, v. 50, no. 3, p. 427–438, doi:10.1046/j.1440-0952.2003.01000.x.

Salmon, M, Kennett, BLN and Saygin, E 2012, Australian Seismological Reference Model (AuSREM): Crustal component: Geophysical Journal International, v. 192, p. 190–206.

Recommended reference

Murdie, RE and Yuan, H 2021, The southwest Yilgarn Moho 2021: Geological Survey of Western Australia, digital data layer.

Pre-Mesozoic interpreted bedrock geology of the southwest Yilgarn, 2021

by

R Quentin de Gromard, TJ Ivanic and I Zibra

Abstract

Introduction

The pre-Mesozoic interpreted bedrock geology map of the southwest Yilgarn (Fig. 1; Geological Survey of Western Australia [GSWA], 2021) integrates legacy data with a substantial volume of new data from multiple datasets acquired under the Accelerated Geoscience Program (AGP). The objective of this interpreted bedrock geology map is to achieve a uniform interpretation of the geology across the southwest of the Yilgarn Craton (south–central part of the South West Terrane of Cassidy et al., 2006). It provides context for known mineral deposits in the region and aims to open new search space in this underexplored and highly prospective portion of the Yilgarn Craton.

This extended abstract is intended to be used in conjunction with the interpreted bedrock geology digital layers and with the other ~600 digital layers provided within the Southwest Yilgarn, 2021 Geological Exploration Package (GSWA, 2021).

The southwest Yilgarn interpreted bedrock geology map area is approximately 450 x 380 km wide and is bounded in the west by the Darling Fault, and in the east by the Southern Cross – Forrestania – Ravensthorpe greenstone belts. It includes the Wongan Hills and Westonia greenstone belts in the north and extends into the Albany–Fraser Orogen in the south. The area encompasses the informal Balingup, Boddington and Lake Grace terranes of Wilde et al. (1996). One of the most significant outcomes of our interpretation is a change in the subdivision of Yilgarn Craton terranes. The nomenclature of Wilde et al. (1996) is not fully adopted here because our interpretation shows that the Lake Grace terrane represents a higher metamorphic grade equivalent to the Youanmi Terrane. The extent of our redefined South West Terrane is nearly identical to the extent of the combined Boddington and Balingup terranes of Wilde et al. (1996). No attempt has been made to subdivide the redefined South West Terrane due to insufficient age data. The Proterozoic Cardup Basin has not been included in this version of the southwest Yilgarn interpreted bedrock geology but may be added in a future iteration of this map. The interpreted bedrock geology map consists of five interpretative layers:

- ‘Terrane boundary’ layer, which consists of the trace of the interpreted terrane boundary between the Youanmi and the South West Terranes based on tracing existing structure lines from the ‘structure line’ layer below.
- ‘Geophysical line’ layer, which consists of lines interpreted from aeromagnetic data. These are to be regarded as form lines and represent the aeromagnetic signature of primary fabrics including bedding and magmatic layering, or secondary fabrics such as tectonic foliation, gneissic layering or attenuated and dismembered layers forming boudin trains.
- ‘Geological line’ layer, which primarily comprises the trace of mafic dykes but also of narrow geological units that are too thin to be represented as polygons, such as felsic dykes and banded iron-formations (BIF).
- ‘Structural line’ layer, which contains faults and shear zones and includes attributes, where known, such as dip estimate, dip direction, kinematic information and inferred maximum and minimum ages.
- ‘Geological polygon’ layer containing the geologically coded map units and, where known, unit names, descriptions and geochemical classification of granites.

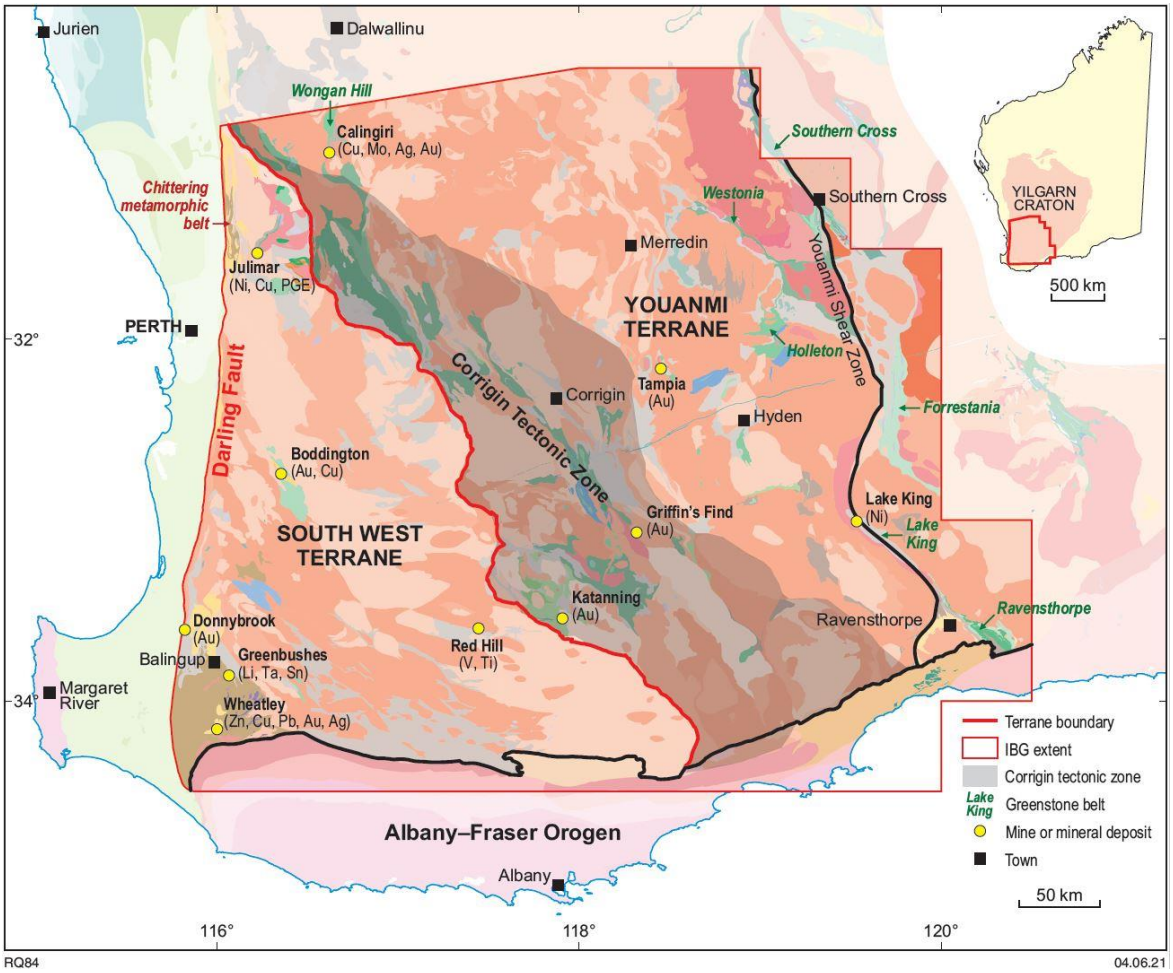

Figure 1. Simplified pre-Mesozoic interpreted bedrock geology (IBG) of the southwest Yilgarn, showing the new mapping produced during the southwest Yilgarn project of the AGP, overlying the 1:500 000-scale state IBG polygon layer. The thick red line shows the location of the redefined terrane boundary between the Youanmi and South West Terranes, the yellow dots show the location of the main mines and mineral deposits west of Youanmi Shear Zone; the main commodities are shown in brackets. To view all layers of the southwest interpreted bedrock geology, see the Southwest Yilgarn, 2021 Geological Exploration Package (GSWA, 2021)

Data

A vast number of features contained within various legacy and AGP datasets and publications have contributed to the making of this interpreted bedrock geology map and are included, where possible, as digital layers on the Southwest Yilgarn, 2021 Geological Exploration Package (GSWA, 2021). These supporting layers include:

- GSWA field observations captured in WAROX (GSWA, 2020a)
- GSWA digital WAROX text searches layer (Ivanic et al., 2021a)
- GSWA digital granite geochemical classification layer (Smithies et al., 2021a)
- GSWA digital greenstone geochemistry layers (Ivanic et al., 2021b)
- GSWA U–Pb zircon geochronology (GSWA, 2020b)
- GSWA Sm–Nd and zircon O isotope maps of Western Australia (Lu et al., 2021a,b)
- GSWA MINEDEX Mines and Mineral deposits layers
- GSWA Metamorphic History records of the southwest Yilgarn (Korhonen et al., 2021)
- legacy GSWA 1: 250 000 surface geology and explanatory notes (including their 1: 250 000 interpreted geology figures)

- existing GSWA interpreted bedrock geology digital layers at 1:100 000 and 1: 500 000 scale
- numerous, georeferenced company maps (GSWA, 2021)
- new, detailed field mapping of the Chittering Metamorphic Belt (at approximately 1:50 000 scale) conducted and compiled by Zibra (2021) was seamlessly incorporated into the southwest Yilgarn interpreted bedrock geology
- aeromagnetic compilation images including multi-scale edges (Brett, 2021; GSWA, 2021). The line spacing of individual available (open file and confidential) surveys ranges from 25 to 400 m over the whole interpreted bedrock geology map area, with over two-thirds of the map area covered by 100 m line spacing or less. The aeromagnetic compilation images employed a 40 x 40 m cell size, optimized for 150 m, or greater, line spacing. Where available, high-resolution surveys were used to obtain the highest confidence level in interpretation of specific areas
- open file gravity data including multi-scale edges (Brett, 2021; GSWA, 2021)
- external publications and theses.

Methods and interpretation

Two field trips were conducted at the start of the project to provide spatial and geological context for all existing data, and in particular, to develop an understanding of deformation style, strain intensity, metamorphic grade and main lithostratigraphic units, and to provide regional context to known mineral deposits.

Over the whole interpreted bedrock geology map area, the uniformity of the data structure and the relatively high density of the individual point datasets has allowed for consistency of geological interpretations during map compilation with a high level of confidence. The geological point datasets were systemically correlated with the gravity and aeromagnetic compilation images (Brett, 2021; GSWA, 2021). The potential field data compilation images, being derived from multiple datasets of different resolution, enabled consistency of interpretation across the whole map area. Correlating mappable polygons from the aeromagnetic dataset from point data was achieved primarily in areas of high point data density, and then extrapolated into the areas of lesser data density. Geological interpretation and a matrix of relative event timing were progressively built during the map compilation process. We systematically recorded crosscutting relationships between the various geological features with the same principles used during field mapping. The compilation over most of the interpreted bedrock geology extent was constructed at between 1:40 000 and 1:65 000 scale and is intended to be best viewed at 1:250 000 scale.

The primary focus was on the central part of the map area, whereas the southern and eastern edges were left practically unchanged from existing 1:100 000 and 1:500 000 mapping; the latter mapping is included in the southwest Yilgarn interpreted bedrock geology for edge matching purposes. For example, the eastern part of the SOUTHERN CROSS 1:100 000 map sheet as well as the Forrestania and Ravensthorpe greenstone belts from GSWA 1:500 000 digital layers were imported from the existing digital compilation and blended into the southwest Yilgarn interpreted bedrock geology.

In the following paragraphs we will describe the layers as they are displayed in the Southwest Yilgarn, 2021 Geological Exploration Package.

Geolines

5922 line segments were interpreted and digitized into the geoline layer ('Interpreted pre-Mesozoic bedrock geology lines, 2021') of the interpreted bedrock geology. This layer largely consists of interpreted mafic dyke segments assigned to 12 different dyke suites or members of such suite (Fig. 2). The mafic dyke compilation is largely based on a previously published statewide dyke layer (Wingate, 2017) on an unpublished compilation (T. Beardsmore, written communication, 2020), and

on recently dated dykes (Stark et al., 2018a,b; Stark et al., 2019). Each line segment is attributed with a code, a unit name, a description and, where available, with an age and a magnetic polarization (either positive or negative). The mafic dykes were entirely (re-)drawn from the high-resolution aeromagnetic dataset, to ensure that crosscutting relationships between dykes and structures were systemically captured and interpreted consistently. The main aeromagnetic images used were the 'TMI_RTP_drape90_colour', the 'TMI_RTP_1VD_colour' and the 'TMI_RTP_1VD_grey' images. Additionally, the 'TMI_AnS_drape' image was used to avoid misinterpreting a negatively magnetized mafic dyke for a demagnetized fault and vice versa. Minor geolines, other than mafic dykes, such as BIF, chert, felsic dykes, pegmatite or quartz veins were are also included in this layer, and mostly in the marginal parts of the southwest Yilgarn interpreted bedrock geology map area.

Twelve mafic dyke suites or members of such suites were identified and digitized (Fig. 2). In relative chronological order, these are:

- A north- to northeast-trending, Archean mafic dyke suite, interpreted to be c. 2640 Ma in age, is here informally named the 'Babakin metadolerite'. This undated suite was identified from aeromagnetic data primarily within the Corrigin Tectonic Zone and is interpreted as a suite of deformed mafic dykes emplaced synchronously with the syn- to post-tectonic intrusions of the c. 2651–2630 Ma low-Ca, P-rich granites. These dykes all have a positive magnetic polarity.
- c. 2615 Ma northeasterly to north-northeasterly trending Yandinilling Dolerite, dated by Stark et al. (2018a). These dykes are largely restricted to the northwest portion of the map area. They crosscut and are not affected by the Corrigin Tectonic Zone and thus form an absolute minimum age for this deformation event. Most of these dykes are 'positive', but few negatively polarized dykes occur.
- c. 2410 Ma westerly to west-southwesterly trending Widgiemooltha Dolerite. Individual dyke segments are commonly 100–200 km long, and occur over most the map area. This dyke swarm hosts some of the widest mafic dykes in the map area, which are locally up to ~600 m wide. Both positive and negative magnetic polarities occur and the age of this magnetic pole reversal was previously bracketed between 2408 ± 3 Ma and 2401 ± 2 Ma for a 'positive' and a 'negative' dyke, respectively (Wingate, 2007; Pisarevsky et al., 2015).
- c. 1888 Ma west-northwesterly trending Boonadgin Dolerite dated by Stark et al. (2019). These dykes mostly occur in the southwest portion of the map area and are almost entirely restricted to the redefined extent of the South West Terrane. These dykes all preserve a positive magnetic polarity.
- c. 1390 Ma north-northwesterly trending Biberkine Dolerite, dated by Stark et al. (2018b). The dykes occur in the western part of the map, and were mostly intruded into the redefined extent of the South West Terrane, but also within the southwestern margin of the Youanmi Terrane. These dykes are emplaced along and parallel to the terrane boundary, and lie parallel to the regional to terrane-scale, north-northwesterly trending, long-wavelength gravity anomaly that underlies the South West Terrane. Both 'positive' and 'negative' dykes occur.
- Dykes of the c. 1210 Ma Marnda Moon Large Igneous Province:
    - The northwesterly trending Boyagin Dolerite. These dykes also largely occur in the redefined extent of the South West Terrane; only minor occurrences were interpreted east of the terrane boundary. These dykes all preserve a positive magnetic polarity.
    - The west-southwesterly trending Gnowangerup–Fraser Dolerite, occurring in the southern portion of the map area, across the Youanmi and South West Terranes, and emplaced parallel to the western Albany–Fraser Orogen margin. Both 'positive' and 'negative' dykes occur.

    - The west-northwesterly trending Wheatbelt Dolerite. These dykes occur in the northern portion of the map area and were mostly intruded into the Youanmi Terrane. These dykes all preserve a positive magnetic polarity.

- The undated northwesterly trending Beenong Dolerite, bracketed between c. 1218 and 541 Ma, occurring in the eastern part of the map area and exclusively within the Youanmi Terrane. These dykes mostly preserve a positive magnetic polarity, only minor 'negative' dykes were identified.
- Undifferentiated Proterozoic mafic dykes mostly occurring in the far southwestern corner of the map are abundant and tightly spaced, all preserving a positive magnetic polarity.
- c. 733 Ma west-northwesterly trending Nindibillup Dolerite, rare and limited to the redefined extent of the Youanmi Terrane, these dykes can be hundreds of kilometres long and preserve both positive and negative magnetic polarity.

Form lines

A total of 7864 form lines interpreted from aeromagnetic data were interpreted and digitized into the geophysics layer (geophys_lne) of the interpreted bedrock geology map. Entirely interpreted from aeromagnetic data, these lines represent the aeromagnetic signature of primary fabrics such as bedding or magmatic foliation or secondary fabrics such as tectonic foliation, folds or boudin trains. This layer should be regarded as a form line interpretation and be primarily used as a representation of the ductile architecture of the crust subsurface. The form lines are particularly useful to estimate strain intensity, to map shear zones by localizing truncations and attenuation of various markers, and interpret the kinematics of faults and shear zones from offsets and drag of primary or secondary layering. Thus, map domains with different geometries of form lines can potentially suggest that these domains experienced differing geological histories.

Structural lines

To understand the structural framework, initially a first-pass, interpreted bedrock geology-wide, structural framework of main shear zones and faults was established. Large-scale faults and shear zones were mostly interpreted using Bouguer gravity (SWYC_grav_drape_), isostatic residual gravity (SWYC_graviso_drape_) and multi-scale edges (Brett, 2021; GSWA, 2021) together with upward continued (Up) images of the reduced to pole (RTP), total magnetic intensity (TMI) data with upward continuation values of 10 km, 1 km and 500 m (SWYC_tmi_RTPUp10km, SWYC_tmi_RTPUp1km, SWYC_tmi_RTPUp500m) variously coloured or as greyscale images as well as the magnetic integral images ('pseudogravity', SWYC_tmi_RTPInt_drape) and magnetic multi-scale edges (Brett, 2021; GSWA, 2021). While the greyscale images best visualize breaks in the data, and are particularly useful in tracing the appropriate location of structures, the coloured images together with the multi-scale edges give an appreciation of the dip direction and dip estimate of particular magnetic horizons. The gravity and magnetic multi-scale edges were used for a semi-quantitative interpretation of dip, dip direction and penetration depth of main structures in order to differentiate between major and minor shear zones. This broad structural framework was then iteratively fine-tuned during the smaller-scale interpretation stages. The semi-quantitative estimate of the dip and dip direction of a particular magnetic horizon or structures was further achieved by interpreting gradients in the magnetic data using aeromagnetic images processed with either a sun overhead illumination or no sun illumination.

A total of 3868 structural lines were interpreted and digitized into the structural line layer ('Interpreted pre-Mesozoic bedrock geology structural lines, 2021'). The very large majority of structural lines were attributed as either 'fault' or 'shear zone' (see below). The few structures attributed as 'fault or shear zone' are a relic from the pre-existing mapping copied into this data package for edge matching purposes and thus only occur on the periphery of the map. Where constraints are known, faults and shear zones are also attributed with dip estimates, dip direction and kinematic attributes as well as maximum and minimum ages. The age constraints were interpreted from crosscutting relationships

of dated geological features, where known. As a result, the structures can be symbolized or colour-coded by structure type or kinematics but also by minimum and/or maximum age (Figs 3–5).

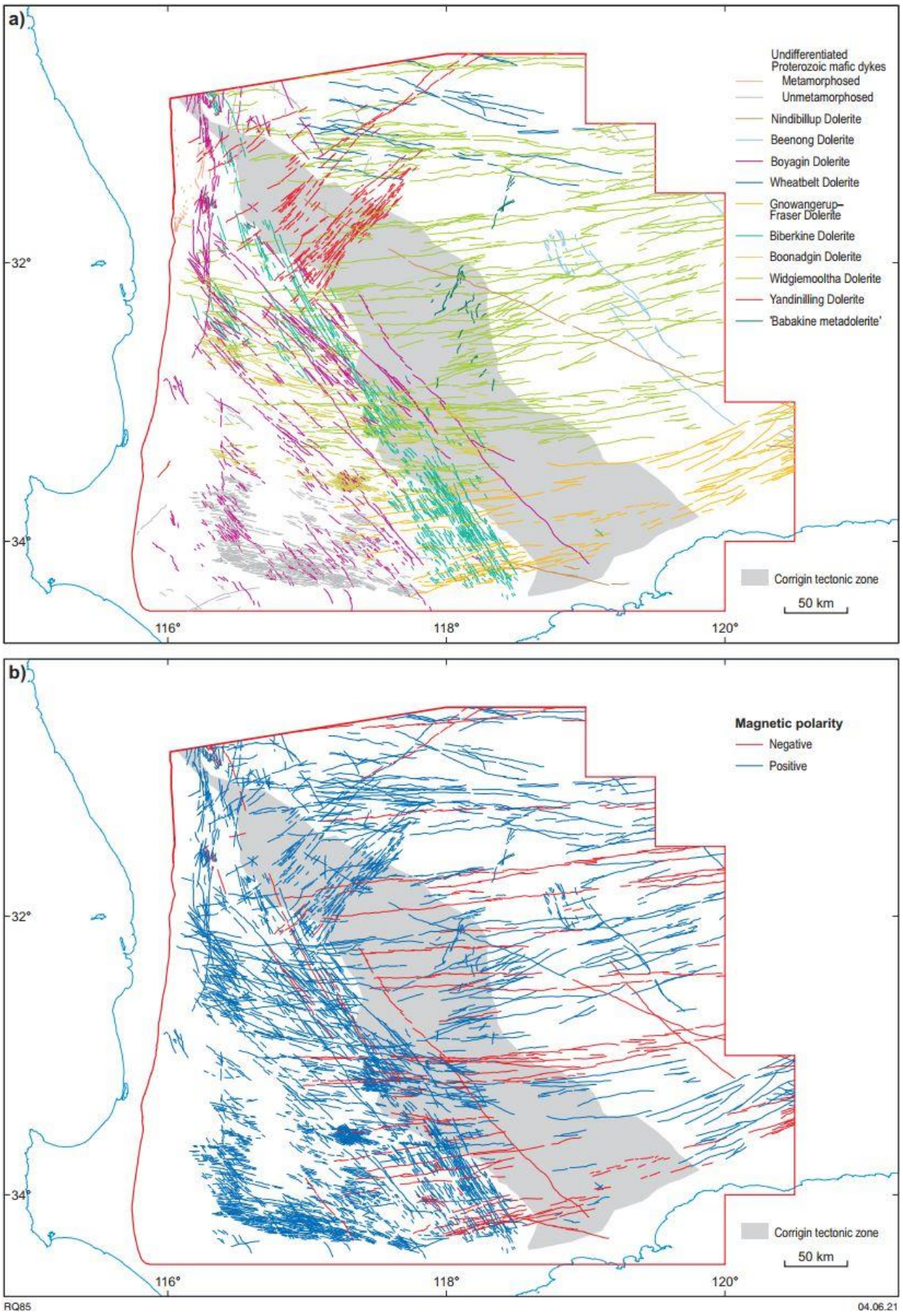

Figure 2. Interpreted mafic dykes colour-coded by: a) name (inverted commas indicate informal name); b) magnetic polarity

Shear zones

Care was taken to differentiate shear zones from faults. For a shear zone to be mapped from aeromagnetic data, it needs to fulfil at least some first-order criteria: they must be wide zones, anastomosed, show curved offsets of magnetic horizons and rotations of magnetic elements towards parallelism, which indicates the high strain portion of the shear zone. They also need to fulfil at least some of the following second-order criteria: show evidence of truncation, folding, attenuation, boudinage and/or magnetite remobilization. Although, a shear zone is defined as a zone of heterogeneously distributed strain relative to its wallrock, the current layer structure for the interpreted bedrock geology requires the structures to be drawn as lines, it was chosen to place the line where truncations occur or where the highest strain portions of the shear zones are interpreted to occur as defined and evidenced by the aeromagnetic form lines mentioned above.

Faults

To satisfy the interpretation of a structure as a fault from the magnetic data alone, the mapped features need to display at least some of the following characteristics; they need to be thin, linear features showing straight offsets, mostly represented by demagnetized zones, locally with a weak and diffuse magnetic response possibly due to minor magnetite/hematite remobilization along the fault. Observations from aeromagnetic interpretation suggest that the faults can act as a propagation medium but also as a barrier to dyke emplacement. As a result, careful, meticulous, and systematic mapping of each fault–dyke intersection was required to assign with some degree of confidence a relative timing between the mapped fault sets and dyke suites and their members. It should be noted that in this interpreted bedrock geology map, only the faults with a cumulative displacement visible in the available magnetic resolution data were mapped, and no attempt has been made to map fracture patterns.

Folds

Fold interpretation from aeromagnetic data was achieved using the principles of structural geophysics (Jessell 2001), using coloured aeromagnetic images processed with either a sun overhead illumination or no sun illumination such as 'SWYC_tmi_RTP_drape90_ps' or 'SWYC_tmi_RTP_colour_ps'. This allows for the semi-quantitative estimate of the dip angle and dip direction of the folded magnetic horizon to be interpreted, as a result one may be able to differentiate between antiforms and synforms, estimate folds interlimb angle and interpret fold orientation, plunge and vergence. These features are attributed where they could be estimated with reasonable confidence.

Structure maps

Because of the way individual lines from the structure line layer are attributed, it is possible to distinguish ductile structures from brittle structures; and by plotting only the interpreted geophysical lines, together with the structures attributed as shear zones, one can obtain a map of the ductile fabrics alone (Fig. 3). Similarly, one can map the brittle structures alone (Fig. 4). The maximum and minimum ages of the structures, interpreted from crosscutting relationships to dated geological units (polygons or lines), could be assigned to about half of all the structure lines and colour-coded according to minimum or maximum ages resulting in a basic structural evolution diagram (Fig. 5).

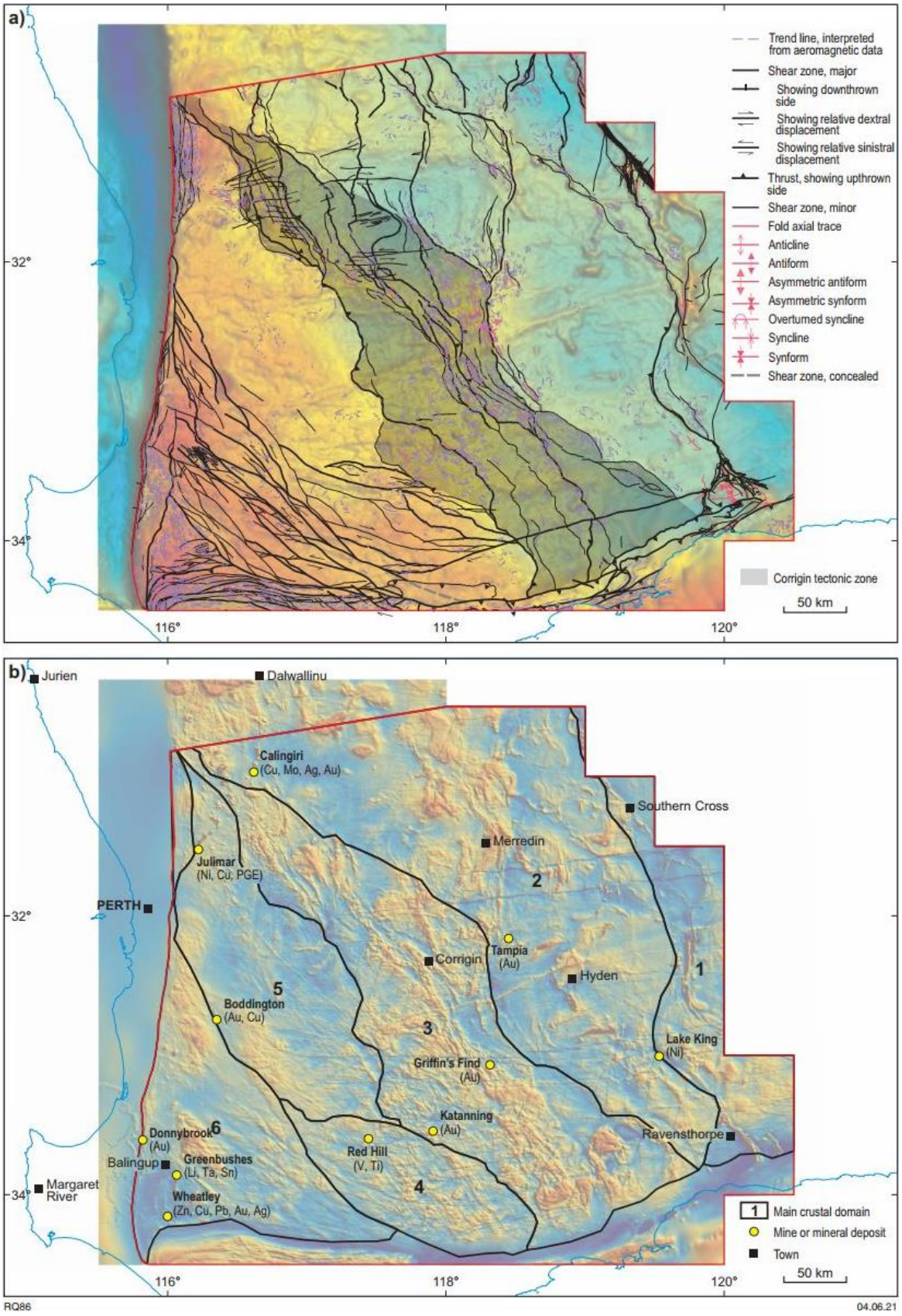

Figure 3. a) Interpreted ductile structures of the southwest Yilgarn displayed over the Bouguer gravity compilation image. The dashed blue lines are form lines interpreted from aeromagnetic data; b) Main crustal domains displayed over the upwards continued (500 m), RTP total magnetic compilation image

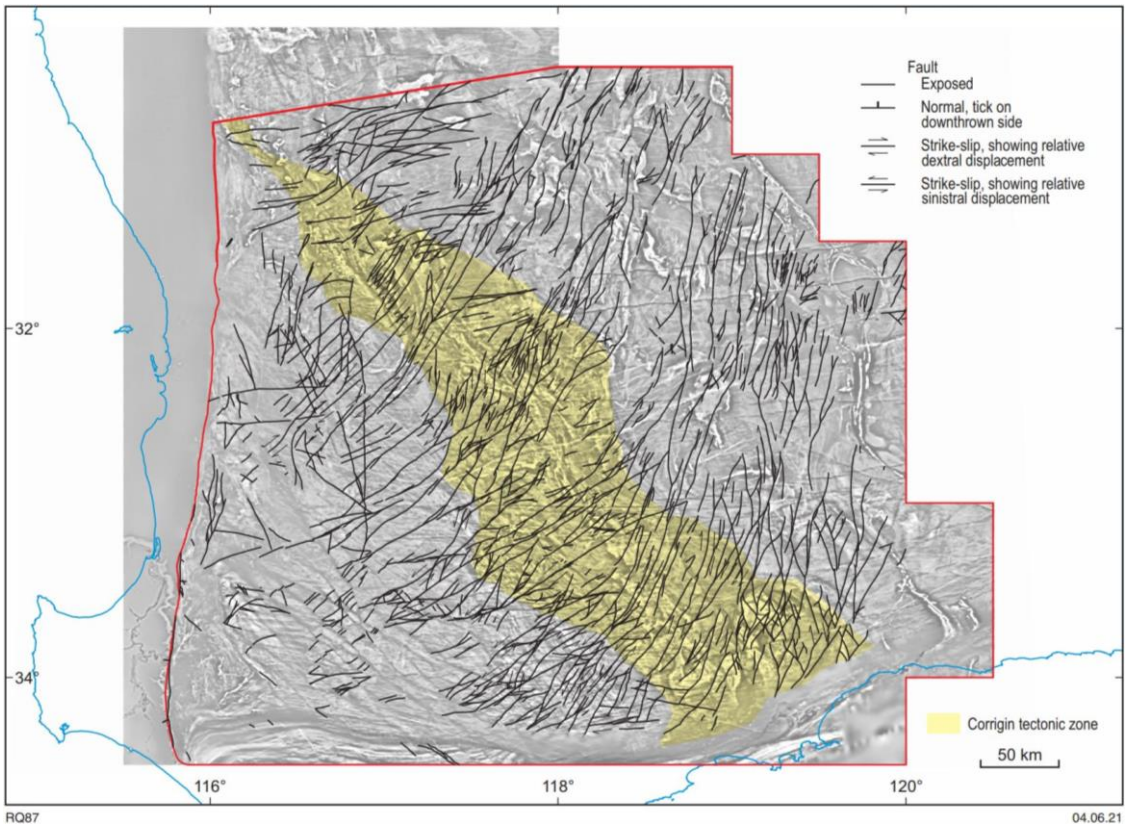

Figure 4. Interpreted brittle structures of the southwest Yilgarn displayed over the upwards continued (500 m), first vertical derivative, RTP total magnetic compilation image

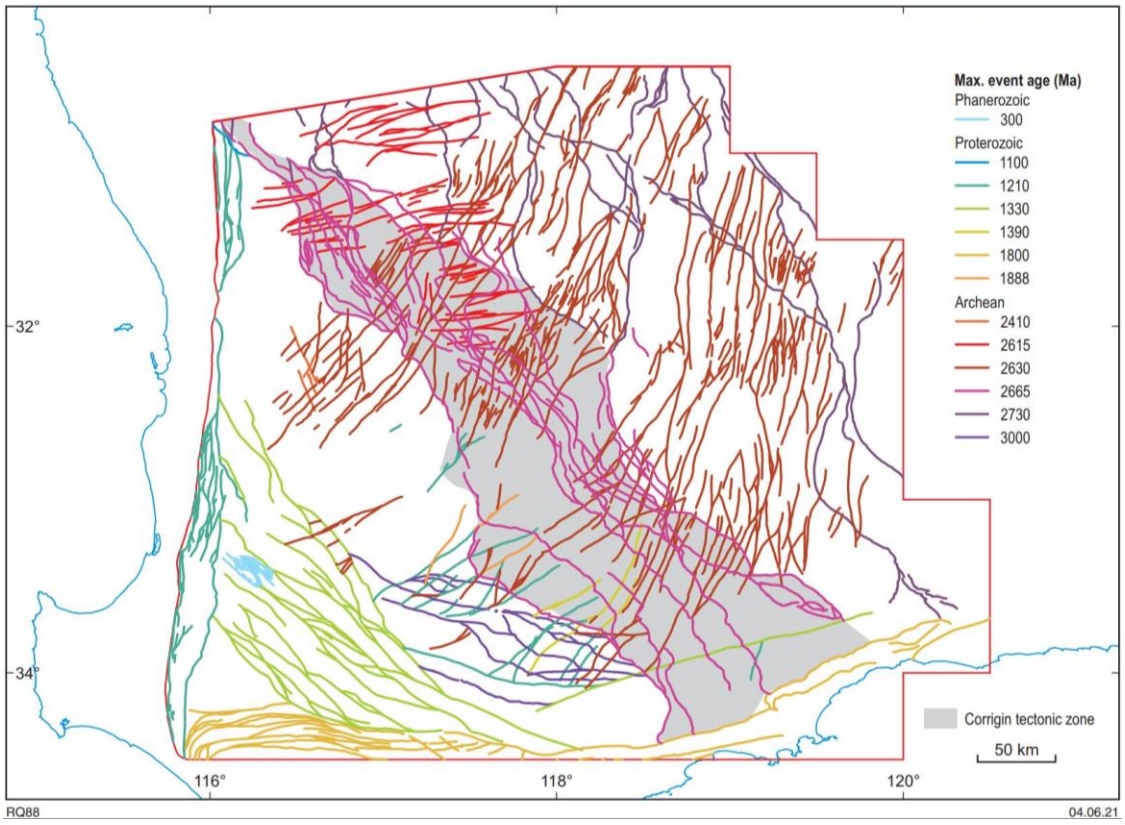

Figure 5. Structures with age data attribution of the southwest Yilgarn colour-coded by maximum age. Thirteen age brackets were defined based on cross-cutting relationships with dated geological units (see text for explanation)

Based on this approach and on crosscutting relationships, we defined 13 relative age brackets for movement along faults and shear zones:

i. 3000–2665 Ma: major west-northwesterly trending shear zones between the Katanning Au region (Fig. 1) and the Albany–Fraser Orogen, and restricted to the South West Terrane. The maximum age is not constrained, only generally attributed to the oldest known gneissic granite in the map area. The minimum age constraint is the maximum age of the Corrigin Tectonic Zone, which truncates the west-northwesterly trending shear zones.

ii. 2730–2665 Ma: major approximately north-striking anastomosing shear zone system of the Youanmi Terrane (i.e. lozenges). The maximum age is that of the earliest age of deformation for the Yilgarn orogeny of Zibra et al. (2017). The minimum age constraint is the maximum age of the Corrigin Tectonic Zone, which truncates and drags sinistrally the north-striking lozenges of the Youanmi Terrane.

iii. 2665–2635 Ma: major northwest-striking sinistral transpressive shear zone system of the Corrigin Tectonic Zone (see Domain 3 of 'Crustal Domain' section below). The maximum and minimum age constraints are defined by the oldest and youngest metamorphic zircons in the Corrigin Tectonic Zone, which also encompass the age range obtained from monazite.

iv. 2630–2410 Ma: prominent set of northeast-striking faults, some individual faults exceeding 200 km, mostly showing dextral shear sense, and cutting across the South West and Youanmi Terranes. These faults affect low-Ca granite plutons dated at c. 2630 Ma but pre-date the c. 2410 Ma Widgiemooltha Dolerite. These faults could therefore be of similar age to the c. 2615 Ma Yandinilling Dolerite dykes.

v. <2615 Ma: east-northeasterly striking shear zones in the northern part of the map affecting the Corrigin Tectonic Zone structures and the c. 2615 Ma Yandinilling Dolerite dykes. No minimum age constraint could be defined.

vi. <2410 Ma: minor set of northwest-striking faults, mostly dextral, restricted to the South West Terrane and affecting the 2410 Ma Widgiemooltha Dolerite.

vii. 1888–1390 Ma: minor set of dominantly sinistral faults affecting the c. 1888 Ma Boonadgin Dolerite dykes but not affecting the c. 1390 Ma Biberkine Dolerite dykes.

viii. 1800–1140 Ma: major east-striking shear zones of the Albany–Fraser Orogen. The maximum age for these shear zones is interpreted to be related to extensional faulting that formed the c. 1800–1590 Ma Barren Basin and the minimum age is likely related to deformation during the c. 1225–1140 Ma Stage II of the Albany–Fraser Orogeny.

ix. <1390 Ma: minor set of mostly sinistral northeasterly to north-northeasterly striking faults, restricted to the southern part of the map area and truncating the redefined terrane boundary between the South West and Youanmi Terranes, affecting the c. 1390 Ma Biberkine Dolerite dykes.

x. 1330–1140 Ma: major northwesterly trending, sinistral, ductile shear zones, restricted to the southern part of the South West Terrane, in the southwestern corner of the map area. These shear zones are interpreted to be Proterozoic in age, as they affect the c. 2610 Ma granites, and are possibly synchronous with compressional or transpressional deformation related to the c. 1390–1140 Ma Albany–Fraser Orogeny. Alternatively, they may be related to the early stages of sinistral transtensional deformation producing the north-trending fabric along the Darling Fault scarp (Zibra, 2021) and the regional-scale sinistral drag of tectonic fabrics of the western end of the western Albany–Fraser Orogen; however, they are truncated by the latest stages of north-trending fabrics parallel to the Darling Fault.

xi. <1210 Ma: minor set of mostly sinistral northeast-trending faults restricted to the South West Terrane affecting the c. 1210 Ma Boyagin Dolerite dykes that probably reactivated the c. 2630–2410 Ma faults of the same orientation.

xii. <1210 Ma: major set of north-trending structures parallel to the Darling Fault scarp, produced during sinistral transtension as identified in the Chittering Metamorphic Belt (Zibra, 2021) and likely producing the regional-scale apparent sinistral drag of tectonic fabrics of the western end of the western Albany–Fraser Orogen. These structures deform north-trending dolerite dykes attributed to the 1210 Ma Boyagin Dolerite suite providing a maximum age of deformation for the sinistral transtensional event. The minimum age is unknown.

xiii. <299 Ma: mostly northwest-trending faults affecting the Carboniferous–Permian Collie Sub-basin in the southwest part of the map that likely reactivated the pre-existing c. 1330–1140 Ma major northwesterly trending, shear zones in the area.

Geology polygons

A total of 1581 polygons were interpreted and digitized into the geology polygon layer ('Interpreted pre-Mesozoic bedrock geology polygons, 2021'). Each polygon is attributed with a code, a unit name, a description, and where available, with maximum and minimum ages and granite geochemistry classification. The main datasets utilized were the WAROX observations (GSWA, 2020a) and WAROX text searches (Ivanic et al., 2021a), the granite geochemistry classification (Smithies et al., 2021), company and GSWA mafic geochemistry, particularly the MgO content to differentiate between mafic and ultramafic rocks (Ivanic et al., 2021b), GSWA zircon U–Pb geochronology data (GSWA, 2020b), external geochronology, GSWA 1:250 000 surface geology maps, MINEDEX Mines and Mineral deposits layers (GSWA, 2021), and various company maps (GSWA, 2021). All these data were integrated and assembled in a uniform interpretation using compilation images of the aeromagnetic and gravity data (GSWA, 2021).

Outlines of the polygons were digitized primarily using various compilation images of the aeromagnetic data, by defining domains of similar texture and intensity. The tilt image ('SWYC_tmi_Tilt_drape_ps') image is particularly useful to delineate areas of similar texture. The various clipped images ('SWYC_tmi_RTP_clipped') were largely used in areas of overall low magnetic intensity to reveal magnetic features otherwise masked by a colour stretching of the aeromagnetic data over too large a range of values. The point datasets were correlated to the combined characteristics of aeromagnetic domains and gravity response (high, medium or low) and the correlation between point data and potential field data was primarily achieved in areas of high point data density. The resulting interpretations were then extrapolated in areas or lesser point data density using primarily the potential field data.

Granites

An extensive granite geochemistry dataset and the resulting granite classification (Smithies et al., 2021) formed the basis for an interpreted granite map. Together with WAROX lithological descriptions, it has been possible to assign aeromagnetic and gravity characteristics for mappable domains of similar geochemical groupings in the aeromagnetic data. The resulting interpretation developed in areas of the highest point data density was then extrapolated to geophysical domains of similar characteristics but with lesser point data density. Each granite polygon was attributed to a particular granite group, allowing the compilation of a granite map (Fig. 6). However, small granite plutons of specific granite class, such as sanukitoids, were not captured as single polygons because it was not possible to individually map polygons from the resolution of the geophysical datasets. As a result, these have been included as minor components within a composite polygon, with the various lithologies present expressed in the legend narrative.

The seven granite geochemical groups represented on the interpreted bedrock geology map are:

i. High Ca, Na to high Na, high Sr/Y: largely consisting of metamorphosed, foliated to gneissic, locally migmatitic tonalite–trondhjemite–granodiorite (TTG). These typically have a low to medium gravity response, low to moderate magnetic intensity and are textureless. In the informal Lake Grace terrane of Wilde et al. (1996), they form an extensive area with a distinctive, shear zone-bounded, oblong crustal domain, similar to lozenge-shape domains in

the northern part of the Youanmi Terrane. The TTGs intrude into greenstones of the Youanmi Terrane, where the greenstones form dismembered rafts 'floating' in a 'sea' of high-Ca granite.

ii. High Ca, Na, low Sr/Y: typically hornblende granodiorite, mostly occurring within the South West Terrane as relatively undeformed intrusions, except for areas of Proterozoic deformation along the Darling Fault scarp.

iii. High Ca, and not further differentiated, either because of insufficient data points or because mixed high and low Sr/Y was not possible to differentiate as unique polygons.

iv. High Ca, K, high Sr/Y: rare occurrences within the Corrigin Tectonic Zone consisting of migmatitic, gneissic TTG.

v. High Ca, K, low Sr/Y: rare occurrences in the northwest corner of the map area of metamorphosed hornblende-bearing granodiorite to monzogranite.

vi. Low Ca, K, low to high Sr/Y: typically weakly foliated porphyritic biotite monzogranite, commonly forming low-density features within the high-Ca granites, with moderate magnetic intensity and a well-developed mottled texture. The c. 2677–2610 Ma low-Ca granites were emplaced synchronously with the c. 2665–2635 Ma deformation and metamorphism of the Corrigin Tectonic Zone. In the Corrigin Tectonic Zone, they occur as sheets emplaced along the footwalls of ductile shear zones; however, their occurrence is not restricted to the Corrigin Tectonic Zone. In the northern part of the map area, outside of the Corrigin Tectonic Zone, they form plutons often emplaced at a triple junction between earlier ductile structures and seem to inflate, overprint and cross-cut these structures. These are interpreted as post-tectonic granites, post-dating the north-trending shear zone system attributed to result from c. 2730–2660 Ma deformation. They also occur as domes within large areas of high-Ca granite, for example, the low-Ca granite pluton exposed at Wave Rock. Emplacement of the low-Ca granite is therefore not the result of orogenesis in the Corrigin Tectonic Zone but more likely related to a thermal event superimposed and potentially fortuitously synchronous with c. 2665–2635 Ma deformation and metamorphism in the Corrigin Tectonic Zone.

vii. Dominantly low Ca, P-rich: commonly monzogranite and syenogranite, rarely granodiorite, typically biotite-bearing and forming high magnetic intensity areas, with a well-developed mottled texture, of low to moderate density. These appear as cogenetic with the low-Ca granites but possibly as later P-rich phases within a low-Ca intrusion cycle. Where they occur in the Corrigin Tectonic Zone, they appear intruded as sheets directly against and along the footwalls of the shear zones and are interpreted as syntectonic granite. Outside of the Corrigin Tectonic Zone, they form concentric zonation with the low-Ca, K, low-Sr/Y group described above and seem to inflate existing post-tectonic low-Ca granites overprinting existing deformation structures.

Greenstones

The dominant datasets used in differentiating polygons and lines of greenstone lithologies were the WAROX database, existing surface mapping (GSWA and external), aeromagnetic texture and intensity and gravity response. The greenstone geochemistry dataset (Ivanic et al., 2021b), is highly focused on isolated drillcore samples, thus it was locally very useful for lithological assignment. The geochemical point data were classified into various geochemical groups and classes and, in a few instances in this interpreted bedrock geology map, it has been possible to assign greenstones based upon these groups.

We assigned greenstone polygon codes either to the South West Terrane or the Youanmi Terrane (i.e. A-lithology-YSW or A-lithology-YYO), and this decision was based primarily on geochronological constraints. For example, the South West Terrane, as we define it, has distinctly younger greenstone depositional ages than the Youanmi Terrane. Mixed lithology codes were used in many instances in both terranes to represent heterogeneous map units or units with fine interlayering, for example

where metasedimentary and metabasaltic rocks were interpreted to be interlayered and lensed together along shear zones, or where abundant metamonzogranite sheets intrude amphibolite.

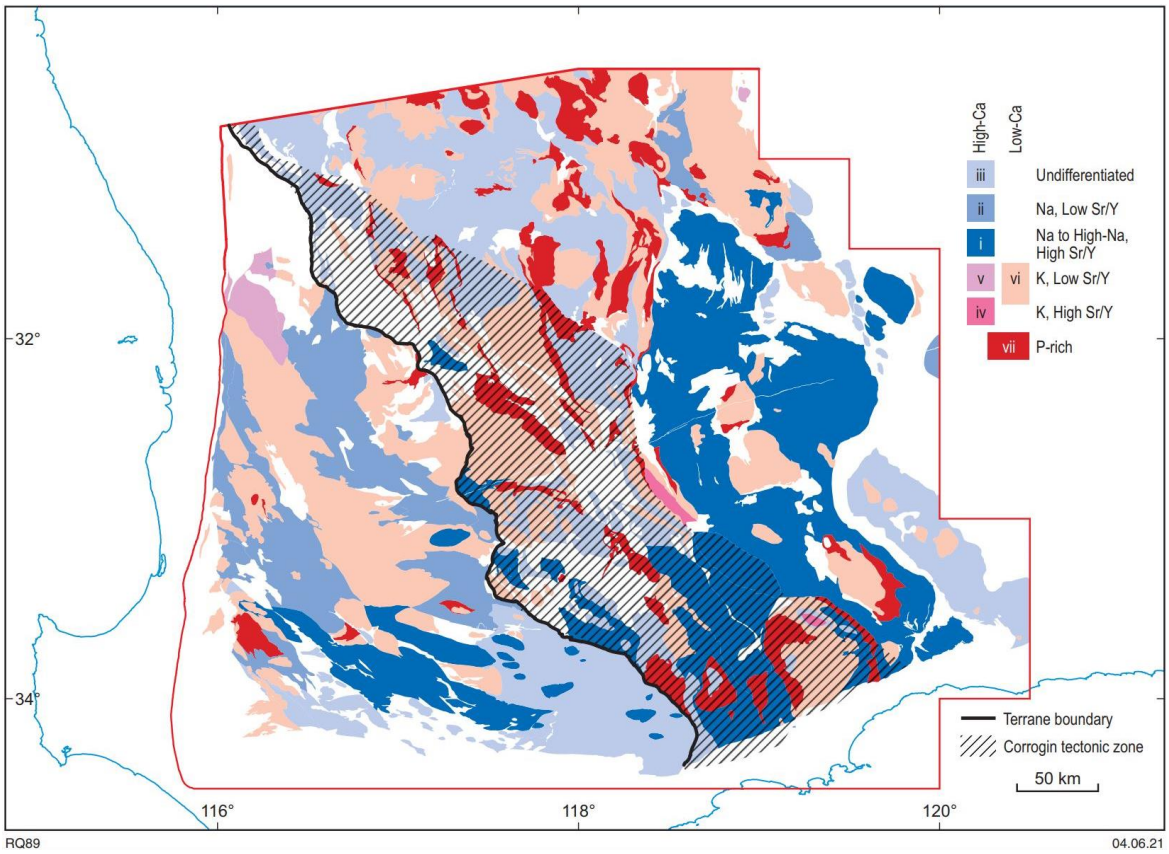

Figure 6. Interpreted granite map of the southwest Yilgarn showing the distribution of mappable polygons of major geochemical granite groups

Even though the terrane boundary itself was drawn along interpreted structures that post-date greenstone deposition, the boundary does appear to separate polygons of distinct greenstone characteristics.

Without a direct record of lithology in the WAROX database, the following list summarizes the ways we differentiated the main groups of greenstones (including their metamorphosed equivalents) in both terranes on the interpreted bedrock geology map:

- Ultramafic volcanic rocks: highly magnetic (typically narrow trend lines), high density, interlayered with mafic volcanic rocks and metasedimentary rocks, generally <45 wt% SiO_2, >18 wt% MgO.
- Mafic volcanic rocks: generally, low magnetic response, moderate density, interlayered with metasedimentary rocks, locally intruded by sills of mafic–ultramafic intrusive rocks, 45–57 wt% SiO_2; <18 wt% MgO.
- Felsic–intermediate volcanic rocks: typically too thin to show a distinct geophysical response, >57 wt% SiO_2.
- Ultramafic intrusive rocks: generally highly magnetic (wider, elongate, irregular shapes compared to BIF), high density, MgO > 18 wt%; often in a belt containing several small circular features; where metamorphosed to high grade, they tend to form ovoid features, 1–10 km across.
- Mafic intrusive rocks: generally low–moderate magnetic intensity, moderate–high gravity response, 6–18 wt% MgO; where Fe rich, they are highly magnetic due to interlayered gabbro and magnetitite; where metamorphosed to high grade, they tend to form ovoid features.

- Siliciclastic sedimentary rocks: generally low magnetic intensity, featureless and low density.
- Chemical sedimentary rocks: extremely highly magnetic, typically thin, narrowly spaced magnetic lines, high density, typically interlayered with mafic volcanic rocks; chert-rich rather than BIF-rich successions are typically too thin to show a distinct geophysical response.

These results are shown in a greenstones map for the interpreted bedrock geology extent (Fig. 7). The lithological assemblages vary across the map and form northwest-trending domains. From southwest to northeast these informal assemblages are:

- Assemblage 1: Greenstone belts at Forrestania, Lake King and Ravensthorpe (Fig. 1) have lithological assemblages more typical of Neoarchean Youanmi Terrane greenstone belts with ultramafic volcanic rocks, mafic volcanic and intrusive rocks, metasedimentary siliciclastic rocks and BIF. Lower proportions of felsic–intermediate volcanic rocks and ultramafic intrusive rocks.
- Assemblage 2: Greenstone belts at Wongan Hills, Westonia and Holleton have lithological assemblages more typical of Mesoarchean Youanmi Terrane greenstone belts with high proportions of each of: mafic volcanic, mafic intrusive rocks and both metasedimentary siliciclastic rocks and BIF and lower proportions of felsic–intermediate volcanic and ultramafic volcanic rocks.
- Assemblage 3: Greenstones in a wide area centred on Narembeen (and similar to the Corrigin Tectonic Zone structural domain) have lithological assemblages comprising granulite-facies mafic intrusive, mafic volcanic and sedimentary rocks and lesser ultramafic rocks. This is more typical of Mesoarchean Youanmi Terrane greenstone belt assemblages, but at higher metamorphic grade.
- Assemblage 4: Greenstones in the Northam area have lithological assemblages comprising BIF interlayered with metamorphosed siliciclastic, mafic volcanic and mafic intrusive rocks. This is similar to Mesoarchean Youanmi Terrane greenstone belt assemblages, but with a higher abundance of metasedimentary rocks.
- Assemblage 5: In the north and east of the South West Terrane the majority of greenstones comprise metamorphosed siliciclastic rocks intruded by mafic–ultramafic sills and plugs.
- Assemblage 6: The Boddington greenstone belt comprises a distinct lithological assemblage of mafic–intermediate volcanic rocks and lesser metasedimentary rocks and ultramafic sills.
- Assemblage 7: In the far west and south of the South West Terrane, the area coincident with the 'Balingup terrane' (Wilde et al., 1996) contains dominant siliciclastic rocks locally with numerous small ultramafic sills.

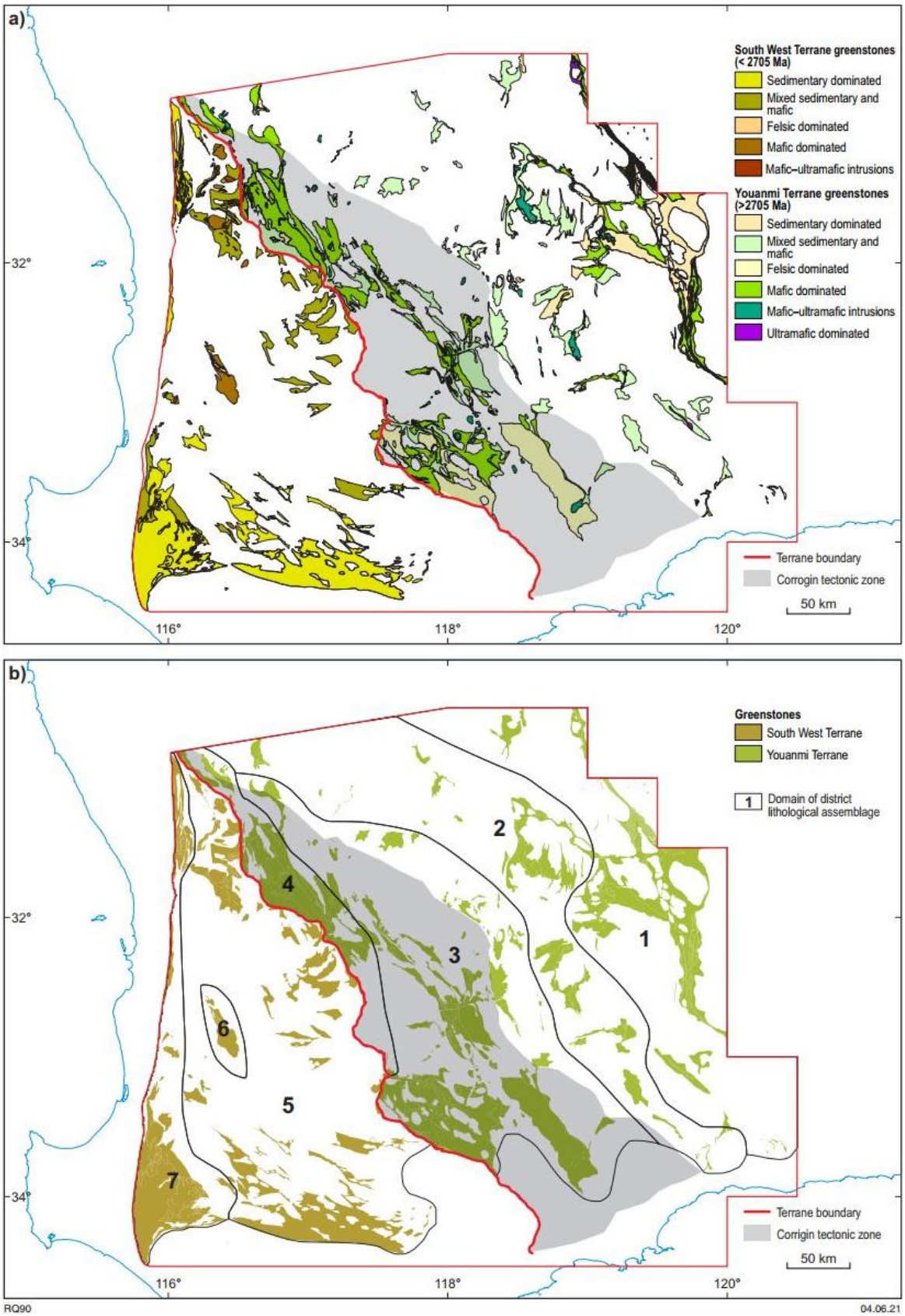

Figure 7. Interpreted greenstone map groups of the South West Terrane and the southwestern Youanmi Terrane. Inset shows numbered domains of distinct lithological assemblages (see text for explanation)

Main findings

Crustal domains

We identify six main shear zone-bounded crustal domains of different geological history across the interpreted bedrock geology area (Fig. 3b); these are:

Domain 1: A greenschist to amphibolite facies domain within the Youanmi Terrane, bounded to the west by the Youanmi Shear Zone. This domain includes characteristic linear and fault-bounded greenstone belts such as Southern Cross, Forrestania, Lake King and Ravensthorpe (Fig. 1). These are intruded by large granitic domes that dominantly show regional-scale sinistral asymmetry.

Domain 2: An amphibolite- to granulite-facies domain within the Youanmi Terrane, bounded to the east by the Youanmi Shear Zone and to the west by the Corrigin Tectonic Zone. This domain contains a shear zone system that anastomoses and forms lozenges of similar shapes and probably of similar geological history to the 2730–2665 Ma north-trending lozenges observed further north in the Youanmi Terrane; however, here the long axes of the lozenges trend north-northwest. This change in orientation from northerly to north-northwesterly trending is interpreted to result from rotation of the long axes of the lozenges (simple shear component) during sinistral drag along the eastern margin of the 2665–2635 Ma sinistral transpressive Corrigin Tectonic Zone (see Domain 3). Domain 2 is largely dominated by gneissic TTGs with high Ca, ±Na and high Sr/Y values (Fig. 6) intruded into Youanmi greenstones. The greenstone associations in this domain occur as dismembered rafts within the gneissic TTGs. Minor porphyritic low-Ca, K, low-Sr/Y biotite monzogranite, such as that observed at Wave Rock near Hyden (Figs 1, 6), form domes within the gneissic TTGs. This domain is interpreted to represent a mid-crustal level exposure.

Domain 3 (the Corrigin Tectonic Zone): A strongly deformed, largely migmatitic, granulite-facies domain forming the southwestern end of the Youanmi Terrane. The area contains a moderately to steeply northeast-dipping foliation, shows abundant tight to isoclinal folds that are dominantly west-verging, and commonly display regional-scale asymmetric boudins indicating sinistral shear sense. The deformation is interpreted to be partitioned into moderately northeast-dipping thrusts and steeply dipping, northwest-striking sinistral shear zones that we interpret to have formed in between 2665 and 2635 Ma. The area hosts a high proportion of migmatitic, gneissic TTGs intruded by syntectonic low-Ca, K, low-Sr/Y and low-Ca, P-rich metamonzogranite and metasyenogranite intruded as tabular sheets along and in the footwalls of northwest-striking shear zones of the Corrigin Tectonic Zone (Fig. 6). The counter clockwise rotation of the lozenges' long axes of Domain 2 along the Corrigin Tectonic Zone, together with the identification of regional-scale, northwest-trending, asymmetric sinistral boudins, and of compressional southwest-verging tectonic fabrics, indicates that deformation was partitioned into moderately northeast-dipping thrusts and steeply dipping, northwest-striking sinistral shear zones. These observations form a strong argument that the Corrigin Tectonic Zone resulted from sinistral transpression. The Corrigin Tectonic Zone is dominated by migmatitic rocks that generally record metamorphic conditions of 5–7 kbar and 700–900 °C, although lower and higher values are also reported (Korhonen et al., 2021). The U–Pb zircon and monazite metamorphic ages for this zone are between c. 2665 and 2635 Ma, interpreted as the age of high-grade metamorphism and likely as the age of deformation. Zircon $\delta^{18}O$ values from c. 2800 to 2641 Ma granitic rocks from the Corrigin Tectonic Zone yielded values ranging between 6.5 and 6.9‰ (Lu et al. 2021b) suggesting significant tectonic burial of supracrustal material into the source region of the c. 2800 to 2641 Ma granite, which is consistent with the underthrusting inferred from the transpressional interpretation for the Corrigin Tectonic Zone.

Domain 4: Potentially a relatively old and deep crustal domain within the otherwise apparently younger South West Terrane. The basement aeromagnetic features within this domain are largely obscured by the very high density of northwesterly to north-northwesterly striking mafic dykes. Mapping the aeromagnetic form lines in the background of these dykes revealed a systematic west-northwesterly striking domain. West-northwesterly trending ovoid features in this domain with

concentric aeromagnetic trend lines and associated with high-Ca, high-Na, and high-Sr/Y granite analyses are interpreted as ovoid TTG plutons (Fig. 6). Major west-northwesterly trending shear zones bound and occur within this domain and are interpreted to pre-date and control the emplacement of the TTG plutons dated at c. 2702 Ma and c. 2669 Ma and are truncated by the northwest-striking major shear zones of the 2665–2635 Ma Corrigin Tectonic Zone. The shear zones bounding this domain control the distribution of exposed high-Ca granites with high Sr/Y values in the South West Terrane. Domain 4 is largely dominated by TTGs with high Ca (± Na) and high Sr/Y, while the high-Ca (± Na) granites of Domains 5 and 6 have almost exclusively low Sr/Y values. Additionally, Domain 4 contains very few low-Ca granites while Domains 5 and 6 are largely dominated by them. Domain 4 also coincides with a high gravity anomaly and we interpret the basement into which the TTG plutons were intruded as a mixed intermediate and mafic gneissic crust, which possibly represents a low crustal level exposure. One major west-northwesterly trending shear zone in this domain is spatially associated with sanukitoid and low-Ca, high-P intrusions and has been found to host Au occurrences. The west-northwesterly trending structures of Domain 4 have likely been reused during the intrusion of the west-northwesterly trending c. 1888 Ma Boonadgin Dolerite dykes.

Domain 5: A domain largely dominated by low-Ca, K, low-Sr/Y biotite monzogranite, a large area of hornblende-bearing granodiorite and minor high-Ca (±Na) granite exclusively with low Sr/Y values. This domain is bounded to the east by the Corrigin Tectonic Zone and to the west by Proterozoic shear zones of the proto-Darling Fault and also includes Julimar (Ni) and Boddington (Au) (Figs 1, 3b). Although unconstrained, the overall metamorphic grade of Domain 5 appears lower than that of the Corrigin Tectonic Zone (i.e. Domain 3); indeed the rock succession at Boddington is at greenschist facies. We interpret this domain as an upper crustal level exposure.

Domain 6: This domain is bounded to the west by the Darling Fault and to the south by the Albany–Fraser Orogen. It includes the Chittering Metamorphic Belt, as well as the sedimentary succession around Balingup and hosts REE-bearing pegmatite at Greenbushes (Figs 1, 3b). It is mainly characterized by the widespread Proterozoic overprint that produced the numerous major shear zones that dissect this domain, either as north-striking shear zones subparallel to the Darling Fault or as closely-spaced, northwest-trending shear zones in the southwest corner of the map area. This domain contains a larger proportion of sedimentary rocks than any other domain, and also contains a young 2615–2610 Ma suite of granite.

Redefined boundary between the Youanmi and South West Terranes

Three significant issues were identified with the previous terrane boundary between the Youanmi and South West Terranes of Cassidy et al. (2006), which:

- cuts geophysical trend lines at a high angle
- does not differentiate between crustal domains with contrasting geological histories
- does not represent a change in lithological assemblages within greenstone belts.

In our new interpretation, the Youanmi Terrane has been extended southwest to include Domain 2, which broadly coincides with the informal Lake Grace terrane of Wilde et al. (1996) and the Corrigin Tectonic Zone (i.e. Domain 3; Figs 1, 3). The terrane boundary with the South West Terrane is now interpreted to lie along the southwestern deformation front of the northwest-trending Corrigin Tectonic Zone, which, together with the informal Lake Grace terrane, are now interpreted to represent an upper amphibolite to granulite facies equivalent to the rest of the Youanmi Terrane. Key variations within many new or updated datasets (Fig. 8) were used to guide interpretation of the new terrane boundary: Nd and O isotopes, the distribution of igneous crystallization ages, the nature of the greenstone belts, mineralization data, granite geochemistry, structural patterns, deformation style and metamorphic history data. Regarding the metamorphic data, nearly all new pressure and temperature data are from samples within the amphibolite- to granulite-facies Youanmi Terrane, but it is clear that there has to be a significant change towards the western portion of the South West Terrane because supracrustal

rocks at Boddington have been identified to be at greenschist facies. Among these datasets, the geochronology of granite and greenstone samples most clearly differentiated the two terranes.

We have identified that Domain 2 is characterized by an anastomosed system of north-northwesterly striking shear zones that collectively form lozenge-shape patterns that closely resemble those of the central and northern parts of the Youanmi Terrane (Fig. 3). The similar lithological associations and geochronology data between Domain 2 and the rest of the Youanmi Terrane strongly suggests that the lozenge patterns affected similarly aged rocks to those in the rest of the Youanmi Terrane, indicating that they also formed during tectonic events occurring between 2730–2665 Ma (Zibra et al. 2017). The lack of lozenge shear zone patterns in the South West Terrane marks a strong difference in structural style and suggests that it shares a different tectonic history.

Similarly, the zircon O isotopes also indicate that the South West and Youanmi Terranes did not experience the same tectonic history (Lu et al. 2021b). The South West Terrane contains zircon dominated by mantle-like $\delta^{18}O$ values (4.7 – 5.9‰), indicating that no significant supracrustal reworking has occurred prior to or during granite generation. By contrast, values from the Youanmi Terrane commonly have $\delta^{18}O$ values over 5.9‰ suggesting at least a minor amount of crustal reworking and supracrustal material burial into the source regions of granites of the amphibolite- to granulite-facies portion of the Youanmi Terrane. The highest zircon O isotopes values ($\delta^{18}O$ up to 6.9‰) in the entire Yilgarn Craton have been obtained from granitic rocks along the proposed terrane boundary between the South West and Youanmi Terranes, possibly indicating that maximum burial of supracrustal material has occurred along this boundary.

The Nd isotope depleted mantle model age (T_{DM2}) map of the project area indicates an overall change to younger model ages (<2.95 Ga) across the terrane boundary towards the southwest, but the shift is not distinct (Lu et al. 2021a). There are several regions within the South West Terrane with >3 Ga Nd model ages, which is similar to the Youanmi Terrane. However, the overall texture of the isotopic map does change to the southwest whereby the domains of similar ages are much smaller. This pattern within the South West Terrane may indicate local Youanmi Terrane basement such as in the area around Boddington, but also a different geological history involving multiple, younger, juvenile input events, which are not known from the Youanmi Terrane.

Magmatic crystallization ages within granitic rocks indicate that >2.8 Ga granitic rocks are restricted to the Youanmi Terrane. Xenocrystic zircons within granitic rocks show that the oldest grains within the South West Terrane are c. 2.8 Ga, whereas 2.9 – 3.1 Ga xenocrystic zircons are widely present in granitic rocks of the Youanmi Terrane (Fig. 8).

Magmatic crystallization ages constraining the age of deposition and mafic magmatism within greenstones differ across the new terrane boundary. Figure 8 shows that the Youanmi Terrane experienced a distinct, older history of greenstone deposition from 2.7 – 3.1 Ga, compared to 2.7 – 2.4 Ga in the South West Terrane. The c. 2.69 Ga 'McCaskill group' in the Youanmi Terrane is very localized and occurs as very low volume slivers, whereas the 2704–2670 Ma Saddleback Group in the South West Terrane is more voluminous and protracted with a higher proportion of volcanic rocks. The 'Balingup supergroup' has poor geochronological constraints:

- Metasandstone at Wheatley has an interpreted maximum depositional age 2646 Ma (Sircombe et al. 2007).
- In the far southwest corner of the South West Terrane, a pelitic gneiss has a 2636 Ma zircon, interpreted as a potential detrital grain (Lu et al. 2015).
- c. 3200 Ma detrital zircons are present in some parts of the stratigraphy (Lu et al. 2016).
- The metasedimentary units to the north are locally cut by a suite of c. 2615 Ma granitic rocks, providing a minimum age constraint.

Thus, while we can say that the 'Balingup supergroup' is different in age (and composition, being very quartzite rich) to anything found in the Youanmi Terrane, further work is required to establish the geological history of the 'Balingup supergroup'.

In terms of mafic–ultramafic intrusive rocks, the geological history of the South West Terrane is independent to the Youanmi Terrane until 2615 Ma (Fig. 8). The 'Julimar' and 'Red Hill' suites at c. 2665 Ma only intrude units of the South West Terrane. Further work is required to test whether these suture across the terrane boundary in the north. If so, they would provide a minimum age for accretion of the two terranes.

Across the project area, the lithological assemblages within greenstones form distinct, northwest-trending domains, where the most significant shift is located at the new terrane boundary between the South West Terrane and the Youanmi Terrane. Overall, this change towards the southwest includes:

- an increase in quartz-rich metasedimentary rocks, including much more abundant quartzite
- an increase in young (c. 2665 Ma), mineralized mafic–ultramafic intrusions
- a decrease in mafic volcanic rocks
- a decrease in BIF
- a decrease in granulite-facies rocks, particularly those with a particularly high thermal gradient (Korhonen et al., 2021).

The revised terrane boundary between the South West Terrane and the Youanmi Terrane represents one of the major divisions within the Yilgarn Craton, second only to the Eastern Goldfields and Youanmi Terrane (Ida Fault). Further work is required to understand the tectonic significance of this boundary and to refine its precise location. Nevertheless, such an important feature provides a crustal-scale (and potentially mantle-tapping) feature to explore for mineral deposits, opening up a corridor of exploration search space.

Stratigraphy, magmatism and mineralization

The reinterpreted terrane boundary presented here indicates a break in the stratigraphy and magmatic history of the South West and Youanmi Terranes (Fig. 8). We consider the new boundary to be a major control on the distribution of several key magmatic suites and stratigraphic units, many of which are mineralized (see details in MINEDEX layer, GSWA, 2021). For example:

- in the South West Terrane:
  - Boddington (Au–Cu–Mo)
  - Julimar (Ni–Cu–PGE)
  - Red Hill (V–Ti)
  - Donnybrook (Au)
  - Wheatley (Zn, Cu, Pb, Au, Ag)
  - Greenbushes (REE)
- and in the Youanmi Terrane (west of the Youanmi Shear Zone):
  - Calingiri (Au–Cu–Mo)
  - Lake King (Ni)
  - Katanning (Au), Tampia (Au) and Griffins Find (Au)
  - iron deposits (Fe), widespread within the Youanmi greenstones.

The magmatism at Boddington, although showing striking similarities with the Kalgoorlie–Kambalda region (Smithies et al., 2021b), is unique in the southwest Yilgarn Craton and we consider it to be a distinct stratigraphic package (in age as well as composition) comprising a higher proportion of intermediate volcanic rocks than anywhere else in the South West Terrane. Further work is required to uncover the total extent of the 'Julimar suite' as we expect several intrusive mafic–ultramafic

geological polygons in a wide area of the South West Terrane may be related. Likewise, further work is required to establish the full extent of the 'Red Hill suite', which may occur as sills in a wide area between Katanning and Northam, including the Coates Siding Gabbro (Ivanic et al., 2021b).

The Donnybrook Au deposit is located in the metasedimentary lithological assemblage 7 and it is possible that similar deposits may exist along strike. At Wheatley, the metasedimentary units hosting mineralization are not exposed and lack of exposure in this part of the South West Terrane means that lithologies and mineralization are unconstrained. The Greenbushes Pegmatite is an outlier in that similar granitic suites are not found in the South West Terrane, but similar rocks may exist in areas under cover.

In the Youanmi Terrane, the c. 3000 Ma, Calingiri mineralization has been linked to particular monzogranite and syenogranite plutons (Outhwaite, 2018) and potentially to the felsic volcanism in the Wongan Hills greenstone belt. The 'Wongan group' and the 'Calingiri suite', part of the Thundelarra Supersuite, are likely to be traceable along a vast area of older Youanmi Terrane greenstones and Yilgarn Craton granitic rocks within the western Yilgarn Craton. In the far northeast of the project area are metamorphosed ultramafic rocks, which, in light of their continuation of the Ravensthorpe – Lake King – Forrestania trend of Ni deposits, are prospective. The Katanning, Tampia and Griffins Find Au deposits lie in proximity to a large volume of granulite-facies mafic–ultramafic rocks. These are exposed in the Corrigin Tectonic Zone and associated structures, often forming circular structures 1–10 km across and interpreted as greenstone 'keels' (e.g. Gee et al., 1986). Immediately north of the terrane boundary, within the southwesternmost Youanmi Terrane, there is a notable linear belt of BIF-hosted Fe deposits (within lithological assemblage 4), but these are typically too thin to yield large deposits.

Conclusion

A pre-Mesozoic interpreted bedrock geology map of the southwest Yilgarn is provided and the wealth of information contained within this map can be displayed in various ways, including mafic dyke maps, structure maps, a granite geochemistry map and a greenstone lithological map. We identify six crustal domains of distinct geological history, also possibly reflecting varying levels of crustal exposure, although further work is required to fully understand this assertion. The most significant outcomes of this work are the redefinition of the terrane boundary between the South West Terrane and the Youanmi Terrane and the ability to provide additional geological background to known deposits of various commodities in the southwest Yilgarn.

The new domains and terranes defined in this work integrate numerous and diverse GSWA and external datasets to present a significantly updated and united geological framework for the southwest Yilgarn. The methodology defined here is capable of dealing with the large and diverse nature of geological data coverage in the Yilgarn. The Pre-Mesozoic interpreted bedrock geology of the southwest Yilgarn, 2021 provides a highly interpreted view of the outcome of this unification process and should be used in parallel with the ~600 geological layers in the Southwest Yilgarn, 2021 Geological Exploration Package (GSWA, 2021). Although further work is required to test and expand this dataset and interpretation of the geological history of the southwest Yilgarn, this work provides a significant leap in geological understanding and can broaden the scope for the exploration of diverse types of mineral deposits.

How to access

The Pre-Mesozoic interpreted bedrock geology map of the southwest Yilgarn is best accessed using GeoVIEW.WA. The digital data are also available as a free download from the Data and Software Centre.

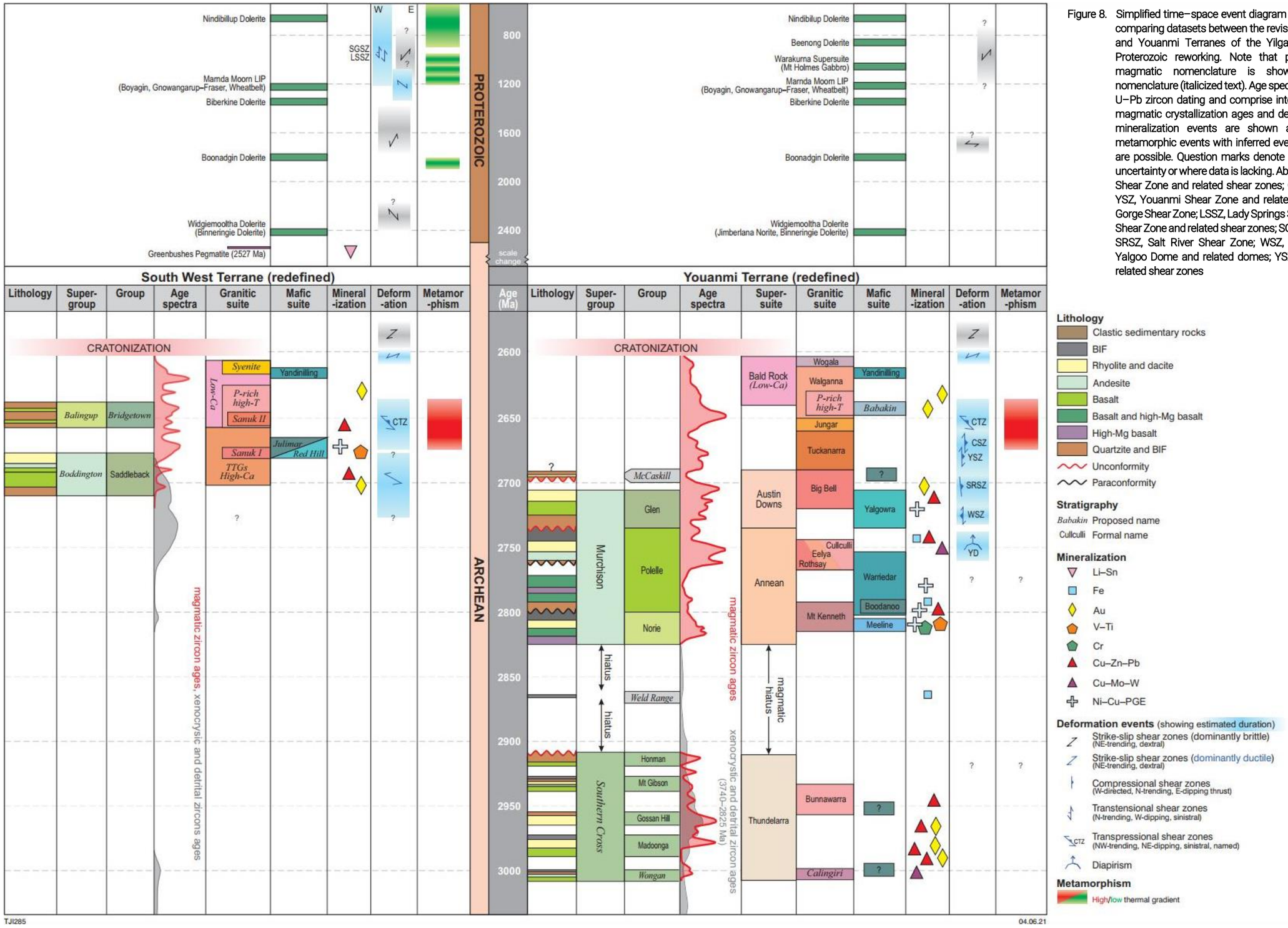

Figure 8. Simplified time–space event diagram and stratigraphic framework comparing datasets between the revised extents of the South West and Youanmi Terranes of the Yilgarn Craton, and subsequent Proterozoic reworking. Note that published stratigraphic and magmatic nomenclature is shown along with proposed nomenclature (italicized text). Age spectra are derived primarily from U–Pb zircon dating and comprise interpreted GSWA and external magmatic crystallization ages and detrital zircon data. Significant mineralization events are shown alongside deformation and metamorphic events with inferred event duration where estimates are possible. Question marks denote features or events with high uncertainty or where data is lacking. Abbreviations: CSZ, Cundimurra Shear Zone and related shear zones; CTZ, Corrigin Tectonic Zone; YSZ, Youanmi Shear Zone and related shear zones; SGSZ, Swan Gorge Shear Zone; LSSZ, Lady Springs Shear Zone; CSZ, Cundimurra Shear Zone and related shear zones; SGSZ, Swan Gorge Shear Zone; SRSZ, Salt River Shear Zone; WSZ, Waroonga Shear Zone; YD, Yalgoo Dome and related domes; YSZ, Youanmi Shear Zone and related shear zones

References

Brett, JW 2021, Multi-scale edges for the southwest Yilgarn from gravity and magnetics: Geological Survey of Western Australia, digital data layer, <www.dmirs.wa.gov.au/geoview>.

Cassidy, KF, Champion, DC, Krapež, B, Barley, ME, Brown, SJA, Blewett, RS, Groenewald, PB and Tyler, IM 2006, A revised geological framework for the Yilgarn Craton, Western Australia: Geological Survey of Western Australia, Record 2006/8, 8p.

Gee, RD, Myers, JS and Trendall, AF 1986, Relation between Archaean high-grade gneiss and granite–greenstone terrain in western Australia: Precambrian Research, v. 33, no. 1, p. 87–102, doi:10.1016/0301-9268(86)90016-1.

Geological Survey of Western Australia 2020a, Compilation of WAROX data, 2020: Geological Survey of Western Australia, Digital Data Package.

Geological Survey of Western Australia 2020b, Compilation of geochronology information, 2020:Geological Survey of Western Australia, Digital Data Package.

Geological Survey of Western Australia 2021, Southwest Yilgarn, 2021: Geological Survey of Western Australia, Geological Exploration Package.

Ivanic, TJ, Kelsey, DE and Duuring, P 2021a, Magmatic and stratigraphic WAROX text search results for the southwest Yilgarn: Geological Survey of Western Australia, digital data layer.

Ivanic, TJ, Lowrey, JR and Smithies, RH 2021b, New geochemical constraints on the mafic and ultramafic rocks of the southwest Yilgarn: Geological Survey of Western Australia, digital data layer.

Jessell, MW 2001, Atlas of Structural Geophysics II: Australian Crustal Research Centre, Journal of the virtual explorer, v. 5. 94p.

Korhonen, FJ, Blereau, ER, Kelsey, DE, Fielding, IOH and Romano, SS 2021, Metamorphic evolution of the southwest Yilgarn: Geological Survey of Western Australia, digital data layer.

Lu, Y, Wingate, MTD, Champion, DC, Smithies, RH, Johnson, SP, Mole, DR, Poujol, M, Zhao, J, Maas, R and Creaser RA 2021a, Samarium–Neodymium isotope map of Western Australia: Geological Survey of Western Australia, digital data layer.

Lu, Y, Wingate, MTD, Smithies, RH, Martin, L, Jeon, H, Champion, DC, Johnson, SP and Mole, DR 2021b, Zircon oxygen isotope map of Western Australia: Geological Survey of Western Australia, digital data layer.

Lu, Y, Wingate, MTD and Bodorkos, S 2016, 184116: quartzite, Polina Road; Geochronology Record 1310: Geological Survey of Western Australia, 4p.

Lu, Y, Wingate, MTD, Kirkland, CL, Goscombe, B and Wyche, S 2015, 198551: pelitic gneiss, Donnelly River; Geochronology Record 1283: Geological Survey of Western Australia, 6p.

Outhwaite, MD 2018, Metamorphosed Mesoarchean Cu–Mo–Ag mineralization: evidence from the Calingiri deposits, southwest Yilgarn Craton: Geological Survey of Western Australia, Report 183, 208p.

Pisarevsky, SA, Waele, BD, Jones, S, Söderlund, U and Ernst, RE 2015, Paleomagnetism and U–Pb age of the 2.4 Ga Erayinia mafic dykes in the south-western Yilgarn, Western Australia: Paleogeographic and geodynamic implications: Precambrian Research, v. 259, p. 222–231, doi:10.1016/j.precamres.2014.05.023.

Sircombe, KN, Cassidy, KFC, Champion, DC and Tripp, G 2007, Compilation of SHRIMP U–Pb geochronological data, Yilgarn Craton, Western Australia, 2004–2006: Geoscience Australia, Record 2007/01, 182p.

Smithies, RH, Lu, Y, Lowrey, J, Ivanic, T, Champion, DC and Wilde, SA 2021a, Variations in granite geochemistry in the southwest Yilgarn. Geological Survey of Western Australia, digital data layer.

Smithies, RH, Lu, Y and Champion, DC 2021b, New geochemical and geochronological constraints on the magmatic evolution of Boddington, southwest Yilgarn: Geological Survey of Western Australia, digital data layer.

Stark, JC, Wilde, SA, Söderlund, U, Li, Z-X, Rasmussen, B and Zi, J-W 2018, First evidence of Archean mafic dykes at 2.62 Ga in the Yilgarn Craton, Western Australia: Links to cratonisation and the Zimbabwe Craton: Precambrian Research, v. 317, p. 1–13.

Stark, JC, Wang, X-C, Denyszyn, SW, Li, Z-X, Rasmussen, B, Zi, J-W, Sheppard, S and Liu, Y 2019, Newly identified 1.89 Ga mafic dyke swarm in the Archean Yilgarn Craton, Western Australia suggests a connection with India: Precambrian Research, v. 329, p. 156–169, 14p., doi:10.1016/j.precamres.2017.12.036.

Stark, JC, Wang, X-C, Li, Z-X, Denyszyn, SW, Rasmussen, B and Zi, J-W 2018, 1.39 Ga mafic dyke swarm in southwestern Yilgarn Craton marks Nuna to Rodinia transition in the West Australian Craton: Precambrian Research, v. 316, p. 291–304, 14p., doi:10.1016/j.precamres.2018.08.014.

Wilde, SA, Middleton, MF and Evans, BJ 1996, Terrane accretion in the southwestern Yilgarn Craton: Evidence from a deep seismic crustal profile: Precambrian Research, v. 78, p. 179–196.

Wingate, MTD 2007, Proterozoic mafic dykes in the Yilgarn Craton, *in* Proceedings of Geoconferences (WA) Inc. Kalgoorlie '07 Conference, 25–27 September 2007, Kalgoorlie, Western Australia *edited by* FP Bierlein and CM Knox-Robinson: Geoscience Australia, Record 2007/14, p. 80–84.

Wingate, MTD 2017, Mafic dyke swarms and large igneous provinces in Western Australia get a digital makeover, *in* GSWA 2017 extended abstracts: promoting the prospectivity of Western Australia: Geological Survey of Western Australia, Record 2017/2, p. 4–8.

Zibra, I, Clos, F, Weinberg, RF and Peternell, M 2017, The c. 2730 Ma onset of the Neoarchean Yilgarn Orogeny: Tectonics, v. 36, no. 9, p. 1787–1813, doi:10.1002/2017TC004562.

Zibra, I, 2021, Lithostructural map of the Chittering Metamorphic Belt. Geological Survey of Western Australia, digital data layer.

Recommended reference

Quentin de Gromard, R, Ivanic, TJ and Zibra, I 2021, Pre-Mesozoic interpreted bedrock geology of the southwest Yilgarn: Geological Survey of Western Australia, digital data layers.

New geochemical and geochronological constraints on the magmatic evolution of Boddington, southwest Yilgarn

by

RH Smithies, Y Lu and DC Champion*

Abstract

A total of 47 legacy and 73 recently acquired whole-rock major and trace element analyses, collected mainly from drillcores at the Boddington Au–(Cu) mine, have been examined and the rocks classified into geochemical groups, with their magmatic crystallization ages constrained by eight new Sensitive High-Resolution Ion Microprobe (SHRIMP) U–Pb zircon dates.

Basaltic rocks (18 samples) are likely part of the Marradong Formation, which forms the older part of the greenstone stratigraphy at Boddington, and can be grouped into low-Th basalts (LTB, terminology of Barnes et al., 2012), LTB transitional to intermediate-Th basalts (ITB) and high-Ti basalts. Compared with typical LTB from the Eastern Goldfields region, the Boddington LTB are more enriched in incompatible trace elements and were derived from a less depleted mantle source. A wide range in Th/Nb ratios of the LTB and ITB suggests the trace element enrichments likely result from crustal contamination, but a subduction-enriched mantle source cannot be discounted.

Felsic volcanic, volcaniclastic and subvolcanic rocks have been divided into three groups (Fig. 1). A large proportion of these samples (n = 44) form a geochemically coherent group consisting of felsic volcanic rocks (mainly andesites and dacites) and diorites. The igneous crystallization age from a dacitic member of this group is 2704 ± 3 Ma (Lu et al., 2020b). Increasing Sr/Y with increasing SiO_2 and positively correlated Nd/Zr and Gd/Yb indicate hornblende fractionation, consistent with the hornblende-rich mineralogy and suggesting a hydrated parental magma. Relatively high $Mg^{\#}$ (~57 at 61 wt% SiO_2, where $Mg^{\#}$ = mol Mg/[mol Mg + mol Fe_{total}]), and high Cr and Ni concentrations (both >>100 ppm at about 60 wt% SiO_2) suggest fractionation from a hydrated mantle-derived magma and a 'sanukitoid-like' composition. Low Sr (<400 ppm) and relatively low light rare earth elements (REE) suggest lower degrees of source enrichment than expected for the source of sanukitoids. Intriguingly, the closest Archean compositional analogue to these rocks are c. 2706 Ma dacites and associated diorites from the Kalgoorlie region of the Eastern Goldfields (Fig. 1; Smithies et al, in prep). Zircon trace element data from the Boddington c. 2700 Ma rocks ('Boddington 2700 Ma syn-ore diorites and dacite' of Lu et al., 2019), are similar to those from calk-alkaline rocks hosting Phanerozoic porphyry-style Cu–Au mineralization.

A second group (four samples including one rhyolite, one andesite and two diorites) compositionally resemble rocks of the Archean tonalite–trondhjemite–granodiorite (TTG) series or modern adakites. The andesite of this group yielded an igneous crystallization age of 2690 ± 2 Ma (Lu et al., 2020a). This c. 2690 Ma group can be distinguished from the c. 2704 Ma magmas in having significantly more fractionated mantle-normalized REE patterns (higher La/Yb ratios), typically more Al-rich compositions (Al_2O_3 > 15 wt% at 70 wt% SiO_2) and higher Sr/Y ratios (>30 cf. <30 for the c. 2704 Ma rocks) albeit still at rather low Sr concentrations (<350 ppm).

* Geoscience Australia, GPO Box 378, Canberra, ACT 2601

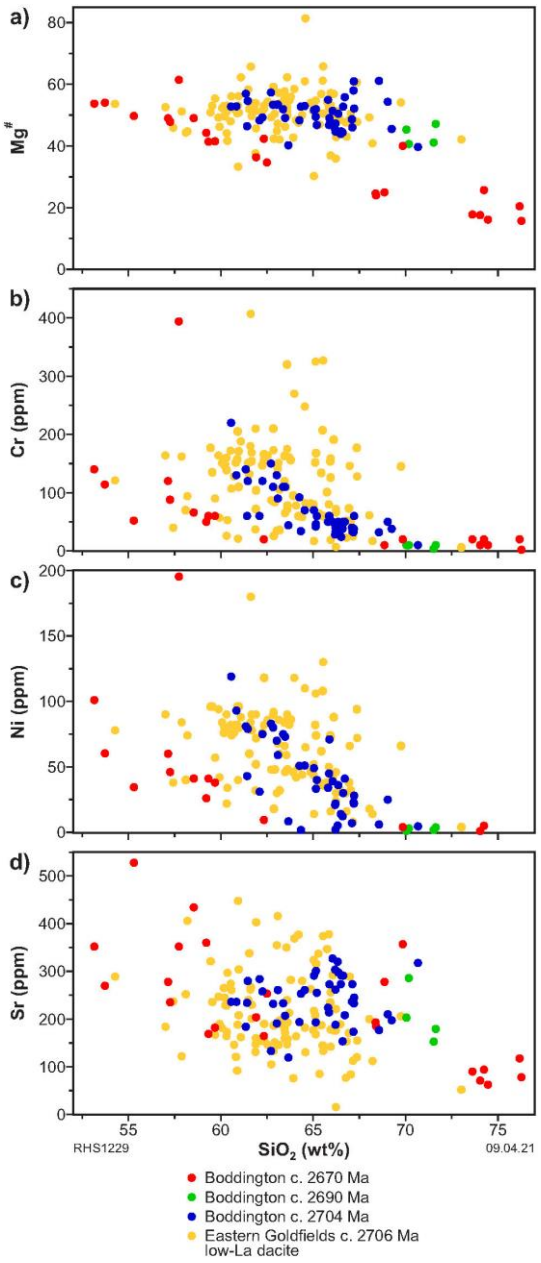

Figure 1. Geochemical variation diagram showing variations in: a) Mg#; b) Cr concentration; c) Ni concentration; d) Sr concentration, against concentration of SiO_2 for felsic rocks from Boddington

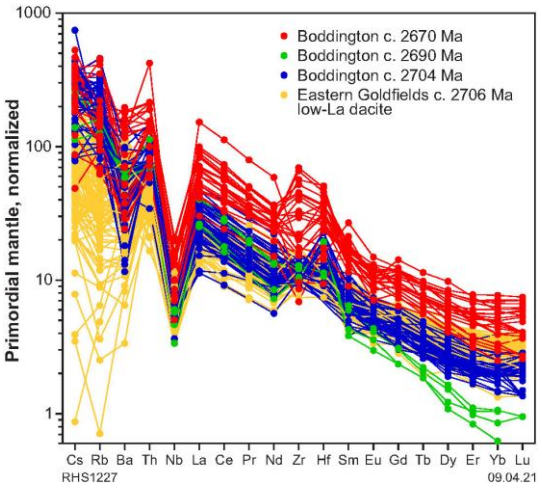

Figure 2. Multi-element spidergrams showing mantle-normalized trace element patterns for felsic rocks from Boddington (normalization after after McDonough et al., 1992)

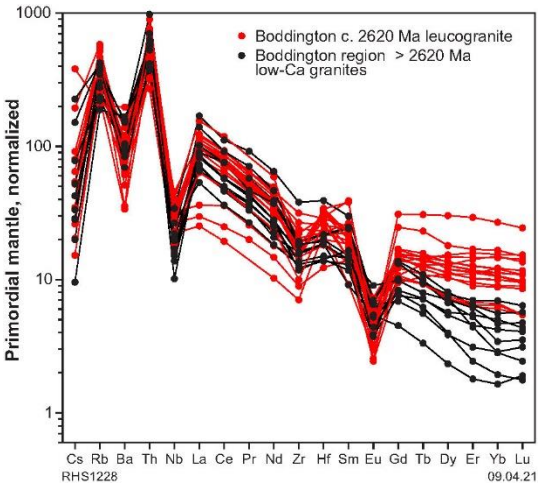

Figure 3. Multi-element spidergrams comparing mantle-normalized trace element patterns for c. 2620 Ma leucogranites that intrude the felsic volcanic rocks at Boddington, with regional low-Ca granites (normalization after after McDonough et al., 1992)

A third group (24 samples of andesite–rhyolite and diorite) includes samples yielding igneous crystallization ages of 2670 ± 3 and 2673 ± 3 Ma (Lu et al., 2020e, 2020f, respectively). These form a relatively geochemically coherent group with mantle-normalized trace element patterns significantly more enriched than those of the c. 2704 Ma rocks (Fig. 2). This group also exhibits variable SiO_2 contents (53.7 – 76.3 wt% SiO_2), with lower MgO, Cr and Ni concentrations at a given SiO_2 content, and has similarities with Phanerozoic basalt–andesite–dacite–rhyolite series, but at slightly elevated Ni and Cr concentrations typical of 'Archean' andesites and dacites (e.g. Barnes and Van Kranendonk, 2014).

Leucogranite intruding the volcanic rocks and diorite at Boddington yielded igneous crystallization ages of 2619 ± 2, 2617 ± 3, and 2617 ± 2 Ma (Lu et al., 2020c, 2020d, 2020g, respectively). From a major element perspective, these are all monzogranitic to syenogranitic low-Ca granites (e.g. Champion and Sheraton, 1997). However, their trace element patterns exhibit strong enrichments in Nb and flat, elevated, middle- to heavy-REE patterns (Fig. 3) that are more characteristic of hot, anhydrous, A-type magmas in extensional settings, but are distinct from the older (c. 2638–2628 Ma) low-Ca granites of the Boddington region. Zircon trace element data from these c. 2620 Ma leucogranites confirm the anhydrous nature of these magmas (Lu et al., 2019).

Perhaps the most significant features of the felsic volcanic rocks and diorites at the Boddington mine are their hydrous and calk-alkaline composition. For the c. 2704 Ma magmas, and possibly also the c. 2690 and 2670 Ma groups, $Mg^{\#}$ and concentrations of Cr and Ni are too high to reflect crustal melting alone and so fractionation from primary magmas derived from hydrated mantle is required. Although the origin of source hydration can be debated, this magmatism is most likely related to a fundamental translithospheric structure, and a long-lived thermal anomaly. The magmatic evolution appears to show striking similarities between the Boddington area and the Kalgoorlie–Kambalda region. In both, mafic volcanism came to an end before the emplacement of a long-lived series of hydrous, hornblende-bearing, enriched, calk-alkaline magmas of variable compositions, which were followed by anhydrous, relatively high-temperature crustal melts.

How to access

The Boddington geochemistry digital data are available on a USB and via the Data and Software Centre.

References

Barnes, SJ and Van Kranendonk, MJ 2014, Archean andesites in the east Yilgarn craton, Australia: products of plume-crust interaction? Lithosphere, v. 6, no. 2, p. 80–92, doi:10.1130/L356.1.

Barnes, SJ, Van Kranendonk, MJ and Sonntag, I 2012, Geochemistry and tectonic setting of basalts from the Eastern Goldfields Superterrane: Australian Journal of Earth Sciences, v. 59, no. 5, p. 707–735.

Champion, DC and Sheraton, JW 1997, Geochemistry and Nd isotope systematics of Archaean granites of the Eastern Goldfields, Yilgarn Craton, Australia: implications for crustal growth processes: Precambrian Research, v. 83, no. 1–3, p. 109–132, doi:10.1016/S0301-9268(97)00007-7.

Lu, Y, Smithies, RH, Wingate, MTD, Evans, NJ, McCuaig, TC, Champion, DC and Outhwaite, M 2019, Zircon fingerprinting of magmatic–hydrothermal systems in the Archean Yilgarn Craton: Geological Survey of Western Australia, Report 197, 22p.

Lu, Y, Wingate, MTD and Smithies, RH 2020a, 236410: meta-andesite, Boddington mine; Geochronology Record 1688: Geological Survey of Western Australia, 4p.

Lu, Y, Wingate, MTD and Smithies, RH 2020b, 236419: meta-andesite, Boddington mine; Geochronology Record 1689: Geological Survey of Western Australia, 4p.

Lu, Y, Wingate, MTD and Smithies, RH 2020c, 236432: porphyritic monzogranite, Boddington mine; Geochronology Record 1690: Geological Survey of Western Australia, 4p.

Lu, Y, Wingate, MTD and Smithies, RH 2020d, 236444: metamonzogranite, Boddington mine; Geochronology Record 1691: Geological Survey of Western Australia, 4p.

Lu, Y, Wingate, MTD and Smithies, RH 2020e, 236452: metagranodiorite, Boddington mine; Geochronology Record 1692: Geological Survey of Western Australia, 4p.

Lu, Y, Wingate, MTD and Smithies, RH 2020f, 236460: hornblende–biotite metatonalite, Boddington mine; Geochronology Record 1693: Geological Survey of Western Australia, 4p.

Lu, Y, Wingate, MTD and Smithies, RH 2020g, 236461: metasyenogranite, Boddington mine; Geochronology Record 1694: Geological Survey of Western Australia, 4p.

McDonough, WF, Sun, S-S, Ringwood, AE, Jagoutz, E and Hofmann, AW 1992, Potassium, rubidium, and cesium in the Earth and Moon and the evolution of the mantle of the Earth. Geochimica Cosmochimica Acta, v. 56, p. 1001–1012.

Smithies et al, in prep, Eastern Goldfields greenstone geochemical barcoding project: geochemical characterization of igneous units from the Ora Banda – Kambalda region: Geological Survey of Western Australia, Report.

Recommended reference

Smithies, RH, Lu, Y and Champion, DC 2021, New geochemical and geochronological constraints on the magmatic evolution of Boddington, southwest Yilgarn: Geological Survey of Western Australia, digital data layer, <https://www.dmirs.wa.gov.au/geoview>.

EXPLORATION INCENTIVE SCHEME

Australian Government
Geoscience Australia

Variations in granite geochemistry in the southwest Yilgarn

by

RH Smithies, Y Lu, J Lowrey, T Ivanic, DC Champion[1] and SA Wilde[2]

Abstract

A dataset is provided comprising 1006 analyses of granitic rocks, compiled from new data, re-analysis of archived samples and literature sources, and is used here to make preliminary comments on regional variations in granite composition across the region encompassed within the southwest Yilgarn Accelerated Geoscience Program. Too few absolute age constraints are available to allow age of intrusion to be considered.

Granitic rocks were primarily classified into high-Ca granites, low-Ca granites, high field strength elements (HFSE) granites and sanukitoids (mafic granites) based on comparisons with compositional fields established by Champion and Sheraton (1997) and Champion and Cassidy (2002). In doing this, a specific group of analyses was identified, usually with high concentrations of TiO_2, P_2O_5, rare earth elements (REE) and HFSE, broadly transitional between low-Ca and HFSE granites, and is referred to here as 'low-Ca, P-rich granite'. Sanukitoid is defined here as a hornblende-bearing rock (or rock series) which, at ~60 wt% silica has a $Mg^{\#}$ >60, Cr and Ni both >100 ppm, and Sr and Ba both >400–500 ppm (e.g. Stern et al., 1989). Several hornblende-bearing intrusions and much of the felsic volcanic rock (all ages) from the Boddington region satisfy most, but not all, of these criteria and are referred to as 'sanukitoid-like'.

A secondary classification scheme based on K_2O/Na_2O and Sr/Y ratios is also applied to the high- and low-Ca granites (Fig. 1).The K_2O/Na_2O ratio can be used as a broad proxy for source composition, or degree of fractionation or partial melting. Strongly sodic granites ($K_2O/Na_2O < 0.6$) are derived from sources with a broadly 'basaltic' composition, whereas potassic granites ($K_2O/Na_2O > 1.0$) are derived from source compositions more evolved than basalt (i.e. they have a recycled, or 'crustal', source component) and/or reflect lower degrees of partial melting and/or higher degrees of fractionation (sodic granites [K_2O/Na_2O 0.6 – 1.0] lie between strongly sodic and potassic granites in this scheme). The Sr/Y ratio can be used as a broad proxy for the depth of melting based on the effect that any plagioclase (Sr bearing) and garnet and hornblende (Y bearing) remaining in the source after melting has on this ratio (e.g. a deep, garnet-rich source yields melts with high Sr/Y). However, water-saturated melting, source enrichment and fractionation/cumulate processes can all complicate any pressure-related interpretations based on Sr/Y ratios.

The newly identified low-Ca, P-rich granite group includes rocks that have some compositional attributes of charnockite-series granites and A-type granites, including enrichments in Ti, P, Fe, Zr and REE. Zircon saturation thermometry (Watson and Harrison, 1983; see Granite geochemistry – Zircon TC layer) shows these to have higher zircon saturation temperatures (a potential proxy for magma temperature) than any other group, including the HFSE granites.

1 Geoscience Australia, GPO Box 378, Canberra, ACT 2601
2 School of Earth and Planetary Sciences, Curtin University, GPO Box U1987, Perth, WA 6845

Granite classification layers

These show that while most groups of granites are spread throughout much of the region, the following generalizations appear valid:

- There is a clear band in the southeastern corner dominated by high-Ca granites (Granite geochemistry – Classification layer). This might be interpreted as a particularly geochemically 'primitive' region of crust.
- A central–western region appears to have a particularly low abundance of high Sr/Y varieties of high-Ca granite compared with surrounding areas. This might be interpreted as a region where melting of basaltic crustal sources happens at a middle- rather than lower crustal level (Granite geochemistry – High Ca classification layer).
- Sanukitoids and sanukitoid-like rocks (including Na- and K-rich diorite/monzodiorite) concentrate in or close to major structures (Granite geochemistry – Sanukitoid classification layer). This might be interpreted to suggest that these are translithospheric structures.
- Low-Ca, P-rich granites concentrate in a southeast-trending band along the eastern edge of the project area (Granite geochemistry – Classification and Granite geochemistry – Low Ca classification layers), potentially reflecting a region characterized by a particularly high thermal gradient. They are sparsely distributed elsewhere.

Granite geochemistry layers

These have been constructed for elements and element ratios that provide information on crustal evolution and/or are of particular economic interest.

- Lithium concentrations (Granite geochemistry – Li layer) do not appear to favour any particular granite type and appear rather randomly spread, although two regions trending north-northwest with higher concentrations of more Li-enriched granites might be discernible along the northeastern edge of the project area and approximating the reinterpreted eastern boundary of the South West Terrane of the Yilgarn Craton.
- Gold concentrations (Granite geochemistry – Au layer: note, only data from aqua regia analyses are shown) are not randomly distributed. Apart from a regional anomaly coinciding with the Boddington Au–Cu mine (not shown as our data contain no aqua regia analyses from Boddington, although fire assay data clearly demonstrate an Au anomaly), higher concentrations occur along the southern margin of the project area, mainly recorded from high-Ca granites and sanukitoids (and related rocks), and in a region trending north-northwest along the northeastern edge of the project area, mainly in low-Ca granites. Looking only at samples with Au concentrations >0.5 ppb (Granite geochemistry – Au >0.5 ppb layer) emphasizes the southern part of the project area as a Au-rich region but shows that large regions within the central half of the project area are devoid of samples with >0.5 ppb Au, except along two north-trending bands, the eastern one broadly coincident with an interpreted fault. The >0.5 ppb data also highlights the southern part of the new eastern structural boundary of the South West Terrane of the Yilgarn Craton, but not the northern part. This, and the low Au concentrations in the central part of the project area, potentially indicates a basement compositional control on the distribution and concentration of Au in granites. However, a more northwesterly trending band of >0.5 ppb samples appears to connect the Katanning region with Boddington, and a similar trend is distinct in the data for Zn (cf. Granite geochemistry – Zn and Zn >77 ppm layers) and Mo (Granite geochemistry – Mo layer) and perhaps to a lesser extent Cu (Granite geochemistry – Cu layer; but see Zn, Cu and Mo below). This probably suggests

that the base and precious metal enrichments in these rocks are not simply (or even largely) magmatic (i.e. they might also relate to post-magmatic hydrothermal alteration).

- Zinc, Cu and Mo concentrations (Granite geochemistry – Zn, – Zn >77 ppm, – Cu, – Cu >32 ppm and – Mo layers) show a similar distribution pattern, with high values concentrating in bands trending northwest and north-northwest. In contrast with Au distribution, apart from these bands, there is no evidence for regions broadly enriched or depleted in these metals. This apparent structural control (see Au, above), strongest for Zn and Mo, is probably best explained in terms of hydrothermal base mental enrichment of granites along major structures, rather than primary magmatic enrichments of these metals. The well-defined northwest Katanning–Boddington trend in the southwest truncates most geophysically defined structural and lithological features of the region, including the newly defined eastern boundary of the South West Terrane of the Yilgarn Craton. However, this trend closely parallels the trend of several Paleoproterozoic to Neoproterozoic dolerite dyke and fault sets, potentially inferring regional post-Archean base metal redistribution.

  Copper represents an exception to this structurally controlled behaviour, and possibly shares some similarity in spatial location with Au. High Cu concentrations (Granite geochemistry – Cu layer) appear to preferentially occur in high-Ca granites or in sanukitoids (and related rocks), often with adjacent granite types showing only background values. These relationships can be interpreted in several ways, including the suggestion that high concentrations of Cu (and perhaps also Au) in sanukitoids and in some high-Ca granites, reflect magmatic values, consistent with the view that sanukitoid-like magmas are compositional (but not necessarily tectonic) analogues of Phanerozoic porphyry Cu (Au) related intrusions, as is consistent with their geochemistry.

- Several strongly incompatible trace elements (Granite geochemistry – Rb, – Ce, – Sn and – Pb layers) and incompatible trace element ratios (Granite geochemistry – Gd/Yb, – Sr/Y, – Rb/Sr and – Eu anomaly layers) show spatial distribution patterns reflecting regional variations in either source composition or melting conditions, or both. The most obvious variations typically either: i) draw a distinction between the southeastern and northwestern halves of the project area, particularly viewing the high-Ca granites, or comparing these with the other granites; ii) identify the low-Ca granites, and in particular the low-Ca, high-P granites, in the northeastern part of the project area as anomalous.

The compositional attributes (in addition to high Au concentrations – see above) that distinguish the southeastern part of the project area from the northwestern part include generally lower concentrations of Sn and Pb, and, particularly in the high-Ca granites, generally higher Eu/Eu* (a measure of the normalized Eu anomaly), Sr/Y and Gd/Yb ratios. This combination can be broadly interpreted to reflect melting of a more primitive source (i.e. more mafic and with less of a reworked component), possibly at generally higher pressures. If true, this reflects a distinct basement compositional province that is truncated by the prominent north-northwesterly structural trend of the project area (e.g. Smithies et al., 2018).

Compared to the southeastern parts of the project area, the northern region also shows broadly higher concentrations of Rb, light REE (e.g. Ce) and heavy REE (e.g. Yb Granite geochemistry – Yb layer) and higher Rb/Sr ratios. This anomalism relates mainly to samples of low-Ca granite, and in particular the low-Ca, high-P granites. Calculated zircon saturation temperatures (Granite geochemistry – Zircon TC layer) (Watson and Harrison, 1983) for the low-Ca granites typically lie between 775 and 875 °C and those for the low-Ca, high-P granites between 850 and 950 °C, whereas those for the other groups rarely exceed 850 °C. The broad range of compositional and mineralogical (broadly anhydrous mineralogy) characteristics of the low-Ca, high-P granites, including high Ti, P, Fe, Zr and REE concentrations, is consistent with high-temperature felsic magmatism, and suggests that

large regions of the northern part of the project area reflect zones of unusually high heat flow — potentially zones of extension.

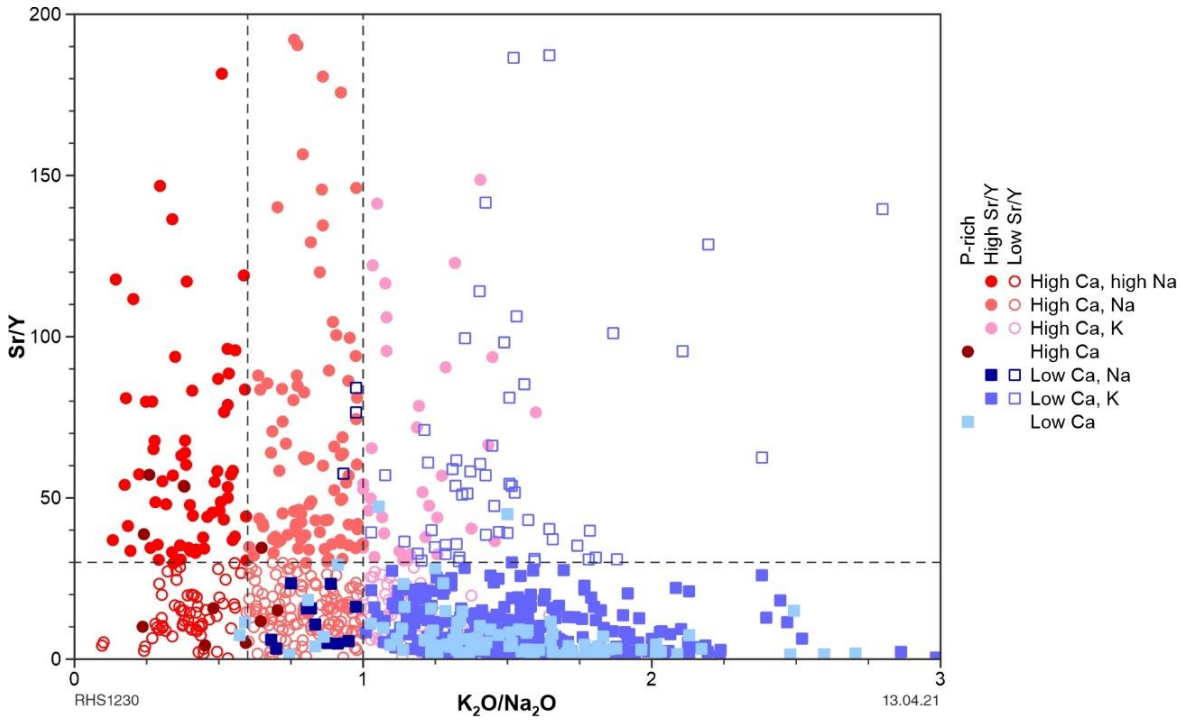

Figure 1. Secondary classification (Sr/Y against K_2O/Na_2O) of high- and low-Ca granites (n = 459 and 470, respectively) in the southwest Yilgarn

How to access

The southwest Yilgarn granite geochemistry digital data are available on a USB and via the Data and Software Centre.

References

Champion, DC and Sheraton, JW 1997, Geochemistry and Nd isotope systematics of Archaean granites of the Eastern Goldfields, Yilgarn Craton, Australia: implications for crustal growth processes: Precambrian Research, v. 83, p. 109–132.

Champion, DC and Cassidy, K 2002, Granites of the northern Eastern Goldfields: their distribution, age, geochemistry, petrogenesis, relationship with mineralisation, and implications for tectonic environment (including a simplified key for discriminating granite groups in the northern Eastern Goldfields), in Characterization and metallogenic significance of Archaean granitoids of the Yilgarn Craton by K Cassidy, D Champion, N McNaughton, I Fletcher, A Whitaker, I Bastrakova and A Budd: Minerals and Energy Research Institute of Western Australia, Report 222, 531p.

Smithies, RH, Lu, Y, Gessner, K, Wingate, MTD and Champion, DC 2018, Geochemistry of Archean granitic rocks in the South West Terrane of the Yilgarn Craton: Geological Survey of Western Australia, Record 2018/10, 13p.

Stern, RA, Hanson, GN and Shirey, SB 1989, Petrogenesis of mantle-derived, LILE-enriched Archean monzodiorites and trachyandesites (sanukitoids) in southwestern Superior Province: Canadian Journal of Earth Sciences, v. 26, p. 1688–1712.

Watson, EB and Harrison, TM 1983, Zircon saturation revisited: Temperature and composition effects in a variety of crustal magma types: Earth and Planetary Science Letters, v. 64, p. 295–304.

Recommended reference

Smithies, RH, Lu, Y, Lowrey, J, Ivanic, T, Champion, DC and Wilde, SA 2021, Variations in granite geochemistry in the southwest Yilgarn: Geological Survey of Western Australia, digital data layer, <http://www.dmirs.wa.gov.au/geoview>.

HyLogger spectral mineralogy of diamond drillcore from the southwest Yilgarn

by

MJ Wawryk and EA Hancock

Abstract

The Geological Survey of Western Australia (GSWA) systematically collects infrared reflectance spectral data from drillcore and other rock samples stored at its Perth and Kalgoorlie Core Libraries, using the GSWA HyLogger-3 system. This instrument collects high-resolution images and reflectance spectral data from the visible-near infrared (VNIR, 380–1000 nm), shortwave infrared (SWIR, 1000–2500 nm) and thermal infrared (TIR, 6000 – 14500 nm) regions (Hancock et al., 2013). Mineral assemblages and physiochemistry are interpreted from diagnostic spectral features produced by electronic transitions and molecular vibrations that occur in most rock-forming minerals, using The Spectral Geologist (TSG) software (Hancock et al., 2013). Derived downhole mineralogical information can be used for a variety of purposes, including defining lithological units, documenting weathering and alteration profiles, and identifying vectors towards mineralization (Hancock and Huntington, 2010).

A mineralogical database has been created using extant HyLogger data for diamond drillcore from the southwest Yilgarn. Original HyLogger datasets were reprocessed to a standard level using TSG version 8.0.7.4 and the latest mineral reference library and full-pattern unmixing algorithms (SWIR: TSAS+ 7.05; TIR: jCLST 7.08). Error measurements and mineral interpretations were obtained from the spectral data using TSG's automated algorithm. A minimum threshold of 0.15 per 8 mm sample was applied to mineral spectral weight percentages for both VNIR–SWIR and TIR spectral unmixing results, and additional scalars were produced that directly measure the wavelengths and depths/heights of spectral absorptions and other characteristics for diagnostic mineral groups. All results were then binned to one-metre intervals downhole, and the derived SWIR and TIR results for individual drillholes were merged to create the final mineralogy database.

How to access

The southwest Yilgarn hyperspectral mineralogy database can be acquired as part of the Southwest Yilgarn, 2021 Geological Exploration Package, which is available on a USB via the DMIRS eBookshop and as a free download from the Data and Software Centre.

References

Hancock, EA, Green, AA, Huntington, JF, Schodlok, MC and Whitbourn, LB 2013, HyLogger-3: Implications of adding thermal-infrared sensing: Geological Survey of Western Australia, Record 2013/3, 24p.

Hancock, EA and Huntington, JF 2010, The GSWA NVCL HyLogger: rapid mineralogical analysis for characterizing mineral and petroleum core: Geological Survey of Western Australia, Record 2010/17, 21p.

Recommended reference

Wawryk, MJ and Hancock, EA 2021, HyLogger spectral mineralogy of diamond drillcore from the southwest Yilgarn, Geological Survey of Western Australia, digital data layer.

Lithostructural map of the Chittering Metamorphic Belt

by

I Zibra

Abstract

A well-exposed, high-strain area along and east of the Darling Fault in the Perth hills, was mapped as part of the southwest Yilgarn Accelerated Geoscience Program. The target area is centered on the Chittering Metamorphic Belt (CMB), which is part of the Balingup sub-terrane* (Wilde et al., 1996), within the South West Terrane of the Yilgarn Craton. The CMB was mapped during the 1970s as part of the initial regional-scale mapping conducted by the Geological Survey of Western Australia (Wilde and Low, 1978) but, since then, has not been the subject of further geological investigations. The first stage of the mapping project presented here included 30 days of fieldwork, spread over the period of October–December 2020. The mapped area has a nearly rectangular shape, with a north–south length of about 85 km, and east–west of about 15–20 km, parallel to the north-trending, prominent morphological feature of the Darling Scarp. The southern end of the mapped area corresponds to the Bells Rapids area, near the suburb of Brigadoon (latitude 31.77°S), while its northern end corresponds to the northern boundary of the PERTH 1:250 000 map sheet, along the Moore River valley, just north of the town of Mogumber (latitude 31.03°S). While the southern part of the CMB, between the Avon Valley and the southern part of the Chittering Valley, is very well exposed (rock exposure up to 50%), outcrop quality and abundance progressively decrease northwards, where the landscape is dominated by gentle hills between vast flat areas. This disparity in rock exposure is reflected on the geological map, which offers more detail and a high density of structural data points in the south, while the compilation of the northern portion relied more heavily on geophysical data. To support and integrate mesoscale observations, about 140 thin sections were prepared from oriented rock chips collected during mapping.

The main target of this mapping exercise was the systematic collection of lithostructural data, to produce a geological map that illustrates:

- the distribution of the main rock types and their field relationships
- information about mesoscale geometry, kinematics, finite strain and relative age of the various deformation fabrics identified in the study area
- microstructural data providing information about deformation temperature for the various deformation fabrics, shear sense for the main shear zones identified in the field, and the relationship between deformation and growth of metamorphic minerals.

The CMB includes a series of high-strain metamorphic rocks that mainly consists of leucocratic gneisses and schists, associated with subordinate mafic gneiss and schist. A north-striking, subvertical foliation and layering are well developed nearly everywhere throughout the CMB. Weakly deformed to undeformed rocks are rare, and are mainly represented by the more competent gabbroic lithologies. The Darling Fault marks the western limit of the CMB (Middleton et al., 1993), while its eastern flank is intruded by Archean granitic gneisses of unknown age, which are poorly exposed, being largely buried under a thick laterite cover. The southern portion of the CMB is intruded by Late-Archean granitic rocks of the c. 2648–2626 Ma Darling Range batholith (Nemchin and Pidgeon, 1997), while its northern portion is juxtaposed to greenstone rocks belonging to the Jimperding greenstone belt (Wilde, 2001). The contact between the two belts is marked by northwest-striking,

* informal name

low-temperature shear zones, which likely experienced local post-Archean reactivations of the high-temperature Archean, northwest-striking fabrics of the Jimperding greenstone belt. Field and geophysical data indicate that the CMB and surrounding granitic rocks are intruded by numerous mafic dykes (P_-mod) that range from gabbro to dolerite, and occur in two main orientations: (i) northeast-striking dykes mainly occur in the southeastern portion of the mapped area, and are likely part of the c. 2615 Ma Yandinilling dyke swarm (Stark et al., 2018); (ii) a dense network of north-striking dykes likely belonging to the c. 1210 Ma Marnda Moorn Large Igneous Province (Wingate, 2017). A dolerite dyke of the Marnda Moorn Large Igneous Province, sampled in Brigadoon, returned a magmatic crystallization age of 1214 ± 5 Ma (Pidgeon and Cook, 2003). In a few localities, due to outcrop conditions, it is unclear whether the exposed mafic gneiss represents sheared dykes, or older mafic rocks associated with the felsic gneisses. On the map, these units are displayed as generic amphibolite (A-mwa-YSW).

Within the group of felsic schists and gneisses of the CMB, the map distinguishes between melanocratic (biotite rich; A-mdnb-YSW) and leucocratic (muscovite rich; A-mdnm-YSW) end-members, and those that are feldspar free, with very high quartz content (i.e. >70%; A-mlsm-YSW). Sillimanite–kyanite and garnet–staurolite varieties are also distinguished (A-mdnk-YSW and A-mdng-YSW, respectively), given their potential usefulness for unravelling the metamorphic evolution of the belt. These units are likely of siliciclastic sedimentary origin although, due to deformation and high-grade metamorphism, the possibility that some of them resulted from metamorphism of weathered igneous rocks cannot be ruled out. In the intensely deformed areas, sillimanite and kyanite are partially to totally replaced by retrograde biotite and muscovite. Therefore, the present-day discontinuous occurrence of aluminosilicate minerals throughout the CMB probably results from bulk chemistry heterogeneities in the protoliths, combined with the effects of heterogeneous retrograde shearing.

Felsic gneisses that retain clues of their igneous origin include augen gneisses (derived from porphyritic granites, A-mgmu-Y) and mylonitic to schistose metagranites (A-mgs-Y), the latter commonly deriving from equigranular protoliths. Here, feldspar zoning is commonly visible in thin section, proving the igneous origin of these gneisses. A distinctive unit of grey microgneiss (A-mdnf-YSW) of granitic composition, exhibiting distinctive magnetite porphyroblasts, dominates the northwestern portion of the belt, and could be of metasedimentary and/or igneous origin. This unit had been previously mapped as granofels, due to the common lack of foliation. In reality, the grey microgneiss is mainly exposed along constrictional, sinistral shear zones (Fig. 1), and therefore mainly occurs as L>S-tectonites to pure L-tectonites, explaining the general lack of planar fabric. A distinctive unit of layered, mylonitized migmatitic gneiss (A-mgii-Y) of bulk granitic composition (and likely igneous origin) mainly occurs in the central and southern part of the map. Migmatitic gneiss is associated with a peculiar unit of layered schist (A-xmvyl-mgsl-YSW) composed of bluish, aphanitic felsic schist of (sub-)volcanic origin, interlayered with leucogranitic and quartz veins.

The well-exposed granitic rocks of the Darling Range batholith are mostly weakly foliated to completely undeformed (A-jgm-mn-Y). In the study area, they are mainly represented by medium- to fine-grained equigranular, two-mica leucogranites, commonly including rafts of migmatitic gneiss and schist, which become more common close to the contacts with the CMB. Strongly foliated to mylonitic equivalents of the same granitic rocks (A-jmgm-mn-Y) occur along the contacts with schist and gneiss of the CMB. The gradual transition between these two end-member varieties is well exposed in the Bells Rapids area.

From a structural viewpoint, the study area is characterized by two major shear zone systems, in addition to the Darling Fault:

- an oblique-slip (normal-sinistral) shear zone marks the eastern boundary of the CMB, juxtaposing the high-strain belt to the low-strain greenstone sequences of the Jimperding greenstone belt, which are exposed at Julimar. This structure is well exposed in the area

between Bells Rapids and Chittering Valley. Its southern portion largely corresponds to the 'Swan Gorge mylonite zone' (Wilde and Low, 1978), and therefore this name is retained here.

- The central–eastern part of the CMB exposes a network of anastomosing, strike-slip sinistral shear zones that mainly occur within augen gneisses and are associated with constrictional fabrics (L>S to pure L-tectonites). This structure is well exposed between Shady Hills and Mogumber; its southern end corresponds to the Lady Springs shear zone (Fig. 1; White et al., 1986), and therefore this name is retained here.

Preliminary microstructural observations suggest that these shear zones developed under greenschist-facies conditions, overprinting higher temperature fabrics. Mafic dykes of the Marnda Moorn Large Igneous Province are sheared along these structures, which were therefore active after c. 1200 Ma, although they may have also had an older shearing history. The migmatitic structures recorded by the CMB are not visible in the surrounding granitic rocks of the Darling Range batholith, and are therefore likely of Archean age. These high- to moderate-temperature shear fabrics are overprinted by north-striking, low-temperature (i.e. <~300 °C) shear zones and faults, which are mostly restricted to the western portion of the CMB and, in the study area, are best exposed along the Darling Scarp, between Bullsbrook and Bells Rapids. Most of these low-temperature structures are steeply west dipping, exhibiting normal kinematics, and are likely part of the Darling Fault.

Overall, the CMB records a multistage geological history spanning from the Archean to the Mesozoic, representing an ideal target for improving our understanding of the evolution of craton margins through time.

Figure 1. Side view of a plurimetric rod of gently south-plunging L-tectonites developed in mylonitic migmatite gneiss, exposed along the Lady Springs shear zone in the central part of the Chittering Valley. Arrow shows the local trend of the stretching lineation, L_{str}

How to access

The data layer forms part of the Pre-Mesozoic interpreted bedrock geology of the southwest Yilgarn map (Quentin de Gromard et al., 2021) and is best accessed using GeoVIEW.WA. This online interactive mapping system allows data to be viewed and searched together with other datasets, including Geological Survey of Western Australia and Geoscience Australia geochronology data, geological maps and mineral exploration datasets. Digital data relating to the Lithostructural map of the Chittering Metamorphic Belt are also available on a USB and via the Data and Software Centre.

References

Middleton, MF, Long, A, Wilde, SA, Dentith, M and Evans, BA 1993, A Preliminary Interpretation of Deep Seismic Reflection and other Geophysical Data from the Darling Fault Zone, Western Australia: Exploration Geophysics, v. 24, 3-4, p. 711–717, doi:10.1071/EG993711.

Nemchin, AA and Pidgeon, RT 1997, Evolution of the Darling Range Batholith, Yilgarn Craton, Western Australia: A SHRIMP zircon study: Journal of Petrology, v. 38, p. 625–649.

Quentin de Gromard, R, Ivanic, TJ and Zibra, I 2021, Pre-Mesozoic interpreted bedrock geology of the southwest Yilgarn, 2021: Geological Survey of Western Australia, digital data layer, <https://www.dmirs.wa.gov.au/geoview>.

Pidgeon, RT and Cook, TJF 2003, 1214 ± 5 Ma dyke from the Darling Range, southwestern Yilgarn Craton, Western Australia: Australian Journal of Earth Sciences, v. 50, p. 769–777.

Stark, JC, Wilde, SA, Söderlund, U, Li, Z-X, Rasmussen, B and Zi, J-W 2018, First evidence of Archean mafic dykes at 2.62 Ga in the Yilgarn Craton, Western Australia: Links to cratonisation and the Zimbabwe Craton: Precambrian Research, v. 317, p. 1–13.

White, SH, Bretan, PG and Rutter, EH 1986, Fault-zone reactivation: kinematics and mechanisms: Philosophical Transactions of the Royal Society A: Mathematical, Physical and Engineering Sciences, v. 317, p. 81–97, doi:10.1098/rsta.1986.0026.

Wilde, SA 2001, Jimperding and Chittering metamorphic belts, Western Australia — a field guide: Geological Survey of Western Australia, Record 2001/12, 24p.

Wilde, SA and Low, GH 1978, Explanatory notes on the Pinjarra 1:250 000 geological sheet, Western Australia: Geological Survey of Western Australia, Record 1978/5, 63p.

Wilde, SA, Middleton, MF and Evans, BJ 1996, Terrane accretion in the southwestern Yilgarn Craton: Evidence from a deep seismic crustal profile: Precambrian Research, v. 78, p. 179–196.

Wingate, MTD 2017, Mafic dyke swarms and large igneous provinces in Western Australia get a digital makeover, in GSWA 2017 Extended abstracts: promoting the prospectivity of Western Australia: Geological Survey of Western Australia, Record 2017/2, p. 4–8.

Recommended reference

Zibra, I 2021, Lithostructural map of the Chittering Metamorphic Belt. Geological Survey of Western Australia, digital data layer, <https://www.dmirs.wa.gov.au/geoview>.

AGP Accelerated Geoscience Program

Statewide critical minerals prospectivity study

Geoscience data for critical mineral discovery in Western Australia

by

TJ Beardsmore, P Duuring, JN Guilliamse, S Kenworthy, S Morin-Ka, J Hogen-Esch and D Then

Abstract

The Geological Survey of Western Australia (GSWA) prioritized its 2020–21 work program towards accelerated delivery of novel geoscience fact and interpretive data, to boost knowledge of the State's geology and mineral prospectivity, and thereby stimulate resources industry exploration activity to aid economic recovery in the wake of the COVID-19 pandemic. This Accelerated Geoscience Program (AGP) comprised five complementary programs or themes considering particular regions (statewide, southwest Yilgarn, far east Yilgarn) or commodity groups (critical minerals, energy systems). An overview of the data package developed for the critical minerals theme is provided here.

Critical minerals are non-fuel commodities that nations deem essential for their manufacturing industries, for which there are no ready substitutes and supply chains are vulnerable to disruption (e.g. USA — Petty, 2018; EU — European Commission, 2020; India – Gupta et al., 2019). The Australian Commonwealth Government identifies 24 'priority' critical minerals or mineral groups that are now, or can possibly be, mined locally and used domestically and exported, to use in manufacturing of technologies to facilitate the transition to a 'low-carbon' world (Austrade-DIIS, 2019, 2020; see Fig. 1).

Western Australia is well placed to capitalize on existing and projected increasing demand for critical minerals. The State is already a significant producer of cobalt, lithium, manganese, rare earth elements (REE), tantalum, titanium and zirconium. It also has known — but undeveloped — resources of antimony, chromium, gallium, graphite, hafnium, magnesium, niobium, platinum group elements (PGE), potash, silica and vanadium. Western Australia presently has no defined resources of other critical minerals such as beryllium, bismuth, gallium, germanium, helium, indium, rhenium and scandium, but is considered prospective for the types of mineral deposits likely to contain them, either as primary or significant accessory components of mineralization (Fig. 1).

The State's long-term economic benefit from critical minerals will depend on continuing discovery and development of additional resources. These will most likely be found in challenging, underevaluated geological environments — for instance as minor components in known deposits, or in undiscovered ores buried beneath significant cover, or even in mining and processing residues. The aim of the Critical Minerals theme has therefore been to apply an understanding of the mineral systems in which critical minerals occur to identify specific geoscience information that can be extracted from GSWA and third-party databases for use in prospectivity and targeting activities. To remain manageable, focus was limited to a few prominent critical minerals, and particular prospective mineralized environments that could contain them (Table 1).

The approach adopted was to define geological features that might indicate fertility of a region for critical minerals, then to extract digital, GIS-based maps showing occurrences of those features from existing databases that could be practicably interrogated or otherwise processed. The goals were to generate a sufficiently comprehensive data package that will be of use to critical (or other) mineral explorers, and to demonstrate the types of information that can be extracted from GSWA geoscience data, and the methodology for achieving this.

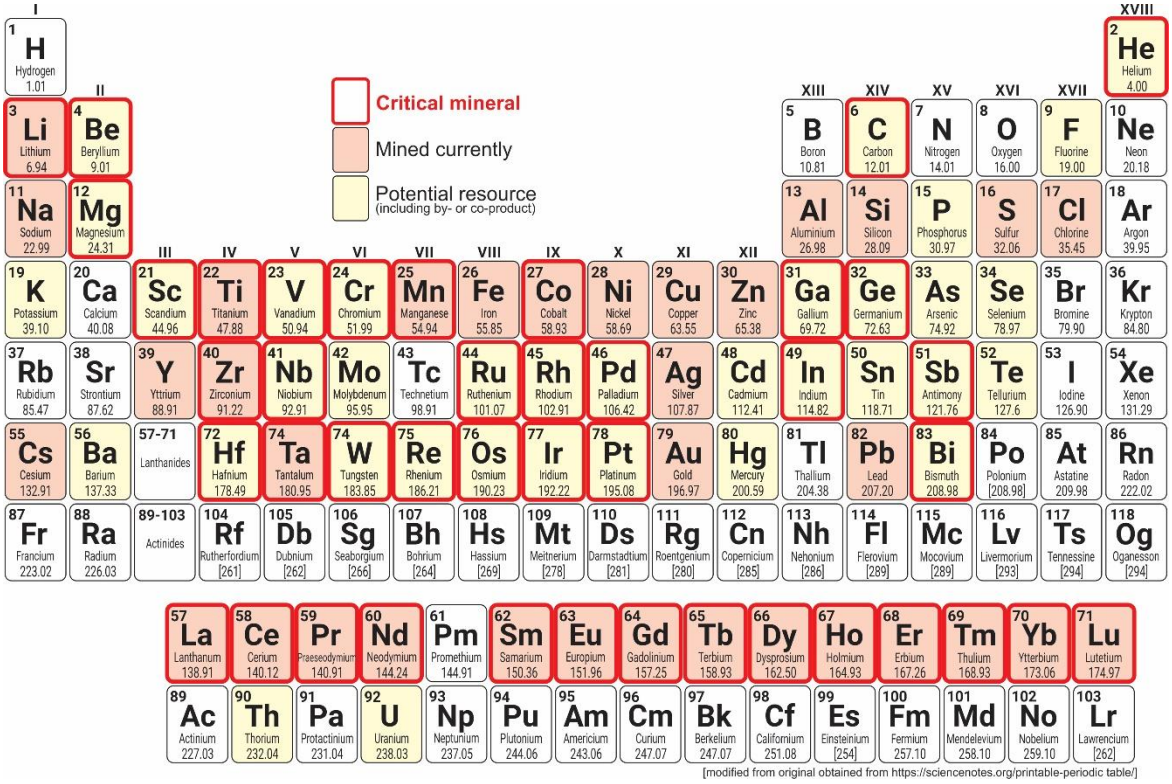

Figure 1. Mined and prospective mineral commodities in Western Australia, with critical minerals highlighted

Table 1. Selected critical minerals and mineralized environments

Critical mineral/group	Mineralized environment
bismuth, germanium, indium	VMS systems (associated with zinc and lead)
graphite	carbonaceous metasediments
lithium (± tin, tantalum, beryllium)	rare-element pegmatites
manganese	sedimentary basins
REE (± tantalum, tungsten, niobium)	carbonatites, kimberlites and lamproites
vanadium, PGE	mafic igneous intrusions
potash	brines in paleochannels and playa lakes
silica	quartz veins

More than 250 individual critical mineral 'fertility indicator' maps have been produced. These maps reflect five broad categories of information — known mineral occurrences, prospective rock types, indicator minerals, geochemical signals, and climate. Maps of similar type and derivation are collectively described in one or other of 20 abstracts (in addition to this one) accompanying the data package, and cited herein.

The locations of known critical mineral occurrences have been extracted from GSWA's MINEDEX database (Morin-Ka et al., 2021a,b). Prospective rock types include those that may either be the hosts for critical minerals, or indicate geological environments that are prospective for critical mineral-bearing mineralization. Maps showing the locations of such rocks were derived from several primary sources of geological mapping. Duuring et al. (2021a) and Duuring and Morin-Ka (2021a,c) extracted maps of prospective rock units from GSWA's interpreted bedrock geology (IBG) maps (Martin et al., 2016 and Morin-Ka, 2021a).

The locations of quartz veins and granitic pegmatites and other small igneous intrusions prospective for critical minerals, which are too small to appear in the GSWA IBG, were digitized from georegistered images of GSWA or third-party fact geology maps (Beardsmore, 2021; Beardsmore and Duuring, 2021), or are reproduced from the GSWA diamond exploration database (Hutchison, 2018a,b; Beardsmore and Hutchison, 2021). Kenworthy and Beardsmore (2021b) describe maps sourced from Geoscience Australia and the WA Department of Water and Environment that show the distributions of Western Australian lakes, paleovalleys and drainage catchments, which are prospective environments for brine-hosted potash and other commodities. Duuring et al. (2021c) have derived maps showing observed locations of outcrops of prospective rock types from GSWA's WAROX database (Riganti et al., 2015).

Also derived from the WAROX database are 'indicator mineral' maps showing the observed occurrences of minerals that are potentially diagnostic either of prospective rock types (Duuring et al, 2021b), or of critical mineral-bearing mineralization or associated alteration (including those that may be part of metamorphosed assemblages; Guilliamse et al., 2021).

Geochemistry is a powerful tool for mineral exploration. Duuring et al. (2021e) have created a Western Australian 'near surface' whole-rock lithogeochemical database by combining harmonized data from the GSWA WACHEM, Geoscience Australia OzCHEM, CRC-LEME 'Laterite' and WAMEX Mineral Exploration 'surface' (soil, stream, rock chip, shallow auger and 'maximum grade in drillhole') datasets. Each component subset of this new database is provided in a separate map layer. Specific lithogeochemical fertility indicator maps have been derived also for rare-element pegmatites and the granites from which they are sourced, for mafic intrusion-hosted vanadium (Duuring et al., 2021d), for basin-hosted manganese (Duuring and Morin-Ka, 2021b), and for VMS systems (Guilliamse and Duuring, 2021).

Three discrete Western Australian well- and bore-water chemistry datasets created by CSIRO have been harmonized and combined, and maps produced to show concentrations of a suite of critical minerals and other analytes (Kenworthy and Beardsmore, 2021a). Such data are useful for exploring for brine-related mineralization in paleovalleys and playa lakes, but can also provide pathfinders to bedrock-hosted mineral deposits.

Long-term climate will influence where commodities dissolved in groundwaters may become particularly concentrated. Maps showing gridded, time averaged rainfall, evaporation, and evapotranspiration data have been obtained from the Bureau of Meteorology (Kenworthy and Beardsmore, 2021c).

The 'merged' IBG map for Western Australia (Morin-Ka, 2021a) is provided as a base layer to the thematic maps, as is a novel statewide 'outcrop geology' map that has been created by extracting portions of the IBG map corresponding to fresh rock outcrops in the GSWA State regolith map (Jakica et al., 2020; Morin-Ka, 2021b). Additionally, the critical minerals data package collects many of these maps into four 'mineral system' themes — basin-hosted manganese, rare-element pegmatites, volcanogenic massive sulfides and mafic intrusion-hosted vanadium — these being mineralization types having significant potential to host critical minerals. The thematic map layers for the 'Rare-element pegmatite' and 'Mafic intrusion-hosted vanadium' mineral systems have also been released via GSWA's Mineral Systems Atlas (www.dmirs.wa.gov.au/mineralsystemsatlas; Morin-Ka et al., 2019).

How to access

The digital GIS maps and associated geoscience data and documents relevant to the critical minerals theme have been compiled into the Critical minerals, 2021 Geological Exploration Package provided on USB via the DMIRS eBookshop, and are also available as a free download from the Data and Software Centre.

References

Austrade-DIIS 2019, Australia's Critical Minerals Strategy (2019), Australian Government, Department of Industry, Innovation and Science, Australian Trade and Investment Commission, <www.industry.gov.au/sites/default/files/2019-03/australias-critical-minerals-strategy-2019.pdf>, viewed 19 May 2021.

Austrade-DIIS 2020, Australian Critical Minerals Prospectus 2020, Australian Government, Department of Industry, Innovation and Science, Australian Trade and Investment Commission, <www.austrade.gov.au/ArticleDocuments/5572/Australian_Critical_Minerals_Prospectus.pdf>, viewed 19 May 2021.

Beardsmore, TJ 2021, Quartz veins in Western Australia: Geological Survey of Western Australia, digital data layers.

Beardsmore, TJ and Duuring, P 2021, Granitic pegmatites in Western Australia: Geological Survey of Western Australia, digital data layers.

Beardsmore, TJ and Hutchison, MT 2021, Carbonatites, kimberlites and lamproites in Western Australia – prospective hosts for rare earth elements: Geological Survey of Western Australia, digital data layers.

Duuring, P and Morin-Ka, S 2021a, Archean greenstone belts in Western Australia: Geological Survey of Western Australia, digital data layers.

Duuring, P and Morin-Ka, S 2021b, Lithogeochemical fertility indicators for manganese oxide mineralization in Western Australia: Geological Survey of Western Australia, digital data layers.

Duuring, P and Morin-Ka, S 2021c, Sedimentary basins in Western Australia: Geological Survey of Western Australia, digital data layers.

Duuring, P, Guilliamse, JN and Morin-Ka, S 2021a, Maps of rock units in Western Australia prospective for selected Critical Minerals (Mn, V, Ni, Co, PGE, Li, Sn, Ta, W): Geological Survey of Western Australia, digital data layers.

Duuring, P, Guilliamse, JN, Morin-Ka, S and Farrell, TR 2021b, Occurrences of minerals in Western Australia diagnostic of rock types prospective for selected Critical Minerals (Li, Ge, In, Ni, PGE, V): Geological Survey of Western Australia, digital data layers.

Duuring, P, Guilliamse, JN, Morin-Ka, S and Farrell, TR 2021c, WAROX observations of rock types prospective for selected Critical Minerals (REE, V, Mn, Ni, PGE, Ge, In, Li, graphite): Geological Survey of Western Australia, digital data layers.

Duuring, P, Guilliamse JN, and Morin-Ka S 2021d, Whole-rock geochemical fertility indicators for lithium and vanadium: Geological Survey of Western Australia, digital data layers.

Duuring, P, Then, D, Howard, D and Morin-Ka 2021e, Western Australian near-surface geochemistry: Geological Survey of Western Australia, digital data layers.

European Commission 2020, Study on the EU's list of Critical Raw Materials – Final Report (2020), 152p., <https://op.europa.eu/en/publication-detail/-/publication/c0d5292a-ee54-11ea-991b-01aa75ed71a1/language-en>, viewed 22 May 2021.

Guilliamse, JN and Duuring, P 2021a, Geochemical pathfinders for volcanogenic massive sulfide (VMS) mineralizing systems in Western Australia: Geological Survey of Western Australia, digital data layers.

Guilliamse, JN, Duuring, P and Farrell, TR 2021, Occurrences of minerals diagnostic of mineralization and alteration prospective for selected Critical Minerals (Li, Ge, In, Ni, PGE, V): Geological Survey of Western Australia, digital data layers.

Gupta, V, Biswas, T and Ganesan, K 2016, Critical non-fuel mineral resources for India's Manufacturing Sector – A vision for 2030: Report, Department of Science and Technology, Government of India, 75p., <https://dst.gov.in/sites/default/files/CEEW_0.pdf>, viewed 22 May 2021.

Hutchison, MT 2018a, Diamond exploration and prospectivity of Western Australia: Geological Survey of Western Australia, Report 179, 70p.

Hutchison, MT 2018b, Data methodologies applied in the Western Australian diamond exploration package: Geological Survey of Western Australia, Record 2017/16, 24p.

Jakica, S, de Souza Kovacs, N, Hogen-Esch, J and Granado, IMT 2020, 1:500 000 State regolith geology of Western Australia — compilation methodologies: Geological Survey of Western Australia, Record 2020/10, 22p.

Kenworthy, S and Beardsmore, TJ 2021a, Hydrogeochemical data from wells and bores in Western Australia: Geological Survey of Western Australia, digital data layers.

Kenworthy, S and Beardsmore, TJ 2021b, Hydrogeological features of Western Australia – Drainage basins, lakes and paleochannels: Geological Survey of Western Australia, digital data layers.

Kenworthy, S and Beardsmore, TJ 2021c, Hydrogeological features of Western Australia – Mean annual rainfall, evaporation and evapotranspiration: Geological Survey of Western Australia, digital data layers.

Martin, DMcB, Hocking, RM, Riganti, A and Tyler, IM 2016, Geological map of Western Australia, 14th edition – Explanatory Notes: Geological Survey of Western Australia, Record 2015/14, 16p.

Morin-Ka, S 2021a, 'GeologyMERGED' – a 'best resolution' interpreted bedrock geology map for Western Australia: Geological Survey of Western Australia, digital data layer.

Morin-Ka, S 2021b, Outcrop geology map of Western Australia: Geological Survey of Western Australia, digital data layer.

Morin-Ka, S, Duuring, P, Guilliamse, JN and Beardsmore, TJ 2021a, Mineralization endowment and style proxies for selected critical mineral occurrences in Western Australia: Geological Survey of Western Australia, digital data layers.

Morin-Ka, S, Ormsby, W and Beardsmore, HJ 2021b, Selected mineralization sites of Western Australia: Geological Survey of Western Australia, digital data layers.

Morin-Ka, S, Duuring, P, Burley, L, Guilliamse, JN and Beardsmore, TJ 2019, Mineral Systems Atlas – a dynamic approach to the delivery of mineral exploration data, *in* GSWA 2019 extended abstracts: Geological Survey of Western Australia, Record 2019/2, p. 9–12.

Petty, TR 2018, Final list of Critical Minerals 2018: US Government, Federal Register, v. 89, no. 97, p. 23295–23296. <https://www.federalregister.gov/documents/2018/05/18/2018-10667/final-list-of-critical-minerals-2018>, viewed 22 May 2021.

Riganti, A, Farrell, TR, Ellis, MJ, Irimies, F, Strickland, CD, Martin, SK and Wallace, DJ, 2015, 125 years of legacy data at the Geological Survey of Western Australia - Capture and delivery: GeoResJ, v. 6, p. 175–194.

Recommended reference

Beardsmore, TJ, Duuring, P, Guilliamse, JN, Kenworthy, S, Morin-Ka, S, Hogen-Esch, J and Then, D 2021, Geoscience data for Critical Mineral discovery in Western Australia: Abstract, Geological Survey of Western Australia Accelerated Geoscience Program, 5p.

Quartz veins in Western Australia

by

TJ Beardsmore

Abstract

Quartz veins can provide important information on the architecture and evolution of the crust — for instance by indicating the presence of significant structures, the rheological behaviour of the crust, or the passage of significant volumes of hydrothermal fluid that might have formed mineral deposits. Quartz veins are also important to the resources industry, certainly as hosts for metalliferous mineralization, but also potentially as resources in their own right, by providing silica for industrial applications such as glass (including optical fibres), mouldings, filtration, coating powders, electronics and solar panels, and more recently for anodes in high-performance lithium ion and "silicon-air" batteries (e.g. Cohn et al., 2009; Dutta and Datta, 2010; Ikonen et al., 2017).

Silica is not commonly regarded as a critical mineral, but its status may change because much is presently obtained from detrital sands, access to which is becoming increasingly problematic due to high demand and competing land use interests. Quartz veins are an obvious alternative silica resource, and it is therefore useful to have easily accessible information on their locations. The mapped occurrences of substantial quartz veins in Western Australia have therefore been manually digitized from the Geological Survey of Western Australia (GSWA) georegistered 1:100 000 or 1:250 000 geological map sheet mosaics (available via the GeoVIEW portal) using whichever source provides the greatest detail, or (in some instances) have been extracted from GSWA 1:100 000-scale GIS data sets, where such data exist and provide additional vein features.

Quartz vein occurrences are provided in two GIS layers — a 'line' version documenting veins of indeterminate width, and a 'polygon' version documenting quartz veins and pods with mappable areal extent. These GIS map layers are attributed using the data schema from the Western Australian 1:100 000 interpreted bedrock geology mapping to permit merging with other GSWA geology data layers, although only a few attributes are currently populated. The maps should be considered as being of a reconnaissance nature only, and no warranty is given that the original mapping comprehensively records all surface outcrops, nor that the quartz contained in any vein is of appropriate 'metallurgical' grade for any particular purpose.

How to access

The Western Australian Quartz vein digital data layers can be acquired as part of the Critical minerals, 2021 Geological Exploration Package, which is provided on USB via the GSWA eBookshop, and is also available to freely download from the Data and Software Centre

References

Cohn, G, Starosvetsky, D, Hagiwara, R, Macdonald, DD and Ein-Eli, Y 2009, Silicon-air batteries: Electrochemistry Communications, v. 11, p. 1916–1918.

Dutta, S and Datta, P 2010, Silicon – A versatile material! Science Reporter, February 2010, p. 40–42.

Ikonen, T, Nissinen, T, Pohjalainen, E, Sorsa, O, Kallio, T and Lehto, V-P 2017, Electrochemically anodized porous silicon: Towards simple and affordable anode material for Li-ion batteries: Scientific Reports, v. 7, 8p., doi:10.1038/s41598-017-08285-3.

Recommended reference

Beardsmore, TJ 2021, Quartz veins in Western Australia: Geological Survey of Western Australia, digital data layers.

Granitic pegmatites in Western Australia

by

TJ Beardsmore and P Duuring

Abstract

Granitic pegmatites are coarse-grained igneous rocks that contain abundant — in some cases giant — crystals with skeletal, graphic or other strongly directional growth habits, or anisotropic layered mineral fabrics (London, 2008). They are important resources of metals critical for the manufacture of advanced (including 'green') technologies (e.g. Be, Cs, Li, Sn, Ta), but are also commonly mined for high-purity quartz, feldspars, kaolinite and white mica for industrial applications such as glass, ceramics, paints, electronics, lubricants, abrasives, refractories, and for gem and museum-quality specimens of many rare minerals.

Granitic pegmatites are typically classified into 'common' and 'rare-element' varieties. The latter are further divided on the basis of element enrichments into three types: LCT (enriched in Li, Cs, Ta, Be, B, F, P, Mn, Ga, Rb, Nb, Sn and Hf), NYF (enriched in Be, Sn, B, Nb>Ta, Ti, Y, REE, Zr, Th, U, Sc and F) and hybrid (having blended rare-element signatures; Černý and Ercit, 2005; Ercit, 2005; London, 2008).

Western Australia is well endowed with large pegmatites (Jacobsen et al., 2007), including many world-class examples of the LCT-type (e.g. Greenbushes, Pilgangoora, Wodgina), but heretofore there has been no easily accessible, digital maps showing pegmatite locations. The mapped occurrences of substantial granitic pegmatite veins and pods in Western Australia have therefore been manually digitized into GIS layers from two principal sources: (i) the Geological Survey of Western Australia (GSWA) georegistered 1:100 000 or 1:250 000 geological map sheet mosaics (available via the GeoVIEW portal); (ii) georegistered resource company maps provided in public announcements to the Australian Securities Exchange — in each case using whichever source provides the greatest detail.

Pegmatite occurrences are provided in four GIS layers - two 'line' versions (one each for GSWA and company data, respectively) documenting dykes of indeterminate width, and two 'polygon' versions (GSWA, company) depicting pegmatite dykes and pods with mappable areal extent. These GIS map layers are structured using the data schema from the Western Australia 1:100 000 interpreted bedrock geology mapping to permit merging with other GSWA geology data layers, but pegmatites are not (yet) classified by type, and only a few attributes are currently populated. The maps should be considered as being of a reconnaissance nature only, and no warranty is given that the original mapping comprehensively records all surface outcrops, nor that the pegmatites contain any particular critical or industrial mineral.

How to access

These data form part of the Critical minerals, 2021 Geological Exploration Package, available via the DMIRS eBookshop

References

Černý, P and Ercit, TS 2005, The classification of pegmatites revisited: The Canadian Mineralogist, v. 43, no. 6, p. 2005–2026, doi:10.2113/gscanmin.43.6.2005.

Ercit, TS 2005, REE-enriched granitic pegmatites, in Rare-element geochemistry and mineral deposits edited by RL Linnen and IM Samson: Geological Association of Canada Short Course Notes 17, p. 175–199.

Jacobsen, MI, Calderwood, MA and Crguric, BA 2007, Guidebook to the pegmatites of Western Australia: Hesperian Press, 394p.

London, D 2008, Pegmatites: Mineralogical Association of Canada, The Canadian Mineralogist Special Publication 10, 347p.

Martin, DMcB 2016, The geological map of Western Australia - past, present and future, in GSWA 2016 extended abstracts: promoting the prospectivity of Western Australia: Geological Survey of Western Australia, Record 2016/2, p. 1–3.

Recommended reference

Beardsmore, TJ and Duuring, P 2021, Granitic pegmatites in Western Australia: Geological Survey of Western Australia, digital data layers.

Carbonatites, kimberlites and lamproites in Western Australia – prospective hosts for rare earth elements

by

TJ Beardsmore and MT Hutchison

Abstract

Particular rock types are known to be prospective as hosts for specific mineral commodities. Carbonatite intrusive complexes are well known for their high rare earth element (REE) contents (e.g. Mount Weld, Western Australia), but elevated REE abundances are also known in other mafic–ultramafic igneous intrusions such as kimberlites (e.g. Redlings [or Jungle Well], Western Australia; Victory Mines Ltd, 2012; Marquee Resources Ltd, 2019) and lamproites (e.g. Argyle, WA; O'Connor, 2019). Such intrusions are generally relatively small and prone to deep weathering (particularly in Western Australia), hence are difficult to locate or recognize during surface geological mapping.

Fortunately, such rocks are also prospective for diamonds, and the recent compilation and evaluation of available Western Australian diamond exploration data by Hutchison (2018a,b) includes three digital map layers showing the locations of carbonatites, kimberlites, lamproites and lamprophyres observed or inferred during resource company exploration and government mapping.

DED_WA_OCCURRENCES provides the locations and physical characteristics of 524 verified discrete intrusions, occurring in clusters or as isolated bodies.

DED_WA_Occurrences_Outlines provides at or near-surface outlines for 215 of these intrusions.

DED_WA_INFERENCES provides the locations and physical characteristics of an additional 24 inferred intrusions.

These maps are now also provided as part of the Critical Minerals Geological Exploration Package. Descriptions of data compilation and verification are provided in Hutchison (2018a, b).

Three additional GIS layers are also provided showing the Geological Survey of Western Australia (GSWA)-mapped distribution of dykes and sills comprising the Gifford Creek (Yangibana) Carbonatite Complex (Slezak and Spandler, 2020). These map layers were manually digitized from the GSWA georegistered 1:100 000 geological map sheet mosaic (specifically the EDMUND sheet number 2150). They are structured using the data schema from the Western Australian 1:100 000 interpreted bedrock geology mapping to permit merging with other GSWA geology data layers, but only a few attributes are currently populated.

All maps should be considered as being of a reconnaissance nature only, and no warranty is given that they comprehensively record all carbonatite, kimberlite and lamproite intrusions in Western Australia, nor that any intrusion contains potentially economic quantities of REE.

How to access

The Carbonatite, kimberlite and lamproite intrusion digital data layers can be acquired as part of the Critical minerals, 2021 Geological Exploration Package, which is provided on USB via the GSWA eBookshop, and are also available to freely download from the Data and Software Centre.

References

Hutchison, MT 2018a, Diamond exploration and prospectivity of Western Australia: Geological Survey of Western Australia, Report 179, 70p.

Hutchison, MT 2018b, Data methodologies applied in the Western Australian diamond exploration package: Geological Survey of Western Australia, Record 2017/16, 24p.

Marquee Resources Ltd 2019, Acquires Redlings Rare Earths Project: Report to Australian Securities Exchange, 25 June 2019, <https://www.asx.com.au/asxpdf/20190625/pdf/4463d30d0cdm08.pdf>, viewed 6 April 2021.

O'Connor, L 2019, Mineralogical and lithological controls on REE in the Argyle Lamproite, Final Report, MRIWA Project M467: Minerals Research Institute of Western Australia, 87p. including appendices.

Slezak, P and Spandler, C 2020, Petrogenesis of the Gifford Creek Carbonatite Complex, Western Australia: Contributions to Mineralogy and petrology, v. 175, no. 28, 23p., doi:10.1007/s00410-020-1666-3.

Victory Mines, 2012, Jungle Well high-grade rare earths confirmed: Report to Australian Securities Exchange, 12 October 2012, <https://www.asx.com.au/asxpdf/20121012/pdf/429bkqnzwvw2sb.pdf>, viewed 6 April 2021.

Recommended reference

Beardsmore, TJ and Hutchison, MT 2021, Carbonatites, kimberlites and lamproites in Western Australia – prospective hosts for rare earth elements: Geological Survey of Western Australia, digital data layers.

Distributions of rock units in Western Australia prospective for selected critical minerals (Li, Mn, Ni, PGE, Sn, Ta, V, W)

by

P Duuring, JN Guilliamse and S Morin-Ka

Abstract

Certain rock types are known to be prospective for specific mineral commodities, either as hosts or as indicators of fertile geological environments. Rock types that are potentially prospective for critical minerals have been selected, including clastic and carbonate-rich sedimentary rocks, and banded iron-formations (potential source areas for the circulation of manganese-rich fluids and the early concentration of Mn [and Fe] ores); pegmatites (hosts for Li, Ta, Sn and W); granites (as potential sources for rare-element pegmatites); and mafic intrusions (prominent hosts for V, Ni, PGE, Cr and Ti).

The spatial distributions of rock units that contain these rock types in Western Australia have been extracted into a number of map layers from the 'GeologyMERGED' State interpreted bedrock geology of Western Australia, 2020 GIS dataset (Morin-Ka, 2021), by querying the DESCRIPTN or ROCKTYPE1 fields using the terms provided in Table 1.

Map polygons for pegmatites, mafic intrusions, and iron formations are tinted in darker or paler colours according to the likelihood that these rock types constitute either substantial or minor components, respectively, in the depicted rock unit. Their relative abundance is indicated by their rock type descriptions in the Geological Survey of Western Australia's Explanatory Notes System (www.dmirs.wa.gov.au/ens).

Additional GIS layers have been created showing the distribution of Western Australian granites categorized by age of emplacement (as determined by geochronology, for potential correlation with pegmatites or rare-element minerals of similar age); of mafic intrusive rocks that are explicitly hornblende free (hence were water poor and more likely to accumulate magnetite and vanadium; Himmelberg and Loney, 1995); and of cumulate magnetitite or chromitite (which may comprise the actual V or Cr ores).

How to access

These data form part of the Critical minerals, 2021 Geological Exploration Package, available via the DMIRS eBookshop. A subset of these data layers (pertaining to the Rare-metal pegmatite, Mafic intrusion-hosted vanadium and Banded iron-formation-hosted mineral systems) can also be obtained from the Mineral Systems Atlas (www.dmirs.wa.gov.au/mineralsystemsatlas) via GeoVIEW.WA, an online interactive mapping and knowledge system that facilitates the location and viewing of geological datasets particularly relevant to mineral deposits in Western Australia (Morin-Ka et al., 2019).

Table 1. Query operations

Operation	Query
Clastic sedimentary rock units are extracted from GeologyMERGED	"ROCKTYPE1" LIKE '%siliciclastic%'
Chemical sedimentary rock units are extracted from GeologyMERGED	"ROCKTYPE1" LIKE '%sed%' AND "ROCKTYPE1" LIKE '%carb%'
Iron-formation-bearing rock units are extracted from GeologyMERGED	LOWER (DESCRIPTN) LIKE LOWER ('%ironstone%') OR LOWER (DESCRIPTN) LIKE LOWER ('%mixed iron formation and mudstone/siltstone%') OR LOWER (DESCRIPTN) LIKE LOWER ('%iron-formation%') OR LOWER (DESCRIPTN) LIKE LOWER ('%meta-iron formation%') OR LOWER (DESCRIPTN) LIKE LOWER ('%metamorphosed iron-formation%') OR LOWER (DESCRIPTN) LIKE LOWER ('%iron formation%') OR LOWER (DESCRIPTN) LIKE LOWER ('%banded iron-formation%') OR LOWER (DESCRIPTN) LIKE LOWER ('%mixed chert and iron formation%') OR LOWER (DESCRIPTN) LIKE LOWER ('%meta-banded iron formation%') OR LOWER (DESCRIPTN) LIKE LOWER ('%granofelsic/hornfelsic meta-iron formation%') OR LOWER (DESCRIPTN) LIKE LOWER ('%gneissose meta-iron formation%') OR LOWER (DESCRIPTN) LIKE LOWER ('%schistose meta-iron formation%') OR LOWER (DESCRIPTN) LIKE LOWER ('%silicified meta-iron formation%') OR LOWER (DESCRIPTN) LIKE LOWER ('%mylonitized meta-iron formation%')
Pegmatite-bearing rock units are extracted from GeologyMERGED	LOWER (DESCRIPTN) LIKE LOWER ('%pegmatite%') OR LOWER (DESCRIPTN) LIKE LOWER ('%metapegmatite%')
Granitic rock units are extracted from GeologyMERGED	LOWER (DESCRIPTN) LIKE LOWER ('%metasyenite%') OR LOWER (DESCRIPTN) LIKE LOWER ('%syenite%') OR LOWER (DESCRIPTN) LIKE LOWER ('%quartz syenite%') OR LOWER (DESCRIPTN) LIKE LOWER ('%quartz alkali feldspar syenite%') OR LOWER (DESCRIPTN) LIKE LOWER ('%alkali feldspar syenite%') OR LOWER (DESCRIPTN) LIKE LOWER ('%alkali feldspar granite%') OR LOWER (DESCRIPTN) LIKE LOWER ('%foliated metagranite%') OR LOWER (DESCRIPTN) LIKE LOWER ('%granitic gneiss%') OR LOWER (DESCRIPTN) LIKE LOWER ('%granitic granofels/hornfels%') OR LOWER (DESCRIPTN) LIKE LOWER ('%granitic rock%') OR LOWER (DESCRIPTN) LIKE LOWER ('%granitic rock; undivided%') OR LOWER (DESCRIPTN) LIKE LOWER ('%granitic schist%') OR LOWER (DESCRIPTN) LIKE LOWER ('%granodiorite%') OR LOWER (DESCRIPTN) LIKE LOWER ('%greisen%') OR LOWER (DESCRIPTN) LIKE LOWER ('%metagranitic rock%') OR LOWER (DESCRIPTN) LIKE LOWER ('%metagranodiorite%') OR LOWER (DESCRIPTN) LIKE LOWER ('%metamonzogranite%') OR LOWER (DESCRIPTN) LIKE LOWER ('%metapegmatite%') OR LOWER (DESCRIPTN) LIKE LOWER ('%metasyenogranite%') OR LOWER (DESCRIPTN) LIKE LOWER ('%monzogranite%') OR LOWER (DESCRIPTN) LIKE LOWER ('%mylonitized metagranitic rock%') OR LOWER (DESCRIPTN) LIKE LOWER ('%pegmatite%') OR LOWER (DESCRIPTN) LIKE LOWER ('%quartz monzodiorite%') OR LOWER (DESCRIPTN) LIKE LOWER ('%quartz monzogabbro%') OR LOWER (DESCRIPTN) LIKE LOWER ('%quartz monzonite%') OR LOWER (DESCRIPTN) LIKE LOWER ('%silicified metagranitic rock%') OR LOWER (DESCRIPTN) LIKE LOWER ('%syenogranite%') AND CODE LIKE '%g%'
Mafic intrusive rock units, layered or otherwise, are extracted from GeologyMERGED	LOWER (DESCRIPTN) LIKE LOWER ('%mafic intrusive rock%') OR LOWER (DESCRIPTN) LIKE LOWER ('%mafic and ultramafic intrusive%') OR LOWER (DESCRIPTN) LIKE LOWER ('%mafic and ultramafic intrusion%') OR LOWER (DESCRIPTN) LIKE LOWER ('%mafic--ultramafic igneous%') OR LOWER (DESCRIPTN) LIKE LOWER ('%gabbro%') OR LOWER (DESCRIPTN) LIKE LOWER ('%norite%') OR

	LOWER (DESCRIPTN) LIKE LOWER ('%anorthosite%') OR **LOWER (DESCRIPTN) LIKE LOWER ('%layered mafic–ultramafic%') OR** **LOWER (DESCRIPTN) LIKE LOWER ('%layered mafic and ultramafic%') OR** LOWER (DESCRIPTN) LIKE LOWER ('%layered mafic--ultramafic%') OR
Magnetitite- and chromitite-bearing rock units are extracted from GeologyMERGED	**LOWER (DESCRIPTN) LIKE LOWER ('%magnetitite%') OR** **LOWER (DESCRIPTN) LIKE LOWER ('%chromitite%')**

References

Himmelberg, GR and Loney, RA 1995, Characteristics and petrogenesis of Alaskan-type ultramafic–mafic intrusions, southeastern Alaska: United States Geological Survey, Professional Paper 1564, 41p.

Morin-Ka, S 2021, 'GeologyMERGED' – a 'best resolution' interpreted bedrock geology map for Western Australia: Geological Survey of Western Australia, digital data layers.

Morin-Ka, S, Duuring, P, Burley, L, Guilliamse, J and Beardsmore, TJ 2019, Mineral Systems Atlas – a dynamic approach to the delivery of mineral exploration data: Extended Abstract, Geological Survey of Western Australia Record 2019/2, p. 9–12.

Recommended reference

Duuring, P, Guilliamse, JN, Morin-Ka, S 2021, Distributions of rock units in Western Australia prospective for selected Critical Minerals (Li, Mn, Ni, PGE, Sn, Ta, V, W): Geological Survey of Western Australia, digital data layers.

Whole-rock geochemical fertility indicators for lithium and vanadium

by

P Duuring, JN Guilliamse and S Morin-Ka

Abstract

The geochemistry of a rock may signal its fertility as a host for metalliferous mineralization. The fertility of pegmatites for rare elements is indicated by elevated abundances of the target elements or their proxies (e.g. Be, Cs, F, Li, Ta and U). Granite fertility for rare-element pegmatites is indicated by elevated element abundances or element ratios that indicate high degrees of magmatic fractionation during crystallization (e.g. Be, Ca, Cs/K, F, Fe, Ga, Ga/Al, La/Yb, Li, Li/Mg, Mg, Nb, Rb, Rb/K, Rb/Sr, SiO_2, Sn, Ta, Ta/Nb, Ti, and total REE). The vanadium content of layered mafic intrusions is the principal chemical indicator of their fertility as hosts for 'orthomagmatic' vanadium (and associated titanium and iron) mineralization.

Geolocated geochemical data for Western Australian pegmatite, granite, and mafic intrusions (including gabbro, norite, anorthosite, magnetitite and chromitite) have been extracted from the 'WACHEMrecalc' component of the statewide 'near-surface geochemistry' dataset (Duuring et al., 2021), using the query terms provided in Table 1.

The 'WACHEMrecalc' database is a derivative of the parent WACHEM database, with additional fields to permit storage of element or element-oxide values calculated from existing data, where such values are not present in WACHEM. The WACHEM database contains whole-rock major element oxide, trace element and isotope geochemistry for rock, unconsolidated surface material (regolith) and drillcore samples collected by the Geological Survey of Western Australia.

How to access

These data form part of the Critical minerals, 2021 Geological Exploration Package, available on a USB via the DMIRS eBookshop.

Reference

Duuring, P, Then, D and Morin-Ka, S 2021, Western Australian near-surface geochemistry: Geological Survey of Western Australia, digital data layers.

Recommended reference

Duuring, P, Guilliamse JN, and Morin-Ka, S, 2021, Whole-rock geochemical fertility indicators for lithium and vanadium: Geological Survey of Western Australia, digital data layers.

Table 1. Query operation

Operation	Query
Pegmatite samples that have been analysed for Be, Cs, F, Li, Ta and U are selected from the WACHEMrecalc database using the query terms, and then individual geochemical maps are generated	LOWER (LITHNAME) LIKE LOWER ('%pegmatite%') OR LOWER (LITHNAME) LIKE LOWER ('%metapegmatite%')
Granitic rock samples that have been analysed for Be, Ca, F, Fe, Ga, Li, Mg, Nb, Rb, SiO2, Sn, Ta, Ti and total REE are first selected from the WACHEMrecalc database using the query terms, Cs/K, Ga/Al, La/Yb, Li/Mg, Rb/K, Rb/Sr and Ta/Nb are calculated and appended, and then individual geochemical maps are generated	LOWER (LITHNAME) LIKE LOWER ('%metasyenite%') OR LOWER (LITHNAME) LIKE LOWER ('%syenite%') OR LOWER (LITHNAME) LIKE LOWER ('%quartz syenite%') OR LOWER (LITHNAME) LIKE LOWER ('%quartz alkali feldspar syenite%') OR LOWER (LITHNAME) LIKE LOWER ('%alkali feldspar syenite%') OR LOWER (LITHNAME) LIKE LOWER ('%alkali feldspar granite%') OR LOWER (LITHNAME) LIKE LOWER ('%foliated metagranite%') OR LOWER (LITHNAME) LIKE LOWER ('%granitic gneiss%') OR LOWER (LITHNAME) LIKE LOWER ('%granitic granofels/hornfels%') OR LOWER (LITHNAME) LIKE LOWER ('%granitic rock%') OR LOWER (LITHNAME) LIKE LOWER ('%granitic rock; undivided%') OR LOWER (LITHNAME) LIKE LOWER ('%granitic schist%') OR LOWER (LITHNAME) LIKE LOWER ('%granodiorite%') OR LOWER (LITHNAME) LIKE LOWER ('%greisen%') OR LOWER (LITHNAME) LIKE LOWER ('%metagranitic rock%') OR LOWER (LITHNAME) LIKE LOWER ('%metagranodiorite%') OR LOWER (LITHNAME) LIKE LOWER ('%metamonzogranite%') OR LOWER (LITHNAME) LIKE LOWER ('%metapegmatite%') OR LOWER (LITHNAME) LIKE LOWER ('%metasyenogranite%') OR LOWER (LITHNAME) LIKE LOWER ('%monzogranite%') OR LOWER (LITHNAME) LIKE LOWER ('%mylonitized metagranitic rock%') OR LOWER (LITHNAME) LIKE LOWER ('%pegmatite%') OR LOWER (LITHNAME) LIKE LOWER ('%quartz monzodiorite%') OR LOWER (LITHNAME) LIKE LOWER ('%quartz monzogabbro%') OR LOWER (LITHNAME) LIKE LOWER ('%quartz monzonite%') OR LOWER (LITHNAME) LIKE LOWER ('%silicified metagranitic rock%') OR LOWER (LITHNAME) LIKE LOWER ('%syenogranite%')
Mafic intrusive rock samples that have been analysed for V are first extracted from the WACHEMrecalc database using the query terms, and then the geochemical map is generated	(LOWER (LITHNAME) LIKE LOWER ('%gabbro%') OR LOWER (LITHNAME) LIKE LOWER ('%norite%') OR LOWER (LITHNAME) LIKE LOWER ('%anorthosite%') OR LOWER (LITHNAME) LIKE LOWER ('%magnetitite%') OR LOWER (LITHNAME) LIKE LOWER ('%chromitite%')) AND NOT LOWER (LITHNAME) LIKE LOWER ('%hornblende gabbro%')

Occurrences of minerals in Western Australia diagnostic of rock types prospective for selected critical minerals (Li, Ge, In, Ni, PGE, V)

by

P Duuring, JN Guilliamse, S Morin-Ka and TR Farrell

Abstract

These maps show the occurrences of minerals that may indicate the presence of particular rock types prospective for critical minerals in Western Australia — exhalative sediments (for Ge and In in VMS), pegmatites or fractionated granites (for Li), and mafic intrusions (for Ni, PGE, V) — using observations recorded in the Geological Survey of Western Australia WAROX database (Table 1).

The WAROX database contains data related to geological observations and samples collected in the field, including outcrop geology, regolith geology, field photographs, geological samples, rock physical properties, petrography, paleontology and geochronology (Riganti et al., 2015).

Some minerals may also indicate fertility for other rock types or commodities, and the maps should be considered in conjunction with complementary maps showing occurrences of minerals diagnostic of critical mineral-prospective mineralization and alteration (Guilliamse and Duuring, 2021).

Table 1. Query operation

Operation	Query
Occurrences of selected carbonate, oxide and sulfate minerals diagnostic of exhalative (or evaporitic) rocks are extracted by querying any field in the WAROX database	Any field = 'ankerite' OR Any field = 'calcite' OR Any field = 'dolomite' OR Any field = 'siderite' OR Any field = 'hematite' OR Any field = 'magnetite' OR Any field = 'anhydrite' OR Any field = 'barite' OR Any field = 'gypsum'
Occurrences of selected minerals diagnostic of rare element pegmatites or fractionated granite are extracted by querying any field in the WAROX database	Any field = 'fluorite' OR Any field = 'topaz' OR Any field = 'tourmaline'
Occurrences of selected "primary" minerals diagnostic of rock types in mafic intrusions are extracted by querying any field in the WAROX database	Any field = 'hornblende' OR Any field = 'olivine' OR Any field = 'clinopyroxene' OR Any field = 'orthopyroxene'

How to access

These data form part of the Critical minerals, 2021 Geological Exploration Package, available on a USB via the DMIRS eBookshop.

Reference

Riganti, A, Farrell, TR, Ellis, MJ, Irimies, F, Strickland, CD, Martin, SK and Wallace, DJ, 2015, 125 years of legacy data at the Geological Survey of Western Australia: Capture and delivery: GeoResJ, v. 6, p. 175-194.

Recommended reference

Duuring, P, Guilliamse, JN, Morin-Ka, S and Farrell, TR 2021, Occurrences of minerals in Western Australia diagnostic of rock types prospective for selected critical minerals (Li, Ge, In, Ni, PGE, V): Geological Survey of Western Australia, digital data layers.

WAROX observations of rock types prospective for selected critical minerals (REE, V, Mn, Ni, PGE, Ge, In, Li, graphite)

by

P Duuring, JN Guilliamse, S Morin-Ka TR Farrell and D Then

Abstract

These data layers show the distribution of rock types that may be prospective for particular mineral commodities, either as hosts or as indicators of fertile geological environments, based on observations of rock types recorded in the Geological Survey of Western Australia WAROX database. Each layer is tailored to show the occurrence of a specific rock type (e.g. pegmatite) (Table 1).

The parent WAROX database contains geoscientific data related to observations and samples collected in the field (Riganti et al., 2015). The data include information about outcrop geology, regolith geology, field photographs, geological samples, rock physical properties, petrography, paleontology and geochronology.

Table 1. Query operation

Operation	Query
WAROX data are queried to select specific rock types from any field in the WAROX database. The occurrences are prospective for a variety of mineralization types (e.g. graphite, diamond, Ni-rich orthomagmatic systems, and REE mineralization)	Any field = 'carbonaceous' OR Any field = "chert" OR Any field = "jasper" OR Any field = 'kimberlite' OR Any field = 'lamproite' OR Any field = 'lamprophyre' OR Any field = 'gabbro' OR Any field = 'norite' OR Any field = 'anorthosite' OR Any field = 'limestone' OR Any field = 'dolostone' OR Any field = 'siliciclastic' OR Any field = 'carbonatite' OR Any field = 'dunite' OR Any field = 'peridotite' OR Any field = 'troctolite'
WAROX data are queried to select chemical sedimentary rocks from the ROCKTYPENAME Field. Chemical sedimentary rocks may indicate basinal settings prospective for manganese mineralization	ROCKTYPENAME = 'metasedimentary carbonate' OR ROCKTYPENAME = 'metasedimentary other chemical' OR ROCKTYPENAME = 'metasedimentary other chemical: meta-iron formation' OR ROCKTYPENAME = 'sedimentary carbonate' OR ROCKTYPENAME = 'sedimentary other chemical or biochemical'
WAROX data are queried to select clastic sedimentary rocks from the ROCKTYPENAME Field. Clastic sedimentary rocks may indicate basinal settings prospective for manganese mineralization	ROCKTYPENAME = 'metasedimentary siliciclastic' OR ROCKTYPENAME = 'metasedimentary siliciclastic: pelite' OR ROCKTYPENAME = 'metasedimentary siliciclastic: psammite' OR ROCKTYPENAME = 'metasedimentary siliciclastic: psammite and pelite; interlayered' OR

	ROCKTYPENAME = 'metasedimentary siliciclastic: psephite' OR ROCKTYPENAME = 'metasedimentary siliciclastic: semipelite' OR ROCKTYPENAME = 'metasedimentary siliciclastic: semipsephite' OR ROCKTYPENAME = 'sedimentary siliciclastic'
WAROX data are queried to select iron formations from the ROCKNAME Field. Jasper and chert layers may be prospective for volcanic-hosted massive sulfide (Ge, In) mineralization	ROCKNAME = 'Ironstone' OR ROCKNAME = 'chemical or biochemical rock; undivided' OR ROCKNAME = 'mixed iron formation and mudstone/siltstone' OR ROCKNAME = 'iron formation' OR ROCKNAME = 'banded iron-formation' OR ROCKNAME = 'mixed chert and iron formation' OR ROCKNAME = 'meta-iron formation' OR ROCKNAME = 'meta-banded iron formation' OR ROCKNAME = 'granofelsic/hornfelsic meta-iron formation' OR ROCKNAME = 'gneissose meta-iron formation' OR ROCKNAME = 'schistose meta-iron formation' OR ROCKNAME = 'silicified meta-iron formation' OR ROCKNAME = 'mylonitized meta-iron formation'
WAROX data are queried to select pegmatites from the ROCKNAME Field, which may be hosts to rare elements	ROCKNAME = 'pegmatite' OR ROCKNAME = 'metapegmatite'
WAROX data are queried to select granitic rocks from the ROCKNAME Field. Granitic rocks may be the primary source of pegmatite intrusions	LOWER (DESCRIPTN) LIKE LOWER ('%metasyenite%') OR LOWER (DESCRIPTN) LIKE LOWER ('%syenite%') OR LOWER (DESCRIPTN) LIKE LOWER ('%quartz syenite%') OR LOWER (DESCRIPTN) LIKE LOWER ('%quartz alkali feldspar syenite%') OR LOWER (DESCRIPTN) LIKE LOWER ('%alkali feldspar syenite%') OR LOWER (DESCRIPTN) LIKE LOWER ('%alkali feldspar granite%') OR LOWER (DESCRIPTN) LIKE LOWER ('%foliated metagranite%') OR LOWER (DESCRIPTN) LIKE LOWER ('%granitic gneiss%') OR LOWER (DESCRIPTN) LIKE LOWER ('%granitic granofels/hornfels%') OR LOWER (DESCRIPTN) LIKE LOWER ('%granitic rock%') OR LOWER (DESCRIPTN) LIKE LOWER ('%granitic rock; undivided%') OR LOWER (DESCRIPTN) LIKE LOWER ('%granitic schist%') OR LOWER (DESCRIPTN) LIKE LOWER ('%granodiorite%') OR LOWER (DESCRIPTN) LIKE LOWER ('%greisen%') OR LOWER (DESCRIPTN) LIKE LOWER ('%metagranitic rock%') OR LOWER (DESCRIPTN) LIKE LOWER ('%metagranodiorite%') OR LOWER (DESCRIPTN) LIKE LOWER ('%metamonzogranite%') OR LOWER (DESCRIPTN) LIKE LOWER ('%metapegmatite%') OR LOWER (DESCRIPTN) LIKE LOWER ('%metasyenogranite%') OR LOWER (DESCRIPTN) LIKE LOWER ('%monzogranite%') OR LOWER (DESCRIPTN) LIKE LOWER ('%mylonitized metagranitic rock%') OR LOWER (DESCRIPTN) LIKE LOWER ('%pegmatite%') OR LOWER (DESCRIPTN) LIKE LOWER ('%quartz monzodiorite%') OR LOWER (DESCRIPTN) LIKE LOWER ('%quartz monzogabbro%') OR LOWER (DESCRIPTN) LIKE LOWER ('%quartz monzonite%') OR LOWER (DESCRIPTN) LIKE LOWER ('%silicified metagranitic rock%') OR LOWER (DESCRIPTN) LIKE LOWER ('%syenogranite%') AND CODE LIKE '%g%'

How to access

These data form part of the Critical minerals, 2021 Geological Exploration Package, available on a USB via the DMIRS eBookshop.

Reference

Riganti, A, Farrell, TR, Ellis, MJ, Irimies, F, Strickland, CD, Martin, SK and Wallace, DJ, 2015, 125 years of legacy data at the Geological Survey of Western Australia: Capture ad delivery: GeoResJ, v. 6, p. 175–194.

Recommended reference

Duuring, P, Guilliamse, JN, Morin-Ka, S, Farrell, TR and Then, D 2021, WAROX observations of rock types prospective for selected critical minerals (REE, V, Mn, Ni, PGE, Ge, In, Li, graphite): Geological Survey of Western Australia, digital data layers.

Archean greenstone belts in Western Australia as possible hosts to rare-element pegmatites

by

P Duuring and S Morin-Ka

Abstract

This data layer shows the distribution of greenstone belts in Western Australia.

Greenstone belts are commonly hosts to rare-element pegmatites because they are both products of collisional tectonic processes. Rare-element pegmatites form in orogenic hinterlands related to plate convergence (Bradley et al., 2017). Arc-related processes control pegmatite generation by decompression melting. The pegmatites are products of extreme fractional crystallization of S-type granites, derived from melting of metasedimentary rocks in continental collision zones (Cerný and Ercit, 2005).

Greenstone belts are derived by querying the parent 1:500 000 State interpreted tectonic units of Western Australia digital map (Table 1), which is sourced from the 1:500 000 State interpreted bedrock geology of Western Australia, 2016 digital map (Martin, 2016). The nomenclature and hierarchy for the tectonic units (Table 2) are based on the Geological Survey of Western Australia's Explanatory Notes System (www.dmirs.wa.gov.au/ens).

Table 1. Query operation

Operation	Query
1:500K Tectonic units are queried, selecting greenstone units from the LITHOLOGY and TSETT_QUAL Fields	LITHOLOGY = 'granite-greenstones' OR TSETT_QUAL = 'granite-greenstone'

Table 2. Legend

Legend	Description
Granite–greenstone	Granite and greenstone belts (i.e. volcano-sedimentary rocks)
Granitic complex	Package of rock containing granite and greenstone
Undivided	No lithological classification

How to access

These data form part of the Critical minerals, 2021 Geological Exploration Package, available via the DMIRS eBookshop, and can also be obtained from the Mineral Systems Atlas via GeoVIEW.WA (www.dmirs.wa.gov.au/mineralsystemsatlas), an online interactive mapping and knowledge system that facilitates the location and viewing of geological datasets particularly relevant to mineral deposits in Western Australia (Morin-Ka et al., 2019).

References

Bradley, DC, McCauley, AD and Stillings, LL 2017, Mineral-deposit model for lithium-cesium-tantalum pegmatites: United States Geological Survey, Reston, VA, Scientific Investigations Report 2010-5070, 58p., doi:10.3133/sir201050700.

Cerný, P and Ercit, TS 2005, The classification of pegmatites revisited: The Canadian Mineralogist, v. 43, no. 6, p. 2005–2026, doi:10.2113/gscanmin.43.6.2005.

Martin, DMcB 2016, The geological map of Western Australia - past, present and future, *in* GSWA 2016 extended abstracts: promoting the prospectivity of Western Australia: Geological Survey of Western Australia, Record 2016/2, p. 1–3.

Morin-Ka, S, Duuring, P, Burley, L, Guilliamse, J and Beardsmore, TJ 2019, Mineral Systems Atlas – a dynamic approach to the delivery of mineral exploration data: Extended Abstract, Geological Survey of Western Australia Record 2019/2, p. 9–12.

Recommended reference

Duuring, P and Morin-Ka, S, 2021, Archean greenstone belts in Western Australia as possible hosts to rare-element pegmatites: Geological Survey of Western Australia, digital data layers.

Lithogeochemical fertility indicators for manganese oxide mineralization in Western Australia

by

P Duuring and S Morin-Ka

Abstract

Manganese (Mn) is one of the 24 commodities recently identified by the Australian Commonwealth Government as critical to the economic development of industrialized countries (Austrade, 2019). Western Australia is a producer of Mn, and it is also highly prospective for the discovery of additional Mn resources. Lithogeochemistry is an important exploration tool, either as a direct detector of Mn mineralization or as an indicator of hydrothermal alteration that is associated with such mineralization.

Geolocated lithogeochemical data relevant to Mn mineralization have been extracted from the Statewide near-surface geochemistry dataset. This is a compilation of such data from Western Australian soil, laterite, stream sediment, and outcrop or drillhole rock specimens, held alternatively in four separate primary databases maintained by the Geological Survey of Western Australia: WACHEM, OZCHEM (WA subset), CRCLEME-laterite, and WAMEX (i.e. the surface rock chip, surface stream sediment, surface shallow drillhole, surface soil, and maximum grade in drillhole). The creation of this 'near surface' dataset is described in more detail by Duuring et al. (2021).

Eight GIS maps show the distribution and abundance of MnO values for each primary data source. An additional four maps depict various element ratios that may reveal possible hydrothermal alteration or other Mn-enrichment process:

1. **MnO/Al_2O_3 index:** a proxy indicating addition of MnO relative to a less mobile element oxide (Al_2O_3), in an altered rock containing these two elements
2. **MnO/(CaO+MgO) index:** a proxy for the dissolution of calcite and dolomite in carbonate-rich rocks, resulting in enrichment of less-soluble MnO
3. **MnO/SiO_2 index:** a proxy for enrichment of MnO in silica-rich sedimentary rocks via the removal of silica (e.g. supergene dissolution of quartz bands in banded iron-formation)
4. **MnO/Fe_2O_{3T} index**: a proxy for oxidation, where a higher ratio indicates increased likelihood that the rock experienced high degrees of oxidation and enrichment in MnO.

All ratios were calculated using combined surface rock chip, surface stream sediment and shallow drillhole 'auger') data from all primary data components, and for MnO/SiO_2 and MnO/Fe_2O_{3T} ratios also surface soil data from WAMEX (which has no Al_2O_3, CaO, and MgO analyses).

A unique legend and colour scheme has been chosen for each geochemical layer to best highlight geochemical trends, with higher element abundance values drawn over lower values to more clearly show spatial gradients.

The use of ratios also 'normalizes' disparate primary datasets obtained from different sample media by varying laboratory procedures, allowing their combination and comparison. Even so, all these indices will be sensitive to precursor rock chemistry, and to the effects of overprinting events such as weathering. These factors need to be taken into consideration when interpreting alteration indices. Alternative methods such as the use of normative and mass balance calculations are recommended (cf. Mathieu, 2018).

How to access

These data form part of the Critical minerals, 2021 Geological Exploration Package, available on a USB via the DMIRS eBookshop.

References

Austrade 2019, Australia's Critical Mineral Strategy (2019), Australian Government, Department of Industry, Innovation and Science, Australian Trade and Investment Commission, viewed 10 May 2021, <www.industry.gov.au/sites/default/files/2019-03/australias-critical-minerals-strategy-2019.pdf>.

Duuring, P, Then, D and Morin-Ka, S 2021, Western Australian near-surface geochemistry: Geological Survey of Western Australia, digital data layers.

Mathieu, L 2018, Quantifying Hydrothermal Alteration: A Review of Methods: Geosciences, v. 8, no. 7, p. 245, doi:10.3390/geosciences8070245.

Recommended reference

Duuring, P and Morin-Ka, S, 2021, Lithogeochemical fertility indicators for manganese oxide mineralization in Western Australia: Geological Survey of Western Australia, digital data layers.

Sedimentary basins in Western Australia as potential repositories for critical minerals

by

P Duuring and S Morin-Ka

Abstract

This data layer shows the distribution of sedimentary basins in Western Australia.

Sedimentary basins can be important repositories for critical mineral resources such as manganese, germanium and indium in clastic- and carbonate-hosted sulfide and oxide deposits, and may also have been sources for the fluids responsible for such mineralization (e.g. Spinks et al., 2018).

Sedimentary basins are derived by querying the parent 1:500 000 State interpreted tectonic units of Western Australia digital map (Table 1). This tectonic units map is itself derived from the digital 1:500 000 State interpreted bedrock geology of Western Australia, 2016 (Martin, 2016) and offshore components adopted from the tectonic divisions in Geoscience Australia's Australian Geological Provinces GIS dataset, and adjusting polygons to seamlessly merge onshore and offshore tectonic elements. The nomenclature and hierarchy for the tectonic units are based on the Geological Survey of Western Australia's Explanatory Notes System (www.dmirs.wa.gov.au/ens).

Table 1. Query operation

Operation	Query
The 1:500 000 tectonic units of Western Australia layer is queried by selecting basins from the TECTSETTIN Field	TECTSETTIN = 'basin'

How to access

These data form part of the Critical minerals, 2021 Geological Exploration Package, available on a USB via the DMIRS eBookshop. The data can also be obtained from the Mineral Systems Atlas via GeoVIEW.WA (www.dmirs.wa.gov.au/mineralsystemsatlas), an online interactive mapping and knowledge system that facilitates the location and viewing of geological datasets particularly relevant to mineral deposits in Western Australia (Morin-Ka et al., 2019).

References

Martin, DMcB 2016, The geological map of Western Australia - past, present and future, *in* GSWA 2016 extended abstracts: promoting the prospectivity of Western Australia: Geological Survey of Western Australia, Record 2016/2, p. 1–3.

Morin-Ka, S, Duuring, P, Burley, L, Guilliamse, J and Beardsmore, TJ 2019, Mineral Systems Atlas – a dynamic approach to the delivery of mineral exploration data *in* GSWA 2019 extended abstracts: advancing the prospectivity of Western Australia: Geological Survey of Western Australia Record 2019/2, p. 9–12

Spinks, S, Thorne, R, Sperling, EA, White, AJR, Armstrong, JT, Brant, F, LeGras, M, Birchall, R and Munday, TJ 2018, Sedimentary Manganese as Precursors to the Supergene Manganese Deposits of the Collier Group; Capricorn Orogen, Western Australia: CSIRO, Perth, Australia, 36p.

Recommended reference

Duuring, P and Morin-Ka, S, 2021, Sedimentary basins in Western Australia as potential repositories for critical minerals: Geological Survey of Western Australia, digital data layers.

Western Australian near-surface geochemistry

by

P Duuring, D Then, D Howard and S Morin-Ka

Abstract

Eight GIS layers depict geochemical data for Western Australian soil, laterite, stream sediment, and outcrop or drillhole rock specimens, extracted from four primary databases maintained by the Geological Survey of Western Australia (GSWA): WACHEM, OZCHEM (WA subset), CRCLEME-laterite, and WAMEX.

WACHEM data were mostly collected by GSWA as part of regular geoscience programs. Most of the 49 123 samples analysed and included here are surface samples from Western Australia, but some are subsurface specimens from drillholes (sample locations are projected to the drillhole collar). Strict quality controls were in place for sampling, rock preparation, and laboratory analysis. The data have high fidelity.

OZCHEM data were collected by Geoscience Australia or its predecessors. Most of the 17 614 samples analysed and here included from Western Australia are surface samples, but some are subsurface specimens from drillholes (sample locations are projected to the drillhole collar). Strict quality controls were applied during sampling, rock preparation, and laboratory analysis. The data have high fidelity.

CRCLEME-laterite samples were collected as part of the 'Astro Yilgarn Regolith' collaborative research project conducted by CSIRO between 1997 and 2000 and sponsored by Astro Mining NL (Cornelius et al., 2005). This publicly available database includes multi-element analyses of 4441 regolith samples from the central Yilgarn Craton. Strict quality controls were applied during sampling, rock preparation, and laboratory analysis. The data have high fidelity.

WAMEX geochemical data are derived from exploration and mining activities in Western Australia and are provided to GSWA by companies as part of their statutory reporting obligations. The complete database includes at least half a billion single or multi-element analyses from a variety of sample media, including surface rock chips, stream sediments, soils, unconsolidated material from shallow drilling, and rock chip or core material from deeper drilling. GSWA applies some quality control measures at the time of data submission, but a proportion of the data are known to be problematic (e.g. errors in unit reporting, multiple field names for the same analyte, incorrect assignment of analyte), and GSWA is progressively identifying and correcting such issues. Only 'near-surface' WAMEX geochemistry and 'maximum grade in drillhole' (projected to surface collar location) are provided in this product release; complete deep drilling geochemistry is not included because of the size of that dataset, and the limitations associated with portraying three-dimensional drillhole data as a two-dimensional map layer.

As part of the Accelerated Geoscience Program, GSWA has also sought to add value to the WACHEM, OZCHEM, CRCLEME-laterite and WAMEX whole-rock geochemical datasets by merging them into a single, internally consistent, interrogable database. This has been done by initially 'harmonizing' the WAMEX geochemistry by extracting as much of the original analytical data as possible into a universal table layout that has unique field names for analytes (e.g. MnO_%) and consistent use of analyte concentration units. The WACHEM, OZCHEM and CRCLEME-laterite datasets were then merged into this universal table layout. Null values for analytes from each dataset have been assigned the numerical value '-9999', and obviously spurious values in WAMEX (those exceeding 100%, and probably indicating originally mis-assigned units) are identified by the value '-6666'. Detection limits were preserved using the '-DLvalue' convention. Finally, appropriate additional fields were added to the universal data table to permit capture of all analytes as element oxide or element

concentrations, and the 'missing' values calculated from the primary data, as required.

The Western Australian near-surface geochemistry GIS layers can be used for generating derivative element abundance and element ratio maps, which are useful for investigating rock and ore-forming geological processes.

How to access

These data form part of the Critical minerals, 2021 Geological Exploration Package, available on a USB via the DMIRS eBookshop.

References

Cornelius, AJ, Cornelius, M, Smith, RE and Shu, L 2005, Laterite geochemical database for the central Yilgarn Craton, Western Australia: Cooperative Research Centre for Landscape Environments and Mineral Exploration (CRC LEME), Open File Report 188, 8p.

Recommended reference

Duuring, P, Then, D, Howard, D and Morin-Ka, S, 2021, Western Australian near-surface geochemistry: Geological Survey of Western Australia, digital data layers.

Geochemical pathfinders for volcanogenic massive sulfide (VMS) mineralizing systems in Western Australia

by

JN Guilliamse and P Duuring

Abstract

This collection of GIS maps shows the distribution and abundance of selected elements or element ratios for rock, soil, stream, and laterite samples from Western Australia. These geochemical data are relevant for mineral exploration because they either directly identify base metal mineralization that may be associated with volcanogenic massive sulfide (VMS) deposits (e.g. Cu, Zn), or they may be considered proxies for hydrothermal fluid alteration associated with such mineralization.

The derivative GIS layers were created using a 'Statewide near-surface geochemistry' database (Duuring et al., 2021) compiled from the primary data collections of Geological Survey of Western Australia (GSWA) WACHEM and WAMEX databases (comprising surface rock chip, surface stream sediment, surface shallow drillhole, surface soil, and maximum grade in drillhole), Geoscience Australia (OZCHEM) and CRC-LEME (laterite geochemistry). A unique legend and colour scheme has been chosen for each geochemical layer to best highlight geochemical trends. Higher element abundance values are drawn over lower values to more clearly show gradients in abundance.

Users of the statewide database should exercise care when comparing element value ranges between different primary datasets. The WACHEM, OZCHEM, and CRC-LEME laterite data are considered to have high fidelity because strict quality controls have been exercised during sampling, sample preparation, laboratory analysis, and reporting. WAMEX geochemical data, however, have been collected by hundreds of companies during exploration and mining activities in Western Australia, and the quality of the data supplied to GSWA is more difficult to guarantee. GSWA applies some quality control measures at the time of data submission, but spurious results are known to be present
(e.g. errors in unit reporting, multiple field names for the same analyte, incorrect assignment of analytes). Samples in each primary dataset will also have been analysed for different suites of elements, using a variety of analytical approaches, at different laboratories. Element ratio maps have been created to normalize some of the systematic data variations arising from use of different laboratories and techniques.

Several element ratios have been calculated using the primary geochemical datasets to evaluate relative changes in element concentrations that are common in VMS mineralizing systems:

1. Cu/Al measures gains in copper vs less mobile aluminium. Copper is commonly elevated in VMS mineralizing systems.
2. Pb/Al measures gains in lead vs less mobile aluminium. Lead is commonly elevated in VMS mineralizing systems.
3. Zn/Al measures gains in zinc vs less mobile aluminium. Zinc is commonly elevated in VMS mineralizing systems.
4. In/Al measures gains in indium vs less mobile aluminium. Indium is commonly elevated in VMS mineralizing systems.

Maps have also been developed to indicate possible hydrothermal alteration associated with VMS mineralization in Western Australia, using several well-established alteration indices based on whole-rock geochemistry:

1. Ishikawa alteration index (AI = 100 x (K_2O + MgO)/(K_2O + MgO + Na_2O + CaO) after Ishikawa et al., 1976): The AI is considered a proxy for the intensity of chlorite and sericite alteration replacing sodic plagioclase and volcanic glass in volcanic rocks. A value of 0 represents an unaltered sample, while a value of 100 indicates a highly altered sample.
2. Chlorite–carbonate–pyrite index (CCPI = 100 x (Fe_2O_{3T*} + MgO)/(Fe_2O_{3T*} + MgO + Na_2O + CaO after Large et al., 2001). The CCPI is considered a proxy for the intensity of chlorite alteration replacing albite, K-feldspar, and sericite, as well as measuring carbonate alteration and enrichment in pyrite, hematite, and magnetite. A value of 0 represents an unaltered sample, while a value of 100 indicates a highly altered sample. Fe_2O_{3T*} = FeO+Fe_2O_3
3. ACNK alteration index (Al_2O_3/(CaO+Na_2O+K_2O) after Hodges and Manojlovic, 1993): the ratio of Al vs Ca+Na+K is a measure of feldspar mineral destruction due to alteration. An index value of greater than 1.6 potentially indicates changes in rock composition associated with hydrothermal alteration (Grunsky, 2013).

All alteration indices will be influenced by precursor rock chemistry and the effects of overprinting by later fluid activity (such as during weathering), and their interpretation requires consideration of such factors. The use of methods such as normalization and mass balance calculations is recommended (cf. Mathieu, 2018). Alteration in sedimentary rocks can be particularly difficult to evaluate because of their potentially large variability in precursor major and trace element compositions. Alteration indices have therefore only been calculated for relatively fresh (little weathered) Western Australian volcanic (including volcaniclastic) rocks and their metamorphic equivalents, from the WACHEM and OZCHEM subsets of the geochemistry database, using the following rock type query criteria.

Table 1. Query operation for geochemical alteration indices

Operation	Query
WACHEM dataset is queried for felsic, intermediate, and mafic volcanic rocks and their Al_2O_3, CaO, Fe_2O_{3T*}, MgO, Na_2O, and K_2O values are used to calculate the ACNK, CCPI, and Ishikawa alteration index values	LOWER (LITHNAME) LIKE LOWER ('%amphibolite derived from volcanic rock%') OR LOWER (LITHNAME) LIKE LOWER ('%andesite%') OR LOWER (LITHNAME) LIKE LOWER ('%basalt'%') OR LOWER (LITHNAME) LIKE LOWER ('%basaltic andesite'%) OR LOWER (LITHNAME) LIKE LOWER ('%dacite%') OR LOWER (LITHNAME) LIKE LOWER ('%dolerite%') OR LOWER (LITHNAME) LIKE LOWER ('%felsic gneiss derived from volcanic rock%') OR LOWER (LITHNAME) LIKE LOWER ('%felsic schist derived from volcanic rock%') OR LOWER (LITHNAME) LIKE LOWER ('%felsic volcanic rock%') OR LOWER (LITHNAME) LIKE LOWER ('%felsic volcaniclastic breccia%') OR LOWER (LITHNAME) LIKE LOWER ('%felsic volcaniclastic breccia-sandstone%') OR LOWER (LITHNAME) LIKE LOWER ('%felsic volcaniclastic conglomerate%') OR LOWER (LITHNAME) LIKE LOWER ('%felsic volcaniclastic granule/pebble breccia%') OR LOWER (LITHNAME) LIKE LOWER ('%felsic volcaniclastic rock%') OR LOWER (LITHNAME) LIKE LOWER ('%felsic volcaniclastic sandstone%') OR LOWER (LITHNAME) LIKE LOWER ('%felsic volcaniclastic sandstone-siltstone%') OR LOWER (LITHNAME) LIKE LOWER ('%felsic volcaniclastic siltstone/mudstone%') OR LOWER (LITHNAME) LIKE LOWER ('%mafic gneiss derived from volcanic rock%') OR LOWER (LITHNAME) LIKE LOWER ('%mafic granofels/hornfels derived from volcanic rock%') OR

	LOWER (LITHNAME) LIKE LOWER ('%mafic schist derived from volcanic rock%') OR LOWER (LITHNAME) LIKE LOWER ('%mafic volcanic rock%') OR LOWER (LITHNAME) LIKE LOWER ('%mafic volcaniclastic breccia%') OR LOWER (LITHNAME) LIKE LOWER ('%mafic volcaniclastic breccia-sandstone%') OR LOWER (LITHNAME) LIKE LOWER ('%mafic volcaniclastic conglomerate%') OR LOWER (LITHNAME) LIKE LOWER ('%mafic volcaniclastic rock%') OR LOWER (LITHNAME) LIKE LOWER ('%mafic volcaniclastic sandstone%') OR LOWER (LITHNAME) LIKE LOWER ('%mafic volcaniclastic sandstone-siltstone%') OR LOWER (LITHNAME) LIKE LOWER ('%mafic volcaniclastic siltstone/mudstone%') OR LOWER (LITHNAME) LIKE LOWER ('%meta-andesite%') OR LOWER (LITHNAME) LIKE LOWER ('%metabasalt%') OR LOWER (LITHNAME) LIKE LOWER ('%metabasaltic andesite%') OR LOWER (LITHNAME) LIKE LOWER ('%metadacite%') OR LOWER (LITHNAME) LIKE LOWER ('%metadolerite%') OR LOWER (LITHNAME) LIKE LOWER ('%metafelsic volcanic rock%') OR LOWER (LITHNAME) LIKE LOWER ('%metamafic volcanic rock%') OR LOWER (LITHNAME) LIKE LOWER ('%metarhyodacite%') OR LOWER (LITHNAME) LIKE LOWER ('%metarhyolite%') OR LOWER (LITHNAME) LIKE LOWER ('%metavolcanic and metavolcaniclastic rock%') OR LOWER (LITHNAME) LIKE LOWER ('%mylonitized metafelsic volcanic rock%') OR LOWER (LITHNAME) LIKE LOWER ('%rhyodacite%') OR LOWER (LITHNAME) LIKE LOWER ('%rhyolite%') OR LOWER (LITHNAME) LIKE LOWER ('%volcanic rock%')
OzCHEM dataset is queried for felsic, intermediate, and mafic volcanic rocks and their Al_2O_3, CaO, Fe_2O_{3T*}, MgO, Na_2O, and K_2O values are used to calculate the ACNK, CCPI, and Ishikawa alteration index values	LOWER (LITHNAME) LIKE LOWER ('%andesite%') OR LOWER (LITHNAME) LIKE LOWER ('%ash tuff%') OR LOWER (LITHNAME) LIKE LOWER ('%basalt%') OR LOWER (LITHNAME) LIKE LOWER ('%basaltic andesite%') OR LOWER (LITHNAME) LIKE LOWER ('%breccia, volcanic%') OR LOWER (LITHNAME) LIKE LOWER ('%dacite%') OR LOWER (LITHNAME) LIKE LOWER ('%dolerite%') OR LOWER (LITHNAME) LIKE LOWER ('%felsic volcanic%') OR LOWER (LITHNAME) LIKE LOWER ('%hyaloclastite%') OR LOWER (LITHNAME) LIKE LOWER ('%ignimbrite%') OR LOWER (LITHNAME) LIKE LOWER ('%intermediate volcanic%') OR LOWER (LITHNAME) LIKE LOWER ('%lapilli tuff%') OR LOWER (LITHNAME) LIKE LOWER ('%latite%') OR LOWER (LITHNAME) LIKE LOWER ('%phonolite%') OR LOWER (LITHNAME) LIKE LOWER ('%rhyodacite%') OR LOWER (LITHNAME) LIKE LOWER ('%rhyolite%') OR LOWER (LITHNAME) LIKE LOWER ('%trachydacite%') OR LOWER (LITHNAME) LIKE LOWER ('%trachyte%') OR LOWER (LITHNAME) LIKE LOWER ('%tuff%') OR LOWER (LITHNAME) LIKE LOWER ('%volcanic rock%') OR LOWER (LITHNAME) LIKE LOWER ('%volcaniclastic rock%')

Particular compositions of felsic volcanic and subvolcanic rocks are considered empirically to be more fertile for VMS mineralization. Lesher et al. (1986) discriminate this VMS fertility using a plot of Zr/Y against Y to define four fields — FI, FII, FIIIa, and FIIIb. Hart et al. (2004) alternatively compare La/Yb against Yb to define five fields — FI, FII, FIIIa, FIIIb, and FIV. In both schemes, felsic rocks falling in the FI field are considered non-prospective, FII-type rocks are also typically barren, but may rarely host VMS deposits, and felsic rocks falling in the FIII and FIV fields are common hosts for VMS mineralization, with the largest deposits typically hosted by FIII-type rocks.

These distinct compositional variations are interpreted to relate to the degree of partial melting of the crust at progressively shallower depths within a rift environment, and varying trace-element partitioning between melts and different coexisting residual mineral phases. Hence, FI magmas form in the deep crust in the presence of garnet residua, FII magmas are mid-crustal melts associated with amphibole–plagioclase bearing residua, and FIII and FIV magmas form at shallowest crustal levels where plagioclase is present, and amphibole and garnet absent (Hart et al., 2004; Guilliamse, 2013). Intrusions at progressively shallower levels in the crust are more conducive to VMS formation because they are more able to provide heat and energy to drive near-surface hydrothermal convection cells.

VMS fertility maps have been generated using the query criteria below to identify relatively fresh (little weathered) Western Australian felsic volcanic rocks and their metamorphic equivalents, from the WACHEM and OZCHEM subsets of the geochemistry database. Volcaniclastic rocks were specifically excluded because their distance from source (hence potential VMS deposit site) could not be determined. Field values for each data point were determined by creating discrimination diagrams in ioGAS. The data was then exported as a excel table with the relevant field added, before being imported into ArcMap and converted into a shapefile.

Table 2. Query operation for felsic fertility discrimination plots

Operation	Query
WACHEM dataset is queried for felsic volcanic rocks and their La, Y, Yb, and Zr values are used to calculate felsic fertility plots	LOWER (LITHNAME) LIKE LOWER ('%dacite%') OR LOWER (LITHNAME) LIKE LOWER ('%felsic schist derived from volcanic rock%') OR LOWER (LITHNAME) LIKE LOWER ('%felsic volcanic rock%') OR LOWER (LITHNAME) LIKE LOWER ('%metadacite%') OR LOWER (LITHNAME) LIKE LOWER ('%metafelsic rock%') OR LOWER (LITHNAME) LIKE LOWER ('%metafelsic volcanic rock%') OR LOWER (LITHNAME) LIKE LOWER ('%metarhyodacite%') OR LOWER (LITHNAME) LIKE LOWER ('%metarhyolite%') OR LOWER (LITHNAME) LIKE LOWER ('%mylonitized metafelsic volcanic rock%') OR LOWER (LITHNAME) LIKE LOWER ('%rhyodacite%') OR LOWER (LITHNAME) LIKE LOWER ('%rhyolite%') OR
OzCHEM dataset is queried for felsic volcanic rocks and their La, Y, Yb, and Zr values are used to calculate felsic fertility plots	LOWER (LITHNAME) LIKE LOWER ('%ash tuff%') OR LOWER (LITHNAME) LIKE LOWER ('%dacite%') OR LOWER (LITHNAME) LIKE LOWER ('%felsic volcanic%') OR LOWER (LITHNAME) LIKE LOWER ('%ignimbrite%') OR LOWER (LITHNAME) LIKE LOWER ('%lapilli tuff%') OR LOWER (LITHNAME) LIKE LOWER ('%rhyodacite%') OR LOWER (LITHNAME) LIKE LOWER ('%rhyolite%') OR LOWER (LITHNAME) LIKE LOWER ('%tuff%')

How to access

These data form part of the Critical minerals, 2021 Geological Exploration Package, available on a USB via the DMIRS eBookshop.

References

Duuring, P, Then, D and Morin-Ka, S 2021, Western Australian near-surface geochemistry: Geological Survey of Western Australia, digital data layers.

Grunsky, EC 2013, Predicting Archaean volcanogenic massive sulphide deposit potential from lithogeochemistry: application to the Abitibi Greenstone Belt: Geochemistry: Exploration, Environment, Analysis, v. 13, p. 317–336.

Guilliamse, JN 2013, Investigation into the potential for volcanic-associated massive sulfide mineralization at Weld Range by using Golden Grove as a comparative model: Geological Survey of Western Australia, Report 141, 67p

Hart, TR, Gibson, HL and Lesher, CM 2004, Trace element geochemistry and petrogenesis of felsic volcanic rocks associated with volcanogenic massive Cu-Zn-Pb sulfide deposits: Economic Geology, v. 99, no. 5, p. 1003–1013.

Hodges, D and Manojlovic, P 1993, Application of lithogeochemistry to exploration for deep VMS deposits in high grade metamorphic rocks, Snow Lake, Manitoba: Journal of Geochemical Exploration, v. 48, no. 2, p. 201–224, doi:10.1016/0375-6742(93)90005-7.

Ishikawa, Y, Sawaguchi, T, Iwaya, S and Horiuchi, M 1976, Delineation of prospecting targets for Kuroko deposits based on modes of volcanism of underlying dacite and alteration haloes: Mining Geology, v. 26, p. 105–117.

Large, RR, Gemmell, JB, Paulick, H and Huston, DL 2001, The alteration box plot: A simple approach to understanding the relationship between alteration mineralogy and lithogeochemistry associated with volcanic-hosted massive sulfide deposits: Economic Geology, v. 96, no. 5, p. 957–971.

Lesher, CM, Goodwin, AM, Campbell, IH and Gorton, MP 1986, Trace-element geochemistry of ore-associated and barren, felsic metavolcanic rocks in the Superior Province, Canada: Canadian Journal of Earth Sciences, v. 23, no. 2, p. 222–237.

Mathieu, L 2018, Quantifying Hydrothermal Alteration: A Review of Methods: Geosciences, v. 8, no. 7, p. 245, doi:10.3390/geosciences8070245.

Recommended reference

Guilliamse, JN and Duuring, P, 2021, Geochemical pathfinders for volcanogenic massive sulfide (VMS) mineralizing systems in Western Australia: Geological Survey of Western Australia, digital data layers.

Occurrences of minerals diagnostic of mineralization or associated alteration prospective for selected critical minerals

by

JN Guilliamse, P Duuring and TR Farrell

Abstract

These map layers show the distributions of minerals in Western Australia that may be indicative of mineralization or associated alteration (or their metamorphosed equivalents) related to critical (and base metal) mineral systems. The data have been extracted from observations recorded in the Geological Survey of Western Australia WAROX database (Riganti et al., 2015), using the queries in Table 1. Each map layer shows a specific mineral.

Some minerals may also indicate fertility for other mineral systems, and the maps should also be considered in conjunction with complementary maps showing occurrences of minerals diagnostic of critical mineral-prospective rock types (Duuring et al., 2021).

Table 1. Query operation

Operation	Query
WAROX data are queried to select particular sulfide minerals from any field in the WAROX database	Any field = 'arsenopyrite' OR Any field = 'bornite' OR Any field = 'chalcocite' OR Any field = 'chalcopyrite' OR Any field = 'cinnabar' OR Any field = 'galena' OR Any field = 'molybdenite' OR Any field = 'pentlandite' OR Any field = 'pyrite' OR Any field = 'pyrrhotite' OR Any field = 'sphalerite' OR Any field = 'stibnite' OR Any field = 'sulfide' OR Any field = 'sulphide' OR Any field = 'tetrahedrite'
For the 'non-sulfide ore minerals' layers, WAROX data are queried to select specific minerals from any field in the WAROX database	Any field = 'ankerite' OR Any field = 'atacamite' OR Any field = 'azurite' OR Any field = 'barite' OR Any field = 'cerrusite' OR Any field = 'cuprite' OR Any field = 'goethite' OR Any field = 'graphite' OR Any field = 'hematite' OR Any field = 'kaolinite' OR

	Any field = 'magnetite' OR Any field = 'malachite' OR Any field = 'manganese' OR Any field = 'Mn oxide' OR Any field = 'montmorillonite' OR Any field = 'pyrolusite' OR Any field = 'pyromorphite' OR Any field = 'visible gold' OR Any field = 'scorodite' OR Any field = 'siderite' OR Any field = 'smectite' OR Any field = 'telluride'
For the 'rare element pegmatite' layers, WAROX data are queried to select specific minerals from any field in the WAROX database	Any field = 'beryl' OR Any field = 'cassiterite' OR Any field = 'columbite' OR Any field = 'lepidolite' OR Any field = 'scheelite' OR Any field = 'spodumene' OR Any field = 'tantalite' OR Any field = 'wolframite'
'Sericitic alteration - Low grade metamorphism' occurrence layers are extracted by querying for selected alteration minerals from any field in the WAROX database	Any field = 'illite' OR Any field = 'quartz' OR Any field = 'whitemica'
'Sericitic alteration - High grade metamorphism' occurrence layers are extracted by querying for selected metamorphic minerals from any field in the WAROX database	Any field = 'biotite' OR Any field = 'cordierite' OR Any field = 'garnet' OR Any field = 'K-feldspar' OR Any field = 'kyanite' OR Any field = 'quartz' OR Any field = 'sillimanite'
'Chloritic alteration - Low grade metamorphism' occurrence layer is extracted by querying for this mineral from any field in the WAROX database	Any field = 'chlorite'
'Chloritic alteration - High grade metamorphism' occurrence layers are extracted by querying for selected metamorphic minerals from any field in the WAROX database	Any field = 'anthophyllite' OR Any field = 'cordierite' OR Any field = 'diopside' Any field = 'garnet' Any field = 'gedrite' OR Any field = 'kyanite' OR Any field = 'orthopyroxene' OR Any field = 'phlogopite' OR Any field = 'prehnite' Any field = 'sillimanite' Any field = 'staurolite' OR Any field = 'wollastonite'

How to access

These data form part of the Critical minerals, 2021 Geological Exploration Package, available on a USB via the DMIRS eBookshop.

References

Duuring, P, Guilliamse, JN and Morin-Ka, S 2021, Distributions of minerals in Western Australia diagnostic of rock types prospective for selected critical minerals (Li, Ge, In, Ni, PGE, V), derived from the GSWA WAROX field observations database: Geological Survey of Western Australia, digital data layers.

Riganti, A, Farrell, TR, Ellis, MJ, Irimies, F, Strickland, CD, Martin, SK and Wallace, DJ, 2015, 125 years of legacy data at the Geological Survey of Western Australia: Capture ad delivery: GeoResJ, v. 6, p. 175–194.

Recommended reference

Guilliamse, JN, Duuring, P and Farrell, TR 2021, Occurrences of minerals diagnostic of mineralization or associated alteration prospective for selected critical minerals: Geological Survey of Western Australia, digital data layers.

Hydrogeochemical data from wells and bores in Western Australia

by

S Kenworthy and TJ Beardsmore

Abstract

Groundwaters in Western Australia can contain economic concentrations of commodities such as potassium, which is a critical mineral used in the production of sulfate of potash for the agricultural industry (e.g. Mernagh et al., 2013). Groundwater geochemistry may also provide vectors to a variety of bedrock mineralization styles (Noble et al., 2011). A knowledge of dissolved mineral loads in groundwaters is therefore crucial in assessing mineral prospectivity.

The Geological Survey of Western Australia (GSWA) provides a 'seamless' database of Western Australian groundwater hydrogeochemistry for a host of cations and anions and other attributes such as pH and electrical conductivity. This database has been derived by harmonizing three separate datasets compiled by the CSIRO for water samples collected from wells and bores throughout a significant portion of the State (Gray and Bardwell, 2016; Gray, 2016; Gray et al 2016). These primary datasets have been selected over other possible sources (for instance GSWA's WAMEX Exploration geochemistry, WA Department of Water and Environmental Regulation, Bureau of Meteorology) because they offer the widest geographic spread, the greatest variety of analytes, and the best internal consistency of analytical suite and technique (even though CSIRO used several commercial and government laboratories that applied several analytical approaches). The merged product provides a robust and accessible hydrogeochemical dataset for Western Australia that includes a csv file tabulation of all data and a suite of 31 GIS layers depicting the concentrations in groundwaters for selected analytes, including a variety of critical minerals.

How to access

The Hydrogeochemistry data from wells and bores in Western Australia data layer can be acquired as part of the Critical Minerals, 2021 Geological Exploration Package, which is provided on USB via the DMIRS eBookshop and is also available as a free download from the Data and Software Centre.

References

Gray, D 2016, Hydrogeochemistry Dataset from Stygofauna Sampling, Pilbara Region, Western Australia, Data Release v1: CSIRO, Data Collection, doi:10.4225/08/575CDF639A59A.

Gray, DJ and Bardwell, N 2016, Hydrogeochemistry of Western Australia: Data Release, Accompanying Notes: CSIRO, Australia, EP156404, 37p.

Gray, D, Noble RRP, Reid, N, Sutton, GJ and Pirlo, MC 2016, Regional Scale Hydrogeochemical Mapping of the Northern Yilgarn Craton, Western Australia: A new Technology for Exploration in Arid Australia: Geochemistry: Exploration, Environment, Analysis, 16, p. 100–115.

Mernagh, TP, Bastrakov, EN, Clarke, JDA, de Caritat, P, English, PM, Howard, FJF, Jaireth, S, Magee, JW, McPherson, AA, Roach, IC, Schroder, IF, Thomas, M and Wilford JR 2013, A review of Australian salt lakes and assessment of their potential for strategic resources: Geoscience Australia, Record 2013/39, 243p.

Noble, RRP, Gray, DJ and Gill, AJ 2011, Field guide for mineral exploration using hydrogeochemical analysis, CSIRO, 56p.

Recommended reference

Kenworthy, S and Beardsmore, TJ 2021, Hydrogeochemical data from wells and bores in Western Australia: Geological Survey of Western Australia, digital data layer.

Hydrogeological features of Western Australia — drainage basins, lakes and paleovalleys

by

S Kenworthy and TJ Beardsmore

Abstract

Groundwaters in Western Australia can contain economic concentrations of commodities such as potassium, which is a critical mineral used in the production of sulfate of potash for the agricultural industry (e.g. Mernagh et al., 2013). Groundwater geochemistry may also be useful as a vector to a variety of bedrock mineralization styles (Noble et al., 2011). Using groundwaters to assess 'mineral prospectivity' requires an understanding of their hydrogeological setting, including features that influence groundwater movement and storage and its interactions with chemical elements in rocks and soils, such as topographic drainage basins ('catchments'), surficial lakes, and paleovalley aquifers. The Geological Survey of Western Australia (GSWA) provides three statewide maps depicting such features, abstracted from existing national public sources and with simplified data fields.

The topographic drainage map for Western Australia has been sourced from the Western Australian Department of Water and Environmental Regulation. The map incorporates the national Division/Basin/Subcatchment hierarchy defined and managed by the Australia Water Resources Council.

Lakes are defined as naturally occurring bodies that are perennially to only periodically filled with mainly static water, surrounded by land. The map of their current distribution in Western Australia has been abstracted from Geoscience Australia's GEODATA TOPO 1:250 000 Series 3 dataset (Catalogue Number 64058).

Paleovalleys and associated playas are dynamic elements of the modern hydrological regime. They initially formed during the Paleocene–Eocene epochs as widespread perennial river and lake systems, when Australia lay well south of its current position and was largely vegetated with warm to cool temperate rainforest. As Australia moved northwards and its climate warmed and dried, the perennial river and lake systems became ephemeral and then dry, and the valleys substantially filled with sediment, leaving the current disaggregated chains of salt lakes and playas along the former valleys. The map of paleovalley distribution has been sourced from Geoscience Australia (Bell et al., 2012).

How to access

The Hydrogeological features of Western Australia data layer can be acquired as part of the Critical minerals, 2021 Geological Exploration Package, which is provided on USB via the DMIRS eBookshop and is also available as a free download from the Data and Software Centre.

References

Bell, JG, Kilgour, PL, English, PM, Woodgate, MF and Lewis, SJ 2012, WASANT Palaeovalley Map - Distribution of Palaeovalleys in Arid and Semi-arid WA-SA-NT, GIS thematic map: Geoscience Australia, Canberra.

Mernagh, TP, Bastrakov, EN, Clarke, JDA, de Caritat, P, English, PM, Howard, FJF, Jaireth, S, Magee, JW, McPherson, AA, Roach, IC, Schroder, IF, Thomas, M and Wilford JR 2013, A review of Australian salt lakes and assessment of their potential for strategic resources: Geoscience Australia, Record 2013/39, 243p.

Noble, RRP, Gray, DJ and Gill, AJ 2011, Field guide for mineral exploration using hydrogeochemical analysis, CSIRO, 56p.

Recommended reference

Kenworthy, S and Beardsmore TJ 2021, Hydrogeological features of Western Australia drainage basins, lakes and paleochannels: Geological Survey of Western Australia, digital data layer.

Hydrogeological features of Western Australia — mean annual rainfall, evaporation and evapotranspiration

by

S Kenworthy and TJ Beardsmore

Abstract

Groundwaters in Western Australia can contain economic concentrations of commodities such as potassium, which is a critical mineral used in the production of potash of sulfate for the agricultural industry (e.g. Mernagh et al., 2013). Groundwater geochemistry may also be useful as a vector to a variety of bedrock mineralization styles (Noble et al., 2011). The current climate regime affects the flux of water and dissolved material in groundwater systems. Rainfall adds water to the ground, and evaporation and evapotranspiration extract it, and the relative influences of these processes determine whether minerals dissolved in groundwater will become diluted or concentrated.

The Geological Survey of Western Australia (GSWA) provides three statewide maps depicting rainfall, evaporation and evapotranspiration across Western Australia. These maps use publicly available data from the Australian Bureau of Meteorology (BoM), subsetted to Western Australia and regridded to 0.05 degrees for consistency.

Rainfall and evaporation maps show gridded average annuals in millimetres over the periods 1981–2010 and 1975–2005, respectively. Data were collected by the BoM at a network of weather stations across Australia, and from Class A pans for evaporation. The evapotranspiration map shows gridded mean annual areal actual values calculated by the BoM using temperature, vapour pressure and solar global exposure data from the period 1961 to 1990. It is the evapotranspiration that actually takes place, under the condition of existing water supply, from an area sufficiently large that the effects of any upwind boundary transitions are negligible and local variations can be integrated to an areal average.

How to access

The Hydrogeological features of Western Australia data layer can be acquired as part of the Critical minerals, 2021 Geological Exploration Package, which is provided on a USB via the DMRIS eBookshop and is also available as a free download from the Data and Software Centre.

References

Mernagh, TP, Bastrakov, EN, Clarke, JDA, de Caritat, P, English, PM, Howard, FJF, Jaireth, S, Magee, JW, McPherson, AA, Roach, IC, Schroder, IF, Thomas, M and Wilford JR 2013, A review of Australian salt lakes and assessment of their potential for strategic resources: Geoscience Australia, Record 2013/39, 243p.

Noble, RRP, Gray, DJ and Gill, AJ 2011, Field guide for mineral exploration using hydrogeochemical analysis, CSIRO, 56p.

Recommended reference

Kenworthy, S and Beardsmore, TJ 2021, Hydrogeological features of Western Australia — mean annual rainfall, evaporation and evapotranspiration: Geological Survey of Western Australia, digital data layer.

GeologyMERGED — a best-resolution interpreted bedrock geology map of Western Australia

by

S Morin-Ka

Abstract

GeologyMERGED is an interpreted bedrock geology map of Western Australia that was created by combining 1:100 000-scale and statewide 1:500 000-scale interpreted bedrock geology data (Martin et al., 2016). It was achieved by cutting the 1:500 000 layer with the polygons from the 1:100 000 layer and merging the two. The final layer is coloured using the symbology from the original layers. An additional field, SOURCE, records the source data as either '500k' or '100k'. The aim of the GeologyMERGED layer was to create a single statewide interpreted bedrock geology map that incorporates geological data at the best available resolution.

How to access

The GeologyMERGED digital data form part of the Critical minerals, 2021 Geological Exploration Package, which is available via the DMIRS eBookshop, and are also available to freely download from the Data and Software Centre. The data can also be obtained via the Mineral Systems Atlas, an online interactive mapping and knowledge system that facilitates the location and viewing of geological datasets particularly relevant to mineral deposits in Western Australia (Morin-Ka et al., 2019).

References

Martin, DMcB, Hocking, RM, Riganti, A and Tyler, IM 2016, Geological map of Western Australia, 14th edition – Explanatory Notes, Geological Survey of Western Australia, Record 2015/14, 16p.

Morin-Ka, S, Duuring, P, Burley, L, Guilliamse, J and Beardsmore, TJ 2019, Mineral Systems Atlas — a dynamic approach to the delivery of mineral exploration data, *in* GSWA 2019 extended abstracts: advancing the prospectivity of Western Australia: Geological Survey of Western Australia, Record 2019/2, p. 9–12.

Recommended reference

Morin-Ka, S, 2021, GeologyMERGED — a best-resolution interpreted bedrock geology map of Western Australia: Geological Survey of Western Australia, digital data layer.

Outcrop geology map of Western Australia, 2020

by

S Morin-Ka

Abstract

The Outcrop geology map of Western Australia shows the distribution and broad lithology of fresh bedrock outcrops in Western Australia. It has been created by extracting all polygons that correspond to fresh rock outcrops (Table 1) from the Geological Survey of Western Australia 1:500 000 State regolith geology map (Jakica et al., 2020), and attributing and symbolizing these polygons according to the interpreted bedrock geology that they intersect with on the GeologyMERGED (1:100 000 and 1:500 000 scales) interpreted bedrock geology map of Western Australia (Martin et al., 2016, Morin-Ka, 2021).

Table 1. Query operation

Regolith filter	*Code*
Exposed geology	CODE LIKE '_X-%'

How to access

These data form part of the Critical minerals, 2021 Geological Exploration Package, available via the DMIRS eBookshop.

References

Jakica, S, de Souza Kovacs, N, Hogen-Esch, J and Granado, IMT 2020, 1:500 000 State regolith geology of Western Australia — compilation methodologies: Geological Survey of Western Australia, Record 2020/10, 22p.

Martin, DMcB, Hocking, RM, Riganti, A and Tyler, IM 2016, Geological map of Western Australia, 14th edition – Explanatory Notes, Geological Survey of Western Australia, Record 2015/14, 16p.

Morin-Ka, S, 2021, GeologyMERGED – a best resolution interpreted bedrock geology map of Western Australia: Geological Survey of Western Australia; digital data layer.

Recommended reference

Morin-Ka, S 2021, Outcrop geology map of Western Australia, 2020: Geological Survey of Western Australia; digital data layer.

Mineralization endowment and style proxies for selected critical mineral occurrences in Western Australia

by

S Morin-Ka, P Duuring and TJ Beardsmore

Abstract

The locations of known in situ mineral commodities provide an important indicator of the prospectivity of a particular region for further discoveries of those commodities. Morin-Ka et al. (2021) describe a collection of maps derived by querying the Geological Survey of Western Australia (GSWA) Mines and mineral deposits database (MINEDEX) by SITE_COMMODITY, to show the known locations of important minerals in Western Australia, including a selection of critical minerals. Each site is categorized according to whether it is a mine, deposit, prospect, occurrence or 'unclassified' (as defined by GSWA; Table 1), and indicates only that a particular commodity is present. There is no information on mineral endowment — nor on the mineral deposit style. The commodity depicted may be just a minor component in a multi-commodity deposit.

Proxies for relative commodity endowment and mineral deposit type can be gleaned by querying MINEDEX for sites where the commodity of interest is listed in SITE_COMMODITY, and categorizing these sites according to the corresponding TARGET_COMMODITY_GROUP (sought-after minerals) or higher-level COMMODITY_GROUP (defined by typical commodity end use). A commodity that is listed as a SITE_COMMODITY is likely to be a significant component of the mineralization if it is also included in the TARGET_COMMODITY_GROUP (e.g. Table 2) name or is a defined component of the COMMODITY_GROUP (Table 3). If it does not appear in TARGET_COMMODITY_GROUP or COMMODITY_GROUP, it is most likely to be only a minor or trace component, or it is expected to be present but its abundance is untested. The TARGET_COMMODITY_GROUP also proxies for mineralization style, as particular commodity associations typically occur in particular mineral deposit types — for instance COPPER-LEAD-ZINC in volcanogenic massive sulfide or carbonate-hosted deposits, or TIN-TANTALUM-LITHIUM in granitic pegmatite-hosted (or associated alluvial) deposits.

Examples of such maps have been created for recorded mines, deposits, prospects and occurrences of the critical minerals manganese, lithium and vanadium. Manganese and lithium sites are categorized by TARGET_COMMODITY_GROUP (Table 2), and vanadium sites by COMMODITY_GROUP (Table 3).

How to access

These data form part of the Critical minerals, 2021 Geological Exploration Package, which is available via the DMIRS eBookshop, and are also available to freely download from the Data and Software Centre. The Selected (critical mineral) mineralization sites digital layers (Morin-Ka et al., 2021) and the MINEDEX database can be accessed via GeoVIEW.WA.

Table 1. Definitions of mineralization site types

Site type	*Definition*
Mine	A deposit that is being mined, was previously mined, or is proposed to be mined
Deposit	A mineral occurrence that is not a mine, but which has probable economic value and has an established resource
Prospect	A mineral occurrence that is not a mine or deposit, where (i) economic grades have been intersected over a significant width and strike length but for which there is not yet a resource; or (ii) there is a working or exploration site that has subeconomic mineral occurrences, but there is no recorded production
Occurrence	A mineral occurrence that is not a mine, deposit or prospect, where a potentially economic mineral has been identified in outcrop, or rock chip or drilling assay results exceed an agreed concentration and size
Unclassified	A mineralization site for which the specified commodity is not reflected in the TARGET_COMMODITY_GROUP, hence there is no confirmation of its presence or abundance, and the SITE_TYPE_DESCRIPTION cannot be applied

Table 2. Target commodity groups relevant for manganese and lithium mineralization sites

TARGET_COMMODITY_GROUP	*Description*
MANGANESE ORE	A mineralization site where Mn is the dominant commodity
IRON ORE	A mineralization site where Fe ore is the dominant commodity, Mn is a relatively minor component
COPPER-LEAD-ZINC	A mineralization site where Cu, Pb and Zn are the dominant commodities, Mn is a relatively minor component
NICKEL	A mineralization site where Ni is the dominant commodity, Mn is a relatively minor component
GOLD	A mineralization site where Au is the dominant commodity, Mn is a relatively minor component
TIN-TANTALUM-LITHIUM	A mineralization site where Li is a major commodity

Table 3. Commodity groups that contain metal commodities, as defined for use in MINEDEX. Manganese, vanadium and lithium are highlighted

COMMODITY_GROUP	*Defined constituent metal commodities*
Steel alloy metal	Co, Cr, **Mn**, Mo, Nb, Ni, Ti, **V**, W
Specialty metal	Bi, Cs, **Li**, Mg, Nb, rare earth elements (REE), Rb, Sc, Sn, Ta, Zr
Base metal	As, Cu, Pb, Sb, Zn
Iron	Fe
Energy	Coal, lignite, Th, U
Precious mineral	Au, Ag, platinum group elements (PGE; Pd, Pt, Rh)

References

Morin-Ka, S, Ormsby, W and Beardsmore, TJ 2021, Selected mineralization sites of Western Australia: Geological Survey of Western Australia; digital dataset, <www.dmirs.wa.gov.au/geoview>.

Recommended reference

Morin-Ka, S, Duuring, P and Beardsmore, TJ 2021, Mineralization style proxies for selected critical mineral occurrences in Western Australia: Geological Survey of Western Australia, digital dataset.

AGP Accelerated Geoscience Program

Energy systems including petroleum, geothermal, and carbon capture and storage

Composite well logs from petroleum wells, Phanerozoic and Neoproterozoic basins of Western Australia

by

DM Brooks and F Irimies

Abstract

The Energy Systems Atlas is a collection of new geological map layers designed to help explorers identify each of the essential elements and processes of a petroleum system: source, reservoir, seal, burial, maturation, stratigraphic framework, structure, trap formation and migration. To help assess well operational information, stratigraphy and lithology, composite well logs from petroleum wells within Western Australia have been compiled from data submitted to the Geological Survey of Western Australia (GSWA). These composite well logs are useful for examining a summary of well operations such as casing points, depths of formation tests, location of sidewall cores, full-hole cores, wireline logs, interpreted lithology and stratigraphy. The composite well logs have been compiled from Well Completion Reports covering the majority of Western Australian sedimentary basins. New composite well logs will be added as they become open file.

The formations and depth intervals of each composite well log and a description of the data is given in the attribute tables in the Energy Systems Atlas. Unless otherwise stated the depths are given as metres measured depth.

How to access

The Energy Systems Atlas is best accessed using the Western Australian Petroleum and Geothermal Information Management System (WAPIMS). This online interactive mapping system allows data to be viewed and searched together with other datasets. The Energy Systems Atlas composite well logs are also available as a data package on request from WAPIMS/requests form.

Recommended reference

Brooks, DM and Irimies, F 2021, Composite well logs from petroleum wells, Phanerozoic and Neoproterozoic basins of Western Australia: Geological Survey of Western Australia, digital dataset, <www.dmirs.wa.gov.au/wapims>.

Core images from petroleum wells, Phanerozoic and Neoproterozoic basins of Western Australia

by

DM Brooks and F Irimies

Abstract

The Energy Systems Atlas is a collection of new geological map layers designed to help explorers identify each of the essential elements and processes of a petroleum system: source, reservoir, seal, burial, maturation, stratigraphic framework, structure, trap formation and migration. To help assess basin stratigraphy and lithology, core images from petroleum wells drilled within the Phanerozoic basins of Western Australia have been compiled from data submitted to the Geological Survey of Western Australia (GSWA). These core images are useful for examining lithology and sedimentary features. The core images have been compiled from various industry reports covering the majority of Western Australian sedimentary basins. New core images will be added when they are received.

The formations and depth intervals of each core image and a description of the data is given in the attribute tables of each core image in the Energy Systems Atlas. Unless otherwise stated the depths are given as metres measured depth.

How to access

The Energy Systems Atlas is best accessed using the Western Australian Petroleum and Geothermal Information Management System (WAPIMS). This online interactive mapping system allows data to be viewed and searched together with other datasets. The Energy Systems Atlas core images are also available as a data package on request from WAPIMS/requests form.

Recommended reference

Brooks, DM and Irimies, F 2021, Core images from petroleum wells, Phanerozoic and Neoproterozoic basins of Western Australia: Geological Survey of Western Australia, digital dataset, <www.dmirs.wa.gov.au/wapims>.

Mud logs from petroleum wells, Phanerozoic and Neoproterozoic basins of Western Australia

by

DM Brooks and F Irimies

Abstract

The Energy Systems Atlas is a collection of new geological map layers designed to help explorers identify each of the essential elements and processes of a petroleum system: source, reservoir, seal, burial, maturation, stratigraphic framework, structure, trap formation and migration. To help assess well operational information, hydrocarbon shows, drilling parameters and lithology, the mud logs from petroleum wells within Western Australia have been compiled from data submitted to the Geological Survey of Western Australia (GSWA). These mud logs are useful for examining a summary of well operations such as casing points, depths of formation tests, drilling parameters such as Rate of Penetration (ROP), weight on bit, mud weight, gas shows through continuous gas monitoring, oil shows from fluorescence observations and well site lithological descriptions. The mud logs have been compiled from Well Completion Reports covering the majority of Western Australian sedimentary basins. New mud logs will be added as they become open file.

The formations and depth intervals of each mud log and a description of the data is given in the attribute tables in the Energy Systems Atlas. Unless otherwise stated the depths are given as metres measured depth.

How to access

The Energy Systems Atlas is best accessed using the Western Australian Petroleum and Geothermal Information Management System (WAPIMS). This online interactive mapping system allows data to be viewed and searched together with other datasets. The Energy Systems Atlas mud logs are also available as a data package on request from WAPIMS/requests form.

Recommended reference

Brooks, DM and Irimies, F 2021, Mud logs from Petroleum wells, Phanerozoic and Neoproterozoic basins of Western Australia: Geological Survey of Western Australia, digital dataset, <www.dmirs.wa.gov.au/wapims>.

Hydrocarbon distribution: oil and gas fields, Phanerozoic and Neoproterozoic basins of Western Australia

by

DM Brooks and F Irimies

Abstract

The Energy Systems Atlas is a collection of new geological map layers designed to help explorers identify each of the essential elements and processes of a petroleum system: source, reservoir, seal, burial, maturation, stratigraphic framework, structure, trap formation and migration. A set of layers have been compiled to show the known distribution of hydrocarbons. This layer is oil and gas fields including operator, joint venture partners, location information and description of reservoir, seal, source, structural play type and hydrocarbons of each field within the Phanerozoic and some Proterozoic basins of Western Australia, which has been compiled from new and legacy data submitted to or generated by the Geological Survey of Western Australia (GSWA). These datasets are useful for assessing trends in oil and gas distribution. The hydrocarbon fields have been compiled from reports submitted to GSWA including from petroleum companies, other government departments, academic institutions and research bodies as well as new analysis arranged by GSWA covering the majority of Western Australian sedimentary basins. New hydrocarbon fields data will be added as they become open file.

The geology of the rocks within the hydrocarbon fields and descriptions of the data and methods of data collection are outlined in the original reports, which are included in the attribute tables for all data in the Energy Systems Atlas. GSWA publications are available from the DMIRS eBookshop. Unless otherwise stated the depths are given as metres measured depth.

How to access

The Energy Systems Atlas is best accessed using the Western Australian Petroleum and Geothermal Information Management System (WAPIMS). This online interactive mapping system allows data to be viewed and searched together with other datasets. The Energy Systems oil and gas fields are also available as a data package on request from WAPIMS/requests form.

Recommended reference

Brooks, DM and Irimies, F 2021, Hydrocarbon distribution: oil and gas fields, Phanerozoic and Neoproterozoic basins of Western Australia: Geological Survey of Western Australia, digital dataset, <www.dmirs.wa.gov.au/wapims>.

Hydrocarbon distribution: oil and gas shows, Phanerozoic and Neoproterozoic basins of Western Australia

by

DM Brooks and F Irimies

Abstract

The Energy Systems Atlas is a collection of new geological map layers designed to help explorers identify each of the essential elements and processes of a petroleum system: source, reservoir, seal, burial, maturation, stratigraphic framework, structure, trap formation and migration. A set of layers have been compiled to show the known distribution of hydrocarbons. This layer comprises hydrocarbon shows including descriptions of fluorescence oil shows and mud log gas measurements within the Phanerozoic and some Proterozoic basins of Western Australia, compiled from new and legacy data submitted to or generated by the Geological Survey of Western Australia (GSWA). These datasets are useful for assessing trends in oil and gas distribution. The hydrocarbon shows originate from reports submitted to GSWA including from petroleum companies, other government departments, academic institutions and research bodies as well as new analyses by GSWA covering the majority of Western Australian sedimentary basins. New hydrocarbon shows data will be added as they become open file.

The geology of the rocks containing hydrocarbon shows and descriptions of the data and methods of data collection are outlined in the original reports, which are included in the attribute tables for all data in the Energy Systems Atlas. GSWA publications are available from the DMIRS eBookshop. Unless otherwise stated the depths are given as metres measured depth.

How to access

The Energy Systems Atlas is best accessed using the Western Australian Petroleum and Geothermal Information Management System (WAPIMS). This online interactive mapping system allows data to be viewed and searched together with other datasets. The Energy Systems hydrocarbon shows are also available as a data package on request from WAPIMS/requests form.

Recommended reference

Brooks, DM and Irimies, F 2021, Hydrocarbon distribution: oil and gas shows, Phanerozoic and Neoproterozoic basins of Western Australia: Geological Survey of Western Australia, digital dataset, <www.dmirs.wa.gov.au/wapims>.

Hydrocarbon distribution: petroleum composition, Phanerozoic and Neoproterozoic basins of Western Australia

by

DM Brooks and F Irimies

Abstract

The Energy Systems Atlas is a collection of new geological map layers designed to help explorers identify each of the essential elements and processes of a petroleum system: source, reservoir, seal, burial, maturation, stratigraphic framework, structure, trap formation and migration. A set of layers have been compiled to show the known distribution of hydrocarbons. This layer shows petroleum composition including a list of percentage of petroleum components analysed from fluid and gas samples including hydrocarbons (C1 to C12+), CO_2, helium, hydrogen, oxygen, nitrogen, H_2S, CO and argon from petroleum wells within the Phanerozoic and some Proterozoic basins of Western Australia. These data have been compiled from new and legacy data submitted to or generated by the Geological Survey of Western Australia (GSWA). Petroleum composition data are useful for assessing trends in the geographic and stratigraphic distribution of oil, hydrocarbon gas and other petroleum components. The compositional data have been compiled from reports submitted to GSWA including from petroleum companies, other government departments, academic institutions and research bodies as well as new analysis arranged by GSWA covering the majority of Western Australian sedimentary basins. New petroleum composition data will be added as they become open file.

The descriptions of the data and methods of data collection and analyses are outlined in the original reports, which are included in the attribute tables for all data in the Energy Systems Atlas. GSWA publications are available from the DMIRS eBookshop. Unless otherwise stated the depths are given as metres measured depth.

How to access

The Energy Systems Atlas is best accessed using the Western Australian Petroleum and Geothermal Information Management System (WAPIMS). This online interactive mapping system allows data to be viewed and searched together with other datasets. The Energy Systems petroleum composition data are also available as a data package on request from WAPIMS/requests form.

Recommended reference

Brooks, DM and Irimies, F 2021, Hydrocarbon distribution: petroleum composition, Phanerozoic and Neoproterozoic basins of Western Australia: Geological Survey of Western Australia, digital dataset, <www.dmirs.wa.gov.au/wapims>.

Rock-Eval pyrolysis, Total Organic Carbon and vitrinite reflection data of hydrocarbon source rocks, Phanerozoic and Neoproterozoic basins of Western Australia

by

DM Brooks and F Irimies

Abstract

The Energy Systems Atlas is a collection of new geological map layers designed to help explorers identify each of the essential elements and processes of a petroleum system: source, reservoir, seal, burial, maturation, stratigraphic framework, structure, trap formation and migration. To help assess the hydrocarbon source rock potential, organic geochemistry data from Rock-Eval pyrolysis, Total Organic Carbon (TOC) and vitrinite reflectance measurements (Vr) within the Phanerozoic and some Proterozoic basins of Western Australia have been compiled from new and legacy data submitted to or generated by the Geological Survey of Western Australia (GSWA). These datasets are useful for assessing petroleum source-rock quality and quantity. The source-rock analyses have been compiled from reports submitted to GSWA including from petroleum companies, other government departments, academic institutions and research bodies as well as new analysis arranged by GSWA covering the majority of Western Australian sedimentary basins. New Rock-Eval, TOC and Vr data will be added when they become open file.

The geology of the source rocks and descriptions of the data and methods of all Rock-Eval, TOC and Vr data are outlined in the original reports, which are included in the attribute tables for all data in the Energy Systems Atlas. GSWA publications are available from eBookshop. Unless otherwise stated the depths are given as metres measured depth.

How to access

The Energy Systems Atlas is best accessed using the Western Australian Petroleum and Geothermal Information Management System (WAPIMS). This online interactive mapping system allows data to be viewed and searched together with other datasets. The Energy Systems Atlas organic geochemistry data are also available as a data package on request from WAPIMS/requests form.

Recommended reference

Brooks, DM and Irimies, F 2021, Rock-Eval pyrolysis, Total Organic Carbon and vitrinite reflection data of hydrocarbon source rocks, Phanerozoic and Neoproterozoic basins of Western Australia: Geological Survey of Western Australia, digital dataset, <www.dmirs.wa.gov.au/wapims>.

Routine Core Analysis data of reservoir rocks, Phanerozoic and Neoproterozoic basins of Western Australia

by

DM Brooks and F Irimies

Abstract

The Energy Systems Atlas is a collection of new geological map layers designed to help explorers identify each of the essential elements and processes of a petroleum system: source, reservoir, seal, burial, maturation, stratigraphic framework, structure, trap formation and migration. To help assess the reservoir potential, Routine Core Analysis (RCA) data including porosity, permeability, grain density, bulk density, lithology, water and oil saturation measurements within the Phanerozoic and some Proterozoic basins of Western Australia have been compiled from new and legacy data submitted to or generated by the Geological Survey of Western Australia (GSWA). These datasets are useful for assessing reservoir quality and quantity. The RCA data have been compiled from reports submitted to GSWA including from petroleum companies, other government departments, academic institutions and research bodies as well as new analysis arranged by GSWA covering the majority of Western Australian sedimentary basins. New RCA data will be added as they become open file.

The geology of the reservoir rocks and descriptions of the data and methods of all RCA data are outlined in the original reports, which are included in the attribute tables for all data in the Energy Systems Atlas. GSWA publications are available from DMIRS eBookshop. Unless otherwise stated the depths are given as metres measured depth.

How to access

The Energy Systems Atlas is best accessed using the Western Australian Petroleum and Geothermal Information Management System (WAPIMS). This online interactive mapping system allows data to be viewed and searched together with other datasets. The Energy Systems Atlas RCA analyses of measured porosity, permeability, bulk and grain density, lithology and pore fluid saturation are also available as a data package on request from WAPIMS/requests form.

Recommended reference

Brooks, DM and Irimies, F 2021, Routine Core Analysis data of reservoir rocks, Phanerozoic and Neoproterozoic basins of Western Australia: Geological Survey of Western Australia, digital dataset, <www.dmirs.wa.gov.au/wapims>.

Well correlations, Phanerozoic and Neoproterozoic basins of Western Australia

by

DM Brooks and F Irimies

Abstract

The Energy Systems Atlas is a collection of new geological map layers designed to help explorers identify each of the essential elements and processes of a petroleum system: source, reservoir, seal, burial, maturation, stratigraphic framework, structure, trap formation and migration. To help assess basin stratigraphy, published well correlations within the Phanerozoic basins of Western Australia have been compiled from new and legacy Geological Survey of Western Australia (GSWA) publications. These correlations are original GSWA interpretations of wireline logs, lithology and biostratigraphy from petroleum and mineral well intersections and outcrop. Well correlations have been compiled from various interpretation reports covering the majority of Western Australian sedimentary basins. New correlations will be added as new stratigraphic interpretation campaigns conclude.

The geology and a description of the data and methods of all well correlations are outlined in the original GSWA publications, which are given in the attribute tables of each correlation in the Energy Systems Atlas. GSWA publications are available from the DMIRS eBookshop. Legacy correlations do not show updates since the year of publication and do not incorporate newer well data. Unless otherwise stated, depth axes are given as metres below sea level and are positive downwards, and distance between wells are given as kilometres or without scale in cases where the well templates are evenly spaced.

How to access

The Energy Systems Atlas is best accessed using the Western Australian Petroleum and Geothermal Information Management System (WAPIMS). This online interactive mapping system allows data to be viewed and searched together with other datasets. The Energy Systems Atlas well correlations are also available as a data package on request from WAPIMS/requests form.

Recommended reference

Brooks, DM and Irimies, F 2021, Well correlations, Phanerozoic and Neoproterozoic basins of Western Australia: Geological Survey of Western Australia, digital dataset, <www.dmirs.wa.gov.au/wapims>.

SEEBASE layers provided in GSWA Reports 182 and 191, and OZ SEEBASE 2020 grid, 2020

by

CM Thomas and Y Zhan

Abstract

The Energy Systems Atlas is a collection of new geological map layers designed to help explorers identify each of the essential elements and processes of a petroleum system: source, reservoir, seal, burial/maturation, structure/trap formation and migration. Basement parameters such as depth and composition are important factors when considering heat flow, and in areas with little to no seismic coverage, depth-to-basement models determined from potential field datasets such as magnetic and gravity serve as good first-pass regional assessments of basin structure. In 2005, Frogtech Geoscience completed the OZ SEEBASE (Structurally Enhanced view of Economic BASEment) project using primarily potential field data with seismic interpretation constraints where possible, resulting in a continental-scale depth-to-basement grid highlighting the structure of Phanerozoic basins across Australia. With the acquisition of new potential field and seismic datasets since then, in 2017–18 the Geological Survey of Western Australia (GSWA) contracted Frogtech Geoscience (now Geognostics Australia) to revise the SEEBASE model of the Carnarvon Basin and the Canning Basin including the extension over the western Amadeus Basin, and to provide interpretations of basement terranes and lithology. The 2017 Canning SEEBASE project (GSWA Report 182) and the 2018 Carnarvon SEEBASE project (GSWA Report 191) have markedly increased the resolution of the Canning and Carnarvon Basin depth-to-basement models compared to the 2005 version, and improved identification of major structures, basement faults and crustal architecture. Geognostics Australia have incorporated the new depth models from these two projects into the latest OZ SEEBASE 2020 grid. The Canning Basin SEEBASE project (2017) also included a heat flow study that will aid geothermal explorers.

How to access

The Energy Systems Atlas is best accessed using the Western Australian Petroleum and Geothermal Information Management System (WAPIMS). This online interactive mapping system allows data to be viewed and searched together with other datasets. Original SEEBASE layers are available as zipped ASCII files or within ArcGIS data packages that can be ordered online via eBookshop for each of the Carnarvon and Canning Basin projects. The OZ SEEBASE 2020 grid and contours are displayed with permission from Geognostics Australia, and updated products will be added when available.

Recommended reference

Thomas, CM and Zhan, Y 2021, SEEBASE layers provided in GSWA Reports 182 and 191, and OZ SEEBASE 2020 grid, 2020: Geological Survey of Western Australia; digital dataset, <https://wapims.dmp.wa.gov.au/WAPIMS/GISMap/Map>.

Subsurface structure maps (two-way time, depth, isopach and two-way time thickness maps), Western Australian basins

by

CM Thomas and Y Zhan

Abstract

The Energy Systems Atlas is a collection of new geological map layers designed to help explorers identify each of the essential elements/processes of a petroleum system: source, reservoir, seal, burial/maturation, structure/trap formation and migration. To help assess basin structure, subsurface structure maps of major geological horizons, including formation boundaries within the Phanerozoic basins of Western Australia, have been compiled from new and legacy Geological Survey of Western Australia (GSWA) publications. These maps are based primarily on original GSWA interpretation of industry and government reflection seismic data tied to well intersections and outcrop. Structure maps have been compiled from various interpretation reports covering the southwest Canning Basin and Broome Platform (Canning Basin), the northern Canning Basin, Officer Basin, Eucla Basin, Bremer Basin, offshore Bonaparte Basin, the Merlinleigh Sub-basin (Southern Carnarvon Basin), the Peedamullah Shelf (Northern Carnarvon Basin), and both the northern and southern Perth Basins. New maps will be added as digitization continues and as new seismic interpretation campaigns conclude. Outlines of salt intrusions mapped from seismic data in the Officer Basin have also been digitized, and the layer will later include other basins as mapping and digitization continues.

The geology and a description of the data and methods of all subsurface structure maps are outlined in the original GSWA publication, which is given in the attribute tables of the contour versions of each map in the Energy Systems Atlas. GSWA publications are available from eBookshop. Some legacy maps were re-gridded and lightly smoothed using digitized versions of the map data presented in the publications. Subsurface maps do not show updates since the year of publication and do not incorporate newer well and seismic data. Unless otherwise stated, depth maps are given as metres below sea level and are positive downwards, and two-way time (TWT) maps are given as milliseconds referenced from median sea level.

How to access

The Energy Systems Atlas is best accessed using the Western Australian Petroleum and Geothermal Information Management System (WAPIMS). This online interactive mapping system allows data to be viewed and searched together with other datasets. The Energy Systems Atlas subsurface structure digital data are also available as free downloads from the Data and Software Centre via Datasets — Statewide spatial datasets — Energy Systems Atlas — Subsurface structure and isopach/thickness maps, as ESRI shapefiles and MapInfo TAB files and as raster grid (.BIL) files.

Recommended reference

Thomas, CM and Zhan, Y 2021, Subsurface structure maps (two-way time, depth, isopach and two-way time thickness maps), Western Australian basins: Geological Survey of Western Australia; digital dataset, <https://wapims.dmp.wa.gov.au/WAPIMS/GISMap/Map>.

Regional salt maps (two-way time, depth, isopach and two-way time thickness maps), Phanerozoic and Neoproterozoic basins of Western Australia

by

Y Zhan and CM Thomas

Abstract

The Energy Systems Atlas is a collection of new geological map layers designed to help explorers identify each of the essential elements and processes of a petroleum system: source, reservoir, seal, burial, maturation, stratigraphic framework, structure, trap formation and migration. A set of regional depth and isopach maps have been compiled to delineate the lateral extents of subsurface salt formations that have potential sealing capacity to trap hydrocarbons, helium and natural hydrogen and possibly be utilized for manufactured hydrogen storage, and as a seal for carbon dioxide sequestration. The currently known subsurface salts are present in the Canning, Officer, Amadeus, Carnarvon and Bonaparte Basins. Some of these salts have been interpreted and mapped by the Geological Survey of Western Australia (GSWA) based on well intersections and reflection seismic data. The maps cover the southern Canning and Officer Basins, and new maps will be added as new interpretation campaigns conclude.

The geology and a description of the data and methods of all subsurface salt structure maps are outlined in the original GSWA publication, which is given in the attribute tables of the contour versions of each map in the Energy Systems Atlas. GSWA publications are available from the DMIRS eBookshop. Some legacy maps were re-gridded and lightly smoothed using digitized versions of the map data presented in the publications. Subsurface maps do not show updates since the year of publication and do not incorporate newer well and seismic data. Unless otherwise stated, depth maps are given as metres below sea level and are positive downwards, and two-way time (TWT) maps are given as milliseconds referenced from median sea level.

How to access

The Energy Systems Atlas is best accessed using the Western Australian Petroleum and Geothermal Information Management System (WAPIMS). This online interactive mapping system allows data to be viewed and searched together with other datasets. The Energy Systems Atlas subsurface salt structure digital data are also available as free downloads from the Data and Software Centre via Datasets — Statewide spatial datasets — Energy Systems Atlas — Subsurface structure and isopach/thickness maps, as ESRI shapefiles and MapInfo TAB files and as raster grid (.BIL) files.

Recommended reference

Zhan, Y and Thomas, CM 2021, Regional salt maps (two-way time, depth, isopach and two-way time thickness maps), Phanerozoic and Neoproterozoic basins of Western Australia: Geological Survey of Western Australia, digital dataset, <www.dmirs.wa.gov.au/wapims>.

RECORD 2021/4

ACCELERATED GEOSCIENCE PROGRAM EXTENDED ABSTRACTS

This Record is published in digital format (PDF) and is available as a free download from the DMIRS website at <www.dmirs.wa.gov.au/GSWApublications>.

Further details of geoscience products are available from:

Information Centre
Department of Mines, Industry Regulation and Safety
100 Plain Street
EAST PERTH WESTERN AUSTRALIA 6004
Phone: +61 8 9222 3459 Email: publications@dmirs.wa.gov.au
www.dmirs.wa.gov.au/GSWApublications